Identifizierung des epidermalen Wachstumsfaktor-Rezeptors als Zielstruktur für Umweltschadstoffe

Inaugural-Dissertation

zur Erlangung des Doktorgrades

der Mathematisch-Naturwissenschaftlichen Fakultät

der Heinrich-Heine-Universität Düsseldorf

vorgelegt von

Natalie Caroline Sondermann

aus Düsseldorf

Düsseldorf, November 2024

aus dem IUF – Leibniz-Institut für umweltmedizinische Forschung GmbH

Gedruckt mit der Genehmigung der

Mathematisch-Naturwissenschaftlichen Fakultät der

Heinrich-Heine-Universität Düsseldorf

Berichterstatter/innen:

1. Promotionsbetreuer: Priv.-Doz. Dr. Thomas Haarmann-Stemmann

2. Mentorin: Prof. Dr. Henrike Heise

Tag der mündlichen Prüfung: **06.03.2025**

Inhaltsverzeichnis

Abstract

A large number of persistent and bioaccumulating pollutants are present in the environment as a result of anthropogenic influences. These are found in the air, in water, in soil, in wild animals and also in humans and can have harmful effects on health. A prominent receptor that initiates the metabolism of many of these environmental pollutants is the aryl hydrocarbon receptor (AHR). Enzymes induced via the AHR signaling pathway can cause detoxification, but also toxic activation of its ligands and thus support the development or progression of certain diseases. In addition, the AHR signaling response has a certain ligand specificity in which, for example, polycyclic aromatic hydrocarbons (PAHs) differ from dioxins and dioxin-like substances (DLCs), among other things by exerting a different influence on another receptor. This is the epidermal growth factor receptor (EGFR), which controls important signaling pathways in homeostasis and the development of various tissues. In this study, not only was the interaction between the AHR and EGFR signaling pathways investigated in more detail, but the EGFR itself was also identified as a direct target structure for exposure-relevant environmental pollutants. It has been observed that dioxins, DLCs, benzotriazole UV stabilizers (BUVs) and polybrominated diphenyl ethers (PBDEs) can bind directly to the extracellular domain of the receptor and inhibit its ligand activation. This can also affect cellular processes such as DNA synthesis or expression of certain target genes. Deepening the understanding of the interaction between AHR and EGFR, along with identifying EGFR as a direct target for a variety of organic pollutants may not only help to understand the development of various diseases but also contribute to the creation of new therapeutic approaches and endpoints for risk assessment of environmental chemicals.

Zusammenfassung

Durch anthropogene Einflüsse liegt eine Vielzahl persistierender und bioakkumulierender Schadstoffe in der Umwelt vor. Diese finden sich in der Luft, in Gewässern, in Böden, in Wildtieren und auch im Menschen und können gesundheitsschädliche Folgen haben. Ein prominenter Rezeptor, der den Metabolismus einer Vielzahl dieser Umweltschadstoffe initiiert, ist der Arylhydrocarbon-Rezeptor (AHR). Über den AHR aktivierte Enzyme können eine Detoxifizierung, jedoch auch eine toxische Aktivierung seiner Liganden bewirken und somit die Entstehung oder das Voranschreiten bestimmter Krankheiten unterstützen. Hinzu kommt, dass die AHR-Signalantwort eine gewisse Ligandenspezifität aufweist, bei der z.B. polyzyklische aromatische Kohlenwasserstoffe (PAKs) sich von Dioxinen und Dioxin-ähnliche Substanzen (DLCs) unterscheiden, u.a. indem sie unterschiedlich Einfluss auf einen weiteren Rezeptor nehmen. Bei diesem handelt es sich um den epidermalen Wachstumsfaktorrezeptor (EGFR), welcher wichtige Signalwege in der Homöostase als auch Entwicklung verschiedener Gewebe steuert. In dieser Arbeit wurde nicht nur die Interaktion zwischen dem AHR- und EGFR-Signalweg genauer untersucht, sondern auch der EGFR selbst als direkte Zielstruktur für expositionsrelevante Umweltschadstoffe identifiziert. So konnte beobachtet werden, dass Dioxine, DLCs, Benzotriazol-UV-Stabilisatoren (BUVs) und polybromierte Diphenylether (PBDEs) direkt an die extrazelluläre Domäne des Rezeptors binden und dessen Liganden-Aktivierung inhibieren können. Dies kann sich auch auf zelluläre Prozesse, wie z.B. die DNA-Synthese oder Expression bestimmter Zielgene, auswirken. Die Vertiefung des Verständnisses der Interaktion zwischen AHR und EGFR sowie die Identifizierung des EGFR als direkte Zielstruktur für eine Vielzahl organischer Schadstoffe kann nicht nur dabei helfen, die Entstehung verschiedener Krankheiten zu verstehen, sondern auch relevant für die Entwicklung neuer therapeutischer Ansätze oder Endpunkte zur Risikobewertung von Umweltchemikalien sein.

1 Einleitung

1.1 Umweltschadstoffe

Unter dem Begriff Umweltverschmutzung versteht man das Einführen von für Organismen schädliche Substanzen in die Umwelt durch hauptsächlich anthropogene Belastungen. Diese Substanzen werden als Kontaminanten oder Umweltschadstoffe bezeichnet. Ihre Expositionswege in Bezug auf den menschlichen Organismus sind divers, da sie beispielsweise im Trinkwasser, der Luft, den Meeren und Seen, im Hausstaub oder in Agrarflächen vorliegen (Butte und Heinzow 2002, Manisalidis et al. 2020). In Abhängigkeit von Dauer und Ausmaß, kann die Exposition gegenüber diesen Umweltschadstoffen ein Risiko für die Gesundheit der Allgemeinbevölkerung darstellen. So gibt es Hochrechnungen von Fuller et al. zufolge seit 2015 jährlich ca. 9 Millionen verfrühte Tode, welche von Umweltschadstoffen verschuldet sind (Fuller et al. 2022).

Eine Umweltschadstoffgruppe von großer Bedeutung sind die polyzyklischen aromatischen Kohlenwasserstoffe (PAKs), welche bei unvollständigen Verbrennungsprozessen von organischem Material entstehen (Yasuda und Takahashi 1998). Diese können sowohl natürlich auftreten, wie beispielsweise bei einem Waldbrand oder einer Vulkaneruption, als auch anthropogen, etwa bei der Nutzung fossiler Brennstoffe oder Prozesse der Stahlindustrie (Yemele et al. 2024). PAKs haben lipophile Eigenschaften und bergen ein hohes Bioakkumulationspotential, wobei sich besonders in aquatischen Vertebraten und Invertebraten toxische Konzentrationen ansammeln können (Honda und Suzuki 2020). Bei Exposition können PAKs sich negativ auf die menschliche Gesundheit auswirken und sowohl akute als auch chronische Effekte hervorrufen. Zu den Auswirkungen akuter PAK-Intoxikation

gehören z.B. Irritationen, Übelkeit oder Diarrhö, während eine chronische Exposition beispielsweise Krebs, Störungen des Immunsystems, respiratorische oder kardiovaskuläre Erkrankungen zufolge haben kann (Mallah et al. 2022). So wird z.B. der wohl am meisten erforschte PAK Benzo(a)pyren (BaP) auch von der Internationalen Agentur für Krebsforschung als karzinogen für Menschen eingestuft (Bull und Collins 2013).

Eine andere bedeutsame Gruppe toxischer Umweltschadstoffe sind die persistenten organischen Schadstoffe (*persistent organic pollutants*; POPs) (Abb. 1). Dabei handelt es sich um synthetische Chemikalien, welche natürlichen Degradierungsprozessen gegenüber sehr resistent sind und somit in der Umwelt persistieren. Hinzu kommt, dass sie einen lipophilen Charakter haben und somit in fettreichen Geweben von Tier und Mensch akkumulieren (Li et al. 2006). Neben den von einzelnen Chemikalien hervorgerufenen Effekten spielen auch Mischungseffekte eine große Rolle. Dies liegt daran, dass Umweltschadstoffe selten isoliert auftreten, sondern eine Exposition und Bioakkumulation verschiedener Schadstoffe im Organismus stattfinden. Solche Mischungseffekte können der Grund dafür sein, dass auch eine nicht-toxische Dosis bestimmter Substanzen beispielsweise das Krebsrisiko signifikant erhöhen kann (Fernandez-Martinez et al. 2020, Fazakas et al. 2024, Keil und O'Brien 2024).

Aufgrund der bekannten Gesundheitsrisiken von POPs und ihrer globalen Verbreitung wurde 2001 das „Stockholmer Übereinkommen über persistente organische Schadstoffe“, auch Stockholm-Konvention, als völkerrechtlich bindende Verbots- und Beschränkungsmaßnahme beschlossen. Ziel dieses Übereinkommens, welches 2004 in Kraft trat, ist die globale Reduktion bzw. Eliminierung von bestimmten POPs zum Schutz der Bevölkerung und verschiedener Ökosysteme. Die initialen zwölf POPs, welche über das Abkommen reguliert wurden, sind als „dreckiges Dutzend“ bekannt,

darunter z.B. Industriechemikalien wie polychlorierte Biphenyle (PCBs) und Dioxine oder Insektizide, wie Dichlordiphenyltrichlorethan (DDT) und Hexachlorbenzol (UNEP 2001). Seit Inkrafttreten kamen noch zahlreiche weitere Chemikalien hinzu, wie zum Beispiel die als Flammschutzmittel verwendeten polybromierten Diphenylether (PBDE) oder der Benzotriazol-UV-Stabilisator (BUV) UV-328 (UNEP 2023a).

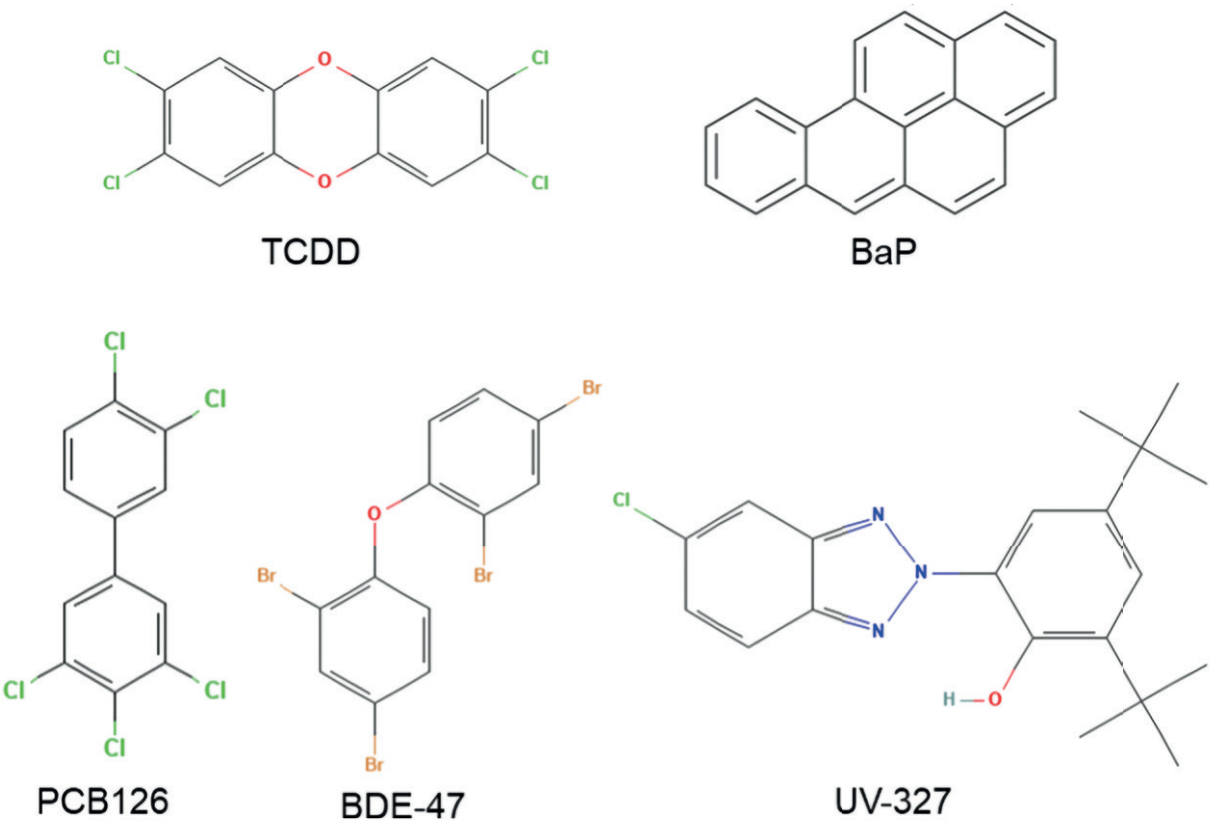

Abb. 1: 2D-Strukturen verschiedener organischer Umweltschadstoffe. Die Strukturen wurden aus der Datenbank PubChem (https://pubchem.ncbi.nlm.nih.gov) übernommen. PubChem IDs: TCDD (15625), BaP (2336), PCB126 (63090), BDE-47(23249466), UV-327 (77470).

Seit Jahren wird die Verteilung und Konzentration von POPs in der Umwelt und in verschiedenen Organismen über zahlreiche Monitoring-Projekte beobachtet (Guardans 2024). Eines der umfassendsten Programme, welches als Teil der Stockholm-Konvention zur Bemessung ihrer Effektivität dient, ist der *Global Monitoring Plan*. Im letzten Report aus 2023 wurden beispielsweise signifikant hohe

Konzentrationen beinahe aller POPs in humaner Muttermilch festgestellt, wobei für die initialen POPs, z.B. PCBs, seit 2000 ein konstant abnehmender Trend verzeichnet wurde. Dennoch ist die Humandatenlage zu POPs sehr limitiert, was die Notwendigkeit von weiterem Biomonitoring und populationsbasierten Studien, insbesondere zur Einschätzung von Langzeitfolgen, unterstreicht (UNEP 2023c). Für eine adäquate Risikoabschätzung wird außerdem ein besseres Verständnis der Wirkmechanismen diverser POPs, insbesondere auf zellulärer und molekularer Ebene, benötigt.

1.2 Dioxine und dioxinähnliche Substanzen (DLCs)

Dioxine und dioxinähnliche Substanzen (*dioxin-like compounds*; DLCs) zeichnen sich strukturell durch ein System von zwei oder drei Benzolringen sowie verschiedene Grade der Chlorierung aus. Zu ihnen gehören polychlorierte Dibenzo-*p*-dioxine (PCDDs), polychlorierte Dibenzofurane (PCDFs) und PCBs, welche sich bei Exposition allesamt negativ auf die menschliche Gesundheit auswirken können (WHO 2019). Eine akute Intoxikation mit Dioxinen und DLCs kann die Leberfunktion einschränken und Chlorakne, eine chronisch-entzündliche Hauterkrankung, verursachen. Zu den Langzeitfolgen einer Exposition gehören z.B. die Schädigung des Nervensystems, Immundefizienz, reprotoxische Effekte oder eine Störung des endokrinen Systems (Marinkovic et al. 2010). Dioxine und DLCs sind lipophil und können über Jahre im Körper verbleiben, wobei für manche PCDFs eine Halbwertzeit von 6 Monaten bis hin zu 20 Jahren berechnet wurde (Schecter et al. 2006, Milbrath et al. 2009). Die ubiquitär vorhandenen Dioxine und DLCs werden hauptsächlich als unerwünschte Nebenprodukte durch anthropogene Prozesse in die Umwelt gebracht (Dopico und Gomez 2015). Dies geschieht in erster Linie über Verbrennungsprozesse,

wie z.B. der Verbrennung von Krankenhausabfällen oder Klärschlamm, der Metallverhüttung sowie der Dieselverbrennung (Kulkarni et al. 2008).

Als toxischste dieser Substanzen gilt 2,3,7,8-Tetrachlordibenzo-*p*-dioxin (TCDD), welches häufig schlicht „Dioxin“ genannt wird (Birnbaum 1994). Dieses wurde 1956 erstmals von Wilhelm Sandermann am Institut für Holzchemie und chemische Technologie des Holzes der Bundesforschungsanstalt für Forst- und Holzwirtschaft synthetisiert. Aufgrund der hohen Akuttoxizität und der kostengünstigen Synthese wurde seinen Entdeckern untersagt, über die Giftwirkung von TCDD zu publizieren. So sollte dessen mögliche Nutzung als militärischer Kampfstoff nicht gefährdet werden. Stattdessen publizierten Sandermann und Kollegschaft die TCDD-Formel „versteckt“, ohne seine besondere Toxizität zu erwähnen, 1957 in seiner Veröffentlichung über Pentachlorphenol. Diese half kurze Zeit später dabei, TCDD als jenes „Supergift“ zu identifizieren, welches als Verunreinigung in chemischen Werken bereits zuvor zu Intoxikationen, u.a. mit starken Hauterkrankungen, geführt hatte (Sandermann 1974, Sandermann 1984). In seiner Publikation von 1974 schildert Sandermann die Folgen polychlorierter aromatischer Verbindungen für die Gesundheit und nennt neben Dermatosen auch die mögliche teratogene, mutagene und kanzerogene Wirkung dieser Substanzen (Sandermann 1974). Dies bestätigen auch aktuellere Studien, welche die Nachwirkungen des Sevesounglücks, einem Chemieunfall mit TCDD-Freisetzung im Jahr 1976, behandeln. Sowohl damalige Anwohner der italienischen Stadt Seveso als auch die darauffolgende Generation weisen eine erhöhte Rate an kardiovaskulären Erkrankungen, Diabetes mellitus und verschiedenen Krebsarten auf. Hinzu kommt eine verminderte Fruchtbarkeit von Männern und Frauen, was die Rolle von TCDD als endokrinem Disruptor unterstreicht (Eskenazi et al. 2018, Consonni et al. 2024). Im Jahr des Sevesounglücks wurde auch

der Mechanismus hinter der Entstehung der TCDD-induzierten Chlorakne näher aufgeschlüsselt, als die Gruppe um Alan Poland herum einen hochaffinen Rezeptor für TCDD entdeckte. Das zunächst als Dixoinrezeptor benannte Signalmolekül ist heute als Arylhydrocarbon-Rezeptor (AHR) bekannt (Poland et al. 1976, Sondermann et al. 2023). Der AHR wird neben Dioxinen auch von PCBs und anderen DLCs aktiviert, wobei TCDD jedoch die höchste Affinität zum Rezeptor aufweist (Kafafi et al. 1993, Zhang et al. 2022). TCDD ist sehr persistent und wird aufgrund der Positionierung seiner vier Chloratome nicht oder nur in sehr geringem Maße durch CYP-Enzyme oxidiert (Sorg et al. 2009). Durch Bindung an den AHR induziert TCDD jedoch CYP-Enzyme, welche aus Mangel eines Elektronenakzeptors Sauerstoff-CYP-Komplexe bilden, welche wiederum über Autooxidation Superoxide freisetzen und letztlich zu einem gesteigerten Level reaktiver Sauerstoffspezies (ROS) führen (Park et al. 1996, Knerr et al. 2006, Albertolle und Peter Guengerich 2018, Wang et al. 2024). Dieser oxidative Stress kann z.B. auch EGFR-abhängige MAPK-Signalwege aktivieren, was zu unkontrollierter Proliferation oder Apoptose führen kann (Son et al. 2013, Murray et al. 2014).

Eine weitere Gruppe DLCs, die von besonderem wissenschaftlichem Interesse ist, bilden die PCBs. Durch das fortlaufende Bestehen von PCBs in der Umwelt und am Arbeitsplatz sowie den damit einhergehenden Gesundheitsrisiken, rückten sie besonders im letzten Jahrzehnt zurück in den Fokus der Forschung (Abafe und Martincigh 2015, Montano et al. 2022). Von besonderer Relevanz war hierbei, dass PCBs vor Einführung der Stockholm-Konvention, jahrelang bei der Produktion zahlreicher Produkte und Materialien verwendet wurden, welche noch heute vor allem in Innenräumen vorfindbar sind (Kohler et al. 2005, Dai et al. 2016). Somit liegt eine PCB-Belastung der Luft und Oberflächen in vielen Innenräumen vor, was zu einer

chronischen Exposition von Individuen mit diesen Substanzen beiträgt (Dai et al. 2016, Montano et al. 2022).

Um die Toxizität von Dioxinen, DLCs und Mischungen aus ihnen besser einschätzen zu können, wurde das System der Toxizitätsäquivalenz (TEQ) entwickelt. Dabei wird die Giftigkeit der Einzelsubstanzen oder Mischungen auf TCDD als giftigste Verbindung dieser Stoffgruppe bezogen (Van den Berg et al. 1998). Erst 2022 nahm die Weltgesundheitsorganisation (WHO) eine Reevaluation dieses Systems vor und betonte hierbei nochmals die enormen Speziesunterschiede hinsichtlich der Effekte von TCDD und DLCs sowie den Mangel an Humandaten (Eaton et al. 2024).

1.3 Polybromierte Diphenylether (PBDEs)

PBDEs werden aufgrund ihrer flammenhemmenden Eigenschaften vor allem als Additive in der Produktion verschiedener Konsumgüter, darunter Baumaterialien, Elektronikartikel oder Textilien, genutzt (Linares et al. 2015). Als Flammschutzmittel können sie den Verbrennungsprozess inhibieren, indem die substituierten Brommoleküle zerfallen und Bromradikale bilden, welche wiederum mit dem Kohlenwasserstoff reagieren und Bromwasserstoff (HBr) bilden. Der in hoher Konzentration freigesetzte Bromwasserstoff neutralisiert die hochenergetischen H- und OH-Radikale, indem er diese durch weniger energetische Bromradikale ersetzt. Der dabei verbrauchte Bromwasserstoff wird dann wiederum durch Reaktion mit Kohlenwasserstoff regeneriert. Dieser Zyklus endothermer Reaktionen wird aufrechterhalten und sorgt über Neutralisierung hochenergetischer Radikale für die Hemmung der Verbrennungsreaktion (Alaee et al. 2003, Morgan 2024).

Sowohl in der Außenluft als auch in Hausstaub, Nahrungsmitteln, Böden, Wasser und Marinegewässern treten PBDEs auf, wobei die wichtigsten humanen Expositionswege

inhalativ, dermal oder über die Nahrungsaufnahme ablaufen. Durch ihren persistenten und lipophilen Charakter akkumulieren sie in Fettgeweben von exponierten Organismen sowie in fetthaltigen tierischen und pflanzlichen Produkten (Fromme et al. 2016, Gomes et al. 2024).

Seit 2004 ist die Produktion von PBDEs über die Stockholm-Konvention reguliert. Trotz dessen gelangen sie weiterhin in die Umwelt, da sie z.B. aus PBDE-haltigen Produkten austreten oder beim Recycling dieser freigesetzt werden können (Sharkey et al. 2020).

1.4 Benzotriazol-UV-Stabilisatoren (BUVs)

BUVs, auch als Phenol-Benzotriazole bekannt, sind stark lipophile Substanzen, welche als Additive zum Schutz vor UV-induzierter Schädigung, wie dem Vergilben oder einer lichtinduzierten Degradierung von Materialien und Produkten, eingesetzt werden (Pavanello et al. 2022). Hierzu eignen sie sich, da sie UV-Strahlen sehr schnell in Wärme umwandeln können (Köhler et al. 2010). BUVs wurden großflächig eingesetzt und könnten beispielsweise auch aus Plastikprodukten, sowohl bei ihrer Produktion als auch Verwendung oder Entsorgung, austreten. Daher sind diese Industriechemikalien weit in unserer Umwelt verbreitet und wurden bereits in verschiedenen Fischen, Meeressäugern, Vögeln und in Humanproben nachgewiesen. Dennoch ist das Wissen über die genauen biologischen Effekte, welche BUVs insbesondere auf Säugetiere haben, trotz ihrer hohen Verbreitung begrenzt (Khare et al. 2023). Aktuell gibt es zumindest Hinweise darauf, dass einige BUVs den AHR aktivieren können (Nagayoshi et al. 2015), immunsuppressive Effekte haben (Kubota et al. 2022), mit Steroidhormonrezeptoren (Zhuang et al. 2017, Feng et al. 2020, He et al. 2022) sowie dem epidermalen Wachstumsfaktor-Rezeptor (*epidermal growth factor*

receptor; EGFR) (Sondermann et al. 2024) interagieren und so die natürliche Homöostase stören könnten.

Aufgrund der bekannten und unbekannten Gefahren, welche von BUVs ausgehen, wurden verschiedene präventive Maßnahmen ergriffen, um ihre weitere Verbreitung einzudämmen. So wurde UV-328 im Jahr 2023 als erstes BUV in die Stockholm-Konvention aufgenommen (UNEP 2023b). Weitere BUVs, wie UV-320, UV-326, UV-327 und UV-350, unterliegen bereits anderen Regulationen zum Risikomanagement (Watanabe und Noma 2010, ECHA 2015, ECHA 2023).

1.5 Arylhydrocarbon-Rezeptor (AHR)

Erstmals identifiziert wurde der AHR im Jahr 1976 von Alan Poland und seinen Kollegen, als sie Versuche mit radioaktiv markiertem TCDD durchführten, welches an das Rezeptormolekül gebunden hat (Poland et al. 1976). Der AHR gehört zu der Familie der Per-Arnt-Sim (PAS)-Transkriptionsfaktoren und weist ein basisches Helix-Loop-Helix Motiv auf. Darüber hinaus hat der AHR zwei PAS-Domänen, PAS-A und PAS-B, wobei die PAS-B-Domäne unter anderem der Ligandenbindung dient (Wu et al. 2013).

In seinem inaktiven Zustand liegt der AHR als Teil eines Multiproteinkomplexes, bestehend aus dem *AHR-interacting protein*, einem Heatshock Protein 90-Dimer, dem Co-Chaperon p23 sowie der Proteintyrosinkinase Src im Zytosol vor (Jia et al. 2019, Paris et al. 2022). Sobald der AHR von einem Liganden gebunden wird, zerfällt dieser Komplex und der AHR transloziert in den Nukleus. Dort bildet er über seine beiden PAS-Domänen ein Heterodimer mit seinem Partnermolekül, dem *AHR-nuclear translocator* (ARNT). Das entstandene Heterodimer bindet wiederum an sogenannte xenobiotisch-responsive Elemente (XRE, 5‘-GCGTG-3‘) in der *Enhancer*-Region der

Zielgene, um den generellen Transkriptionsapparat zu rekrutieren und anschließend die Genexpression zu induzieren (Wu et al. 2013, Avilla et al. 2020). Die am besten untersuchten Zielgene des AHR/ARNT-Komplexes kodieren für die Cytochrom P450 (CYP)-Enzyme CYP1A1, CYP1A2 und CYP1B1, welche die Detoxifizierung der AHR-aktivierenden Subtanzen vorantreiben (Nebert und Karp 2008, Ye et al. 2019). Auf der anderen Seite können CYP-Enzyme jedoch auch zur metabolischen Aktivierung von AHR-Liganden und der Entstehung von oxidativem Stress beitragen, was wiederum zu Schäden an DNA oder anderen Makromolekülen führen kann. So ist beispielsweise bekannt, dass AHR-defiziente Mäuse im Gegensatz zu ihren AHR-profizienten Wurfgeschwistern keine Hauttumore bilden, nachdem sie mit dem AHR-Agonisten BaP behandelt wurden, was durch die verminderte CYP1A-Expression in diesen Tieren begründet wurde (Shimizu et al. 2000). Das PAK Dibenzo[a,l]pyrene konnte hingegen auch in AHR-defizienten Mäusen weiterhin über CYP1B1 metabolisiert werden, sodass im Vergleich zur AHR-profizienten Kontrollgruppe ein Drittel der Tiere weiterhin Tumore entwickelte. Zudem wurde festgestellt, dass CYP1B1 sowohl in AHR-profizienten und -defizienten Mäusen konstitutiv exprimiert wurde (Nakatsuru et al. 2004). Tatsächlich sind CYP1A1 und CYP1B1 beispielsweise dafür verantwortlich, dass das Prokarzinogen BaP im Körper zum karzinogenen Benzo[a]pyren-7,8-dihydroxy-9,10-epoxid metabolisiert wird. Dies geschieht über eine initiale Epoxidierung von BaP durch besagte CYP1-Monooxygenasen, gefolgt von einer Hydrolyse über Epoxidhydrolasen und anschließend einer weiteren CYP1-katalysierten Epoxidierung, welche den DNA-reaktiven Metaboliten bildet (Xue und Warshawsky 2005, Reed et al. 2018).

Zwar ist bekannt, dass die Effekte des AHR liganden-, gewebe- und zellspezifisch sind, doch viele der expliziten AHR-Antworten wurden noch nicht genau aufgeschlüsselt.

Darüber hinaus ist der AHR auch in zahlreichen anderen Signalwegen involviert, wodurch das AHR-vermittelte Signaling nochmal an Komplexität gewinnt. Einige wichtige Signalmoleküle, deren Wege sich mit dem AHR überschneiden, sind der EGFR oder Transkriptionsfaktor NF-κB (*nuclear factor 'kappa-light-chain-enhancer' of activated B-cells*) (Sondermann et al. 2023). Somit ist anzunehmen, dass auch die von AHR-Liganden vermittelten Gesundheitsschäden über weitere Moleküle vermittelt oder verstärkt werden. Zwar ist die Relevanz des AHR bei der Entstehung von TCDD-induzierten Gesundheitsschäden unumstritten (Mimura und Fujii-Kuriyama 2003), jedoch scheint der Rezeptor nicht allein für diese Effekte verantwortlich zu sein (Sorg 2014). So deuten zumindest erste Hinweise darauf hin, dass auch die Bindung von TCDD an die extrazelluläre Domäne (*extracellular domain*; ECD) des EGFR, und die daraus resultierende Inhibierung des Rezeptors, z.B. zur Pathogenese von Chlorakne beitragen könnten (Vogeley et al. 2022).

1.6 Epidermaler Wachstumsfaktor-Rezeptor (EGFR)

Der humane EGFR gehört zur ErbB-Familie der Rezeptorproteinkinasen (RTKs), welche aus dem EGFR (ErbB1), ErbB2, ErbB3 und ErbB4 besteht. All diese Proteine sind membranständig und haben eine intra- sowie extrazelluläre Domäne (Burgess 2008, Roskoski 2014). Sollte eines dieser Proteine in der menschlichen Entwicklung fehlen, tritt aufgrund von Defekten im Gehirn oder Herzen der Tod bereits embryonal oder sehr früh postnatal ein. Doch auch eine Überexpression oder Mutation eines der Rezeptoren hat fatale Auswirkungen, wie z.B. Lungenkrebs (Burgess 2008). Der EGFR-Signalweg reguliert in Säugetieren das Wachstum, Überleben, Proliferation sowie Differenzierung von Zellen. Dies macht ihn zu einem der am meisten erforschten Signalwege, wobei 2005 beispielsweise das gesamte bis dato bekannte System des

EGFR-Signalings mit 211 Reaktionen und 322 agierenden Proteinen zusammengefasst wurde (Oda et al. 2005).

In Abwesenheit eines Liganden liegt der EGFR als Monomer vor, wobei die ECD als kompakte Struktur (*tethered*) besteht. Sobald ein Ligand bindet, ändert der Rezeptor seine Konformation und die ECD klappt sich aus (*untethered*) (Kozer et al. 2011). Die EGFR ECD setzt sich aus vier Domänen zusammen, wobei Liganden, wie z.B. der epidermale Wachstumsfaktor (*epidermal growth factor*; EGF), zwischen Domäne I und III binden (Ferguson 2008) (Abb. 2). Nach Ligandenbindung wird ein Homodimer aus zwei EGFR-Molekülen oder ein Heterodimer mit einem anderen Mitglied der ErbB-Familie gebildet. Daraufhin findet eine Autophosphorylierung der intrazellulären Domänen statt, was wiederum das Downstream-Signaling steuert und anschließend erfolgt die Internalisierung des Rezeptors sowie seiner Degradierung bzw. seines Recyclings (Schlessinger 2000, Dawson et al. 2005, Oda et al. 2005, Henriksen et al. 2013).

Die Internalisierung des EGFR wird hauptsächlich über das Protein Clathrin gesteuert, wobei der internalisierte EGFR nicht degradiert, sondern recycelt wird und zur Plasmamembran zurückkehrt. Dies führt zu einer konstanten Rezeptorverfügbarkeit und ermöglichst eine vermehrte EGFR-Aktivierung (Sigismund et al. 2008). Daneben gibt es auch eine Clathrin-unabhängige Internalisierung des EGFR, bei welcher der Rezeptor ubiquitiniert und anschließend degradiert wird. Dies funktioniert über eine Bindung des aktiven EGFR durch das Growth Factor Receptor-bound Protein 2, welches ein Src-Homolog ist, und die E3 Ubiquitinligase Cbl rekrutiert. Dieser Prozess

führt zu einer verminderten EGFR-Aktivität (Sigismund et al. 2005, Orth et al. 2006, Tomas et al. 2014).

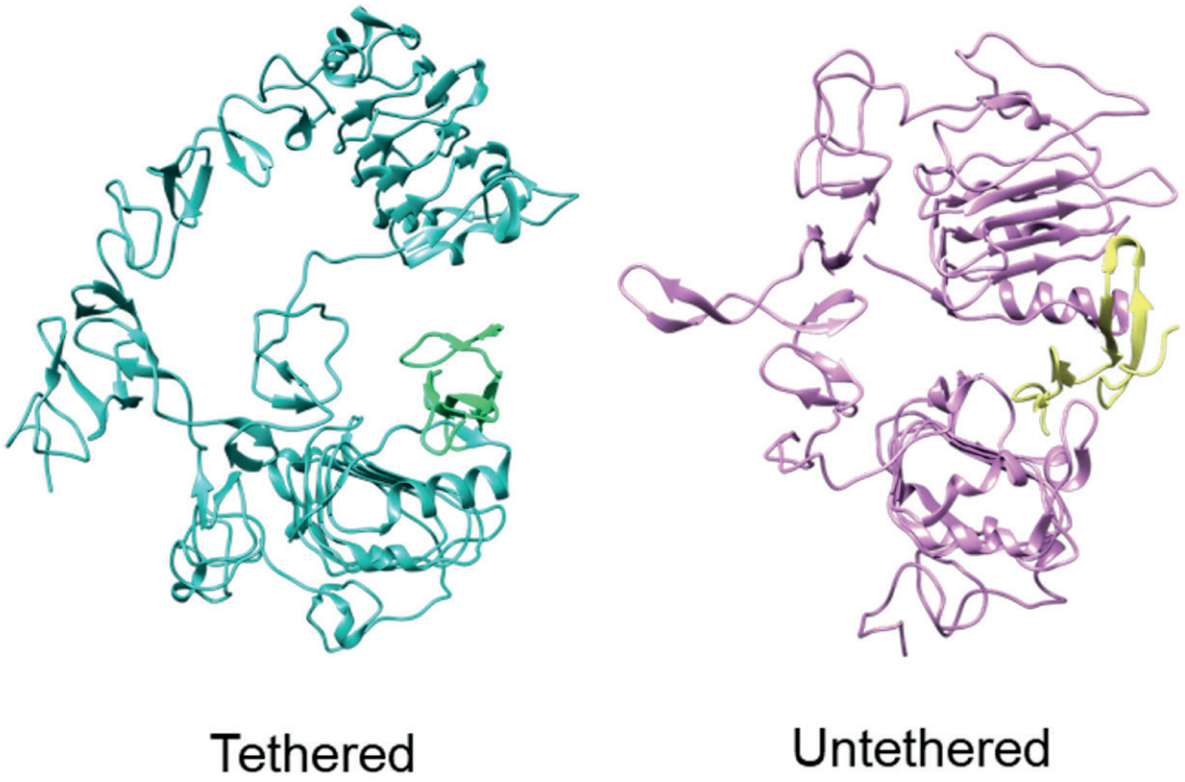

Abb. 2: EGF-gebundenes EGFR-Monomer in den zwei Konformationen *tethered* und un*tethered*. EGF bindet den EGFR zwischen Domäne I und III. Links: EGFR (türkis), EGF (grün.) Rechts: EGFR (lila), EGF (gelb). Kristallstrukturen der EGFR:EGF-Komplexe wurden aus der Protein Data Bank heruntergeladen. PDB ID links: 1nql, rechts: 1ivo (Homodimerstruktur, ein EGFR- und EGF-Molekül wurden für die Darstellung entfernt). Visualisiert als Schleifendarstellung mit UCSF Chimera.

Es sind aktuell sieben agonistische Liganden des EGFR bekannt: EGF, *Transforming Growth Factor-α* (TGFA), *Heparin-binding EGF-like Growth Factor*, Amphiregulin (AREG), Betacellulin, Epiregulin (EREG) und Epigen. Sie unterscheiden sich alle in ihrer Funktionsweise, wobei z.B. drei dieser Liganden auch ErbB4 binden, keiner von ihnen jedoch ErbB2 oder ErbB3 (Singh et al. 2016). Zwar stimulieren alle sieben Liganden nach EGFR-Aktivierung dieselben nachgeschalteten Proteine, jedoch können sie zu verschiedenen Signalantworten im selben Zelltypen führen. Dabei ist

noch nicht vollends verstanden, wie diese ligandenspezifischen Muster zustande kommen (Saito et al. 2004, Streicher et al. 2007, Wilson et al. 2012, Ronan et al. 2016). Hinzu kommt, dass das komplizierte System hinter dem EGFR-Signaling durch Crosstalk mit anderen ErbB-Familienmitgliedern (Holbro und Hynes 2004) und weiteren RTKs (z.B. *Vascular Endothelial Growth Factor Receptor*; VEGFR) (Larsen et al. 2011) sowie assoziierten Kinasen (z.B. Januskinasen) (Andl et al. 2004) in seiner Komplexität weiter zunimmt.

Zu den wichtigsten EGFR-abhängigen Signalwegen gehören *Mitogen-activated Protein Kinase* (MAPK) RAS-RAF-MEK1/2-ERK1/2 und AKT-PI3K-mTOR (Burgess 2008). Der MAPK-Signalweg ist essentiell für die Regulation von Zellproliferation und -überleben, während AKT-PI3K-mTOR für Wachstum, Apoptoseresistenz, Migration und Invasion von Zellen wichtig ist (Scaltriti und Baselga 2006, Freudlsperger et al. 2011). So ist es naheliegend, dass eine Dysregulation des EGFR und seiner nachgeschalteten Signalwege schwerwiegende Folgen für die Zell- und Gewebehomöostase haben kann.

Da der EGFR in zahlreichen Krebserkrankungen überexprimiert oder konstitutiv aktiviert ist, stellt er ein prominentes Ziel in der Entwicklung von inhibierenden Arzneimitteln zur Behandlung von Krebs dar (Gschwind et al. 2004, Guo et al. 2015, Santos et al. 2021). Während einige dieser Medikamente die intrazelluläre ATP-Bindestelle des Rezeptors besetzen (Beyett et al. 2022), binden monoklonale Antikörper, wie z.B. Cetuximab, an dessen ECD (Harding und Burtness 2005). Wenn Cetuximab den EGFR bindet, kann er nicht mehr durch endogene Liganden aktiviert werden, jedoch internalisiert der Antikörper-Rezeptor-Komplex und sorgt so für eine Degradierung des EGFR (Harding und Burtness 2005, Sung et al. 2023).

In Mausstudien stellte man fest, dass eine EGFR-Defizienz nicht nur die neuronale Entwicklung behinderte, sondern auch Defekte im Epithelgewebe, und somit der Entwicklung von Haut und Haarfolikeln, auftraten (Fowler et al. 1995, Lee und Threadgill 2009). Auch eine Inhibierung des EGFR kann Einfluss auf die normale Homöostase der Haut nehmen. So treten beispielsweise bei einer therapeutischen Krebsbehandlung mit EGFR-Inhibitoren in 45 – 100 % der Patienten kutane Nebenwirkungen auf. Hierzu gehören z.B. papulopustulöse Ausschläge, Entzündungen, Verlust des Haupthaars oder trockene und juckende Haut (Lacouture 2006). Interessanterweise sind der EGFR und seine Liganden in Läsionen der chronisch-inflammatorischen Hauterkrankung Psoriasis überexprimiert, was durch die Hyperstimulation und -proliferation von Keratinozyten begründet werden könnte. Ebenso kann eine Behandlung mit EGFR-Inhibitoren antiproliferative Effekte haben und sich so positiv auf die hyperproliferierenden Psoriasis-Läsionen auswirken (Wang et al. 2019).

Auch Umweltschadstoffe können Einfluss auf den EGFR nehmen. So können beispielsweise Feinstaub, welcher in der Regel u.a. mit PAKs belastet ist, oder Zigarettenrauch zu Mutationen des EGFR beitragen und somit zur Entwicklung von Lungenkrebs beitragen (Torres-Duran et al. 2017, Han et al. 2023). Darüber hinaus zeigen aktuelle Studien, dass verschiedene organische Umweltschadstoffe direkt mit dem EGFR interagieren und so auch Einfluss auf das Downstream-Signaling nehmen können. Gezeigt wurde dies z.B. für Dioxine und DCLs (Hardesty et al. 2018, Vogeley et al. 2022), Bisphenol S (Ticiani et al. 2021, Ticiani et al. 2023), BUVs (Sondermann et al. 2024) und PBDEs (Manuskript 2.4).

1.7 Interaktion zwischen AHR und EGFR

Die erste bekannte Interaktion zwischen AHR und EGFR wurde im Jahr 1982 veröffentlicht. Dort wurde beschrieben, dass BaP und andere PAKs nicht nur den AHR aktivieren, sondern auch die Bindung von EGF an den EGFR inhibieren würden. So beobachteten sie nach Behandlung mit PAKs eine Abnahme von radioaktiv markiertem EGF an der Plasmamembran. (Ivanovic und Weinstein 1982). Ebenso führte eine Exposition mit TCDD zu einer verminderten Anreicherung von radioaktiv gelabeltem EGF an der Plasmamembran bzw. dem EGFR (Madhukar et al. 1984, Hudson et al. 1985). Während die PAK-induzierten Effekte, vermutlich durch EGFR-Recycling, nur transient zu einer Abnahme der EGF:EGFR-Bindung führten (Karenlampi et al. 1983), hielt der TCDD-induzierte Effekt in menschlichen Keratinozyten vier Tage (Hudson et al. 1985) und in der Rattenleber 40 Tage lang an (Madhukar et al. 1984). Ein anderer Faktor, der hier Einfluss nehmen könnte, ist die zusätzliche Bindung von DLCs an den EGFR, was die Internalisierung des Rezeptors inhibiert (Hardesty et al. 2018).

Eine Aktivierung des EGFR über den AHR-Signalweg findet z.B. auf transkriptioneller Ebene statt, da z.B. AREG und EREG über die XRE-abhängige Genexpression induziert werden können (Du et al. 2005, Patel et al. 2006, John et al. 2014). In Bezug auf die Untersuchungen, welche nach Behandlung mit AHR-Liganden eine Abnahme von radioaktiv gelabeltem EGF feststellten, könnte auch dies eine Erklärung sein. So ist es vorstellbar, dass EGFR-Liganden, deren Expression über den AHR aktiviert wurde, die radioaktiv gelabelten Liganden verdrängt haben. Des Weiteren gibt es Hinweise darauf, dass Src, welches nach AHR-Aktivierung aus dem Multiproteinkomplex freigesetzt wird, den EGFR und ERK1/2 aktivieren kann (Xie et al. 2012). So soll Src z.B. Metalloproteinasen aktivieren, welche membrangebundene

EGFR-Liganden freisetzen können (Noma et al. 2007). Dieser Vorgang wird auch als *Ectodomain Shedding* bezeichnet.

Diese AHR-vermittelte EGFR-Aktivierung kann auch pathologische Folgen haben. So ist z.B. bekannt, dass die PAK-induzierte AHR-Aktivierung bei Rauchern zu einer Steigerung der AREG-Expression führen kann, wodurch wiederum die Proliferation zunimmt, was einen prokarzinogenen Effekt haben kann (Shao et al. 2003, Du et al. 2005). Ähnliches wurden mit TCDD in humanen Brustkrebszellen beobachtet, wobei die Expression von EGFR-Liganden dort einen inhibierenden Effekt auf die Apoptose hatte, welcher mit einer zusätzlichen Zugabe eines AHR-Antagonisten aufgehoben werden konnte. Dies untermauert die AHR-Abhängigkeit dieser TCDD-induzierten und EGFR-vermittelten Tumorpromotion (Shao et al. 2003).

Bei einer Co-Behandlung von Keratinozyten mit EGF und TCDD stellten Sutter und Kollegen fest, dass die TCDD-induzierte Expression von CYP1A1 und CYP1B1 vermindert wurde. Im weiteren Verlauf ihrer Untersuchungen fanden sie heraus, dass sowohl der AHR- als auch EGFR-Signalweg den transkriptionellen Co-Aktivator CBP/p300 nutzen, wodurch eine Konkurrenz entsteht. Darüber hinaus beobachteten sie, dass die Behandlung mit einem EGFR-Inhibitor die AHR-induzierte Differenzierung von Keratinozyten steigerte, während eine Behandlung mit EGF diese verminderte (Sutter et al. 2009). Ähnliche Beobachtungen machte die Gruppe rund um Aby Joiakim, welche feststellte, dass eine Co-Behandlung von humanen Brustkrebszellen mit TCDD und einem EGFR-Inhibitor zu einer gesteigerten CYP1-Expression führte (Joiakim et al. 2016).

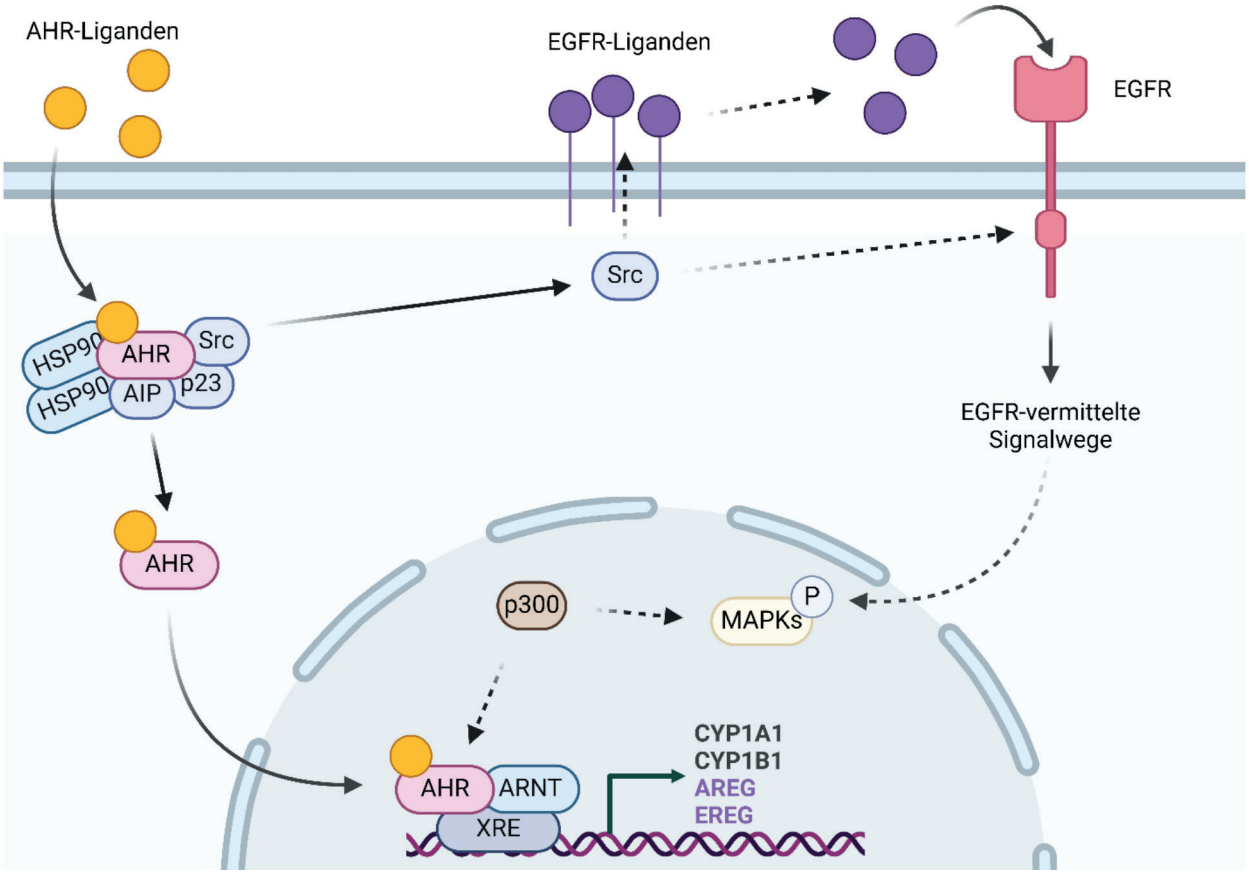

Abb. 3: Interaktionen zwischen dem Aryl-Hydrocarbon-Rezeptor (AHR) und dem epidermalen Wachstumsfaktor-Rezeptor (EGFR). Inaktiv liegt der AHR in einem Multiproteinkomplex, bestehend aus einem HSP90-Dimer, AIP, p23 und Src, im Zytosol vor. Sobald ein Ligand bindet, zerfällt der Komplex und der AHR translozíert in den Nukleus. Dort bildet er ein Heterodimer mit seinem Partnermolekül *AHR-nuclear translocator* (ANRT), welches an die xenobiotisch-responsive Elemente (XRE) bindet und die Transkription von Zielgenen, wie z.B. Cytochrom P450 (CYP)-Enzymen und EGFR-Liganden wie Amphiregulin (AREG) und Epiregulin (EREG), aktiviert wird. Beim Zerfall des Multiproteink omplexes wird ebenfalls Src frei, welches über einen Vorgang namens *Ectodomain-Shedding* membrangebundene EGFR-Liganden freisetzen kann. Darüber hinaus kann Src selbst den EGFR und nachgeschaltete Signalwege aktivieren. Im Nukleus liegt zudem der transkriptionelle Co-Aktivator p300 vor, um welchen der AHR- und EGFR- bzw. *Mitogen-activated Protein Kinase* (MAPK)-Signalweg konkurrieren. / Abbildung erstellt mit BioRender.com

Zusammenfassend sind drei verschiedene Wege bekannt, auf denen sich der AHR- und EGFR-Signalweg kreuzen: (1) die EGFR-Aktivierung durch das aus dem AHR-Multiproteinkomplex freigesetzte Src (z.B. über das *Ectodomain-Shedding* von EGFR-Liganden), (2) die AHR-induzierte Genexpression von EGFR-Liganden, (3) die Konkurrenz um den gemeinsamen Co-Aktivator CBP/p300 (Abb. 3).

1.8 Ziel der Thesis

Das übergeordnete Ziel dieser Thesis ist, die Rolle des EGFR, genauer gesagt seiner ECD, als Zielstruktur für verschiedene organische Umweltschadstoffe auf zellulärer Ebene besser zu verstehen. Ein zusätzlicher Fokus wurde hierbei auf den AHR gelegt, um die wechselseitige Beziehung beider Rezeptoren zueinander und mögliche Konsequenzen von Mischungseffekten weiter aufzuschlüsseln. Diese mechanistischen Erkenntnisse sollen dabei helfen, gesundheitsschädliche Auswirkungen organischer Umweltschadstoffe besser zu verstehen und womöglich auch präventive Konzepte zu entwickeln. Zusätzlich ist die Interaktion von Substanzen, die nicht akut toxisch sind, mit dem EGFR von besonderem Interesse für die strukturelle Entwicklung neuer Medikamente, die gegen den EGFR gerichtet sind. Darüber hinaus könnte ein besseres Verständnis dieser Interaktionen von Umweltschadstoffen mit dem Rezeptor auch bei der Entwicklung neuer Ansätze für die Gefährdungs- und Risikobeurteilung von Nutzen sein.

Innerhalb dieses übergeordneten Ziels wurden folgende Punkte im Rahmen der hier vorliegenden Dissertation untersucht (Abb. 4):

1. Die unterschiedliche Wirkung von PAKs und DLCs hinsichtlich der AHR-vermittelten EGFR-Aktivierung

2. Mechanistische Untersuchungen der direkten Interaktion von BUVs mit der EGFR ECD sowie deren Auswirkungen auf nachgeschaltete Signalwege

3. Die Auswirkungen von PBDEs auf die Liganden-induzierte EGFR-Aktivierung sowie die EGFR-gesteuerte transkriptionelle Aktivität des AHR

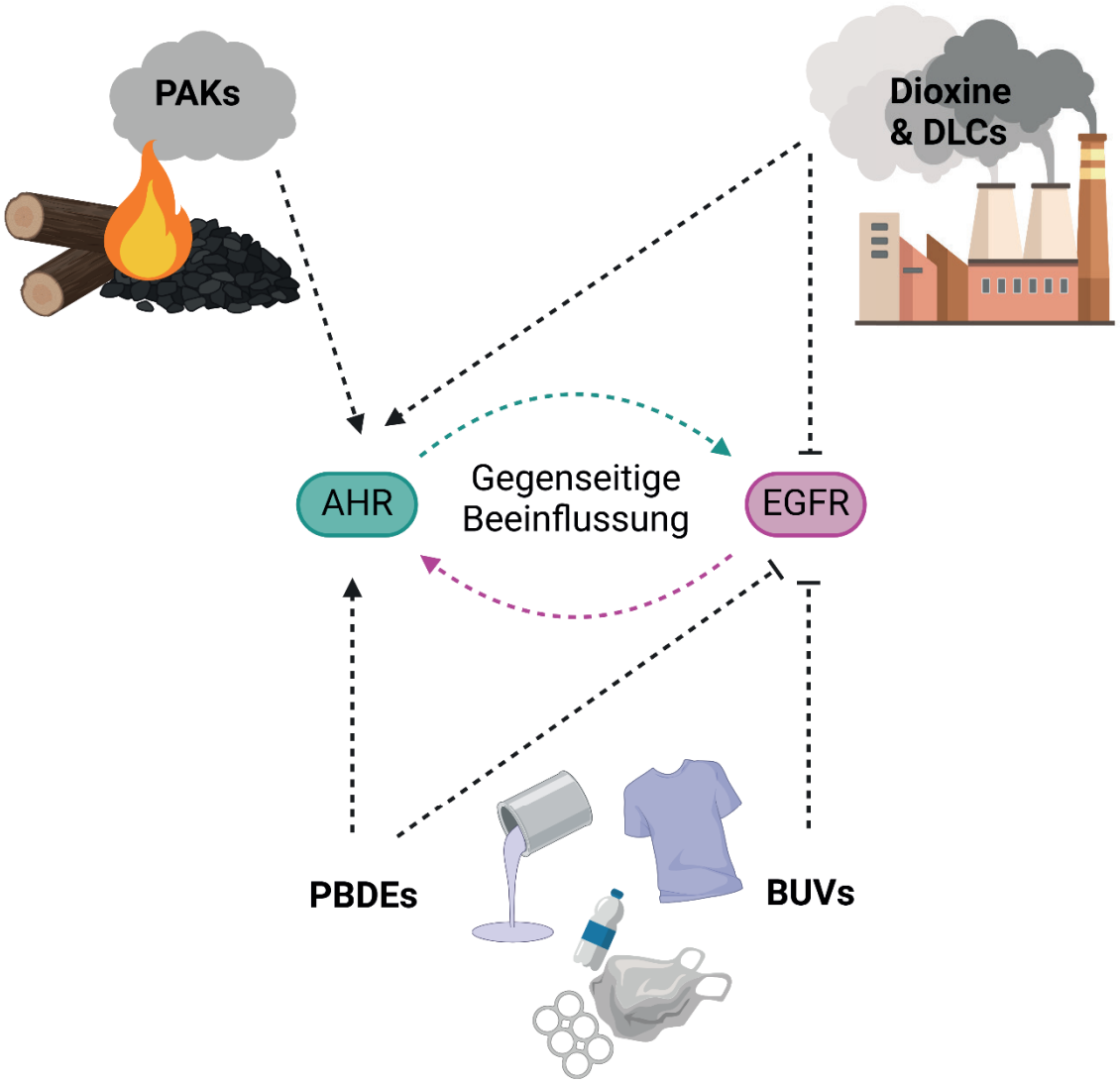

Abb. 4: Gemeinsame Darstellung der untersuchten Hypothesen. Untersucht wurden (1) die ligandenspezifischen Wirkungen von DLCs und PAKs auf den AHR-EGFR-Crosstalk, (2) die Interaktion von BUVs mit der ECD des EGFR und deren Bedeutung für die Rezeptoraktivierung und EGFR-gesteuerte Signalwege und (3) die mechanistischen Auswirkungen von PBDEs auf den EGFR und transkriptionelle Aktivität des AHR. / Abbildung erstellt mit BioRender.com

2 Manuskripte

Im Folgenden sind die vier Publikationen angefügt, bei welchen ich als Erst- oder Co-Autorin beteiligt war.

Bei der ersten Publikation (2.1) handelt es sich um ein Review, welches die vielseitigen Funktionen des AHR außerhalb des kanonischen Signalweges samt den pathologischen Konsequenzen genauer beleuchtet.

Die zweite Publikation (2.2) handelt von den verschiedenen Funktionsweisen von PAKs und DLCs in Bezug auf die AHR- und EGFR-Signalantwort. Hier wurde der EGFR, bzw. seine ECD, als Interaktionspartner für verschiedene halogenierte organische Schadstoffe identifiziert.

Die dritte Publikation (2.3) behandelt die Interaktion von BUVs mit der ECD des EGFR sowie dessen Downstream-Signaling. Dabei wurde die Rolle der EGFR ECD als Zelloberflächenrezeptor für organische Umweltschadstoffe nochmal untermauert.

Beim vierten Manuskript (2.4) wurde untersucht, wie PBDEs sich auf die Liganden-induzierte EGFR-Aktivierung sowie die Aktivierung von AHR-Zielgenen bei einer Co-Behandlung mit AHR-Liganden auswirken.

2.1 Functions of the aryl hydrocarbon receptor (AHR) beyond the canonical AHR/ARNT signaling pathway

Natalie C. Sondermann, Sonja Faßbender, Frederick Hartung, Anna M. Hätälä, Katharina M. Rolfes, Christoph F.A. Vogel, Thomas Haarmann-Stemmann

Neben dem klassischen kanonischen AHR/ARNT-Signalweg, kann es je nach Liganden, Zelltyp und Gewebe zu verschiedenen Signalantworten kommen, bei denen der AHR mit anderen Transkriptionsfaktoren und Signalmolekülen interagiert. Dieser Artikel gibt einen Überblick über einige der wichtigsten nicht-kanonischen AHR-Funktionen und Interaktionen mit anderen Signalwegen, welche das Zellschicksal, Immunantworten, die Anpassung an Sauerstoffkonzentrationen und oxidativen Stress sowie die Ubiquitinierung und den proteasomalen Abbau beeinflussen. Zudem wird ein Fokus auf die Pathogenität der verschiedenen Interaktionen mit dem AHR gelegt, um das Potential der AHR-Modulation für Krankheitsprävention und -behandlung hervorzuheben.

Journal:	Biochemical Pharmacology
Impact Factor:	5,3 (2024)
Beitrag zur Veröffentlichung:	40 %
	Konzept, Literaturrecherche, Verfassen von Zusammenfassung, Einleitung, EGFR-Kapitel und Fazit, Visualisierung aller Kapitel, Editieren
Art der Autorenschaft:	Erstautorenschaft
Status der Publikation:	Veröffentlicht am 15.12.2022

Biochemical Pharmacology 208 (2023) 115371

Contents lists available at ScienceDirect

Biochemical Pharmacology

journal homepage: www.elsevier.com/locate/biochempharm

Review

Functions of the aryl hydrocarbon receptor (AHR) beyond the canonical AHR/ARNT signaling pathway

Natalie C. Sondermann [a], Sonja Faßbender [a], Frederick Hartung [a], Anna M. Hätälä [a], Katharina M. Rolfes [a], Christoph F.A. Vogel [b], Thomas Haarmann-Stemmann [a,*]

[a] IUF – Leibniz Research Institute for Environmental Medicine, 40225 Düsseldorf, Germany
[b] Department of Environmental Toxicology and Center for Health and the Environment, University of California, Davis, CA 95616, USA

ARTICLE INFO

Keywords:
Aryl hydrocarbon receptor
Immune response
Non-canonical signaling
Signal transduction
Transcription factor
Ubiquitination

ABSTRACT

The aryl hydrocarbon receptor (AHR) is a ligand-dependent transcription factor regulating adaptive and maladaptive responses toward exogenous and endogenous signals. Research from various biomedical disciplines has provided compelling evidence that the AHR is critically involved in the pathogenesis of a variety of diseases and disorders, including autoimmunity, inflammatory diseases, endocrine disruption, premature aging and cancer. Accordingly, AHR is considered an attractive target for the development of novel preventive and therapeutic measures. However, the ligand-based targeting of AHR is considerably complicated by the fact that the receptor does not always follow the beaten track, i.e. the canonical AHR/ARNT signaling pathway. Instead, AHR might team up with other transcription factors and signaling molecules to shape gene expression patterns and associated physiological or pathophysiological functions in a ligand-, cell- and micromilieu-dependent manner. Herein, we provide an overview about some of the most important non-canonical functions of AHR, including crosstalk with major signaling pathways involved in controlling cell fate and function, immune responses, adaptation to low oxygen levels and oxidative stress, ubiquitination and proteasomal degradation. Further research on these diverse and exciting yet often ambivalent facets of AHR biology is urgently needed in order to exploit the full potential of AHR modulation for disease prevention and treatment.

1. Introduction

Since its initial identification by Alan Poland's group in 1976, the aryl hydrocarbon receptor (AHR) and its signaling pathways have been and still are a highly relevant research topic in toxicology [1]. Poland had interest in the mechanisms behind the occurrence of industrially acquired acne, called chloracne, in factory workers producing the herbicide 2,4,5-trichlorophenol (2,4,5-T) [2]. As others before, they found unwanted side products like 2,3,7,8-tetrachlorodibenzo-*p*-dioxin (TCDD) to be the acnegenic factor [3]. These findings ultimately led to the idea to synthesize radiolabeled TCDD, followed by the discovery of its receptor molecule AHR [1]. Of note, several investigations of the

Abbreviations: AHR, aryl hydrocarbon receptor; AHRR, aryl hydrocarbon receptor repressor; AKR, aldo-keto reductase; AP-1, activator protein-1; AR, androgen receptor; ARE, antioxidant response element; AREG, amphiregulin; ARNT, aryl hydrocarbon receptor nuclear translocator; BaP, benzo[*a*]pyrene; BMDC, bone marrow-derived dendritic cell; CCL, chemokine (C-C-motif) ligand; COX-2, cyclooxygenase-2; CUL4B, cullin 4B; CYP, cytochrome P450; DC, dendritic cell; ECD, extracellular domain; EGF, epidermal growth factor; EGFR, epidermal growth factor receptor; EPO, erythropoietin; ER, estrogen receptor; FICZ, 6-formylindolo[3,2-*b*]carbazole; GST, glutathione *S*-transferase; HIF-1α, hypoxia-inducible factor 1α; HRE, hypoxia-responsive element; IDO, indolamine-2,3-dioxygenase; IFN, interferon; IL, interleukin; JAK, janus-kinase; KEAP1, Kelch-like ECH-associated protein 1; KYN, kynurenine; LPS, lipopolysaccharide; MAF, musculoaponeurotic fibrosarcoma; MAPK, mitogen-activated protein kinase; MMP-1, matrix metalloproteinase-1; NF-κB, nuclear factor kappa-light-chain-enhancer of activated B cells; NQO1, NADPH:quinone oxidoreductase-1; NRF2, nuclear factor erythroid 2-related factor 2; PAH, polycyclic aromatic hydrocarbon; PCB, polychlorinated biphenyl; PHD2, prolyl hydroxylase domain-containing protein 2; PKC, protein kinase C; PM, particulate matter; POI, protein of interest; PPARγ, peroxisome proliferator-activated receptor γ; PROTAC, proteolysis targeting chimera; ROS, reactive oxygen species; RTK, receptor tyrosine kinase; SLE, systemic lupus erythematosus; STAT, signal transducer and activator of transcription; 2,4,5-T, 2,4,5-trichlorophenol; TCDD, 2,3,7,8-tetrachlorodibenzo-*p*-dioxin; TGF, transforming growth factor; Th17, T helper 17 cells; TLR, Toll-like receptor; TNF, tumor necrosis factor; TPH, tryptophan hydroxylase-1; Tregs, regulatory T cells; VEGF, vascular endothelial growth factor; XRE, xenobiotic-responsive element.

* Corresponding author.
E-mail address: thomas.haarmann-stemmann@iuf-duesseldorf.de (T. Haarmann-Stemmann).

https://doi.org/10.1016/j.bcp.2022.115371
Received 1 October 2022; Received in revised form 28 November 2022; Accepted 29 November 2022
Available online 15 December 2022

laboratory of Daniel Nebert assessing the inducibility of aryl hydroxylase activity by environmental chemicals in genetically different, responsive and non-responsive mouse strains [4–6], preceded this landmark discovery. The critical relevance of AHR for the adverse health effects induced by dioxins is illustrated by several chemical incidents, such as the Seveso disaster in 1976, an explosion of a 2,4,5-T production reactor setting free high amounts of TCDD in a densely populated area nearby [7], the widespread usage of TCDD-contaminated defoliants, in particular Agent Orange, a mixture of 2,4-dichlorophenoxyacetic acid and 2,4,5-T, during Operation Ranch Hand in Vietnam [8] or the dioxin poisoning of the Ukrainian presidential candidate Viktor Yushchenko in 2004 [9].

Since its first description as a cellular signaling molecule that mediates the toxicity of dioxins and related compounds, the mechanistic details and facets of its major signaling route, the so-called canonical AHR signaling pathway, have been elucidated [10–12]. Briefly, in the absence of a ligand, AHR is part of a cytosolic multiprotein complex consisting of AHR-interacting protein (also known as ARA9 or XAP2), a heat shock protein 90 dimer and co-chaperone p23. In addition, an association of the protein tyrosine kinase c-Src with the cytosolic AHR multiprotein complex has been observed in several cell-types [13–15]. Upon ligand-binding, this complex dissociates and AHR translocates into the nucleus where it dimerizes with the AHR nuclear translocator (ARNT). The resulting dimer then binds to xenobiotic-responsive elements (XRE) in the enhancer region of target genes to recruit components of the general transcription machinery and induce their expression [10–12]. The probably best examined target genes of the AHR/ARNT complex encode for cytochrome P450 (CYP) 1A1, CYP1A2 and CYP1B1, xenobiotic-metabolizing enzymes that oxidize the invading (AHR-activating) chemical to enhance its polarity and enable its detoxification *via* the conjugating enzyme system.

However, CYP1-catalyzed reactions may lead to the formation of reactive metabolites and the generation of oxidative stress which can harm the tissue by damaging the DNA and/or other cellular macromolecules. In fact, AHR-deficient mice were found to be resistant against polycyclic aromatic hydrocarbon (PAH)-initiated tumors, a phenomenon which was attributed to the attenuated expression of CYP1 isoforms in the respective animals [16,17]. Furthermore, gene and protein levels of AHR are frequently elevated in various types of cancer, including brain, breast, lung and pancreatic cancer [18]. Also, it was observed that transgenic mice expressing a constitutively active AHR develop gastric tumors [19]. Yet, the role of AHR in cancer is highly complex since oncogenic as well as tumor-suppressive effects of the receptor have been observed [20]. For example, it was shown that AHR-deficiency in mice had a promoting effect on liver tumors, indicating that AHR acts as a tumor suppressor [21]. Additionally, there is evidence that AHR activation is associated with malignant progression and poor survival in glioblastoma patients [22]. However, this multilateral role of AHR in cancer is also critical to the design of AHR-targeted cancer therapeutics, concerning molecular and pharmacological approaches. Currently, there are first clinical trials in progress for the AHR inhibitors BAY2416964 and IK-175 recruiting participants with uncurable solid cancers to assess their tolerability and toxicity profile [23,24]. However, given the complexity of modulating AHR activity in cancer, it should be considered that under certain circumstances, not only AHR antagonists but also agonists may be useful as cancer therapeutics [25].

Furthermore, the AHR is expressed by a number of immune cells, e.g. T helper 17 (Th17) cells and regulatory T (Tregs) cells [10]. Activation of AHR in Th17 cells leads to the production of cytokine interleukin (IL)-22 [26] which is linked to pro-inflammatory processes such as cutaneous inflammation, psoriasis or Crohn's disease [27–29]. Since it has been demonstrated that TCDD treatment leads to immunotoxicity in $Ahr^{+/+}$ but not $Ahr^{-/-}$ mice, as the latter are resistant to TCDD-induced immunosuppression [30], IL-22 production appears to be downstream of AHR [31]. Moreover, activation of AHR by its ligands modulates T cell differentiation and Treg function, contributing to antigen-presenting cell response [32]. A recent study also suggested AHR to be an important regulator for inflammatory diseases, showing that it protects against allergic airway inflammation by controlling cell autophagy [33]. In May 2022, a cream containing 1 % of the AHR agonist tapinarof received its first approval by the US FDA for the topical treatment of the immune-related skin diseases plaque psoriasis in adults [34]. Thus, concomitant with its effects on immune response, AHR may also serve as a target for new therapeutic approaches concerning autoimmune disease [35]. A study from August 2022 for example suggests that AHR might be an interesting target for the therapy of rheumatoid arthritis, as its ubiquitination seems to be involved in an imbalance of Th17/Treg cells [36]. On top of this, AHR is also thought to be involved in COVID-19 hypoxia formation via upregulation of the expression of mucins and hence accumulation of alveolar mucus affecting the blood-gas-barrier [37].

Once considered only a mediator of the toxicity of dioxins, the field of AHR research moved into many different directions. Meanwhile, the multiple tissue-, organ-, and ligand-specific functions and seemingly paradox responses of AHR are still not fully understood. As AHR has recently sparked even more clinical intertest as a target [34,38–40], its complex non-canonical functions should urgently move more sharply into the focus of basic and preclinical research. This review article aims to provide a clear and concise overview of some of the most interesting and potentially important non-canonical AHR signaling events and functions, specifically taking the impact on the development of new pharmacological approaches into account. For that purpose, this review article will first focus on AHR's involvement in major signaling cascades controlling cell function and fate, including the epidermal growth factor receptor (EGFR), janus kinase (JAK)/signal transducer and activator of transcription (STAT) as well as the nuclear factor kappa-light-chain-enhancer of activated B cells (NF-κB). Further, pathways involved in cellular adaptation towards low oxygen levels and oxidative stress will be addressed with regard to hypoxia-inducible factor 1 alpha (HIF-1α) and nuclear factor erythroid 2-related factor 2 (NRF2). Subsequently, the function of AHR beyond its role as a transcription factor will be discussed with a focus on E3 ubiquitin ligase activity.

2. EGFR signaling pathways

The EGFR is a receptor tyrosine kinase (RTK) of the ErbB family and plays a key role in embryonic development and physiology [41]. As EGFR has an intra- and extracellular domain to bind ligands, activation can occur *via* both ways. This activation includes receptor *trans*-autophosphorylation, the hetero- or homodimerization with a member of the ErbB family or another EGFR molecule and the recruitment of signaling proteins or adaptors [41]. Its downstream signaling includes the mitogen-activated protein kinase (MAPK) RAS- RAF- MEK1/2-ERK1/2 and AKT-PI3K-mTOR pathways as well as protein kinase C (PKC), STAT, SRC and NF-κB. Moreover, EGFR is a well-known oncogenic protein and involved in the pathogenesis of several cancers, commonly carrying a mutation that leads to a constitutive activation of the receptor [42,43]. Thus, EGFR plays an important role in several cellular processes such as proliferation, differentiation and apoptosis.

The seemingly first AHR-related interaction with the EGFR was described in 1982 suggesting that benzo[*a*]pyrene (BaP) and other PAHs may not only activate AHR but also inhibit binding of EGFR by its ligand, the epidermal growth factor (EGF) [44]. Since then, it has been repeatedly reported that an exposure to AHR agonists interferes with the binding of radiolabeled EGF to the plasma membrane [45–47]. The underlying molecular mechanism may involve an AHR ligand-mediated enforcement of EGFR internalization either by stimulating a phosphorylation of the RTK *via* c-Src or by inducing the release of growth factors that bind to EGFR extracellular domain (ECD). However, in contrast to PAHs that, presumably due to recycling of EGFR, only cause a transient decline [46,47], TCDD reduces the EGF-binding capacity of the plasma membrane for up to 4 days in human keratinocytes [47] and 40 days in rat liver [45]. In 2022, we published a mechanistic study which may

serve to better understand the interaction between different AHR ligands and EGFR internalization [48]. Briefly, we found that treatment of human keratinocytes with PAHs, i.e. BaP and benzo[*k*]fluoranthene, causes a biphasic stimulation of EGFR phosphorylation and downstream MEK/ERK signal transduction. Whereas the early peak, occurring approximately after 15 min after treatment, this seems to be due to a direct c-Src-mediated phosphorylation of EGFR at residue Y845 (Fig. 1), the second temporally delayed peak of EGFR/ERK activation (approximately 2 h after treatment) involves extracellular events, i.e. the release of growth factors. Specifically, this process is driven by the c-Src-dependent sequential activation of PKC and metalloproteinases resulting in the ectodomain shedding of cell surface-bound EGFR ligands, in particular of amphiregulin (AREG) and transforming growth factor (TGF)-α (Fig. 1). These polypeptide growth factors then bind to the ECD of EGFR and initiate dimerization and autophosphorylation of the RTK at various tyrosine residues, including Y1068 and Y1137 [48]. Importantly, bulk RNAseq analyses indicated that this second wave of EGFR-dependent signal transduction seems to be responsible for the major differences in the gene expression profile in BaP- *versus* polychlorinated biphenyl (PCB) 126-exposed keratinocytes [48]. In fact, we were able to show that binding of dioxin-like compounds, including PCB126 and TCDD, induces similar AHR-dependent and c-Src-driven signaling events culminating in the shedding of EGFR ligands from the plasma membrane. However, dioxin-like compounds stimulate EGFR signal transduction only early (15 min) but not late (2 h) after treatment. *In silico* as well as further experimental work revealed that dioxin-like compounds bind to the ECD of EGFR directly and thereby inhibit an activation of the RTK by growth factors [48,49].

Apart from non-canonical signaling events, the ligand-activated AHR has been found to induce the expression of several EGFR ligands (Fig. 1), including epiregulin and AREG, in an XRE-dependent manner [50,51]. Other investigators reported that tobacco smoke induces the expression of AREG in oral epithelial cells *via* a non-canonical AHR pathway involving the cAMP – protein kinase A signaling axis [52]. However, Lemjabbar *et al.* identified tobacco smoke to stimulate the proliferation of lung epithelial cells by promoting the metalloprotease-mediated ectodomain shedding of AREG [53]. Hence, depending on ligand, cell type and context, AHR may affect EGFR signal transduction via canonical and non-canonical signaling events or a combination of both.

The laboratory of Thomas Sutter reported an inhibition of the TCDD-induced expression of *CYP1A1* and *CYP1B1* upon co-treatment of epidermal keratinocytes with EGF. Results from further mechanistic experiments indicated that both pathways compete for the common transcriptional co-activator CBP/p300. Accordingly, the AHR-mediated keratinocyte differentiation was also inhibited by EGF while co-treatment with an EGFR inhibitor promoted differentiation [54]. Hence, these results suggest that EGFR activation might interfere with activation of AHR or at least its canonical signaling pathway *via* transrepression. This observation is supported by another study, reporting that a pharmacological inhibition of EGFR amplifies the TCDD-induced expression of CYP1 isoforms [55].

Taken together, four different mechanisms of AHR-EGFR-crosstalk have been described so far: (I) AHR-dependent activation of EGFR via release of c-Src, (II) AHR-induced expression of EGFR ligands leading to EGFR activation, (III) AHR-dependent ectodomain shedding of EGFR ligands leading to auto- or paracrine EGFR activation and (IV) the competition for common transcriptional co-activators.

2.1. Pathological consequences of crosstalk between AHR and EGFR

The EGFR is an integral part of multiple signaling pathways controlling tissue homeostasis and disease. Hence, the crosstalk between EGFR and the chemosensor AHR might be a signaling route by which environmental pollutants, drugs or other exogenous chemicals harm cellular functions and tissue integrity. In fact, numerous studies have reported that a modulation of EGFR function by AHR-stimulating factors drives the pathogenesis of diseases, in particular of various types of cancer.

In smokers, the AHR-mediated increased *AREG* expression results in enhanced cell proliferation and contributes to the procarcinogenic effects of tobacco smoke [52,56]. Moreover, in breast cancer cells, TCDD increased EGFR ligand expression resulting in activation of downstream EGFR signaling and thereby inhibition of apoptosis. Interestingly, this effect could be reversed by addition of the AHR antagonist 3′-methoxy-4′-nitroflavone, suggesting an AHR-driven tumor promoting effect [57].

AHR activation and subsequent non-canonical EGFR signaling are also critically involved in the cellular UVB stress response. UVB radiation leads to the formation of the endogenous AHR ligand 6-formylindolo[3,2-*b*]carbazole (FICZ) in the skin and further to a c-Src-dependent EGFR internalization and downstream activation of ERK [58]. In contrast to TCDD, which *per se* activates similar signaling events, FICZ is rapidly metabolized by CYP1 isoforms and, accordingly, causes a transient activation of AHR signaling pathways [59]. However, amongst others, the UVB-induced activation of this AHR signaling cascade leads to an induction of proinflammatory cyclooxygenase-2 (COX-2) [58,60], a modulation of DNA damage-dependent stress responses [61,62], and skin tumor formation [62].

Similar to UVB irradiation [60], exposure to cigarette smoke leads to

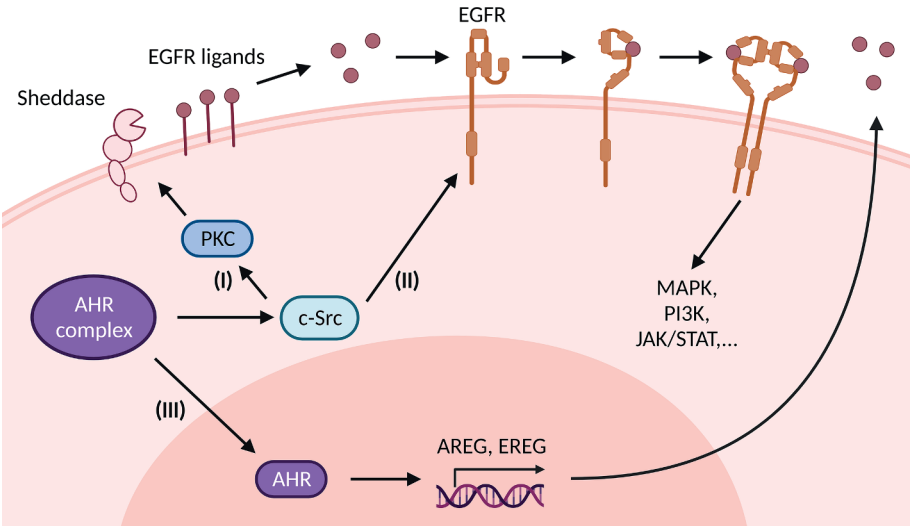

Fig. 1. Ligand-activated AHR activates EGFR and downstream signaling. The ligand-driven dissociation of AHR complex leads to the release of c-Src which can (I) directly activate the epidermal growth factor receptor (EGFR) by phosphorylating its intracellular domain, and (II) sequentially activate protein kinase C (PKC) and sheddases resulting in ectodomain shedding of cell surface-bound EGFR ligands. In addition, nuclear AHR transactivates genes encoding EGFR ligands, such as amphiregulin (AREG) and epiregulin (EREG) (III). Independently from its mode of activation, i.e. ligand-binding or intracellular phosphorylation, the EGFR monomer changes its conformation from tethered to untethered and forms a hetero- or homodimer leading to activation of downstream signaling pathways like MAPK, PI3K or JAK/STAT.

the induction of the AHR-dependent genes *CYP1A1*, *CYP1B1* and matrix metalloproteinase-1 (*MMP-1*) [63]. MMP-1 is also induced in the skin of smokers [64] where it leads to collagen breakdown in the dermis, tissue remodeling and promotion of skin aging [65]. In line with that, a knockdown of *MMP-1* resulted in inhibition of the progression of colorectal cancer *via* suppression of the PI3K/AKT signaling pathway downstream of EGFR. This suggests an involvement of AHR-induced MMP-1 in the EGFR-regulated promotion of malignant behavior in colorectal cancer [66]. It has also been shown that EGF induces MMP-1 secretion through EGFR-mediated MAPK signaling, again leading to increased proliferation [67].

A study from 2022 has shown that BaP exposure leads to aggravated TGF-α and MUC5AC expression in an asthma model [68]. MUC5AC is one of the mucins closely related to asthma [69] as it leads to pronounced secretion and accumulation of mucus which blocks the airway and results in breathing difficulties [70]. It was suggested that BaP-induced AHR activation would lead to production of reactive oxygen species (ROS) which activated EGFR and MAPK signaling [68]. The AHR-mediated upregulation of mucins and accumulation of alveolar mucus was also connected to hypoxia and inflammation in COVID-19 patients. Particularly, interferon (IFN)-β and IFN-γ induced mucin expression in an AHR-dependent manner. Concomitant with this, AHR inhibition led to improvement of the lung function in SARS-CoV-2-infected mice [37].

There already are several therapeutics targeting EGFR and its complex signaling pathways, including monoclonal antibodies or inhibitors, which commonly show skin toxicity as a side effect. This often forces the discontinuation of the respective drug [42]. Further, it seems that many EGFR-dependent effects in diseases are also enforced by AHR-driven EGFR ligand expression and/or membrane shedding. Due to the dynamic crosstalk between EGFR and AHR, when developing therapeutics targeting EGFR signaling, AHR should also be taken into consideration as a possible target or co-target – and *vice versa*. This could possibly lead to reduction of unwanted side effects such as development of drug resistance or other adverse reactions directed at specific tissues or cellular compartments.

3. JAK/STAT pathway

The JAK/STAT pathway transduces signals from the cell surface to the nucleus and, amongst others, is critically involved in the regulation of innate and adaptive immune responses [71]. Accordingly, an aberrant activation of JAK/STAT signaling is associated with the pathogenesis of multiple diseases, including chronic inflammatory diseases, autoimmunity and cancer [72–75]. The molecular mechanisms of JAK/STAT signaling pathways are well characterized. Briefly, members of the JAK family, i.e. JAK1, JAK2, JAK3 and tyrosine kinase 2 in humans, are bound to the intracellular domain of transmembrane cytokine receptors or receptor tyrosine kinases (e.g. EGFR). Upon activation by cytokines or IFNs, the cytokine receptors dimerize or multimerize, leading to a mutual JAK-mediated phosphorylation of specific tyrosine residues in the intracellular domain of the cytokine receptors. These novel phosphotyrosine residues serve as docking sites for the Src-homology 2 (SH2) domain of STAT molecules. After binding to the phosphorylated cytokine receptor, JAKs phosphorylate a C-terminal tyrosine residue in the STAT proteins to form another SH2-binding motif. The latter is reciprocally recognized by two STAT proteins, leading to the formation of a STAT dimer. This dimer translocates to the nucleus and acts as a transcription factor by binding to certain DNA motifs in the enhancer region of target genes. The human genome encodes seven mammalian STAT family members, i.e. STAT1, STAT2, STAT3, STAT4, STAT5A, STAT5B, and STAT6.

In 2004, two independent studies were first to report an impact of AHR on STAT signaling. Nukaya *et al.* showed that a treatment of B6 mice with 3-methylcholanthrene resulted in an AHR-dependent reduction of JAK2 expression in the liver, which was associated by a decreased DNA-binding activity of STAT5 [76]. In the other study, Takanage *et al.* reported that the AHR agonist β-naphthoflavone attenuates the astrocytic differentiation of glioma cells by inhibiting the expression of IL-6 and downstream STAT3 activation [77]. Hence, AHR seems to control the expression of stimulating cytokines and pathway components to alter JAK/STAT activity and associated cellular consequences. In fact, AHR is known to regulate the expression of various JAK/STAT-stimulating cytokines, including IL-2 [78], IL-10 [79], IL-21 [79], IL-22 [31] and others, *via* different pathways. For instance, AHR cooperates with the NF-κB subunit RelA/p65 at the IL-6 promoter [80], whereas in lipopolysaccharide (LPS)-treated macrophages AHR sequentially activates c-Src and STAT3 to induce the expression of IL-10 [81]. Moreover, due to parameters such as physicochemical properties of the ligand, cell type, tissue and microenvironment, AHR may either induce or inhibit the expression of these cytokines, as illustrated for instance by IL-6 [82,83] and IL-33 [84,85]. Importantly, the interrelationship between AHR and JAK/STAT signaling pathways is mutual and much more complex than a unilateral regulation of mediators and signaling molecules (Fig. 2).

In fact, activated STAT1, STAT2 and STAT3 have been reported to bind to the promoter of the *AHR* gene and induce its transcription (Fig. 2). Upon stimulation of human hepatoma cells with IL-6-type cytokines, STAT3 binds to a STAT-responsive element approximately 2 kilobase pairs 5′-upstream of the transcription initiation site of the *AHR* gene [86]. This STAT-responsive element is not conserved in the murine *Ahr* gene, but another functional STAT-binding motif in it has been identified [87]. In murine astrocytes, IFN-β activates JAK1 and tyrosine kinase 2 resulting in the formation of the IFN-stimulated gene factor 2, a trimolecular complex consisting of STAT1, STAT2 and IFN regulatory factor 9, which binds to an IFN-response element in the murine promoter sequence of *Ahr* to induce its expression [88]. Another study reported an activation of the AHR system in B cells by IL-4 [89]. While the authors found that IL-4 induces *AHR* expression in a STAT6-dependent manner, the underlying molecular mechanism of the observed nuclear translocation and target gene induction of AHR in response to the cytokine treatment remains less clear.

However, apart from the transcriptional level, STAT proteins facilitate AHR activation by altering tryptophan metabolism (Fig. 2). In human chronic lymphocytic leukemia cells, for instance, IFN-γ induces the expression of indolamine-2,3-dioxygenase (IDO) 1 through the JAK/STAT1 signaling pathway [90]. IDO1 oxidizes tryptophan to *N*-formylkynurenine which is subsequently converted by aryl formamidase to kynurenine (KYN) [91]. KYN and several of its metabolites, including kynurenic acid and xanthurenic acid, serve as low affinity agonists of AHR [82,92,93]. Importantly, AHR activation by KYN was found to resemble the effects of TCDD treatment in mice, i.e. an induction of immunosuppressive Treg cells [92,94,95]. In 2011, Michael Platten and his team identified KYN as an endogenous AHR ligand that is constitutively generated in human brain tumors and responsible for the suppression of antitumor immune responses and the promotion of cancer cell survival and motility [22]. In lung cancer, an autocrine signaling loop consisting of the stimulation of AHR activity by KYN, an AHR-mediated upregulation of IL-6, a stimulation of STAT3 and the associated induction of KYN-producing IDO1 has been described [96]. A similar way of interaction has been identified to be responsible for the exhaustion of $CD8^+$ T cells in the tumor microenvironment. High levels of IL-2 lead to an activation of STAT5, which subsequently induces the expression of tryptophan hydroxylase-1 (TPH). This enzyme converts tryptophan to 5-hydroxytryptophan, another metabolite that serves as an AHR agonist. The resulting activation of AHR signaling leads to an upregulation of inhibitory receptors (e.g. CD39, PD-1) and a downregulation of IFN-γ and tumor necrosis factor (TNF)-α levels and thus to dysfunctional $CD8^+$ T cells [97]. Interestingly, *Il-2* is an established target gene of AHR in mice [78], suggesting that there might be an another signaling loop.

Taken together, these studies provide evidence that IL-2-, IL-6- and

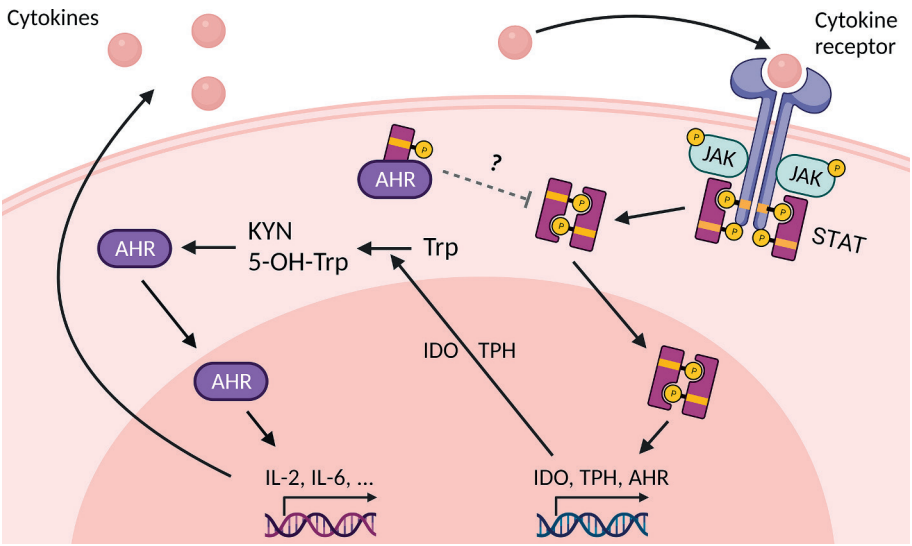

Fig. 2. Crosstalk of JAK/STAT and AHR. AHR and the signal transducer and activator of transcription (STAT) can induce and repress each other. The phosphorylated STAT forms a dimer which can translocate into the nucleus and induce transcription of target genes including AHR, indoleamine 2,3-dioxygenase (IDO) and tryptophan hydroxylase (TPH). IDO and TPH catalyze the metabolism of tryptophan (Trp) into kynurenine (KYN) and 5-OH-Trp, respectively, which can serve as AHR agonists. AHR activation leads to expression of several cytokines, e.g. IL-2 and IL-6, which bind to cytokine receptors and thereby stimulate the sequential phosphorylation of Janus kinases (JAK) and STATs resulting in the release of STATs from the cell surface receptor. Interestingly, AHR can also form a cytosolic heterodimer with a phosphorylated STAT molecule, i.e. STAT, which is thought to repress the formation and nuclear translocation of the phosphorylated STAT dimer.

IFN-triggered JAK/STAT signaling pathways control the expression and activity of AHR (Fig. 2). *Vice versa*, the AHR system can potentially interfere with JAK/STAT signaling pathways by acting as a transcription factor controlling the expression of cytokines, protein kinases, etc. In addition, AHR can directly interact with STAT molecules to either induce or repress their transcriptional activity (Fig. 2). In peritoneal macrophages, both *Ahr*- as well as *Stat1*-deficiency enhances the induction of pro-inflammatory IL-6 in response to LPS treatment [98]. Further mechanistic data, including results from chromatin immunoprecipitation assays, point to the idea that a tripartite complex consisting of AHR, STAT1 and NF-κB subunit p50 is bound to the *Il-6* promoter and represses its transactivation. However, it is worth mentioning that meanwhile, additional mechanisms through which AHR may dampen IL-6 expression in LPS-exposed macrophages have been identified [99]. In T cells, AHR was found to facilitate the polarization towards proinflammatory Th17 cells by inhibiting STAT1 phosphorylation which blocks the competing T helper 1 cell differentiation pathway [100]. Remarkably, Th17-polarizing conditions (IL-6 plus TGF-β) induced the AHR-mediated generation of Th17 cells in the absence of exogenous ligands [100]. Given that, later on a critical involvement of STAT3 in the AHR-dependent differentiation of $CD4^+$ T cells into Th17 cells has been reported [101], a STAT3- and IDO1-dependent production of endogenous tryptophan-derived ligands might serve as an explanation for this observation. However, in contrast to the enforced polarization towards Th17 cell differentiation upon AHR-mediated STAT1 inhibition, the same mechanism was reported to impair Th17 differentiation and promote Tregs in a model for idiopathic pneumonia syndrome [102]. In this model, AHR represses the transcription of the activator protein-1 (AP-1) subunit JUND by preventing the binding of STAT1 to the respective gene promoter, resulting in a reduced expression of IL-6 and the associated polarization of $CD4^+$ T cells toward Th17 cells. Accordingly, KYN-mediated activation of AHR induces immunosuppression and thereby attenuates the pneumonia-related symptoms [102]. This discrepancy between the two studies describing the AHR as an inducer of Th17 cells *versus* an inducer of Tregs has been previously discussed [94,95,103] and may not necessarily solely depend on the structural and biochemical properties of the AHR ligand but also on the applied dose [104]. An inhibitory effect of the IDO1-AHR axis on STAT1 activity has also been observed in a mouse model for melanoma, in which IFN-γ induces dormancy in tumor-repopulating cells by stimulating an iDO-1-driven activation of AHR [105]. This leads to an upregulation of the AHR target and cell cycle inhibitor $p27^{KIP1}$ [106] which subsequently physically interacts with STAT1, thereby causing a switch from the apoptosis to the dormancy program in the malignant cells [105].

In summary, the existing body of literature provides compelling evidence for a mutual interaction of AHR and STAT family transcription factors on various levels, including transcriptional control, induction of signaling mediators and protein–protein interaction. STAT proteins may critically contribute to the impact of the AHR on multiple immune cells, including macrophages and various T cell populations and thereby determine the downstream pro- or anti-inflammatory outcome. In fact, in numerous types of cancer, including melanoma, oral squamous cell carcinoma, lung cancer and glioblastoma, AHR and JAK/STAT signaling pathways seemingly cooperate to repress anti-tumor immune responses and facilitate tumor growth and progression [96,97,101,107,108]. In contrast to this clear trend observed in malignant diseases, there is also compelling evidence for anti-inflammatory consequences of the AHR-JAK/STAT crosstalk, for instance in the context of central nervous system inflammation and inflammatory bowel disease [88,109]. In conclusion, the currently rather limited amount of available experimental data elucidating the interplay between AHR-dependent and JAK/STAT signaling pathways, emphasizes the urgent need for a deeper functional characterization of this crosstalk. This is necessary to assess whether targeting of the JAK/STAT system supports or counteracts AHR-manipulating therapeutic approaches for certain pathological conditions and *vice versa*.

4. The NF-κB family signaling pathway and crosstalk with AHR

The NF-κB family of transcription factors regulates the expression of numerous cytokines and immune response genes [110]. NF-κB is critically involved in biological processes, including apoptosis, cell differentiation, immunity and diseases such as autoimmunity or cancer [111]. Considering the physiological and pathological roles of AHR, a significant overlap with the NF-κB signaling pathway becomes evident [112]. When considering AHR as a transcription factor interacting with NF-κB signaling and modulating immune responses, it is crucial to understand its role in diseases based on immune modulatory effects.

The activity of NF-κB is induced by many cytokines and inflammatory signals in a time- and concentration-dependent manner [113]. Early studies have shown that cytokines also affect the activity of AHR-regulated drug-metabolizing enzymes. For instance, treatment with TNF-α clearly suppressed the activity of hepatic CYP-dependent drug metabolism in mice [114]. Subsequent studies noticed suppression of TCDD-induced *Cyp1a1* and *Cyp1a2* mRNA expression after treatment of isolated rat hepatocytes with IL-1β [115]. In line with this, the acute phase protein IL-6 suppressed the gene expression of *CYP1A1*, *CYP1A2* and *CYP3A3* in human hepatoma cells [116]. These early observations

strongly indicate that NF-κB activated by inflammatory cytokines interferes with AHR signaling and thereby shapes target gene expression and the associated biological outcome.

The activation of NF-κB changes the expression and activity of AHR and *vice versa*. One of the first studies reporting a crosstalk between AHR and proteins of the NF-κB family was published by Tian *et al.* describing the physical interaction of AHR with NF-κB RelA causing a mutual repression of both signaling pathways [117]. In their study, the authors treated mouse hepatoma cells with TNF-α to activate NF-κB and focused on the AHR-mediated induction of CYP1A1 which was significantly repressed after TNF-α treatment. Further, they found that TNF-α-induced NF-κB binding activity was suppressed when Hepa1c1c7 cells were treated with TCDD. Mechanistically, the ligand-dependent activation of AHR induces histone H4 acetylation at the TATA box of the *Cyp1a1* promoter region, which was inhibited by TNF-α-induced NF-κB activity [118].

Further studies have shown that AHR interacts with the NF-κB component RelA which supported the TCDD-mediated induction of IL-6, plasminogen activator inhibitor-2, FAS ligand and c-myc [119–122]. Dinatale *et al.* found that the AHR-mediated amplifying effects on NF-κB signaling requires the AHR/ARNT-heterodimer for the synergistic activation of IL-6 following IL-1β and TCDD treatment. This may involve the dismissal of co-repressors by DNA-bound AHR [119]. The AHR-dependent expression of FasL in thymic stromal cells was found to be regulated through TCDD-mediated activation of the NF-κB subunits p50 and p65 on the *Fasl* promoter [123]. Another mechanism was described for the expression of *C-MYC* in breast cancer cells, where RelA and AHR together bind to NF-κB elements and induce the transcription of *C-MYC* [122].

Conversely, AHR was also identified to suppress NF-κB-mediated gene expression. For instance, the expression of the Ig heavy chain was repressed through the interactions of NF-κB and AHR at a DNA replication-related element and an overlapping κB element [124]. The acute phase protein serum amyloid A was found to be suppressed by the interaction of the activated AHR with RelA, but DNA binding was not involved [125]. Alvaro Puga's group concluded that TCDD-mediated activation of AHR and induction of CYP1A1 leads to the generation of an oxidative stress signal which enhances NF-κB and AP-1 DNA-binding activity. [126]. Interestingly, the enhanced binding activity of the NF-κB complex was found to be formed by p50/p50 complexes which could be responsible for the inhibitory effect of AHR on NF-κB activity. Another study reported an inhibition of IgM expression by TCDD in LPS-activated B cells, which was associated with an AHR-dependent decreased DNA-binding activity of AP-1 but not of NF-κB [127].

Besides RelA, several studies reported an interaction of AHR with the NF-κB member RelB [128–131]. We identified RelB to physically interact with AHR and bind on a previously unrecognized RelB/AHR-responsive element in the promoter of the *IL-8* gene to induce its expression [132]. Further, a ligand-independent activation of AHR *via* protein kinase A triggers its nuclear translocation and the induction of IL-8. Therefore, this mechanism was described as the non-canonical AHR pathway which involves ligand-independent activation and interaction with proteins other than ARNT, such as RelB.

Similarly, the expression of other chemokines including the B-cell activating factor of the TNF family, B-lymphocyte chemoattractant and chemokine (C—C—motif) ligand (CCL) 1 was also found to involve the binding of RelB/AHR-complexes to the promoter of these genes, suggesting a new regulatory function of AHR [128]. The RelB/AHR-responsive element identified on the promoter of *IL-8* is similar to DNA-binding sequences recognized by RelB/p52 dimers in regulatory sequences of the above organogenic chemokine genes [133]. Moreover, AHR signaling can alter the differentiation of mouse bone marrow-derived dendritic cells (BMDC), which involves activation of NF-κB RelB and the AHR-dependent induction of the immune-regulatory enzyme IDO [134,135]. The expression of the cytokines IL-10 and CCL18/DC-CK1 was inhibited by TCDD, but IL-10 was induced in LPS-activated BMDC and in spleen of B6 mice [135,136]. The induction of IDO as well as anti-inflammatory IL-10 in LPS-activated BMDC could critically contribute to the immunosuppressive effect of TCDD. In this context, it is interesting to note that IL-10 was found to protect from colitis [137] and treatment with TCDD may improve colitis in mice associated with an increased number of Tregs [138]. Further, the expression of IL-12A, a key cytokine for Th1 differentiation, was suppressed when TLR4-activated human primary dendritic cells (DCs) were treated with TCDD [139]. This was confirmed in a study using mouse peritoneal macrophages showing that activation of AHR decreased protein levels of pro-inflammatory IL-6 and IL-12 after activation with LPS/IFN-γ [140]. Mechanistically, AHR activation promoted RelA/p65 protein degradation, thus causing the decreased cytokine levels. Besides the interaction of AHR with RelB, studies have demonstrated that ARNT interacts with RelB to regulate expression of the TNF receptor family member CD30 [141]. Since ARNT can dimerize with the AHR repressor (AHRR), the study suggests that AHRR may also affect activity of NF-κB RelB and the expression of cytokines as shown in transgenic mice overexpressing AHRR [142–144]. Interestingly, Ovrevik *et al.* found that ARNT suppressed the expression of RelB which was associated with a decreased expression of IL-8 in human bronchial epithelial BEAS-2B cells [145].

In summary, these studies indicate that the synergistic or inhibitory effects resulting from the interaction of AHR with NF-κB signaling may involve various mechanisms. This includes physical interaction of members of the AHR pathway with subunits of the NF-κB family and combinatorial effects of AHR and NF-κB elements located on promoters of specific target genes.

4.1. Dysregulation of Toll-like receptor responses through AHR signaling

Ligands of the Toll-like receptor (TLR) family are strong activators of NF-κB signaling. Multiple studies have shown that AHR may interfere with responses triggered by pathogens including the TLR4 ligand LPS [112]. Moreover, AHR-deficiency was found to increase the sensitivity of mice towards LPS toxicity including septic shock [120]. Further studies showed that exposure of AHR-deficient mice to LPS, cigarette smoke or crystalline silica triggers an increased inflammation in the lungs associated with increased NF-κB activity [146,147]. On the other hand, exposure to an AHR antagonist significantly inhibited the LPS shock in mice, including a reduced lethality and inflammatory signaling [148]. This finding is in line with our observation that overexpression of AHRR in mice suppressed LPS-induced toxicity and lethality [143]. Possible mechanisms of AHR's role in LPS shock were discussed with regard to the immunosuppressive function of an AHR-iDO-mediated pathway, emphasizing the importance of enhanced IDO activity for the establishment of life-threatening conditions in sepsis [149]. The hypothesis of the AHR-iDO-mediated pathway in sepsis is supported by findings showing that AHR activation synergistically increases the LPS-induced expression of IDO1 and IDO2 [139,150].

Studies with *AHR*$^{-/-}$ mice showed that AHR-deficiency modified the expression of LPS-induced cytokines along with the DNA-binding activity of NF-κB, C/EBPβ and AP-1 in lung and liver [151]. The effects of AHR and TLR ligands in humans were examined in primary DCs derived from human blood monocytes. It was shown that human DCs are very sensitive towards low doses of LPS [139] and that TLR-activated DCs express higher levels of AHR and are more sensitive towards the effects of AHR ligands. Treatment with AHR ligands led to a synergistic or antagonistic effect of the TLR-triggered response in DCs depending on the specific target gene. The effect of AHR ligands in activated DCs involved the expression of RelB and were altered by the specific TLR ligand used to activate DCs. In a study with BMDC from wildtype and RelB-deficient mice, RelB-involvement in ligand-dependent effects on AHR signaling was confirmed [150]. Similar results were received from a study using BEAS-2B cells [145]. The authors found that AHR suppressed activation of RelA stimulated by TNF-α or polyinosinic:

polycytidylic acid. However, activation of AHR induced IL-8 expression, but AHR suppressed the expression of IL-8 and CCL5 when cells were activated by the TLR ligand polyinosinic:polycytidylic acid. The authors concluded that AHR may stimulate or suppress NF-κB signaling and that anti-inflammatory effects of AHR possibly involve additional pathways besides the interaction with NF-κB. The dose-dependent induction of *IL-8* by TCDD described in human DCs [139] is supported by a study demonstrating increased levels of IL-8 in blood of asthmatic children with high PCB serum levels [152].

A synergistic induction of CCL20 was observed in peritoneal macrophages exposed to LPS and AHR ligands [153]. The authors concluded that this was due to both, LPS-mediated increase of AHR levels and a potent tandem AHR-binding site upstream from the transcriptional start site of *CCL20*. Recently, we found that both, a XRE consensus site and a RelBAHRE-binding element located on the promoter of the *IL-22* gene, are necessary to mediate the synergistic effects of AHR and TLR ligands on the expression of this cytokine [31]. Furthermore, an exposure to particulate matter (PM) collected from traffic-related air pollution and wildfires activated AHR and NF-κB signaling, leading to a robust induction of IL-22. The results are in line with a study investigating the expression of IL-33 after exposure to PM collected from tunnel dust [154]. IL-33 is a critical factor in the development of asthma and was induced in macrophages treated with PM samples derived from the tunnel. The analysis of the PM composition indicated that the concentration of PAHs and endotoxins are important factors in the AHR-/TLR-dependent induction of IL-33.

As described earlier [153], levels of AHR mRNA and protein were enhanced by various TLR ligands in DCs and thymus of B6 mice [155]. A functional NF-κB-binding element was identified upstream of the transcription start site of the *AHR* gene indicating an important role of RelA/p50 in the transcriptional regulation of AHR [155]. These results demonstrated for the first time that NF-κB RelA is a critical component regulating the expression of AHR and downstream target gene expression. These findings have important implications regarding the effect of inflammatory stimuli and cytokines that activate NF-κB and induce AHR expression during activation and differentiation of immune cells. The results may provide a possible mechanism of the rapid increase of AHR levels after T cell activation described in previous studies [95,103]. This rapid upregulation of AHR, which also occurs upon activation of murine splenocytes, murine B cells [156] and human B cells [157], may contribute to the enhanced sensitivity of leukocytes towards a modulation by dioxin and dioxin-like compounds. Additionally, the type of TLR response activated through the specific TLR agonist may direct the outcome of AHR interaction with NF-κB subunits and the regulatory or immunogenic response. Further, this involves not only a single gene, but a number or a group of genes will be affected by the AHR/NF-κB-crosstalk. The altered innate immune responses and dysregulation of TLR signaling by AHR are likely to be the key steps in triggering chronic inflammatory diseases as well as modulation of antiviral responses during infection (Fig. 3).

In summary, these findings show that simultaneous activation of AHR and NF-κB signaling pathways leads to synergistic or antagonistic effects on specific target genes by integrating signals of canonical and non-canonical AHR pathways.

4.2. Consequences of AHR and NF-κB interaction in pathology

Many chemotherapeutics are metabolized by AHR-regulated CYP isoforms [158,159]. As described above, inflammatory cytokines can change the expression and activity of CYP enzymes and therefore the metabolism of various drugs. Consequently, changes in the activity of CYP enzymes may ultimately result in clinical endpoints [160]. For instance, altered CYP activities may modify chemotherapeutics exposure and affect the treatment response in cancer patients [161]. In fact, AHR-regulated CYP1 isoforms are primarily responsible for the metabolism of the anti-cancer drugs vemurafenib and imiquimod [162,163]. Alterations in CYP activity also play a critical role in the onset and progression of various diseases including cancer, metabolic disorders and hepatic as well as cardiovascular diseases [160,164–167]. Hence, by attenuating CYP expression and enzyme activity, inflammatory signaling pathways may contribute to adverse health effects.

Inflammatory DCs and macrophages exhibit an increased expression and activity of AHR. Elevated copy numbers of *AHR* were detected in two disease models, i.e. rheumatoid arthritis and allergic airway

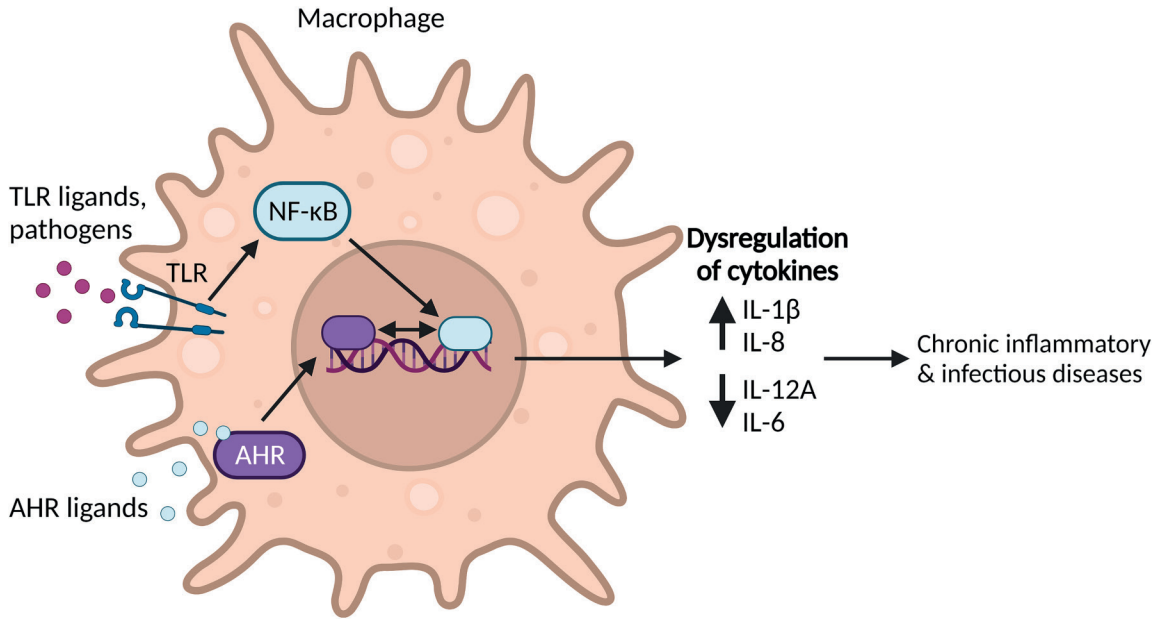

Fig. 3. Dysregulation of Toll-like receptor responses through AHR signaling. In the macrophage, interaction between AHR and nuclear factor kappa-light-chain-enhancer of activated B cells (NF-κB) can regulate immune response and inflammation via transcriptional inhibition and activation of cytokines and chemokines. If the Toll-like receptor (TLR) is bound by ligands or pathogens it leads to the nuclear translocation of NF-κB, whereas ligand-binding of AHR leads to the nuclear translocation of AHR. When both NF-κB and AHR are activated, a dysregulation of transcription of cytokines can occur, e.g. leading to an increase of interleukin (IL)-1β and -8 and a decrease of IL-12A and -6. This favors occurrence of chronic inflammatory and infectious diseases.

inflammation [155]. Further, an increased level of IL-8, an attractant for neutrophils, was found in the blood of asthmatic children which correlated with high PCB serum levels [152]. These data support previous studies showing that AHR activation (*via* TCDD, PCBs) and activation of NFκB through LPS *in vitro* or under chronic inflammatory conditions, like asthma, can synergistically increase target gene expression, such as *IL-8*, in children [168].

The AHR is known to be involved in the pathology of autoimmune diseases, such as rheumatoid arthritis, colitis, and systemic lupus erythematosus (SLE) [169–171]. Interestingly, AHR activation by apoptotic cells was found to depend on interactions between AHR and TLR9 which can inhibit disease progression of SLE in mice [169]. Accordingly, the loss of AHR or deficiency of TLR9 might contribute and accelerate SLE in this mouse model. On the other hand, a synergistic interaction between the shared epitope and the AHR pathway triggered by NFκB signaling has been described to cause a robust increase in arthritis severity in mice [172]. These studies underline the importance of the crosstalk between AHR and NF-κB as a mechanism in the development of autoimmune diseases.

Over the last two decades, numerous reports have shown that the AHR plays an important role in regulating immune responses and that exposure to AHR-activating ligands and toxicants contributes to the promotion of immune system disorders and the development of chronic inflammatory diseases [10,173]. Although AHR ligands and NF-κB stimulation through pathogens or other inflammatory stimuli very specifically activate only one of the two pathways, there is significant crosstalk when both signaling pathways are activated (Fig. 3). The communication between AHR and NF-κB is evidently critical for the immune response, but the type and strength may vary depending upon factors like the length, intensity and timing of the signal, as well as cell-specific receptor distribution. The cross-regulation between these two signaling axes suggests that NF-κB- and AHR-dependent signaling could be viewed within the context of a unique signaling system. It mediates signaling from both pathogen-/inflammatory and ligand-based stimuli that may regulate physiological function and which, if dysregulated, may contribute to pathology of chronic diseases and impact host defenses against infectious diseases. The NF-κB and AHR signaling pathways may run independently in parallel, however, their crosstalk creates multiple opportunities for modulating or fine-tuning of responses to different signals. Such fine-tuning is important as the immune system has to be active enough to fight pathogens or cancer, but should not be hyperactivated and result in chronic inflammatory diseases.

5. HIF-1α and AHR: Interdependence and crosstalk

The Nobel Prize in Physiology or Medicine 2019 was awarded to Gregg Semenza, Sir Peter Ratcliffe and William Kaelin for their joint discovery of hypoxia-inducible factor (HIF)-1α and its functionality under cellular oxygen shortage [174–176]. Of note, the identified co-factor HIF-1β turned out identical to the already known AHR co-factor ARNT. AHR, ARNT, and HIF-1α all belong to the group of basic helix-loop-helix/Per-Arnt-Sim proteins which act as environment-sensing heterodimeric transcription factors [177] governing adaptation to changing external conditions.

HIF-1α function is crucial under physiologic conditions including embryogenesis [178–180] or during anaerobic activity [181,182], but also under pathologic conditions like infection and cancer [180,183,184]. Under normoxic conditions (~21 % O_2), the HIF-1α protein is constantly degraded by the proteasome: Oxygen-dependent HIF-prolyl hydroxylases permit binding of the von Hippel–Lindau protein to hydroxylated HIF-1α, leading to ubiquitination and subsequent degradation by the proteasome [174,176,185]. Under hypoxia (~0,1–1 % O_2/0 % O_2 is termed anoxia), these enzymes are inactive, allowing accumulation of HIF-1α and activation via dimerization with ARNT to induce transcription by binding to hypoxia-responsive elements (HRE) on nuclear DNA (Fig. 4) [175,186].

There is clear long-standing evidence from independent studies that HIF-1α and AHR activities are interdependent [187–190] in different tissues, indicating a functional crosstalk between their pathways in conditions as diverse as obesity, glioblastoma, prostate cancer, nephrocalcinosis, autoimmune hepatitis and affecting processes like T cell and macrophage differentiation as well as blood–brain barrier function [87,191–199]. However, this issue has rarely been addressed systematically [200]: While a majority of studies suggests downregulation of AHR function through HIF-1α activation and *vice versa* [201–203], they almost exclusively investigated the function of TCDD, and more physiologic means of AHR activation have been even more scarcely addressed. The modes of interaction can be competitive or counteracting, but could possibly also be additive or compensatory under certain circumstances (Fig. 4). The specific effect may depend on contextual factors ranging from the specific tissue or cell type or pathway trigger to biochemical properties like ARNT availability, binding preference and other parameters. Importantly, it has been reported that ARNT is influenced by both hypoxia and hypoxia mimetics [204,205]. The skin has been a subject to hypoxia research, since especially the avascular epidermis is mildly hypoxic with constant low HIF-1α activity [206–208]. Of note, loss of ARNT in epidermal keratinocytes causes skin barrier failure in neonatal mice [209–211]

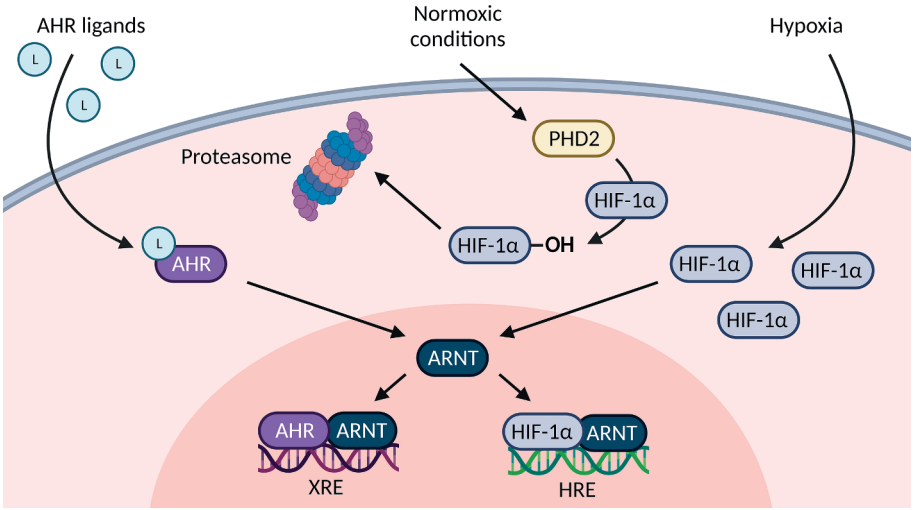

Fig. 4. Crosstalk of HIF-1α and AHR. Activated AHR and hypoxia-inducible factor 1 alpha (HIF-1α) both translocate into the nucleus and dimerize with ARNT which results in binding to either xenobiotic response elements (XRE) or hypoxia responsive elements (HRE) in the enhancer/promoter region of respective target genes. Under normoxic conditions, prolyl hydroxylase domain-containing protein 2 (PHD2) executes hydroxylation of HIF-1α resulting in constant proteasomal degradation of HIF-1α. Under hypoxia, HIF-1α can accumulate and then translocate into the nucleus where it then dimerizes with ARNT. Depending on cell-type and tissue, a competition for ARNT may result in the suppression of the AHR pathway when the HIF-1α pathway is activated or *vice versa*.

associated with dysregulation of processes like synthesis of ceramides [212], a group of lipids implicated in oxidative stress balance [213] which in turn is also mediated by ARNT [214]. Since both keratinocyte-specific *HIF-1α*$^{-/-}$ and *AHR*$^{-/-}$ mice are viable without an overt phenotype [215–217], these findings underline (I) the importance of cooperative function of HIF-1α and AHR in epidermal keratinocytes and (II) may hint toward the involvement of other ARNT-dependent factors and/or (III) possible compensatory or aberrant pathway activation. Though a majority of studies demonstrates interaction of HIF-1α and AHR via ARNT (Fig. 4), others have argued that cells harbor a relative excess of ARNT not limiting its availability to dimerization partners [218], which also include HIF-2α, AHRR and others [177]. Other molecules proposed in HIF-1α-AHR crosstalk are microRNAs [197] and the proteins NCoA-2 [219] and p23 [203].

Among prototypical targets induced by HIF-1α activity are the vascular endothelial growth factor (VEGF), erythropoietin (EPO) and Glut-1 [220,221] which contribute to metabolic adaptation to hypoxia and improvement of oxygen availability: VEGF induces endothelial vessel growth, EPO is a growth factor for erythrocytes and Glut-1, encoded by the *SLC2A1* gene, is an important membrane transport protein enabling the cellular import of glucose and other monosaccharides as well as ascorbic acid. Further, numerous other genes are modulated which can be grouped into inflammation/immune defense, proliferation, tumor promotion/cancer therapy resistance [222]. Taken together, HIF-1α-dependent processes promote cellular survival under stress through oxygen shortage.

The normal oxygen level is tissue-specific and low tissue oxygen availability is not necessarily pathologic: Intermediate O_2 levels are termed physoxia (range ~ 1–13 % O_2, medium values ~ 5 % O_2) [223]. HIF-1α is typically stabilized under hypoxic conditions (below 1 % O_2) which arise during high cell proliferation or metabolic activity including embryogenic development, inflammatory processes, physical strain and tumor growth. Further, numerous diseases ranging from respiratory infection over allergic asthma to COPD, besides consuming chronic diseases or placental insufficiency, can increase oxygen demands and/or restrict oxygen availability to the organism. Moreover, ischemia caused by vessel occlusions or tissue damage can induce regional hypoxia.

The HIF-1α pathway can also be upregulated under normoxic (resp. physoxic) conditions [224] through numerous triggers including LPS [225] or pro-inflammatory cytokines, such as IL-6, IL-18 and TNF-α, as well as thrombin [226], glucose [227], angiotensin II [228], cholesterol [229], hyperthermia [230] and UVB radiation [231–233]. A state of normoxic pathologic HIF-1α activation, which occurs in conditions including type II diabetes and cancer, is sometimes referred to as pseudohypoxia. The associated increase in cellular glycolysis is termed the Warburg effect [234,235]. The contextual nature of the HIF-1α pathway trigger will also activate specific other pathways with important implications regarding functional crosstalk.

In this regard, crosstalk of HIF-1α with AHR could be particularly important during UVB-dependent processes like DNA repair, apoptosis and proliferation in epidermal keratinocytes which are essentially dependent on AHR activity [58,61,62]. Intriguingly, HIF-1α may have contrastive effects on non-melanoma skin cancer (arising from keratinocytes) as opposed to melanoma [236–238], which is not fully investigated to date. Moreover, during UVB-induced immunosuppression to contact hypersensitivity, AHR and HIF-1α appear to take opposing roles in keratinocytes [216,239].

Experimentally, hypoxic stabilization of HIF-1α can be achieved by hypoxia mimetics like cobalt chloride or dimethyloxalylglycine [240] which inhibit the HIF-1α-degrading hydroxylases. Also, several HIF inhibitors are available, of which some are specific for HIF-1α [241,242], but others may also target HIF-2α [243]. It should not be neglected that some ligands of AHR vs HIF-1α may have unexpected indirect effects to modulate the other pathway [244].

The HIF-1α target EPO has a long history of therapeutic use for anemia [245], but also in sports doping [246]. Newer drugs include HIF stabilizers like roxadustat and similar HIF-prolyl hydroxylase inhibitors [247,248], which also achieve erythropoiesis besides other hypoxia-mimetic effects. Another presumably hypoxia-mimetic drug class are SGLT2 inhibitors, which palliate diabetic kidney disease and heart failure while improving erythropoiesis [249]. HIF-1α modulation is of particularly high relevance for ophthalmology of both the anterior (cornea) and posterior (retina) eye segments [250,251] and it should be noted that also the AHR is implicated in ocular diseases with some implications for HIF-1α crosstalk, e.g. in the context of cigarette smoking [252]. Blockade of the HIF-1α target VEGF by bevacizumab (Avastin®) is approved for treatment of several advanced solid tumors (lung, colon, breast, kidney, ovary, uterus) [253] and the similar drug ranibizumab (Lucentis®) is in use for ocular diseases involving pathologic angiogenesis [254,255]. Numerous novel approaches of HIF inhibition for advanced or refractory cancers are in clinical development stages [256]. Since AHR activation is implicated in tumor development due to its pro-proliferative impact [20], it would be worthwhile to further assess the role of HIF-1α-AHR interaction not only in cancer pathogenesis but also with regard to therapy schemes. Another field of possible future therapeutic HIF-1α utilization is the promotion of neuronal/axonal regeneration [257,258], in which AHR kinetics are also implicated [259].

An interesting approach to non-pharmacologic application of the HIF-1α pathway is hypoxic preconditioning: While uncontrolled chronic or also episodic hypoxia can be harmful, e.g. due to chronic heart failure resp. obstructive sleep apnea, controlled intermittent hypoxic training has proven beneficial health effects on the cardiovascular system and even confers protection against tissue damage from ischemic events [260,261]. These are similar to the effects of high-altitude training in professional sports. While HIF-1α is activated during ischemic events, reperfusion therapy is accompanied by additional secondary tissue damage involving inflammatory processes and ROS release in the impacted tissue. Novel literature suggests that AHR activation may play a pivotal role in this pathogenesis and suggests that AHR inhibition may pose a therapeutic strategy to mitigate ischemia–reperfusion damage in brain, myocardium and kidney [262–264].

6. NRF2 signaling

Living organisms have a fine-tuned system for maintaining a well-defined low steady-state level of oxidative stress, i.e. ROS production and elimination are well balanced. The term “oxidative stress” was first defined as a technical term by Helmut Sies in 1985 [265]. In this context, the formation of ROS can be initiated by aerobic metabolic processes, endogenous defense mechanisms, exogenous noxious agents and photobiological processes. Thereby, the main sources of ROS are leakage of the mitochondrial respiratory chain as well as CYP-mediated oxidations (phenomenon of “uncoupling”) [11]. Aldo-keto reductases (AKRs), a family of cytosolic NADPH-dependent oxidoreductases, were also suggested to be involved in the metabolic activation of PAHs and an associated generation of ROS. Moreover, several other enzymes were described and summarized in a review by Haarmann-Stemmann and coworkers to stimulate ROS production in an AHR-dependent manner (e.g., NADPH oxidases, COX-2) [11]. Klicken oder tippen Sie hier, um Text einzugeben.Interestingly, already in the beginnings of the 1990s, there was evidence that AHR activation is involved in the generation of ROS as well as the antioxidant stress response [266,267] (Fig. 5). Besides phase I xenobiotic-metabolizing enzymes, also phase II detoxifying enzymes (i.e. glutathione S-transferase, UDP-glucuronosyltransferase, sulfotransferase and *N*-acetyltransferase) are induced by canonical AHR/ARNT signaling. Moreover, there is evidence that AHR interacts with several regulators of the antioxidant stress response affecting the induction of antioxidants as well as antioxidative enzymes (i.e. catalase, glutathione peroxidase, superoxide dismutase and other peroxidases).

These regulators include transcription-factors such as NF-κB [268], AP-1 [269], β-catenin [270], proliferator-activated receptor γ (PPARγ) [271] and the master regulator NRF2, which is a member of the Cap-*N*-

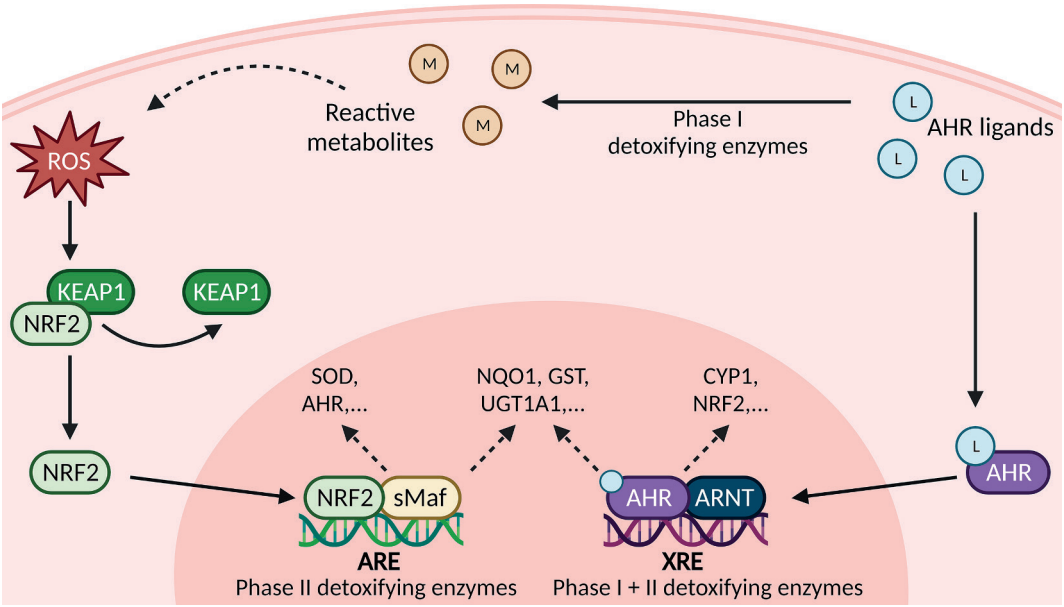

Fig. 5. NRF2-AHR-crosstalk. Ligand-activation of AHR results in its nuclear translocation where it dimerizes with ARNT and, amongst others, induces the transcription of xenobiotic-responsive element (XRE)-regulated phase I and II detoxifying enzymes, and NRF2. Phase I detoxifying enzymes convert AHR ligands into reactive metabolites which again can lead to the formation of reactive oxygen species (ROS). ROS can trigger the dissociation of the cytosolic NRF2-KEAP1-complex resulting in the nuclear translocation of NRF2 and its subsequent dimerization with small Maf proteins. This results in the expression of antioxidative response elements (ARE)-controlled phase II detoxifying enzymes, as well as AHR. Moreover, the AHR and NRF2 target gene batteries partially overlap, the gene expression of NQO1, GST or UGT1A1, for instance, is under control of both pathways.

Collar protein family [272]. In addition to several enzymes introduced above, other cytoprotective proteins such as heme oxygenase-1 and NADPH:quinone oxidoreductase-1 (NQO-1) are under the control of the NRF2/Kelch-like ECH-Associated Protein 1 (KEAP1) signaling pathway [273]. Under basal conditions, NRF2 is bound in the cytosol to the adaptor protein KEAP1 [274,275]. Here, KEAP1 serves as an adapter protein linking NRF2 to a cullin-3-mediated ubiquitination and thus proteasomal degradation [276]. In addition, activation of NRF2 occurs predominantly by a conformational change of KEAP1. Thus, it has been shown that the redox-sensitive cysteine residues of KEAP1 are able to react with and oxidize ROS, thereby preventing a cullin-3-mediated ubiquitination and proteasomal degradation of NRF2 [277]. Moreover, ROS have been described to activate specific kinases (PKC, PI3K, MAPK) that phosphorylate NRF2, resulting in an attenuation of NRF2-KEAP1 interaction and inhibition of proteasomal degradation of NRF2 (Fig. 5) [278,279]. Upon activation, NRF2 shuttles into the nucleus and forms a heterodimer with so-called small musculoaponeurotic fibrosarcoma (MAF) proteins. This dimer then binds to the antioxidant response element (ARE) in the promoter region and enhances target gene expression (Fig. 5) [280].

Metabolic activation of procarcinogens initiated by AHR and downstream CYP1 monooxygenases is well known to play a significant role in the human body regarding the development of malignant diseases. Besides this, several enzyme systems involved in the metabolism of xenobiotics initiated by AHR activation lead to the generation of ROS and thus to oxidative stress, activating the NRF2-signaling pathway (Fig. 5).

Apart from the described indirect crosstalk of AHR and NRF2 (Fig. 5), Miao and colleagues showed that the *NRF2* gene is a direct target of the canonical AHR signaling pathway containing multiple XREs in its promoter region [281]. Consequently, knockdown of *AHR* results in a decreased expression of NRF2 and thereby attenuates the induction of the antioxidant stress response. In contrast to this, it was reported that NRF2 expression and activity controls AHR expression [282,283]. Besides this, expression of genes encoding phase II detoxifying enzymes are induced in response to various environmental factors to counteract the deleterious effects of potentially reactive intermediates. Especially the NRF2/KEAP1 signaling pathway is responsible for their induction. However, there appears to be some overlap with target genes of AHR that include *NQO1* [284], glutathione S-transferases (*GST*) [285,286] and some glucuronosyltransferases [287–289]. In addition, Tsuji *et al.* could prove that treatment of keratinocytes with ketoconazole not only results in an activation of AHR and the corresponding stimulation of *CYP1A1* gene expression but also in an increased induction of *NRF2* and *NQO1* expression. Interestingly, the NRF2 activity stimulated by AHR in ketoconazole-treated primary keratinocytes was independent of ROS [290]. Instead, an involvement of EGFR, a downstream signal transduction of the MEK/ERK signaling pathway and a corresponding phosphorylation of NRF2 and an attenuation of the NRF2/KEAP1 interaction was suggested [272]. In addition, in a recent study we found that PAHs induce AKR1C3 expression in an AHR- EGFR-, MEK/ERK- and NRF2-dependent manner. Specifically, we showed that BaP upregulates AKR1C3 expression via the AHR-EGFR-NRF2 axis, independently of CYP1A1 activity and the associated production of ROS and genotoxic metabolites [48]. But there are also studies showing that it is possible to inhibit AHR activity while stimulating the NRF2/KEAP1 antioxidative system that especially seemed to be important when it comes to metabolic activation of PAHs [291–296]. Interestingly, a treatment with chrysoeriol and curcumin resulted in an inhibition of CYP1A activities and reduced the formation of DNA-adducts induced by BaP metabolites as well as 7,12-dimethylbenz[*a*]anthracene in MCF-7 breast cancer cells [291,292]. Another study demonstrated that curcumin altered BaP-induced activation and DNA-binding of AHR. In fact, they observed enhanced NRF2 stimulation and an associated increased gene expression of *GST* and *NQO1* with improved detoxification of BaP [293]. There are far more publications pointing to this antithetical activation of AHR and NRF2. In addition, cinnamaldehyde was shown to have an inhibitory function on AHR while having antioxidative capacity, mediated by a stimulation of NRF2 and heme oxygennase-1 expression [297]. This described dual function may point to a suitable modulation of AHR and NRF2 signaling, probably as a good tool to protect tissues, in particular those which are frequently exposed to environmentally or lifestyle-

derived AHR ligands (e.g. liver and skin) against the metabolic activation and thus tumor-initiating potency of pro-carcinogenic chemicals. Beyond that, it might also be beneficial for the treatment of disorders related to oxidative stress such as dioxin intoxication, acne and vitiligo as suggested by Furue and co-workers [297]. Beside this, others could show that ROS inhibits the catalytic activity of CYP1A1 and therefore might inhibit the metabolic degradation of AHR ligands. Specifically, it was shown that arsenic-treated mice as well as cells and a corresponding increase of ROS resulted in an accumulation of FICZ and an accompanied upregulation of *Cyp1a1* gene expression [298,299]. In addition, increasing ROS levels induced by glutathione deprivation or in the absence of functional NRF2 correlate with an increased expression and activity of AHR in normal and malignant mammary cells. AHR activation thereby fosters the expression of *AREG* and therefore activation of the EGFR. Subsequent experiments revealed that AHR inhibition sensitized human breast cancer cells to erlotinib and might be an attractive target to change the tumor microenvironment [300]. However, it should be considered that erlotinib itself is a substrate for CYP1A1, so inhibition of AHR/upregulation of CYP1A1 might reinforce an accumulation of erlotinib and would result in an improved impact of erlotinib [301].

Several MAF-proteins, belonging to the family of leucine zipper nuclear transcription factors, were described to have a different impact on transcription of different eukaryotic genes. Thereby, it was demonstrated by Dhakshinamoorthy *et al.* that overexpression of c-MAF has a negative influence on the gene expression of ARE mediated detoxifying enzymes in HepG2 cells. In particular, it was demonstrated that by forming homodimers or heterodimers with MAFG, c-MAF represses ARE-mediated NQO1 expression [302]. Interestingly, an interaction between AHR and c-MAF could also be reported. There, Apetoh *et al.* demonstrated that the AHR interacts with c-MAF to promote IL-27-induced differentiation of Type 1 regulatory T cells [79]. For this reason, it might be possible that the activity of NRF2 could be influenced by an interaction of AHR and c-MAF. Thus, it would be conceivable that other transcription factors and/or signaling pathways may have an impact on the interaction of AHR- and NRF2-signaling pathway and not only in terms of the antioxidant stress response.

7. The AHR as a ligand-dependent E3 ubiquitin ligase

While the AHR is infamous for its function as a ligand-activated transcription factor, some studies regarding the toxicity of dioxins and related compounds have shown that the AHR also mediates estrogenic [303,304], anti-estrogenic [305,306] and androgenic effects [307]. The underlying mechanisms were unclear and could not be explained exclusively by CYP1-mediated degradation of steroid hormones or the CYP19A (aromatase)-catalyzed synthesis of the estrogen receptor (ER)-ligand 17β-estradiol. In 2003, Ohtake and co-workers showed that dioxins exert estrogenic effects through the association of ligand-activated AHR/ARNT to unliganded ER [308]. Additionally, Wormke *et al.* revealed that TCDD induces the proteasome-dependent degradation of endogenous ER-α [309]. Based on this observation, a novel ubiquitin ligase complex was identified. This complex is initiated by ligand activation of the AHR and targets sex steroid receptors [310]. Nevertheless, mechanistic insights into the regulation of both AHR functions remained unclear until 2017, when Luecke-Johansson and co-workers described how the AHR switches between its functions as a transcription factor and an E3 ubiquitin ligase [311].

One of the most important regulators of cellular homeostasis is the ubiquitin proteasome system which specifically degrades targeted proteins [312,313]. In a first step, an activating enzyme (E1) transfers a ubiquitin molecule to a ubiquitin-conjugating enzyme (E2). Ubiquitin protein ligases (E3) recognize specific degradation signals and are therefore responsible for substrate specificity. With the help of an E3 ligase, the E2 enzyme conjugates one or more ubiquitin molecules to the target protein, followed by proteasomal degradation [312,313]. The AHR-associated E3 ligase complex, denoted $CUL4B^{AHR}$, is composed of the scaffold protein Cullin 4B (CUL4B), damaged-DNA binding protein 1, RING-box protein 1, transducin-β-like protein 3 and the proteasomal 19S particle [310]. Upon ligand-activation of the AHR, it initiates assembly of the $CUL4B^{AHR}$ complex and serves as a substrate-specific adapter protein within the complex (Fig. 6). Then, the availability of ARNT determines the functionality of AHR: when ARNT is available, the AHR functions as a ligand-activated transcription factor and activates the canonical AHR signaling pathway. However, when ARNT is occupied by other proteins, such as the AHRR, the AHR functions as an E3 ligase and induces assembly of the $CUL4B^{AHR}$ complex [311]. Subsequently, substrate proteins are targeted for proteasomal degradation (Fig. 6). Target proteins of the $CUL4B^{AHR}$ complex include ER-α, ER-β and androgen receptor (AR) [310,314]. It was also shown that PPARγ, a transcription factor and important regulator of adipogenesis, is targeted by the $CUL4B^{AHR}$ complex for proteasomal degradation [315]. Moreover, β-catenin, which is a transcription factor downstream from the WNT signaling pathway, has been reported as target protein [316]. Canonical WNT/β-catenin signaling pathway is a key regulator of embryonic development and adult tissue homeostasis [317]. While β-catenin degradation by the $CUL4B^{AHR}$ complex was shown in mouse intestine, other working groups could not find evidence for β-catenin degradation in mouse hepatoma cells despite evidence of physical interaction of AHR and β-catenin. This suggests that AHR/β-catenin interaction, or rather the AHR function as an E3 ligase, may not only be ligand-dependent but also tissue-specific. Interestingly, the AHR was found to induce the ubiquitin-proteasomal and lysosomal degradation of RelA/p65 in mouse peritoneal macrophages [140]. However, whether this process involves AHR's function as a E3 ubiquitin ligase requires further investigation.

Importantly, upon its ligand-induced nuclear translocation and the subsequent transactivation of target genes, AHR itself becomes degraded [318,319]. Even though this has been known for many years, details about the degradation process only became evident in 2021. Rijo and co-workers demonstrated that the $CUL4B^{AHR}$ complex and TCDD-inducible poly(ADP-ribose) polymerase collaborate in ligand-induced AHR degradation. Knockdown of *CUL4B* in mouse embryonic fibroblasts partially prevented AHR degradation by TCDD, while additional knockdown of TCDD-inducible poly(ADP-ribose) polymerase completely abolished ligand-induced AHR degradation [320].

Due to the fact that the canonical transcriptional activity and E3-ligase activity of the AHR are in a close relation with each other, it should be considered that molecular targeting of the AHR by classical chemical ligands does also affect other signaling pathways, such as ER, AR, PPARγ and WNT/β-catenin signaling. A dysregulation of these major signaling pathways may contribute to the development of diseases, such as cancer [321–324]. However, the bifunctionality of the AHR gives rise to the opportunity of utilizing the E3 ligase activity of AHR as a new target. Faber *et al.* summarize the targeted modulation of the AHR in inflammatory gastrointestinal indications and give guidance for drug development in their latest review [39]. Particularly, the Proteolysis targeting chimera (PROTAC) technology is a promising tool that may substitute classical small molecule-based inhibitors [39,325,326]. PROTACs are (hetero-)bifunctional molecules consisting of two domains that are joined by a linker. One domain interacts with an E3 ubiquitin ligase and the other binds the protein of interest (POI), bringing the E3 and POI into spatial proximity, resulting in the targeted degradation of the POI by the proteasome [326,327]. PROTAC technology even allows the targeting of so far undruggable proteins and, in contrast to gene editing approaches, it usually does not cause misinterpretations arising from genetic compensation or spontaneous mutations. Just recently, the first PROTACs, for instance targeting AR in prostate cancer (ARV-110), ER in breast cancer (ARV-471) and Bruton's tyrosine kinase in B cell malignancies (NX-2127), have entered clinical testing in humans [327]. First PROTACs targeting the AHR [328], but also first attempts to use the AHR as an E3 ligase to degrade target proteins [329], have already been described. As the AHR has been recognized as a pharmacological target

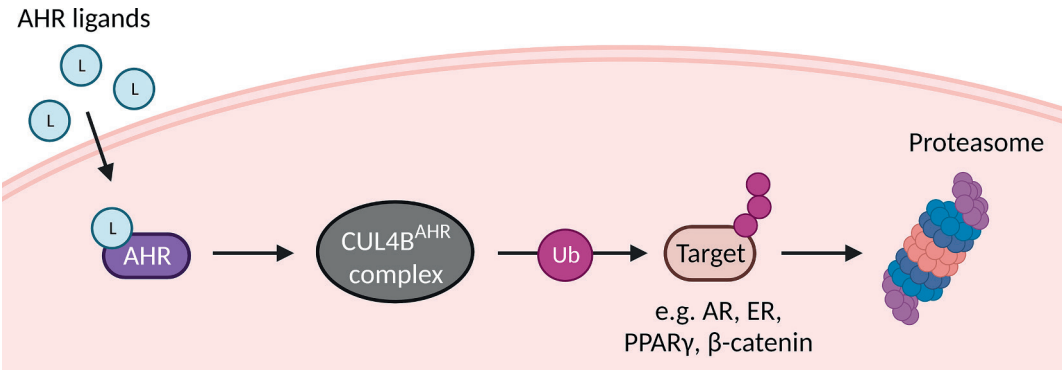

Fig. 6. AHR acts as a ligand-dependent E3 ubiquitin ligase. Upon ligand-activation, AHR and the E3 ubiquitin ligase Cullin 4B (CUL4B) can from a cytosolic complex which ubiquitinates and thereby targets various proteins, including androgen receptor (AR), estrogen receptor (ER), peroxisome proliferator-activated receptor γ (PPARγ) and β-catenin, to proteasomal degradation. This process presumably takes place when the AHR binding partner ARNT is absent.

by many researchers in recent years, approaches such as PROTACs hold great promise for future research of new treatment strategies for various diseases.

8. Conclusion

While the canonical pathway of AHR is well documented, gaps remain in the bigger picture of AHR-related crosstalk with other signaling proteins. The multiple non-canonical events and functions of AHR are expressed by diverse organ-, tissue- and ligand-specific effects. As described in this review article, AHR is indirectly involved in processes concerning proliferation, differentiation, apoptosis, adaptation to low oxygen levels, oxidative stress, ubiquitination and proteasomal degradation. Even though this already covers a broad spectrum of unquestionably relevant functions, even more AHR crosstalk events have been observed. One of them is the TGF-β/SMAD pathway which seems to negatively regulate canonical AHR signaling [330]. Another interesting non-canonical AHR crosstalk concerns the circadian signaling pathways. Here, ligand-activated AHR can influence the amplitude and phase of rhythms in circadian clock genes, hormones and behavior [331]. Moreover, AHR expression and activity has a critical impact on the self-renewal and maintenance of stem cells and their subsequent differentiation in a tissue-specific manner. Specifically, AHR controls the expression of several pluripotency factors (e.g. OCT4, NANOG) and interacts with multiple signaling pathways (e.g. Wnt/β-catenin, Notch) and epigenetic gene regulatory mechanisms (e.g. DNA methylation) [332–334]. However, deepening the knowledge on non-canonical AHR signaling and further unravelling the potentially even more faceted network following upon AHR activation could contribute to a better understanding of many different physiological and pathological processes. Importantly, this would especially benefit the development of new AHR-targeted therapeutic approaches.

CRediT authorship contribution statement

Natalie C. Sondermann: Conceptualization, Writing – original draft, Writing – review & editing, Visualization. **Sonja Faßbender:** Writing – original draft, Writing – review & editing. **Frederick Hartung:** Writing – original draft, Writing – review & editing. **Anna M. Hätälä:** Writing – original draft, Writing – review & editing. **Katharina M. Rolfes:** Writing – original draft, Writing – review & editing. **Christoph F.A. Vogel:** Writing – original draft, Writing – review & editing. **Thomas Haarmann-Stemmann:** Conceptualization, Writing – original draft, Writing – review & editing, Supervision.

Declaration of Competing Interest

The authors declare that they have no known competing financial interests or personal relationships that could have appeared to influence the work reported in this paper.

Acknowledgements

NCS and FH are supported by the Jürgen Manchot Foundation. Research of SF is supported by the Deutsche Forschungsgemeinschaft (FA1468/2-1, FA1468/2-2). CFAV is supported by the National Institute of Environmental Health Sciences of the National Institutes of Health (R01ES029126, R01ES032827). Research in the laboratory of THS is supported by the Deutsche Forschungsgemeinschaft (HA 7346/2-2). The scheme shown in the figure was created with BioRender software (www.biorender.com; agreement numbers HM24OFNLD, TQ24OFNH3K, ZU24OFN6I4, VN24OFNB44, ST24PA4ZKF, DF24OFNNQD and HT24OFNJ20).

References

[1] A. Poland, E. Glover, A.S. Kende, Stereospecific, high affinity binding of 2,3,7,8-tetrachlorodibenzo-p-dioxin by hepatic cytosol, J. Biol. Chem. 251 (16) (1976) 4936–4946.
[2] A.P. Poland, D. Smith, G. Metter, P. Possick, A health survey of workers in a 2,4-D and 2,4,5-T plan with special attention to chloracne, porphyria cutanea tarda, and psychologic parameters, Arch. Environ. Health 22 (3) (1971) 316–327.
[3] J. Kimmig, K.H. Schulz, Occupational acne (so-called chloracne) due to chlorinated aromatic cyclic ethers, Dermatologica 115 (4) (1957) 540–546.
[4] D.W. Nebert, J.E. Gielen, Genetic regulation of aryl hydrocarbon hydroxylase induction in the mouse, Fed. Proc. 31 (4) (1972) 1315–1325.
[5] J.E. Gielen, F.M. Goujon, D.W. Nebert, Genetic regulation of aryl hydrocarbon hydroxylase induction. II. Simple Mendelian expression in mouse tissues in vivo, J. Biol. Chem. 247 (4) (1972) 1125–1137.
[6] A.P. Poland, E. Glover, J.R. Robinson, D.W. Nebert, Genetic expression of aryl hydrocarbon hydroxylase activity. Induction of monooxygenase activities and cytochrome P1–450 formation by 2,3,7,8-tetrachlorodibenzo-p-dioxin in mice genetically "nonresponsive" to other aromatic hydrocarbons, J. Biol. Chem. 249 (17) (1974) 5599–5606.
[7] B. Eskenazi, M. Warner, P. Brambilla, S. Signorini, J. Ames, P. Mocarelli, The Seveso accident: A look at 40 years of health research and beyond, Environ. Int. 121 (2018) 139-71-84.
[8] A.T. Patterson, B.H. Kaffenberger, R.A. Keller, D.M. Elston, Skin diseases associated with Agent Orange and other organochlorine exposures, J. Am. Acad. Dermatol. 74 (1) (2016) 143–170.
[9] O. Sorg, M. Zennegg, P. Schmid, R. Fedosyuk, R. Valikhnovskyi, O. Gaide, V. Kniazevych, J.H. Saurat, 2,3,7,8-tetrachlorodibenzo-p-dioxin (TCDD) poisoning in Victor Yushchenko: identification and measurement of TCDD metabolites, Lancet 374 (9696) (2009) 1179–1185.
[10] V. Rothhammer, F.J. Quintana, The aryl hydrocarbon receptor: an environmental sensor integrating immune responses in health and disease, Nat. Rev. Immunol. 19 (3) (2019) 184–197.
[11] C.F.A. Vogel, L.S. Van Winkle, C. Esser, T. Haarmann-Stemmann, The aryl hydrocarbon receptor as a target of environmental stressors - Implications for pollution mediated stress and inflammatory responses, Redox Biol. 34 (2020), 101530.
[12] M.N. Avilla, K.M.C. Malecki, M.E. Hahn, R.H. Wilson, C.A. Bradfield, The Ah Receptor: Adaptive Metabolism, Ligand Diversity, and the Xenokine Model, Chem. Res. Toxicol. 33 (4) (2020) 860–879.

[13] Y. Jia, Y. Tao, C. Lv, Y. Xia, Z. Wei, Y. Dai, Tetrandrine enhances the ubiquitination and degradation of Syk through an AhR-c-src-c-Cbl pathway and consequently inhibits osteoclastogenesis and bone destruction in arthritis, Cell Death Dis. 10 (2) (2019) 38.

[14] G. Manni, G. Mondanelli, G. Scalisi, M.T. Pallotta, D. Nardi, E. Padiglioni, R. Romani, V.N. Talesa, P. Puccetti, F. Fallarino, M. Gargaro, Pharmacologic Induction of Endotoxin Tolerance in Dendritic Cells by L-Kynurenine, Front. Immunol. 11 (2020) 292.

[15] A. Paris, N. Tardif, F.M. Baietti, C. Berra, H.M. Leclair, E. Leucci, M.D. Galibert, S. Corre, The AhR-SRC axis as a therapeutic vulnerability in BRAFi-resistant melanoma, EMBO Mol. Med. (2022) e15677.

[16] Y. Shimizu, Y. Nakatsuru, M. Ichinose, Y. Takahashi, H. Kume, J. Mimura, Y. Fujii-Kuriyama, T. Ishikawa, Benzo[a]pyrene carcinogenicity is lost in mice lacking the aryl hydrocarbon receptor, PNAS 97 (2) (2000) 779–782.

[17] Y. Nakatsuru, K. Wakabayashi, Y. Fujii-Kuriyama, T. Ishikawa, K. Kusama, F. Ide, Dibenzo[A, L]pyrene-induced genotoxic and carcinogenic responses are dramatically suppressed in aryl hydrocarbon receptor-deficient mice, Int. J. Cancer 112 (2) (2004) 179–183.

[18] A. Paris, N. Tardif, M.D. Galibert, S. Corre, AhR and Cancer: From Gene Profiling to Targeted Therapy, Int. J. Mol. Sci. 22 (2) (2021).

[19] P. Andersson, J. McGuire, C. Rubio, K. Gradin, M.L. Whitelaw, S. Pettersson, A. Hanberg, L. Poellinger, A constitutively active dioxin/aryl hydrocarbon receptor induces stomach tumors, PNAS 99 (15) (2002) 9990–9995.

[20] I.A. Murray, A.D. Patterson, G.H. Perdew, Aryl hydrocarbon receptor ligands in cancer: Friend and foe, Nat. Rev. Cancer 14 (12) (2014) 801–814.

[21] Y. Fan, G.P. Boivin, E.S. Knudsen, D.W. Nebert, Y. Xia, A. Puga, The aryl hydrocarbon receptor functions as a tumor suppressor of liver carcinogenesis, Cancer Res. 70 (1) (2010) 212–220.

[22] C.A. Opitz, U.M. Litzenburger, F. Sahm, M. Ott, I. Tritschler, S. Trump, T. Schumacher, L. Jestaedt, D. Schrenk, M. Weller, M. Jugold, G.J. Guillemin, C. L. Miller, C. Lutz, B. Radlwimmer, I. Lehmann, A. von Deimling, W. Wick, M. Platten, An endogenous tumour-promoting ligand of the human aryl hydrocarbon receptor, Nature 478 (7368) (2011) 197–203.

[23] Bayer, A First-in-Humans Dose Finding Study for an Aryl Hydrocarbon Receptor Inhibitor (AhRi) in Patients With Advanced Cancer. ClinicalTrials.gov identifier: NCT04069026. Updated August 4. 2022. Accessed August 15, 2022. https://clinicaltrials.gov/ct2/show/NCT04069026.

[24] Ikena Oncology, A Phase 1a/b Study of IK-175 as a Single Agent and in Combination With Nivolumab in Patients With Locally Advanced or Metastatic Solid Tumors and Urothelial Carcinoma. ClinicalTrials.gov Identifier: NCT04200963. Updated February 4, 2022. Accessed August 15, 2022. https://clinicaltrials.gov/ct2/show/NCT04200963.

[25] S. Narasimhan, E. Stanford Zulick, O. Novikov, A.J. Parks, J.J. Schlezinger, Z. Wang, F. Laroche, H. Feng, F. Mulas, S. Monti, D.H. Sherr, Towards Resolving the Pro- and Anti-Tumor Effects of the Aryl Hydrocarbon Receptor, Int. J. Mol. Sci. 19 (5) (2018).

[26] L. Dumoutier, E. Van Roost, G. Ameye, L. Michaux, J.C. Renauld, IL-TIF/IL-22: genomic organization and mapping of the human and mouse genes, Genes Immun. 1 (8) (2000) 488–494.

[27] S.J. Aujla, Y.R. Chan, M. Zheng, M. Fei, D.J. Askew, D.A. Pociask, T.A. Reinhart, F. McAllister, J. Edeal, K. Gaus, S. Husain, J.L. Kreindler, P.J. Dubin, J. M. Pilewski, M.M. Myerburg, C.A. Mason, Y. Iwakura, J.K. Kolls, IL-22 mediates mucosal host defense against Gram-negative bacterial pneumonia, Nat. Med. 14 (3) (2008) 275–281.

[28] K. Wolk, E. Witte, E. Wallace, W.D. Döcke, S. Kunz, K. Asadullah, H.D. Volk, W. Sterry, R. Sabat, IL-22 regulates the expression of genes responsible for antimicrobial defense, cellular differentiation, and mobility in keratinocytes: a potential role in psoriasis, Eur. J. Immunol. 36 (5) (2006) 1309–1323.

[29] K. Wolk, S. Kunz, E. Witte, M. Friedrich, K. Asadullah, R. Sabat, IL-22 increases the innate immunity of tissues, Immunity 21 (2) (2004) 241–254.

[30] B.A. Vorderstrasse, L.B. Steppan, A.E. Silverstone, N.I. Kerkvliet, Aryl hydrocarbon receptor-deficient mice generate normal immune responses to model antigens and are resistant to TCDD-induced immune suppression, Toxicol. Appl. Pharmacol. 171 (3) (2001) 157–164.

[31] Y. Ishihara, S.Y. Kado, K.J. Bein, Y. He, A.A. Pouraryan, A. Urban, T. Haarmann-Stemmann, C. Sweeney, C.F.A. Vogel, Aryl Hydrocarbon Receptor Signaling Synergizes with TLR/NF-kappaB-Signaling for Induction of IL-22 Through Canonical and Non-Canonical AhR Pathways, Front Toxicol 3 (2021), 787360.

[32] C.A. O'Driscoll, J.D. Mezrich, The Aryl Hydrocarbon Receptor as an Immune-Modulator of Atmospheric Particulate Matter-Mediated Autoimmunity, Front. Immunol. 9 (2018) 2833.

[33] J. Wang, Y. Zhao, X. Zhang, W. Tu, R. Wan, Y. Shen, Y. Zhang, R. Trivedi, P. Gao, Type II alveolar epithelial cell aryl hydrocarbon receptor protects against allergic airway inflammation through controlling cell autophagy, Front. Immunol. 13 (2022), 964575.

[34] S.J. Keam, Tapinarof Cream 1%: First Approval, Drugs (2022).

[35] C. Esser, A. Rannug, B. Stockinger, The aryl hydrocarbon receptor in immunity, Trends Immunol. 30 (9) (2009) 447–454.

[36] W. Wang, T. Xiang, Y. Yang, Z. Wang, J. Xie, E3 Ubiquitin Ligases STUB1 Contributes to the Th17/Treg Imbalance via the Ubiquitination of Aryl Hydrocarbon Receptor in Rheumatoid Arthritis, Clin. Exp. Immunol. (2022).

[37] Y. Liu, J. Lv, J. Liu, M. Li, J. Xie, Q. Lv, W. Deng, N. Zhou, Y. Zhou, J. Song, P. Wang, C. Qin, W.M. Tong, B. Huang, Mucus production stimulated by IFN-AhR signaling triggers hypoxia of COVID-19, Cell Res. 30 (12) (2020) 1078–1087.

[38] T. Guarnieri, Hypothesis: Emerging Roles for Aryl Hydrocarbon Receptor in Orchestrating CoV-2-Related Inflammation, Cells 11 (4) (2022).

[39] S.C. Faber, T.S. Lahoti, E.R. Taylor, L. Lewis, J.M. Sapiro, V. Toledo Sales, Y. P. Dragan, B.D. Jeffy, Current Therapeutic Landscape and Safety Roadmap for Targeting the Aryl Hydrocarbon Receptor in Inflammatory Gastrointestinal Indications, Cells 11 (10) (2022).

[40] A.Y. Grishanova, M.L. Perepechaeva, Aryl Hydrocarbon Receptor in Oxidative Stress as a Double Agent and Its Biological and Therapeutic Significance, Int. J. Mol. Sci. 23 (12) (2022).

[41] K. Oda, Y. Matsuoka, A. Funahashi, H. Kitano, A comprehensive pathway map of epidermal growth factor receptor signaling, Mol. Syst. Biol. 1 (2005) (2005) 0010.

[42] P. Wee, Z. Wang, Epidermal Growth Factor Receptor Cell Proliferation Signaling Pathways, Cancers 9 (5) (2017) 52.

[43] K. Shostak, A. Chariot, EGFR and NF-kappaB: partners in cancer, Trends Mol. Med. 21 (6) (2015) 385–393.

[44] V. Ivanovic, I.B. Weinstein, Benzo[a]pyrene and other inducers of cytochrome p 1–450 inhibit binding of epidermal growth factor to cell surface receptors, Carcinogenesis 3 (5) (1982) 505–510.

[45] B.V. Madhukar, D.W. Brewster, F. Matsumura, Effects of in vivo-administered 2,3,7,8-tetrachlorodibenzo-p-dioxin on receptor binding of epidermal growth factor in the hepatic plasma membrane of rat, guinea pig, mouse, and hamster, PNAS 81 (23) (1984) 7407–7411.

[46] S.O. Kärenlampi, H.J. Eisen, O. Hankinson, D.W. Nebert, Effects of cytochrome P1–450 inducers on the cell-surface receptors for epidermal growth factor, phorbol 12,13-dibutyrate, or insulin of cultured mouse hepatoma cells, J. Biol. Chem. 258 (17) (1983) 10378–10383.

[47] L.G. Hudson, W.A. Toscano Jr., W.F. Greenlee, Regulation of epidermal growth factor binding in a human keratinocyte cell line by 2,3,7,8-tetrachlorodibenzo-p-dioxin, Toxicol. Appl. Pharmacol. 77 (2) (1985) 251–259.

[48] C. Vogeley, N.C. Sondermann, S. Woeste, A.A. Momin, V. Gilardino, F. Hartung, M. Heinen, S.K. Maaß, M. Mescher, M. Pollet, K.M. Rolfes, C.F.A. Vogel, A. Rossi, D. Lang, S.T. Arold, M. Nakamura, T. Haarmann-Stemmann, Unraveling the differential impact of PAHs and dioxin-like compounds on AKR1C3 reveals the EGFR extracellular domain as a critical determinant of the AHR response, Environ. Int. 158 (2022).

[49] J.E. Hardesty, L. Al-Eryani, B. Wahlang, K.C. Falkner, H. Shi, J. Jin, B.J. Vivace, B. P. Ceresa, R.A. Prough, M.C. Cave, Epidermal Growth Factor Receptor Signaling Disruption by Endocrine and Metabolic Disrupting Chemicals, Toxicol. Sci. 162 (2) (2018) 622–634.

[50] R.D. Patel, D.J. Kim, J.M. Peters, G.H. Perdew, The aryl hydrocarbon receptor directly regulates expression of the potent mitogen epiregulin, Toxicol. Sci. 89 (1) (2006) 75–82.

[51] K. John, T.S. Lahoti, K. Wagner, J.M. Hughes, G.H. Perdew, The Ah receptor regulates growth factor expression in head and neck squamous cell carcinoma cell lines, Mol. Carcinog. 53 (10) (2014) 765–776.

[52] B. Du, N.K. Altorki, L. Kopelovich, K. Subbaramaiah, A.J. Dannenberg, Tobacco smoke stimulates the transcription of amphiregulin in human oral epithelial cells: evidence of a cyclic AMP-responsive element binding protein-dependent mechanism, Cancer Res. 65 (13) (2005) 5982–5988.

[53] H. Lemjabbar, D. Li, M. Gallup, S. Sidhu, E. Drori, C. Basbaum, Tobacco smoke-induced lung cell proliferation mediated by tumor necrosis factor alpha-converting enzyme and amphiregulin, J. Biol. Chem. 278 (28) (2003) 26202–26207.

[54] C.H. Sutter, H. Yin, Y. Li, J.S. Mammen, S. Bodreddigari, G. Stevens, J.A. Cole, T. R. Sutter, EGF receptor signaling blocks aryl hydrocarbon receptor-mediated transcription and cell differentiation in human epidermal keratinocytes, Proc. Natl. Acad. Sci. 106(11) (2009) 4266-4271.

[55] A. Joiakim, P.A. Mathieu, C. Shelp, J. Boerner, J.J. Reiners Jr., Epidermal Growth Factor Receptor Kinase Inhibitors Synergize with TCDD to Induce CYP1A1/1A2 in Human Breast Epithelial MCF10A Cells, Drug Metab. Dispos. 44 (5) (2016) 665–671.

[56] J. Shao, S.B. Lee, H. Guo, B.M. Evers, H. Sheng, Prostaglandin E2 stimulates the growth of colon cancer cells via induction of amphiregulin, Cancer Res. 63 (17) (2003) 5218–5223.

[57] J.W. Davis Jr., A.D. Burdick, F.T. Lauer, S.W. Burchiel, The aryl hydrocarbon receptor antagonist, 3'methoxy-4'nitroflavone, attenuates 2,3,7,8-tetrachlorodibenzo-p-dioxin-dependent regulation of growth factor signaling and apoptosis in the MCF-10A cell line, Toxicol. Appl. Pharmacol. 188 (1) (2003) 42–49.

[58] E. Fritsche, C. Schäfer, C. Calles, T. Bernsmann, T. Bernshausen, M. Wurm, U. Hübenthal, J.E. Cline, H. Hajimiragha, P. Schroeder, L.O. Klotz, A. Rannug, P. Fürst, H. Hanenberg, J. Abel, J. Krutmann, Lightening up the UV response by identification of the arylhydrocarbon receptor as a cytoplasmatic target for ultraviolet B radiation, PNAS 104 (21) (2007) 8851–8856.

[59] L. Bergander, E. Wincent, A. Rannug, M. Foroozesh, W. Alworth, U. Rannug, Metabolic fate of the Ah receptor ligand 6-formylindolo[3,2-b]carbazole, Chem. Biol. Interact. 149 (2–3) (2004) 151–164.

[60] J. Tigges, T. Haarmann-Stemmann, C.F.A. Vogel, A. Grindel, U. Hubenthal, H. Brenden, S. Grether-Beck, G. Vielhaber, W. Johncock, J. Krutmann, E. Fritsche, The new aryl hydrocarbon receptor antagonist E/Z-2-benzylindene-5,6-dimethoxy-3,3-dimethylindan-1-one protects against UVB-induced signal transduction, J, Invest. Dermatol. 134 (2) (2014) 556–559.

[61] K. Frauenstein, U. Sydlik, J. Tigges, M. Majora, C. Wiek, H. Hanenberg, J. Abel, C. Esser, E. Fritsche, J. Krutmann, T. Haarmann-Stemmann, Evidence for a novel anti-apoptotic pathway in human keratinocytes involving the aryl hydrocarbon receptor, E2F1, and checkpoint kinase 1, Cell Death Differ. 20 (10) (2013) 1425–1434.

[62] M. Pollet, S. Shaik, M. Mescher, K. Frauenstein, J. Tigges, S.A. Braun, K. Sondenheimer, M. Kaveh, A. Bruhs, S. Meller, B. Homey, A. Schwarz, C. Esser, T. Douki, C.F.A. Vogel, J. Krutmann, T. Haarmann-Stemmann, The AHR represses nucleotide excision repair and apoptosis and contributes to UV-induced skin carcinogenesis, Cell Death Differ. 25 (10) (2018) 1823–1836.
[63] Y. Ono, K. Torii, E. Fritsche, Y. Shintani, E. Nishida, M. Nakamura, Y. Shirakata, T. Haarmann-Stemmann, J. Abel, J. Krutmann, A. Morita, Role of the aryl hydrocarbon receptor in tobacco smoke extract-induced matrix metalloproteinase-1 expression, Exp. Dermatol. 22 (5) (2013) 349–353.
[64] C. Lahmann, J. Bergemann, G. Harrison, A.R. Young, Matrix metalloproteinase-1 and skin ageing in smokers, Lancet 357 (9260) (2001) 935–936.
[65] H. Tanaka, Y. Ono, S. Nakata, Y. Shintani, N. Sakakibara, A. Morita, Tobacco smoke extract induces premature skin aging in mouse, J. Dermatol. Sci. 46 (1) (2007) 69–71.
[66] K. Wang, J. Zheng, J. Yu, Y. Wu, J. Guo, Z. Xu, X. Sun, Knockdown of MMP-1 inhibits the progression of colorectal cancer by suppressing the PI3K/Akt/c-myc signaling pathway and EMT, Oncol. Rep. 43 (4) (2020) 1103–1112.
[67] H.R. Ancha, R.R. Kurella, C.A. Stewart, G. Damera, B.P. Ceresa, R.F. Harty, Histamine stimulation of MMP-1(collagenase-1) secretion and gene expression in gastric epithelial cells: role of EGFR transactivation and the MAP kinase pathway, Int. J. Biochem. Cell Biol. 39 (11) (2007) 2143–2152.
[68] Y. Sun, X. Miao, L. Zhu, J. Liu, Y. Lin, G. Xiang, X. Wu, X. Wang, Z. Ni, S. Li, Autocrine TGF-alpha is associated with Benzo(a)pyrene-induced mucus production and MUC5AC expression during allergic asthma, Ecotoxicol. Environ. Saf. 241 (2022), 113833.
[69] J.V. Fahy, B.F. Dickey, Airway mucus function and dysfunction, N. Engl. J. Med. 363 (23) (2010) 2233–2247.
[70] L.R. Bonser, L. Zlock, W. Finkbeiner, D.J. Erle, Epithelial tethering of MUC5AC-rich mucus impairs mucociliary transport in asthma, J. Clin. Invest. 126 (6) (2016) 2367–2371.
[71] A.V. Villarino, Y. Kanno, J.J. O'Shea, Mechanisms and consequences of Jak-STAT signaling in the immune system, Nat. Immunol. 18 (4) (2017) 374–384.
[72] A. Salas, C. Hernandez-Rocha, M. Duijvestein, W. Faubion, D. McGovern, S. Vermeire, S. Vetrano, N. Vande Casteele, JAK-STAT pathway targeting for the treatment of inflammatory bowel disease, Nat. Rev. Gastroenterol. Hepatol. 17 (6) (2020) 323–337.
[73] K. Welsch, J. Holstein, A. Laurence, K. Ghoreschi, Targeting JAK/STAT signalling in inflammatory skin diseases with small molecule inhibitors, Eur. J. Immunol. 47 (7) (2017) 1096–1107.
[74] D.M. Schwartz, M. Bonelli, M. Gadina, J.J. O'Shea, Type I/II cytokines, JAKs, and new strategies for treating autoimmune diseases, Nat. Rev. Rheumatol. 12 (1) (2016) 25–36.
[75] H.T. Tzeng, I.T. Chyuan, J.H. Lai, Targeting the JAK-STAT pathway in autoimmune diseases and cancers: A focus on molecular mechanisms and therapeutic potential, Biochem. Pharmacol. 193 (2021), 114760.
[76] M. Nukaya, Y. Takahashi, F.J. Gonzalez, T. Kamataki, Aryl hydrocarbon receptor-mediated suppression of GH receptor and Janus kinase 2 expression in mice, FEBS Lett. 558 (1–3) (2004) 96–100.
[77] H. Takanaga, T. Yoshitake, E. Yatabe, S. Hara, M. Kunimoto, Beta-naphthoflavone disturbs astrocytic differentiation of C6 glioma cells by inhibiting autocrine interleukin-6, J. Neurochem. 90 (3) (2004) 750–757.
[78] M.S. Jeon, C. Esser, The murine IL-2 promoter contains distal regulatory elements responsive to the Ah receptor, a member of the evolutionarily conserved bHLH-PAS transcription factor family, J. Immunol. 165 (12) (2000) 6975–6983.
[79] L. Apetoh, F.J. Quintana, C. Pot, N. Joller, S. Xiao, D. Kumar, E.J. Burns, D. H. Sherr, H.L. Weiner, V.K. Kuchroo, The aryl hydrocarbon receptor interacts with c-Maf to promote the differentiation of type 1 regulatory T cells induced by IL-27, Nat. Immunol. 11 (9) (2010) 854–861.
[80] B.D. Hollingshead, T.V. Beischlag, B.C. Dinatale, P. Ramadoss, G.H. Perdew, Inflammatory signaling and aryl hydrocarbon receptor mediate synergistic induction of interleukin 6 in MCF-7 cells, Cancer Res. 68 (10) (2008) 3609–3617.
[81] J. Zhu, L. Luo, L. Tian, S. Yin, X. Ma, S. Cheng, W. Tang, J. Yu, W. Ma, X. Zhou, X. Fan, X. Yang, J. Yan, X. Xu, C. Lv, H. Liang, Aryl Hydrocarbon Receptor Promotes IL-10 Expression in Inflammatory Macrophages Through Src-STAT3 Signaling Pathway, Front. Immunol. 9 (2018) 2033.
[82] B.C. DiNatale, I.A. Murray, J.C. Schroeder, C.A. Flaveny, T.S. Lahoti, E. M. Laurenzana, C.J. Omiecinski, G.H. Perdew, Kynurenic acid is a potent endogenous aryl hydrocarbon receptor ligand that synergistically induces interleukin-6 in the presence of inflammatory signaling, Toxicol. Sci. 115 (1) (2010) 89–97.
[83] B.A. Jensen, R.J. Leeman, J.J. Schlezinger, D.H. Sherr, Aryl hydrocarbon receptor (AhR) agonists suppress interleukin-6 expression by bone marrow stromal cells: an immunotoxicology study, Environ. Health 2 (1) (2003) 16.
[84] Y. Ishihara, T. Haarmann-Stemmann, N.Y. Kado, C.F.A. Vogel, Interleukin 33 Expression Induced by Aryl Hydrocarbon Receptor in Macrophages, Toxicol. Sci. 170 (2) (2019) 404–414.
[85] G. Tsuji, A. Hashimoto-Hachiya, V.H. Yen, S. Miake, M. Takemura, Y. Mitamura, T. Ito, M. Murata, M. Furue, T. Nakahara, Aryl Hydrocarbon Receptor Activation Downregulates IL-33 Expression in Keratinocytes via Ovo-Like 1, J. Clin. Med. 9 (3) (2020).
[86] N. Stobbe-Maicherski, S. Wolff, C. Wolff, J. Abel, U. Sydlik, K. Frauenstein, T. Haarmann-Stemmann, The interleukin-6-type cytokine oncostatin M induces aryl hydrocarbon receptor expression in a STAT3-dependent manner in human HepG2 hepatoma cells, FEBS J. 280 (24) (2013) 6681–6690.
[87] I.D. Mascanfroni, M.C. Takenaka, A. Yeste, B. Patel, Y. Wu, J.E. Kenison, S. Siddiqui, A.S. Basso, L.E. Otterbein, D.M. Pardoll, F. Pan, A. Priel, C.B. Clish, S. C. Robson, F.J. Quintana, Metabolic control of type 1 regulatory T cell differentiation by AHR and HIF1-alpha, Nat. Med. 21 (6) (2015) 638–646.
[88] V. Rothhammer, I.D. Mascanfroni, L. Bunse, M.C. Takenaka, J.E. Kenison, L. Mayo, C.C. Chao, B. Patel, R. Yan, M. Blain, J.I. Alvarez, H. Kebir, N. Anandasabapathy, G. Izquierdo, S. Jung, N. Obholzer, N. Pochet, C.B. Clish, M. Prinz, A. Prat, J. Antel, F.J. Quintana, Type I interferons and microbial metabolites of tryptophan modulate astrocyte activity and central nervous system inflammation via the aryl hydrocarbon receptor, Nat. Med. 22 (6) (2016) 586–597.
[89] G. Tanaka, S. Kanaji, A. Hirano, K. Arima, A. Shinagawa, C. Goda, S. Yasunaga, K. Ikizawa, Y. Yanagihara, M. Kubo, Y. Kuriyama-Fujii, Y. Sugita, A. Inokuchi, K. Izuhara, Induction and activation of the aryl hydrocarbon receptor by IL-4 in B cells, Int. Immunol. 17 (6) (2005) 797–805.
[90] C.G. Atene, S. Fiorcari, N. Mesini, S. Alboni, S. Martinelli, M. Maccaferri, G. Leonardi, L. Potenza, M. Luppi, R. Maffei, R. Marasca, Indoleamine 2, 3-Dioxygenase 1 Mediates Survival Signals in Chronic Lymphocytic Leukemia via Kynurenine/Aryl Hydrocarbon Receptor-Mediated MCL1 Modulation, Front. Immunol. 13 (2022), 832263.
[91] M. Platten, E.A.A. Nollen, U.F. Rohrig, F. Fallarino, C.A. Opitz, Tryptophan metabolism as a common therapeutic target in cancer, neurodegeneration and beyond, Nat. Rev. Drug Discov. 18 (5) (2019) 379–401.
[92] J.D. Mezrich, J.H. Fechner, X. Zhang, B.P. Johnson, W.J. Burlingham, C. A. Bradfield, An interaction between kynurenine and the aryl hydrocarbon receptor can generate regulatory T cells, J. Immunol. 185 (6) (2010) 3190–3198.
[93] O. Novikov, Z. Wang, E.A. Stanford, A.J. Parks, A. Ramirez-Cardenas, E. Landesman, I. Laklouk, C. Sarita-Reyes, D. Gusenleitner, A. Li, S. Monti, S. Manteiga, K. Lee, D.H. Sherr, An Aryl Hydrocarbon Receptor-Mediated Amplification Loop That Enforces Cell Migration in ER-/PR-/Her2- Human Breast Cancer Cells, Mol. Pharmacol. 90 (5) (2016) 674–688.
[94] C.J. Funatake, N.B. Marshall, L.B. Steppan, D.V. Mourich, N.I. Kerkvliet, Cutting edge: activation of the aryl hydrocarbon receptor by 2,3,7,8-tetrachlorodibenzo-p-dioxin generates a population of CD4+ CD25+ cells with characteristics of regulatory T cells, J. Immunol. 175 (7) (2005) 4184–4188.
[95] F.J. Quintana, A.S. Basso, A.H. Iglesias, T. Korn, M.F. Farez, E. Bettelli, M. Caccamo, M. Oukka, H.L. Weiner, Control of T(reg) and T(H)17 cell differentiation by the aryl hydrocarbon receptor, Nature 453 (7191) (2008) 65–71.
[96] U.M. Litzenburger, C.A. Opitz, F. Sahm, K.J. Rauschenbach, S. Trump, M. Winter, M. Ott, K. Ochs, C. Lutz, X. Liu, N. Anastasov, I. Lehmann, T. Hofer, A. von Deimling, W. Wick, M. Platten, Constitutive IDO expression in human cancer is sustained by an autocrine signaling loop involving IL-6, STAT3 and the AHR, Oncotarget 5 (4) (2014) 1038–1051.
[97] Y. Liu, N. Zhou, L. Zhou, J. Wang, Y. Zhou, T. Zhang, Y. Fang, J. Deng, Y. Gao, X. Liang, J. Lv, Z. Wang, J. Xie, Y. Xue, H. Zhang, J. Ma, K. Tang, Y. Fang, F. Cheng, C. Zhang, B. Dong, Y. Zhao, P. Yuan, Q. Gao, H. Zhang, F. Xiao-Feng Qin, B. Huang, IL-2 regulates tumor-reactive CD8(+) T cell exhaustion by activating the aryl hydrocarbon receptor, Nat. Immunol. 22 (3) (2021) 358–369.
[98] A. Kimura, T. Naka, T. Nakahama, I. Chinen, K. Masuda, K. Nohara, Y. Fujii-Kuriyama, T. Kishimoto, Aryl hydrocarbon receptor in combination with Stat1 regulates LPS-induced inflammatory responses, J. Exp. Med. 206 (9) (2009) 2027–2035.
[99] K. Masuda, A. Kimura, H. Hanieh, N.T. Nguyen, T. Nakahama, I. Chinen, Y. Otoyo, T. Murotani, A. Yamatodani, T. Kishimoto, Aryl hydrocarbon receptor negatively regulates LPS-induced IL-6 production through suppression of histamine production in macrophages, Int. Immunol. 23 (10) (2011) 637–645.
[100] A. Kimura, T. Naka, K. Nohara, Y. Fujii-Kuriyama, T. Kishimoto, Aryl hydrocarbon receptor regulates Stat1 activation and participates in the development of Th17 cells, PNAS 105 (28) (2008) 9721–9726.
[101] X. Liu, H. Hu, H. Fan, D. Zuo, Z. Shou, Y. Liao, Z. Nan, Q. Tang, The role of STAT3 and AhR in the differentiation of CD4+ T cells into Th17 and Treg cells, Medicine (Baltimore) 96 (17) (2017) e6615.
[102] S.M. Lee, C.E. Kim, H.Y. Park, E.H. Yoon, H.J. Won, J.M. Ahn, N.Z.N. Nguyen, M. Kim, W.H. Jang, W.S. Lee, M.S. Kang, M. Jeong, H. Yun, S. Park, S. Wu, D. H. Kim, B. Kwon, S.K. Seo, Aryl hydrocarbon receptor-targeted therapy for CD4+ T cell-mediated idiopathic pneumonia syndrome in mice, Blood 139 (22) (2022) 3325–3339.
[103] M. Veldhoen, K. Hirota, A.M. Westendorf, J. Buer, L. Dumoutier, J.C. Renauld, B. Stockinger, The aryl hydrocarbon receptor links TH17-cell-mediated autoimmunity to environmental toxins, Nature 453 (7191) (2008) 106–109.
[104] A.K. Ehrlich, J.M. Pennington, W.H. Bisson, S.K. Kolluri, N.I. Kerkvliet, TCDD, FICZ, and Other High Affinity AhR Ligands Dose-Dependently Determine the Fate of CD4+ T Cell Differentiation, Toxicol. Sci. 161 (2) (2018) 310–320.
[105] Y. Liu, X. Liang, X. Yin, J. Lv, K. Tang, J. Ma, T. Ji, H. Zhang, W. Dong, X. Jin, D. Chen, Y. Li, S. Zhang, H.Q. Xie, B. Zhao, T. Zhao, J. Lu, Z.W. Hu, X. Cao, F. X. Qin, B. Huang, Blockade of IDO-kynurenine-AhR metabolic circuitry abrogates IFN-gamma-induced immunologic dormancy of tumor-repopulating cells, Nat. Commun. 8 (2017) 15207.
[106] S.K. Kolluri, C. Weiss, A. Koff, M. Gottlicher, p27(Kip1) induction and inhibition of proliferation by the intracellular Ah receptor in developing thymus and hepatoma cells, Genes Dev. 13 (13) (1999) 1742–1753.
[107] J.E. Kenison, Z. Wang, K. Yang, M. Snyder, F.J. Quintana, D.H. Sherr, The aryl hydrocarbon receptor suppresses immunity to oral squamous cell carcinoma through immune checkpoint regulation, PNAS 118 (19) (2021).
[108] M.C. Takenaka, G. Gabriely, V. Rothhammer, I.D. Mascanfroni, M.A. Wheeler, C. C. Chao, C. Gutierrez-Vazquez, J. Kenison, E.C. Tjon, A. Barroso, T. Vandeventer, K.A. de Lima, S. Rothweiler, L. Mayo, S. Ghannam, S. Zandee, L. Healy, D. Sherr,

M.F. Farez, A. Prat, J. Antel, D.A. Reardon, H. Zhang, S.C. Robson, G. Getz, H. L. Weiner, F.J. Quintana, Control of tumor-associated macrophages and T cells in glioblastoma via AHR and CD39, Nat. Neurosci. 22 (5) (2019) 729–740.
[109] K. Nakajima, Y. Maekawa, K. Kataoka, C. Ishifune, J. Nishida, H. Arimochi, A. Kitamura, T. Yoshimoto, S. Tomita, S. Nagahiro, K. Yasutomo, The ARNT-STAT3 axis regulates the differentiation of intestinal intraepithelial TCRalphabeta (+)CD8alphaalpha(+) cells, Nat. Commun. 4 (2013) 2112.
[110] S. Mitchell, J. Vargas, A. Hoffmann, Signaling via the NFkappaB system, Wiley Interdiscip. Rev. Syst. Biol. Med. 8 (3) (2016) 227–241.
[111] K. Taniguchi, M. Karin, NF-kappaB, inflammation, immunity and cancer: coming of age, Nat. Rev. Immunol. 18 (5) (2018) 309–324.
[112] F. Matsumura, C.F. Vogel, Evidence supporting the hypothesis that one of the main functions of the aryl hydrocarbon receptor is mediation of cell stress responses, Biol. Chem. 387 (9) (2006) 1189–1194.
[113] M. Son, A.G. Wang, H.L. Tu, M.O. Metzig, P. Patel, K. Husain, J. Lin, A. Murugan, A. Hoffmann, S. Tay, NF-kappaB responds to absolute differences in cytokine concentrations, Sci. Signal. 14 (666) (2021).
[114] P. Ghezzi, B. Saccardo, M. Bianchi, Recombinant tumor necrosis factor depresses cytochrome P450-dependent microsomal drug metabolism in mice, Biochem. Biophys. Res. Commun. 136 (1) (1986) 316–321.
[115] C.W. Barker, J.B. Fagan, D.S. Pasco, Interleukin-1 beta suppresses the induction of P4501A1 and P4501A2 mRNAs in isolated hepatocytes, J. Biol. Chem. 267 (12) (1992) 8050–8055.
[116] Y. Fukuda, N. Ishida, T. Noguchi, A. Kappas, S. Sassa, Interleukin-6 down regulates the expression of transcripts encoding cytochrome P450 IA1, IA2 and IIIA3 in human hepatoma cells, Biochem. Biophys. Res. Commun. 184 (2) (1992) 960–965.
[117] Y. Tian, S. Ke, M.S. Denison, A.B. Rabson, M.A. Gallo, Ah receptor and NF-kappaB interactions, a potential mechanism for dioxin toxicity, J. Biol. Chem. 274 (1) (1999) 510–515.
[118] S. Ke, A.B. Rabson, J.F. Germino, M.A. Gallo, Y. Tian, Mechanism of suppression of cytochrome P-450 1A1 expression by tumor necrosis factor-alpha and lipopolysaccharide, J. Biol. Chem. 276 (43) (2001) 39638–39644.
[119] B.C. DiNatale, J.C. Schroeder, L.J. Francey, A. Kusnadi, G.H. Perdew, Mechanistic insights into the events that lead to synergistic induction of interleukin 6 transcription upon activation of the aryl hydrocarbon receptor and inflammatory signaling, J. Biol. Chem. 285 (32) (2010) 24388–24397.
[120] H. Sekine, J. Mimura, M. Oshima, H. Okawa, J. Kanno, K. Igarashi, F.J. Gonzalez, T. Ikuta, K. Kawajiri, Y. Fujii-Kuriyama, Hypersensitivity of aryl hydrocarbon receptor-deficient mice to lipopolysaccharide-induced septic shock, Mol. Cell Biol. 29 (24) (2009) 6391–6400.
[121] N.P. Singh, M. Nagarkatti, P.S. Nagarkatti, Role of dioxin response element and nuclear factor-kappaB motifs in 2,3,7,8-tetrachlorodibenzo-p-dioxin-mediated regulation of Fas and Fas ligand expression, Mol. Pharmacol. 71 (1) (2007) 145–157.
[122] D.W. Kim, L. Gazourian, S.A. Quadri, R. Romieu-Mourez, D.H. Sherr, G. E. Sonenshein, The RelA NF-kappaB subunit and the aryl hydrocarbon receptor (AhR) cooperate to transactivate the c-myc promoter in mammary cells, Oncogene 19 (48) (2000) 5498–5506.
[123] I.A. Camacho, N. Singh, V.L. Hegde, M. Nagarkatti, P.S. Nagarkatti, Treatment of mice with 2,3,7,8-tetrachlorodibenzo-p-dioxin leads to aryl hydrocarbon receptor-dependent nuclear translocation of NF-kappaB and expression of Fas ligand in thymic stromal cells and consequent apoptosis in T cells, J. Immunol. 175 (1) (2005) 90–103.
[124] C.E. Sulentic, J.S. Kang, Y.J. Na, N.E. Kaminski, Interactions at a dioxin responsive element (DRE) and an overlapping kappaB site within the hs4 domain of the 3'alpha immunoglobulin heavy chain enhancer, Toxicology 200 (2–3) (2004) 235–246.
[125] R.D. Patel, I.A. Murray, C.A. Flaveny, A. Kusnadi, G.H. Perdew, Ah receptor represses acute-phase response gene expression without binding to its cognate response element, Lab. Invest. 89 (6) (2009) 695–707.
[126] A. Puga, S.J. Barnes, C. Chang, H. Zhu, K.P. Nephew, S.A. Khan, H.G. Shertzer, Activation of transcription factors activator protein-1 and nuclear factor-kappaB by 2,3,7,8-tetrachlorodibenzo-p-dioxin, Biochem. Pharmacol. 59 (8) (2000) 997–1005.
[127] J. Suh, Y.J. Jeon, H.M. Kim, J.S. Kang, N.E. Kaminski, K.H. Yang, Aryl hydrocarbon receptor-dependent inhibition of AP-1 activity by 2,3,7,8-tetra-chlorodibenzo-p-dioxin in activated B cells, Toxicol. Appl. Pharmacol. 181 (2) (2002) 116–123.
[128] C.F. Vogel, E. Sciullo, F. Matsumura, Involvement of RelB in aryl hydrocarbon receptor-mediated induction of chemokines, Biochem. Biophys. Res. Commun. 363 (3) (2007) 722–726.
[129] J. Bankoti, B. Rase, T. Simones, D.M. Shepherd, Functional and phenotypic effects of AhR activation in inflammatory dendritic cells, Toxicol. Appl. Pharmacol. 246 (1–2) (2010) 18–28.
[130] B. Memari, M. Bouttier, V. Dimitrov, M. Ouellette, M.A. Behr, J.H. Fritz, J. H. White, Engagement of the Aryl Hydrocarbon Receptor in Mycobacterium tuberculosis-Infected Macrophages Has Pleiotropic Effects on Innate Immune Signaling, J. Immunol. 195 (9) (2015) 4479–4491.
[131] R.L. Salisbury, C.E. Sulentic, The AhR and NF-kappaB/Rel Proteins Mediate the Inhibitory Effect of 2,3,7,8-Tetrachlorodibenzo-p-Dioxin on the 3' Immunoglobulin Heavy Chain Regulatory Region, Toxicol. Sci. 148 (2) (2015) 443–459.
[132] C.F. Vogel, E. Sciullo, W. Li, P. Wong, G. Lazennec, F. Matsumura, RelB, a new partner of aryl hydrocarbon receptor-mediated transcription, Mol. Endocrinol. 21 (12) (2007) 2941–2955.
[133] G. Bonizzi, M. Bebien, D.C. Otero, K.E. Johnson-Vroom, Y. Cao, D. Vu, A.G. Jegga, B.J. Aronow, G. Ghosh, R.C. Rickert, M. Karin, Activation of IKKalpha target genes depends on recognition of specific kappaB binding sites by RelB:p52 dimers, EMBO J. 23 (21) (2004) 4202–4210.
[134] C.F. Vogel, S.R. Goth, B. Dong, I.N. Pessah, F. Matsumura, Aryl hydrocarbon receptor signaling mediates expression of indoleamine 2,3-dioxygenase, Biochem. Biophys. Res. Commun. 375 (3) (2008) 331–335.
[135] C.F. Vogel, D. Wu, S.R. Goth, J. Baek, A. Lollies, R. Domhardt, A. Grindel, I. N. Pessah, Aryl hydrocarbon receptor signaling regulates NF-kappaB RelB activation during dendritic-cell differentiation, Immunol. Cell Biol. 91 (9) (2013) 568–575.
[136] C.F. Vogel, W.L. Chang, S. Kado, K. McCulloh, H. Vogel, D. Wu, T. Haarmann-Stemmann, G. Yang, P.S. Leung, F. Matsumura, M.E. Gershwin, Transgenic Overexpression of Aryl Hydrocarbon Receptor Repressor (AhRR) and AhR-Mediated Induction of CYP1A1, Cytokines, and Acute Toxicity, Environ Health Perspect 124 (7) (2016) 1071–1083.
[137] D.C. Ranatunga, A. Ramakrishnan, P. Uprety, F. Wang, H. Zhang, J.B. Margolick, C. Brayton, J.H. Bream, A protective role for human IL-10-expressing CD4+ T cells in colitis, J. Immunol. 189 (3) (2012) 1243–1252.
[138] J.M. Benson, D.M. Shepherd, Aryl hydrocarbon receptor activation by TCDD reduces inflammation associated with Crohn's disease, Toxicol. Sci. 120 (1) (2011) 68–78.
[139] S. Kado, W.L.W. Chang, A.N. Chi, M. Wolny, D.M. Shepherd, C.F.A. Vogel, Aryl hydrocarbon receptor signaling modifies Toll-like receptor-regulated responses in human dendritic cells, Arch. Toxicol. 91 (5) (2017) 2209–2221.
[140] O. Dominguez-Acosta, L. Vega, E. Estrada-Muniz, M.S. Rodriguez, F.J. Gonzalez, G. Elizondo, Activation of aryl hydrocarbon receptor regulates the LPS/IFNgamma-induced inflammatory response by inducing ubiquitin-proteosomal and lysosomal degradation of RelA/p65, Biochem. Pharmacol. 155 (2018) 141–149.
[141] C.W. Wright, C.S. Duckett, The aryl hydrocarbon nuclear translocator alters CD30-mediated NF-kappaB-dependent transcription, Science 323 (5911) (2009) 251–255.
[142] C.F.A. Vogel, T. Haarmann-Stemmann, The aryl hydrocarbon receptor repressor - More than a simple feedback inhibitor of AhR signaling: Clues for its role in inflammation and cancer, Curr Opin Toxicol 2 (2017) 109–119.
[143] C.F.A. Vogel, Y. Ishihara, C.E. Campbell, S.Y. Kado, A. Nguyen-Chi, C. Sweeney, M. Pollet, T. Haarmann-Stemmann, J.M. Tuscano, A Protective Role of Aryl Hydrocarbon Receptor Repressor in Inflammation and Tumor Growth, Cancers (Basel) 11 (5) (2019).
[144] C.F.A. Vogel, G. Lazennec, S.Y. Kado, C. Dahlem, Y. He, A. Castaneda, Y. Ishihara, C. Vogeley, A. Rossi, T. Haarmann-Stemmann, J. Jugan, H. Mori, A.D. Borowsky, M.A. La Merrill, C. Sweeney, Targeting the Aryl Hydrocarbon Receptor Signaling Pathway in Breast Cancer Development, Front. Immunol. 12 (2021), 625346.
[145] J. Ovrevik, M. Lag, V. Lecureur, D. Gilot, D. Lagadic-Gossmann, M. Refsnes, P. E. Schwarze, T. Skuland, R. Becher, J.A. Holme, AhR and Arnt differentially regulate NF-kappaB signaling and chemokine responses in human bronchial epithelial cells, Cell Commun. Signal 12 (2014) 48.
[146] C.A. Beamer, B.P. Seaver, D.M. Shepherd, Aryl hydrocarbon receptor (AhR) regulates silica-induced inflammation but not fibrosis, Toxicol. Sci. 126 (2) (2012) 554–568.
[147] T.H. Thatcher, S.B. Maggirwar, C.J. Baglole, H.F. Lakatos, T.A. Gasiewicz, R. P. Phipps, P.J. Sime, Aryl hydrocarbon receptor-deficient mice develop heightened inflammatory responses to cigarette smoke and endotoxin associated with rapid loss of the nuclear factor-kappaB component RelB, Am. J. Pathol. 170 (3) (2007) 855–864.
[148] G.E. Muku, T.S. Lahoti, I.A. Murray, M.A. Podolsky, K.J. Smith, T.D. Hubbard, G. Kuzu, K. Gowda, S.G. Amin, G.H. Perdew, Ligand-mediated cytoplasmic retention of the Ah receptor inhibits macrophage-mediated acute inflammatory responses, Lab. Invest. 97 (12) (2017) 1471–1487.
[149] E. Wirthgen, A. Hoeflich, Endotoxin-Induced Tryptophan Degradation along the Kynurenine Pathway: The Role of Indolamine 2,3-Dioxygenase and Aryl Hydrocarbon Receptor-Mediated Immunosuppressive Effects in Endotoxin Tolerance and Cancer and Its Implications for Immunoparalysis, J. Amino Acids 2015 (2015), 973548.
[150] Y. Ishihara, S.Y. Kado, C. Hoeper, S. Harel, C.F.A. Vogel, Role of NF-kB RelB in Aryl Hydrocarbon Receptor-Mediated Ligand Specific Effects, Int. J. Mol. Sci. 20 (11) (2019).
[151] D. Wu, W. Li, P. Lok, F. Matsumura, C.F. Vogel, AhR deficiency impairs expression of LPS-induced inflammatory genes in mice, Biochem. Biophys. Res. Commun. 410 (2) (2011) 358–363.
[152] M. Tsuji, C.F. Vogel, C. Koriyama, S. Akiba, T. Katoh, T. Kawamoto, F. Matsumura, Association of serum levels of polychlorinated biphenyls with IL-8 mRNA expression in blood samples from asthmatic and non-asthmatic Japanese children, Chemosphere 87 (11) (2012) 1228–1234.
[153] T.S. Lahoti, J.A. Boyer, A. Kusnadi, G.E. Muku, I.A. Murray, G.H. Perdew, Aryl Hydrocarbon Receptor Activation Synergistically Induces Lipopolysaccharide-Mediated Expression of Proinflammatory Chemokine (c-c motif) Ligand 20, Toxicol. Sci. 148 (1) (2015) 229–240.
[154] N. Ishihara, T. Okuda, H. Hagino, A. Oguro, Y. Tani, H. Okochi, C. Tokoro, Y. Fujii-Kuriyama, K. Itoh, C.F.A. Vogel, Y. Ishihara, Involvement of polycyclic aromatic hydrocarbons and endotoxin in macrophage expression of interleukin-33 induced by exposure to particulate matter, J. Toxicol. Sci. 47 (5) (2022) 201–210.
[155] C.F. Vogel, E.M. Khan, P.S. Leung, M.E. Gershwin, W.L. Chang, D. Wu, T. Haarmann-Stemmann, A. Hoffmann, M.S. Denison, Cross-talk between aryl

hydrocarbon receptor and the inflammatory response: a role for nuclear factor-kappaB, J. Biol. Chem. 289 (3) (2014) 1866–1875.
[156] R.S. Marcus, M.P. Holsapple, N.E. Kaminski, Lipopolysaccharide activation of murine splenocytes and splenic B cells increased the expression of aryl hydrocarbon receptor and aryl hydrocarbon receptor nuclear translocator, J. Pharmacol. Exp. Ther. 287 (3) (1998) 1113–1118.
[157] L.L. Allan, D.H. Sherr, Constitutive activation and environmental chemical induction of the aryl hydrocarbon receptor/transcription factor in activated human B lymphocytes, Mol. Pharmacol. 67 (5) (2005) 1740–1750.
[158] U.M. Zanger, M. Schwab, Cytochrome P450 enzymes in drug metabolism: regulation of gene expression, enzyme activities, and impact of genetic variation, Pharmacol. Ther. 138 (1) (2013) 103–141.
[159] M. Mescher, T. Haarmann-Stemmann, Modulation of CYP1A1 metabolism: From adverse health effects to chemoprevention and therapeutic options, Pharmacol. Ther. 187 (2018) 71–87.
[160] D.W. Nebert, K. Wikvall, W.L. Miller, Human cytochromes P450 in health and disease, Philos. Trans. R. Soc. Lond. B Biol. Sci. 368 (1612) (2013) 20120431.
[161] R.L.I. Crake, M.R. Strother, E. Phillips, M.P. Doogue, M. Zhang, C.M.A. Frampton, B.A. Robinson, M.J. Currie, Influence of serum inflammatory cytokines on cytochrome P450 drug metabolising activity during breast cancer chemotherapy: a patient feasibility study, Sci. Rep. 11 (1) (2021) 5648.
[162] M. Mescher, J. Tigges, K.M. Rolfes, A.L. Shen, J.S. Yee, C. Vogeley, J. Krutmann, C.A. Bradfield, D. Lang, T. Haarmann-Stemmann, The Toll-like receptor agonist imiquimod is metabolized by aryl hydrocarbon receptor-regulated cytochrome P450 enzymes in human keratinocytes and mouse liver, Arch. Toxicol. 93 (7) (2019) 1917–1926.
[163] K.M. Rolfes, N.C. Sondermann, C. Vogeley, J. Dairou, V. Gilardino, R. Wirth, S. Meller, B. Homey, J. Krutmann, D. Lang, M. Nakamura, T. Haarmann-Stemmann, Inhibition of 6-formylindolo[3,2-b]carbazole metabolism sensitizes keratinocytes to UVA-induced apoptosis: Implications for vemurafenib-induced phototoxicity, Redox Biol. 46 (2021), 102110.
[164] D.W. Nebert, T.P. Dalton, The role of cytochrome P450 enzymes in endogenous signalling pathways and environmental carcinogenesis, Nat. Rev. Cancer 6 (12) (2006) 947–960.
[165] F. Li, W. Zhu, F.J. Gonzalez, Potential role of CYP1B1 in the development and treatment of metabolic diseases, Pharmacol. Ther. 178 (2017) 18–30.
[166] T. Yi, J. Wang, K. Zhu, Y. Tang, S. Huang, X. Shui, Y. Ding, C. Chen, W. Lei, Aryl Hydrocarbon Receptor: A New Player of Pathogenesis and Therapy in Cardiovascular Diseases, Biomed Res. Int. 2018 (2018) 6058784.
[167] R.H. Elbekai, A.O. El-Kadi, Cytochrome P450 enzymes: central players in cardiovascular health and disease, Pharmacol. Ther. 112 (2) (2006) 564–587.
[168] R. Charrad, W. Kaabachi, A. Rafrafi, A. Berraies, K. Hamzaoui, A. Hamzaoui, IL-8 Gene Variants and Expression in Childhood Asthma, Lung 195 (6) (2017) 749–757.
[169] R. Shinde, K. Hezaveh, M.J. Halaby, A. Kloetgen, A. Chakravarthy, T. da Silva Medina, R. Deol, K.P. Manion, Y. Baglaenko, M. Eldh, S. Lamorte, D. Wallace, S. B. Chodisetti, B. Ravishankar, H. Liu, K. Chaudhary, D.H. Munn, A. Tsirigos, M. Madaio, S. Gabrielsson, Z. Touma, J. Wither, D.D. De Carvalho, T.L. McGaha, Apoptotic cell-induced AhR activity is required for immunological tolerance and suppression of systemic lupus erythematosus in mice and humans, Nat. Immunol. 19 (6) (2018) 571–582.
[170] I. Monteleone, F. Pallone, G. Monteleone, Aryl hydrocarbon receptor and colitis, Semin. Immunopathol. 35 (6) (2013) 671–675.
[171] N.T. Nguyen, T. Nakahama, T. Kishimoto, Aryl hydrocarbon receptor and experimental autoimmune arthritis, Semin. Immunopathol. 35 (6) (2013) 637–644.
[172] J. Fu, S.V. Nogueira, V.V. Drongelen, P. Coit, S. Ling, E.F. Rosloniec, A. H. Sawalha, J. Holoshitz, Shared epitope-aryl hydrocarbon receptor crosstalk underlies the mechanism of gene-environment interaction in autoimmune arthritis, PNAS 115 (18) (2018) 4755–4760.
[173] N.B. Marshall, N.I. Kerkvliet, Dioxin and immune regulation: emerging role of aryl hydrocarbon receptor in the generation of regulatory T cells, Ann. N. Y. Acad. Sci. 1183 (2010) 25–37.
[174] G.L. Wang, G.L. Semenza, General involvement of hypoxia-inducible factor 1 in transcriptional response to hypoxia, PNAS 90 (9) (1993) 4304–4308.
[175] S.M. Wood, J.M. Gleadle, C.W. Pugh, O. Hankinson, P.J. Ratcliffe, The role of the aryl hydrocarbon receptor nuclear translocator (ARNT) in hypoxic induction of gene expression, Studies in ARNT-deficient cells, J Biol Chem 271 (25) (1996) 15117–15123.
[176] M. Ohh, C.W. Park, M. Ivan, M.A. Hoffman, T.Y. Kim, L.E. Huang, N. Pavletich, V. Chau, W.G. Kaelin, Ubiquitination of hypoxia-inducible factor requires direct binding to the beta-domain of the von Hippel-Lindau protein, Nat. Cell Biol. 2 (7) (2000) 423–427.
[177] B.E. McIntosh, J.B. Hogenesch, C.A. Bradfield, Mammalian Per-Arnt-Sim proteins in environmental adaptation, Annu. Rev. Physiol. 72 (2010) 625–645.
[178] S.L. Dunwoodie, The role of hypoxia in development of the Mammalian embryo, Dev. Cell 17 (6) (2009) 755–773.
[179] L.E. Kotch, N.V. Iyer, E. Laughner, G.L. Semenza, Defective vascularization of HIF-1alpha-null embryos is not associated with VEGF deficiency but with mesenchymal cell death, Dev. Biol. 209 (2) (1999) 254–267.
[180] H.E. Ryan, J. Lo, R.S. Johnson, HIF-1 alpha is required for solid tumor formation and embryonic vascularization, EMBO J. 17 (11) (1998) 3005–3015.
[181] M.E. Lindholm, H. Rundqvist, Skeletal muscle hypoxia-inducible factor-1 and exercise, Exp. Physiol. 101 (1) (2016) 28–32.
[182] T. Abe, Y. Kitaoka, D.M. Kikuchi, K. Takeda, O. Numata, T. Takemasa, High-intensity interval training-induced metabolic adaptation coupled with an increase in Hif-1alpha and glycolytic protein expression, J. Appl. Physiol. (1985) 119(11) (2015) 1297-302.
[183] J. Rius, M. Guma, C. Schachtrup, K. Akassoglou, A.S. Zinkernagel, V. Nizet, R. S. Johnson, G.G. Haddad, M. Karin, NF-kappaB links innate immunity to the hypoxic response through transcriptional regulation of HIF-1alpha, Nature 453 (7196) (2008) 807–811.
[184] T. Cramer, Y. Yamanishi, B.E. Clausen, I. Forster, R. Pawlinski, N. Mackman, V. H. Haase, R. Jaenisch, M. Corr, V. Nizet, G.S. Firestein, H.P. Gerber, N. Ferrara, R. S. Johnson, HIF-1alpha is essential for myeloid cell-mediated inflammation, Cell 112 (5) (2003) 645–657.
[185] R.K. Bruick, S.L. McKnight, A conserved family of prolyl-4-hydroxylases that modify HIF, Science 294 (5545) (2001) 1337–1340.
[186] L. Slemc, T. Kunej, Transcription factor HIF1A: downstream targets, associated pathways, polymorphic hypoxia response element (HRE) sites, and initiative for standardization of reporting in scientific literature, Tumour Biol. 37 (11) (2016) 14851–14861.
[187] J.E. Kim, Y.Y. Sheen, Inhibition of 2,3,7,8-tetrachlorodibenzo-p-dioxin (TCDD)-stimulated Cyp1a1 promoter activity by hypoxic agents, Biochem. Pharmacol. 59 (12) (2000) 1549–1556.
[188] K. Gradin, J. McGuire, R.H. Wenger, I. Kvietikova, M.L. Fhitelaw, R. Toftgard, L. Tora, M. Gassmann, L. Poellinger, Functional interference between hypoxia and dioxin signal transduction pathways: competition for recruitment of the Arnt transcription factor, Mol. Cell Biol. 16 (10) (1996) 5221–5231.
[189] M. Gassmann, I. Kvietikova, A. Rolfs, R.H. Wenger, Oxygen- and dioxin-regulated gene expression in mouse hepatoma cells, Kidney Int. 51 (2) (1997) 567–574.
[190] W.K. Chan, G. Yao, Y.Z. Gu, C.A. Bradfield, Cross-talk between the aryl hydrocarbon receptor and hypoxia inducible factor signaling pathways. Demonstration of competition and compensation, J. Biol. Chem. 274 (17) (1999) 12115–12123.
[191] M. Myre, P. Imbeault, Persistent organic pollutants meet adipose tissue hypoxia: does cross-talk contribute to inflammation during obesity? Obes. Rev. 15 (1) (2014) 19–28.
[192] H. Asai, J. Hirata, A. Hirano, K. Hirai, S. Seki, M. Watanabe-Akanuma, Activation of aryl hydrocarbon receptor mediates suppression of hypoxia-inducible factor-dependent erythropoietin expression by indoxyl sulfate, Am. J. Physiol. Cell Physiol. 310 (2) (2016) C142–C150.
[193] M. Vuerich, R. Harshe, L.A. Frank, S. Mukherjee, B. Gromova, E. Csizmadia, I.A. M. Nasser, Y. Ma, A. Bonder, V. Patwardhan, S.C. Robson, M.S. Longhi, Altered aryl-hydrocarbon-receptor signalling affects regulatory and effector cell immunity in autoimmune hepatitis, J. Hepatol. 74 (1) (2021) 48–57.
[194] G. Gabriely, M.A. Wheeler, M.C. Takenaka, F.J. Quintana, Role of AHR and HIF-1alpha in Glioblastoma Metabolism, Trends Endocrinol Metab 28 (6) (2017) 428–436.
[195] E.L. Button, D.C. Bersten, M.L. Whitelaw, HIF has Biff - Crosstalk between HIF1a and the family of bHLH/PAS proteins, Exp. Cell Res. 356 (2) (2017) 141–145.
[196] W.A. Fritz, T.M. Lin, R.E. Peterson, The aryl hydrocarbon receptor (AhR) inhibits vanadate-induced vascular endothelial growth factor (VEGF) production in TRAMP prostates, Carcinogenesis 29 (5) (2008) 1077–1082.
[197] X. Yang, H. Liu, T. Ye, C. Duan, P. Lv, X. Wu, J. Liu, K. Jiang, H. Lu, H. Yang, D. Xia, E. Peng, Z. Chen, K. Tang, Z. Ye, AhR activation attenuates calcium oxalate nephrocalcinosis by diminishing M1 macrophage polarization and promoting M2 macrophage polarization, Theranostics 10 (26) (2020) 12011–12025.
[198] M. Zhang, Y. Hu, F. Yang, J. Zhang, J. Zhang, W. Yu, M. Wang, X. Lv, J. Li, T. Bai, F. Chang, Interaction between AhR and HIF-1 signaling pathways mediated by ARNT/HIF-1beta, BMC Pharmacol. Toxicol. 23 (1) (2022) 26.
[199] A. Jacob, S. Potin, B. Saubamea, D. Crete, J.M. Scherrmann, E. Curis, C. Peyssonnaux, X. Decleves, Hypoxia interferes with aryl hydrocarbon receptor pathway in hCMEC/D3 human cerebral microvascular endothelial cells, J. Neurochem. 132 (4) (2015) 373–383.
[200] S.U. Vorrink, F.E. Domann, Regulatory crosstalk and interference between the xenobiotic and hypoxia sensing pathways at the AhR-ARNT-HIF1alpha signaling node, Chem. Biol. Interact. 218 (2014) 82–88.
[201] S.U. Vorrink, E.H. Sarsour, A.K. Olivier, L.W. Robertson, P.C. Goswami, F. E. Domann, PCB 126 perturbs hypoxia-induced HIF-1alpha activity and glucose consumption in human HepG2 cells, Exp. Toxicol. Pathol. 66 (8) (2014) 377–382.
[202] S.U. Vorrink, P.L. Severson, M.V. Kulak, B.W. Futscher, F.E. Domann, Hypoxia perturbs aryl hydrocarbon receptor signaling and CYP1A1 expression induced by PCB 126 in human skin and liver-derived cell lines, Toxicol. Appl. Pharmacol. 274 (3) (2014) 408–416.
[203] A. Salminen, Mutual antagonism between aryl hydrocarbon receptor and hypoxia-inducible factor-1alpha (AhR/HIF-1alpha) signaling: Impact on the aging process, Cell. Signal. 99 (2022), 110445.
[204] M. Wolff, W. Jelkmann, J. Dunst, R. Depping, The Aryl Hydrocarbon Receptor Nuclear Translocator (ARNT/HIF-1beta) is influenced by hypoxia and hypoxia-mimetics, Cell. Physiol. Biochem. 32 (4) (2013) 849–858.
[205] M. Mandl, R. Depping, Hypoxia-inducible aryl hydrocarbon receptor nuclear translocator (ARNT) (HIF-1beta): is it a rare exception? Mol. Med. 20 (2014) 215–220.
[206] B. Bedogni, S.M. Welford, D.S. Cassarino, B.J. Nickoloff, A.J. Giaccia, M. B. Powell, The hypoxic microenvironment of the skin contributes to Akt-mediated melanocyte transformation, Cancer Cell 8 (6) (2005) 443–454.
[207] A.T. Boutin, A. Weidemann, Z. Fu, L. Mesropian, K. Gradin, C. Jamora, M. Wiesener, K.U. Eckardt, C.J. Koch, L.G. Ellies, G. Haddad, V.H. Haase, M. C. Simon, L. Poellinger, F.L. Powell, R.S. Johnson, Epidermal sensing of oxygen is essential for systemic hypoxic response, Cell 133 (2) (2008) 223–234.

[208] M. Stucker, A. Struk, P. Altmeyer, M. Herde, H. Baumgartl, D.W. Lubbers, The cutaneous uptake of atmospheric oxygen contributes significantly to the oxygen supply of human dermis and epidermis, J. Physiol. 538 (Pt 3) (2002) 985–994.
[209] S. Geng, A. Mezentsev, S. Kalachikov, K. Raith, D.R. Roop, A.A. Panteleyev, Targeted ablation of Arnt in mouse epidermis results in profound defects in desquamation and epidermal barrier function, J. Cell Sci. 119 (Pt 23) (2006) 4901–4912.
[210] A. Wondimu, L. Weir, D. Robertson, A. Mezentsev, S. Kalachikov, A. A. Panteleyev, Loss of Arnt (Hif1beta) in mouse epidermis triggers dermal angiogenesis, blood vessel dilation and clotting defects, Lab. Invest. 92 (1) (2012) 110–124.
[211] E.D. Robertson, L. Weir, M. Romanowska, I.M. Leigh, A.A. Panteleyev, ARNT controls the expression of epidermal differentiation genes through HDAC- and EGFR-dependent pathways, J. Cell Sci. 125 (Pt 14) (2012) 3320–3332.
[212] S. Takagi, H. Tojo, S. Tomita, S. Sano, S. Itami, M. Hara, S. Inoue, K. Horie, G. Kondoh, K. Hosokawa, F.J. Gonzalez, J. Takeda, Alteration of the 4-sphingenine scaffolds of ceramides in keratinocyte-specific Arnt-deficient mice affects skin barrier function, J. Clin. Invest. 112 (9) (2003) 1372–1382.
[213] C. Garcia-Ruiz, A. Colell, M. Mari, A. Morales, J.C. Fernandez-Checa, Direct effect of ceramide on the mitochondrial electron transport chain leads to generation of reactive oxygen species. Role of mitochondrial glutathione, J. Biol. Chem. 272 (17) (1997) 11369–11377.
[214] C. Gu, J. Gonzalez, T. Zhang, S. Kamel-Reid, R.A. Wells, The aryl hydrocarbon receptor nuclear translocator (ARNT) modulates the antioxidant response in AML cells, Leuk. Res. 37 (12) (2013) 1750–1756.
[215] K. Haas, H. Weighardt, R. Deenen, K. Kohrer, B. Clausen, S. Zahner, P. Boukamp, W. Bloch, J. Krutmann, C. Esser, Aryl hydrocarbon receptor in keratinocytes is essential for murine skin barrier integrity, J. Invest. Dermatol. (2016).
[216] S. Fassbender, K. Sondenheimer, M. Majora, J. Schindler, F.V. Opitz, M. Pollet, T. Haarmann-Stemmann, J. Krutmann, H. Weighardt, Keratinocytes Counteract UVB-Induced Immunosuppression in Mice Via HIF-1a Signaling, J, Invest. Dermatol. (2021).
[217] C. Peyssonnaux, A.T. Boutin, A.S. Zinkernagel, V. Datta, V. Nizet, R.S. Johnson, Critical role of HIF-1alpha in keratinocyte defense against bacterial infection, J, Invest. Dermatol. 128 (8) (2008) 1964–1968.
[218] R.S. Pollenz, N.A. Davarinos, T.P. Shearer, Analysis of aryl hydrocarbon receptor-mediated signaling during physiological hypoxia reveals lack of competition for the aryl hydrocarbon nuclear translocator transcription factor, Mol. Pharmacol. 56 (6) (1999) 1127–1137.
[219] C.H. Tsai, C.H. Li, P.L. Liao, Y.W. Cheng, C.H. Lin, S.H. Huang, J.J. Kang, NcoA2-Dependent Inhibition of HIF-1alpha Activation Is Regulated via AhR, Toxicol. Sci. 148 (2) (2015) 517–530.
[220] Y. Benita, H. Kikuchi, A.D. Smith, M.Q. Zhang, D.C. Chung, R.J. Xavier, An integrative genomics approach identifies Hypoxia Inducible Factor-1 (HIF-1)-target genes that form the core response to hypoxia, Nucleic Acids Res. 37 (14) (2009) 4587–4602.
[221] A.A. Tirpe, D. Gulei, S.M. Ciortea, C. Crivii, I. Berindan-Neagoe, Hypoxia: Overview on Hypoxia-Mediated Mechanisms with a Focus on the Role of HIF Genes, Int. J. Mol. Sci. 20 (24) (2019).
[222] R. Ghosh, P. Samanta, R. Sarkar, S. Biswas, P. Saha, S. Hajra, A. Bhowmik, Targeting HIF-1alpha by Natural and Synthetic Compounds: A Promising Approach for Anti-Cancer Therapeutics Development, Molecules 27 (16) (2022).
[223] S. Soni, Y.S. Padwad, HIF-1 in cancer therapy: two decade long story of a transcription factor, Acta Oncol. 56 (4) (2017) 503–515.
[224] F. Cimmino, M. Avitabile, V.A. Lasorsa, A. Montella, L. Pezone, S. Cantalupo, F. Visconte, M.V. Corrias, A. Iolascon, M. Capasso, HIF-1 transcription activity: HIF1A driven response in normoxia and in hypoxia, BMC Med. Genet. 20 (1) (2019) 37.
[225] J.P. Li, F.Y. Li, A. Xu, B. Cheng, S.W. Tsao, M.L. Fung, W.K. Leung, Lipopolysaccharide and hypoxia-induced HIF-1 activation in human gingival fibroblasts, J. Periodontol. 83 (6) (2012) 816–824.
[226] A. Kuschel, P. Simon, S. Tug, Functional regulation of HIF-1alpha under normoxia–is there more than post-translational regulation? J. Cell. Physiol. 227 (2) (2012) 514–524.
[227] T. Isoe, Y. Makino, K. Mizumoto, H. Sakagami, Y. Fujita, J. Honjo, Y. Takiyama, H. Itoh, M. Haneda, High glucose activates HIF-1-mediated signal transduction in glomerular mesangial cells through a carbohydrate response element binding protein, Kidney Int. 78 (1) (2010) 48–59.
[228] E.L. Page, G.A. Robitaille, J. Pouyssegur, D.E. Richard, Induction of hypoxia-inducible factor-1alpha by transcriptional and translational mechanisms, J. Biol. Chem. 277 (50) (2002) 48403–48409.
[229] S. Anavi, M. Hahn-Obercyger, Z. Madar, O. Tirosh, Mechanism for HIF-1 activation by cholesterol under normoxia: a redox signaling pathway for liver damage, Free Radic. Biol. Med. 71 (2014) 61–69.
[230] E.J. Moon, P. Sonveaux, P.E. Porporato, P. Danhier, B. Gallez, I. Batinic-Haberle, Y.C. Nien, T. Schroeder, M.W. Dewhirst, NADPH oxidase-mediated reactive oxygen species production activates hypoxia-inducible factor-1 (HIF-1) via the ERK pathway after hyperthermia treatment, PNAS 107 (47) (2010) 20477–20482.
[231] H.R. Rezvani, S. Dedieu, S. North, F. Belloc, R. Rossignol, T. Letellier, H. de Verneuil, A. Taieb, F. Mazurier, Hypoxia-inducible factor-1alpha, a key factor in the keratinocyte response to UVB exposure, J. Biol. Chem. 282 (22) (2007) 16413–16422.
[232] L. Wunderlich, G. Paragh, N.M. Wikonkal, G. Banhegyi, S. Karpati, J. Mandl, UVB induces a biphasic response of HIF-1alpha in cultured human keratinocytes, Exp. Dermatol. 17 (4) (2008) 335–342.
[233] Y.S. Cho, C.H. Kim, J.W. Park, Involvement of HIF-1alpha in UVB-induced epidermal hyperplasia, Mol. Cells 28 (6) (2009) 537–543.
[234] Y. Hayashi, A. Yokota, H. Harada, G. Huang, Hypoxia/pseudohypoxia-mediated activation of hypoxia-inducible factor-1alpha in cancer, Cancer Sci. 110 (5) (2019) 1510–1517.
[235] J. Song, X. Yang, L.J. Yan, Role of pseudohypoxia in the pathogenesis of type 2 diabetes, Hypoxia (Auckl) 7 (2019) 33–40.
[236] K. Nys, H. Maes, A.M. Dudek, P. Agostinis, Uncovering the role of hypoxia inducible factor-1alpha in skin carcinogenesis, Biochim. Biophys. Acta 1816 (1) (2011) 1–12.
[237] I. Seleit, O.A. Bakry, D.R. Al-Sharaky, R.A.A. Ragab, S.A. Al-Shiemy, Evaluation of Hypoxia Inducible Factor-1alpha and Glucose Transporter-1 Expression in Non Melanoma Skin Cancer: An Immunohistochemical Study, J. Clin. Diagn. Res. 11 (6) (2017) EC09-EC16.
[238] M. Malekan, M.A. Ebrahimzadeh, F. Sheida, The role of Hypoxia-Inducible Factor-1alpha and its signaling in melanoma, Biomed. Pharmacother. 141 (2021), 111873.
[239] F. Navid, A. Bruhs, W. Schuller, E. Fritsche, J. Krutmann, T. Schwarz, A. Schwarz, The Aryl hydrocarbon receptor is involved in UVR-induced immunosuppression, J, Invest. Dermatol. 133 (12) (2013) 2763–2770.
[240] J. Munoz-Sanchez, M.E. Chanez-Cardenas, The use of cobalt chloride as a chemical hypoxia model, J. Appl. Toxicol. 39 (4) (2019) 556–570.
[241] E. Miranda, I.K. Nordgren, A.L. Male, C.E. Lawrence, F. Hoakwie, F. Cuda, W. Court, K.R. Fox, P.A. Townsend, G.K. Packham, S.A. Eccles, A. Tavassoli, A cyclic peptide inhibitor of HIF-1 heterodimerization that inhibits hypoxia signaling in cancer cells, J. Am. Chem. Soc. 135 (28) (2013) 10418–10425.
[242] I. Mylonis, G. Chachami, G. Simos, Specific Inhibition of HIF Activity: Can Peptides Lead the Way? Cancers (Basel) 13 (3) (2021).
[243] T. Yu, B. Tang, X. Sun, Development of Inhibitors Targeting Hypoxia-Inducible Factor 1 and 2 for Cancer Therapy, Yonsei Med. J. 58 (3) (2017) 489–496.
[244] E. Terzuoli, M. Puppo, A. Rapisarda, B. Uranchimeg, L. Cao, A.M. Burger, M. Ziche, G. Melillo, Aminoflavone, a ligand of the aryl hydrocarbon receptor, inhibits HIF-1alpha expression in an AhR-independent fashion, Cancer Res. 70 (17) (2010) 6837–6848.
[245] L.T. Goodnough, T.G. Monk, G.L. Andriole, Erythropoietin therapy, N. Engl. J. Med. 336 (13) (1997) 933–938.
[246] C. Reichel, G. Gmeiner, Erythropoietin and analogs, Handb. Exp. Pharmacol. 195 (2010) 251–294.
[247] S. Dhillon, Roxadustat: First Global Approval, Drugs 79 (5) (2019) 563–572.
[248] K. Hirota, HIF-alpha Prolyl Hydroxylase Inhibitors and Their Implications for Biomedicine: A Comprehensive Review, Biomedicines 9 (5) (2021).
[249] V. Vallon, S. Verma, Effects of SGLT2 Inhibitors on Kidney and Cardiovascular Function, Annu. Rev. Physiol. 83 (2021) 503–528.
[250] L. Cheng, H. Yu, N. Yan, K. Lai, M. Xiang, Hypoxia-Inducible Factor-1alpha Target Genes Contribute to Retinal Neuroprotection, Front. Cell. Neurosci. 11 (2017) 20.
[251] M.P. Nicholas, N. Mysore, Corneal neovascularization, Exp. Eye Res. 202 (2021), 108363.
[252] C.L. Hammond, E. Roztocil, V. Gupta, S.E. Feldon, C.F. Woeller, More than Meets the Eye: The Aryl Hydrocarbon Receptor is an Environmental Sensor, Physiological Regulator and a Therapeutic Target in Ocular Disease, Front. Toxicol. 4 (2022), 791082.
[253] J. Garcia, H.I. Hurwitz, A.B. Sandler, D. Miles, R.L. Coleman, R. Deurloo, O. L. Chinot, Bevacizumab (Avastin(R)) in cancer treatment: A review of 15 years of clinical experience and future outlook, Cancer Treat. Rev. 86 (2020), 102017.
[254] V.S. Dedania, S.J. Bakri, Current perspectives on ranibizumab, Clin. Ophthalmol. 9 (2015) 533–542.
[255] E. Allen, A. Keir, Ranibizumab-The jury is still out, Acta Paediatr. 111 (3) (2022) 698–699.
[256] J. Fallah, B.I. Rini, H.I.F. Inhibitors, Status of Current Clinical Development, Curr. Oncol. Rep. 21 (1) (2019) 6.
[257] S. An, M. Zhou, Z. Li, M. Feng, G. Cao, S. Lu, L. Liu, Administration of CoCl2 Improves Functional Recovery in a Rat Model of Sciatic Nerve Transection Injury, Int. J. Med. Sci. 15 (13) (2018) 1423–1432.
[258] Y. Cho, J.E. Shin, E.E. Ewan, Y.M. Oh, W. Pita-Thomas, V. Cavalli, Activating Injury-Responsive Genes with Hypoxia Enhances Axon Regeneration through Neuronal HIF-1alpha, Neuron 88 (4) (2015) 720–734.
[259] R. Di Giaimo, T. Durovic, P. Barquin, A. Kociaj, T. Lepko, S. Aschenbroich, C.T. Breunig, M. Irmler, F.M. Cernilogar, G. Schotta, J.S. Barbosa, D. Trumbach, E.V. Baumgart, A.M. Neuner, J. Beckers, W. Wurst, S.H. Stricker, J. Ninkovic, The Aryl Hydrocarbon Receptor Pathway Defines the Time Frame for Restorative Neurogenesis, Cell Rep 25(12) (2018) 3241–3251 e5.
[260] A. Navarrete-Opazo, G.S. Mitchell, Therapeutic potential of intermittent hypoxia: a matter of dose, Am. J. Physiol. Regul. Integr. Comp. Physiol. 307 (10) (2014) R1181–R1197.
[261] F.R. Sharp, R. Ran, A. Lu, Y. Tang, K.I. Strauss, T. Glass, T. Ardizzone, M. Bernaudin, Hypoxic preconditioning protects against ischemic brain injury, NeuroRx 1 (1) (2004) 26–35.
[262] J.I. Kwon, H. Heo, S.J. Ham, Y.J. Chae, D.W. Lee, S.T. Kim, J. Min, Y.S. Sung, K. W. Kim, Y. Choi, D.C. Woo, C.W. Woo, Aryl hydrocarbon receptor antagonism before reperfusion attenuates cerebral ischaemia/reperfusion injury in rats, Sci. Rep. 10 (1) (2020) 14906.
[263] J.X. Wang, B.B. Wang, S.Z. Yuan, K. Xue, J.S. Zhang, A.J. Xu, Blocking the Aryl Hydrocarbon Receptor Alleviates Myocardial Ischemia/Reperfusion Injury in Rats, Curr, Med. Sci. (2022).
[264] T. Eleftheriadis, G. Pissas, G. Filippidis, V. Liakopoulos, I. Stefanidis, Reoxygenation induces reactive oxygen species production and ferroptosis in

renal tubular epithelial cells by activating aryl hydrocarbon receptor, Mol. Med. Rep. 23 (1) (2021).
[265] H. Sies, Oxidative Stress: Introductory Remarks, in: H. Sies (Ed.), Oxidative Stress, Academic Press, London, 1985, pp. 1–8.
[266] H.J. Prochaska, P. Talalay, Regulatory mechanisms of monofunctional and bifunctional anticarcinogenic enzyme inducers in murine liver, Cancer Res. 48 (17) (1988) 4776–4782.
[267] S.J. Stohs, Oxidative stress induced by 2,3,7,8-tetrachlorodibenzo-p-dioxin (TCDD), Free Radic. Biol. Med. 9 (1) (1990) 79–90.
[268] H. Shi, J. Liu, H. Gao, Benzo(alpha)pyrene induces oxidative stress and inflammation in human vascular endothelial cells through AhR and NF-kappaB pathways, Microvasc. Res. 137 (2021), 104179.
[269] C. Dietrich, Antioxidant Functions of the Aryl Hydrocarbon Receptor, Stem Cells Int. 2016 (2016) 7943495.
[270] A. Braeuning, C. Kohle, A. Buchmann, M. Schwarz, Coordinate regulation of cytochrome P450 1a1 expression in mouse liver by the aryl hydrocarbon receptor and the beta-catenin pathway, Toxicol. Sci. 122 (1) (2011) 16–25.
[271] M.G. Borland, P. Krishnan, C. Lee, P.P. Albrecht, W. Shan, M.T. Bility, C. B. Marcus, J.M. Lin, S. Amin, F.J. Gonzalez, G.H. Perdew, J.M. Peters, Modulation of aryl hydrocarbon receptor (AHR)-dependent signaling by peroxisome proliferator-activated receptor beta/delta (PPARbeta/delta) in keratinocytes, Carcinogenesis 35 (7) (2014) 1602–1612.
[272] T. Haarmann-Stemmann, J. Abel, E. Fritsche, J. Krutmann, The AhR-Nrf2 pathway in keratinocytes: on the road to chemoprevention? J, Invest. Dermatol. 132 (1) (2012) 7–9.
[273] M. Schafer, S. Werner, Nrf2–A regulator of keratinocyte redox signaling, Free Radic. Biol. Med. 88 (Pt B) (2015) 243–252.
[274] P. Moi, K. Chan, I. Asunis, A. Cao, Y.W. Kan, Isolation of NF-E2-related factor 2 (Nrf2), a NF-E2-like basic leucine zipper transcriptional activator that binds to the tandem NF-E2/AP1 repeat of the beta-globin locus control region, PNAS 91 (21) (1994) 9926–9930.
[275] K. Itoh, N. Wakabayashi, Y. Katoh, T. Ishii, K. Igarashi, J.D. Engel, M. Yamamoto, Keap1 represses nuclear activation of antioxidant responsive elements by Nrf2 through binding to the amino-terminal Neh2 domain, Genes Dev. 13 (1) (1999) 76–86.
[276] A. Kobayashi, M.I. Kang, H. Okawa, M. Ohtsuji, Y. Zenke, T. Chiba, K. Igarashi, M. Yamamoto, Oxidative stress sensor Keap1 functions as an adaptor for Cul3-based E3 ligase to regulate proteasomal degradation of Nrf2, Mol. Cell Biol. 24 (16) (2004) 7130–7139.
[277] T. Yamamoto, T. Suzuki, A. Kobayashi, J. Wakabayashi, J. Maher, H. Motohashi, M. Yamamoto, Physiological significance of reactive cysteine residues of Keap1 in determining Nrf2 activity, Mol. Cell Biol. 28 (8) (2008) 2758–2770.
[278] K. Nakaso, H. Yano, Y. Fukuhara, T. Takeshima, K. Wada-Isoe, K. Nakashima, PI3K is a key molecule in the Nrf2-mediated regulation of antioxidative proteins by hemin in human neuroblastoma cells, FEBS Lett. 546 (2–3) (2003) 181–184.
[279] H.C. Huang, T. Nguyen, C.B. Pickett, Phosphorylation of Nrf2 at Ser-40 by protein kinase C regulates antioxidant response element-mediated transcription, J. Biol. Chem. 277 (45) (2002) 42769–42774.
[280] K. Itoh, T. Chiba, S. Takahashi, T. Ishii, K. Igarashi, Y. Katoh, T. Oyake, N. Hayashi, K. Satoh, I. Hatayama, M. Yamamoto, Y. Nabeshima, An Nrf2/small Maf heterodimer mediates the induction of phase II detoxifying enzyme genes through antioxidant response elements, Biochem. Biophys. Res. Commun. 236 (2) (1997) 313–322.
[281] W. Miao, L. Hu, P.J. Scrivens, G. Batist, Transcriptional regulation of NF-E2 p45-related factor (NRF2) expression by the aryl hydrocarbon receptor-xenobiotic response element signaling pathway: direct cross-talk between phase I and II drug-metabolizing enzymes, J. Biol. Chem. 280 (21) (2005) 20340–20348.
[282] S. Shin, N. Wakabayashi, V. Misra, S. Biswal, G.H. Lee, E.S. Agoston, M. Yamamoto, T.W. Kensler, NRF2 modulates aryl hydrocarbon receptor signaling: influence on adipogenesis, Mol. Cell Biol. 27 (20) (2007) 7188–7197.
[283] A. Anwar-Mohamed, O.S. Degenhardt, M.A. El Gendy, J.M. Seubert, S. R. Kleeberger, A.O. El-Kadi, The effect of Nrf2 knockout on the constitutive expression of drug metabolizing enzymes and transporters in C57Bl/6 mice livers, Toxicol. In Vitro 25 (4) (2011) 785–795.
[284] P. Nioi, M. McMahon, K. Itoh, M. Yamamoto, J.D. Hayes, Identification of a novel Nrf2-regulated antioxidant response element (ARE) in the mouse NAD(P)H: quinone oxidoreductase 1 gene: reassessment of the ARE consensus sequence, Biochem. J 374 (Pt 2) (2003) 337–348.
[285] J.D. Hayes, J.U. Flanagan, I.R. Jowsey, Glutathione transferases, Annu. Rev. Pharmacol. Toxicol. 45 (2005) 51–88.
[286] T.H. Rushmore, C.B. Pickett, Transcriptional regulation of the rat glutathione S-transferase Ya subunit gene. Characterization of a xenobiotic-responsive element controlling inducible expression by phenolic antioxidants, J. Biol. Chem. 265 (24) (1990) 14648–14653.
[287] M.F. Yueh, Y.H. Huang, A. Hiller, S. Chen, N. Nguyen, R.H. Tukey, Involvement of the xenobiotic response element (XRE) in Ah receptor-mediated induction of human UDP-glucuronosyltransferase 1A1, J. Biol. Chem. 278 (17) (2003) 15001–15006.
[288] S. Kalthoff, U. Ehmer, N. Freiberg, M.P. Manns, C.P. Strassburg, Coffee induces expression of glucuronosyltransferases by the aryl hydrocarbon receptor and Nrf2 in liver and stomach, Gastroenterology 139(5) (2010) 1699–710, 1710 e1–2.
[289] P.A. Munzel, S. Schmohl, F. Buckler, J. Jaehrling, F.T. Raschko, C. Kohle, K. W. Bock, Contribution of the Ah receptor to the phenolic antioxidant-mediated expression of human and rat UDP-glucuronosyltransferase UGT1A6 in Caco-2 and rat hepatoma 5L cells, Biochem. Pharmacol. 66 (5) (2003) 841–847.
[290] G. Tsuji, M. Takahara, H. Uchi, T. Matsuda, T. Chiba, S. Takeuchi, F. Yasukawa, Y. Moroi, M. Furue, Identification of ketoconazole as an AhR-Nrf2 activator in cultured human keratinocytes: the basis of its anti-inflammatory effect, J, Invest. Dermatol. 132 (1) (2012) 59–68.
[291] H. Takemura, H. Nagayoshi, T. Matsuda, H. Sakakibara, M. Morita, A. Matsui, T. Ohura, K. Shimoi, Inhibitory effects of chrysoeriol on DNA adduct formation with benzo[a]pyrene in MCF-7 breast cancer cells, Toxicology 274 (1–3) (2010) 42–48.
[292] H.P. Ciolino, P.J. Daschner, T.T. Wang, G.C. Yeh, Effect of curcumin on the aryl hydrocarbon receptor and cytochrome P450 1A1 in MCF-7 human breast carcinoma cells, Biochem. Pharmacol. 56 (2) (1998) 197–206.
[293] R. Garg, S. Gupta, G.B. Maru, Dietary curcumin modulates transcriptional regulators of phase I and phase II enzymes in benzo[a]pyrene-treated mice: mechanism of its anti-initiating action, Carcinogenesis 29 (5) (2008) 1022–1032.
[294] D. Kalpana Deepa Priya, R. Gayathri, D. Sakthisekaran, Role of sulforaphane in the anti-initiating mechanism of lung carcinogenesis in vivo by modulating the metabolic activation and detoxification of benzo(a)pyrene, Biomed. Pharmacother. 65(1) (2011) 9–16.
[295] Y. Zhang, T.W. Kensler, C.G. Cho, G.H. Posner, P. Talalay, Anticarcinogenic activities of sulforaphane and structurally related synthetic norbornyl isothiocyanates, PNAS 91 (8) (1994) 3147–3150.
[296] Y.P. Hwang, E.H. Han, J.H. Choi, H.G. Kim, K.J. Lee, T.C. Jeong, E.S. Lee, H. G. Jeong, Chemopreventive effects of Furan-2-yl-3-pyridin-2-yl-propenone against 7,12-dimethylbenz[a]anthracene-inducible genotoxicity, Toxicol. Appl. Pharmacol. 228 (3) (2008) 343–350.
[297] H. Uchi, M. Yasumatsu, S. Morino-Koga, C. Mitoma, M. Furue, Inhibition of aryl hydrocarbon receptor signaling and induction of NRF2-mediated antioxidant activity by cinnamaldehyde in human keratinocytes, J. Dermatol. Sci. 85 (1) (2017) 36–43.
[298] A. Mohammadi-Bardbori, L. Vikstrom Bergander, U. Rannug, A. Rannug, NADPH Oxidase-Dependent Mechanism Explains How Arsenic and Other Oxidants Can Activate Aryl Hydrocarbon Receptor Signaling, Chem. Res. Toxicol. 28 (12) (2015) 2278–2286.
[299] E. Wincent, J. Bengtsson, A. Mohammadi Bardbori, T. Alsberg, S. Luecke, U. Rannug, A. Rannug, Inhibition of cytochrome P4501-dependent clearance of the endogenous agonist FICZ as a mechanism for activation of the aryl hydrocarbon receptor, PNAS 109 (12) (2012) 4479–4484.
[300] S.P. Kubli, C. Bassi, C. Roux, A. Wakeham, C. Göbl, W. Zhou, S.M. Jafari, B. Snow, L. Jones, L. Palomero, K.L. Thu, L. Cassetta, D. Soong, T. Berger, P. Ramachandran, S.P. Baniasadi, G. Duncan, M. Lindzen, Y. Yarden, C. Herranz, C. Lazaro, M.F. Chu, J. Haight, P. Tinto, J. Silvester, D.W. Cescon, A. Petit, S. Pettersson, J.W. Pollard, T.W. Mak, M.A. Pujana, P. Cappello, C. Gorrini, AhR controls redox homeostasis and shapes the tumor microenvironment in BRCA1-associated breast cancer, Proc. Natl. Acad. Sci. 116(9) (2019) 3604–3613.
[301] A.G. Bart, E.E. Scott, Structures of human cytochrome P450 1A1 with bergamottin and erlotinib reveal active-site modifications for binding of diverse ligands, J. Biol. Chem. 293 (50) (2018) 19201–19210.
[302] S. Dhakshinamoorthy, A.K. Jaiswal, c-Maf negatively regulates ARE-mediated detoxifying enzyme genes expression and anti-oxidant induction, Oncogene 21 (34) (2002) 5301–5312.
[303] D. Brauze, J.S. Crow, D. Malejka-Giganti, Modulation by β-naphthoflavone of ovarian hormone dependent responses in rat uterus and liver in vivo, Can. J. Physiol. Pharmacol. 75 (8) (1997) 1022–1029.
[304] D.R. Boverhof, J.C. Kwekel, D.G. Humes, L.D. Burgoon, T.R. Zacharewski, Dioxin induces an estrogen-like, estrogen receptor-dependent gene expression response in the murine uterus, Mol. Pharmacol. 69 (5) (2006) 1599–1606.
[305] B. Astroff, B. Eldridge, S. Safe, Inhibition of the 17β-estradiol-induced and constitutive expression of the cellular protooncogene c-fos by 2,3,7,8-tetrachlor-odibenzo-p-dioxin (TCDD) in the female rat uterus, Toxicol. Lett. 56 (3) (1991) 305–315.
[306] D.R. Boverhof, L.D. Burgoon, K.J. Williams, T.R. Zacharewski, Inhibition of estrogen-mediated uterine gene expression responses by dioxin, Mol. Pharmacol. 73 (1) (2008) 82–93.
[307] T.M. Lin, K. Ko, R.W. Moore, U. Simanainen, T.D. Oberley, R.E. Peterson, Effects of aryl hydrocarbon receptor null mutation and in utero and lactational 2,3,7,8-tetrachlorodibenzo-p-dioxin exposure on prostate and seminal vesicle development in C57BL/6 mice, Toxicol. Sci. 68 (2) (2002) 479–487.
[308] F. Ohtake, K. Takeyama, T. Matsumoto, H. Kitagawa, Y. Yamamoto, K. Nohara, C. Tohyama, A. Krust, J. Mimura, P. Chambon, J. Yanagisawa, Y. Fujii-Kuriyama, S. Kato, Modulation of oestrogen receptor signalling by association with the activated dioxin receptor, Nature 423 (6939) (2003) 545–550.
[309] M. Wormke, M. Stoner, B. Saville, K. Walker, M. Abdelrahim, R. Burghardt, S. Safe, The aryl hydrocarbon receptor mediates degradation of estrogen receptor alpha through activation of proteasomes, Mol. Cell Biol. 23 (6) (2003) 1843–1855.
[310] F. Ohtake, A. Baba, I. Takada, M. Okada, K. Iwasaki, H. Miki, S. Takahashi, A. Kouzmenko, K. Nohara, T. Chiba, Y. Fujii-Kuriyama, S. Kato, Dioxin receptor is a ligand-dependent E3 ubiquitin ligase, Nature 446 (7135) (2007) 562–566.
[311] S. Luecke-Johansson, M. Gralla, H. Rundqvist, J.C. Ho, R.S. Johnson, K. Gradin, L. Poellinger, A Molecular Mechanism To Switch the Aryl Hydrocarbon Receptor from a Transcription Factor to an E3 Ubiquitin Ligase, Mol. Cell Biol. 37 (13) (2017).
[312] A. Hershko, A. Ciechanover, The ubiquitin system, Annu. Rev. Biochem 67 (1998) 425–479.
[313] D. Nandi, P. Tahiliani, A. Kumar, D. Chandu, The ubiquitin-proteasome system, J. Biosci. 31 (1) (2006) 137–155.

[314] F. Ohtake, A. Baba, Y. Fujii-Kuriyama, S. Kato, Intrinsic AhR function underlies cross-talk of dioxins with sex hormone signalings, Biochem. Biophys. Res. Commun. 370 (4) (2008) 541–546.
[315] H. Dou, Y. Duan, X. Zhang, Q. Yu, Q. Di, Y. Song, P. Li, Y. Gong, Aryl hydrocarbon receptor (AhR) regulates adipocyte differentiation by assembling CRL4B ubiquitin ligase to target PPARgamma for proteasomal degradation, J. Biol. Chem. 294 (48) (2019) 18504–18515.
[316] K. Kawajiri, Y. Kobayashi, F. Ohtake, T. Ikuta, Y. Matsushima, J. Mimura, S. Pettersson, R.S. Pollenz, T. Sakaki, T. Hirokawa, T. Akiyama, M. Kurosumi, L. Poellinger, S. Kato, Y. Fujii-Kuriyama, Aryl hydrocarbon receptor suppresses intestinal carcinogenesis in ApcMin/+ mice with natural ligands, PNAS 106 (32) (2009) 13481–13486.
[317] J. Liu, Q. Xiao, J. Xiao, C. Niu, Y. Li, X. Zhang, Z. Zhou, G. Shu, G. Yin, Wnt/beta-catenin signalling: function, biological mechanisms, and therapeutic opportunities, Signal Transduct. Target. Ther. 7 (1) (2022) 3.
[318] B.J. Roberts, M.L. Whitelaw, Degradation of the basic helix-loop-helix/Per-ARNT-Sim homology domain dioxin receptor via the ubiquitin/proteasome pathway, J. Biol. Chem. 274 (51) (1999) 36351–36356.
[319] Q. Ma, K.T. Baldwin, 2,3,7,8-tetrachlorodibenzo-p-dioxin-induced degradation of aryl hydrocarbon receptor (AhR) by the ubiquitin-proteasome pathway. Role of the transcription activaton and DNA binding of AhR, J. Biol. Chem. 275 (12) (2000) 8432–8438.
[320] M.P. Rijo, S. Diani-Moore, C. Yang, P. Zhou, A.B. Rifkind, Roles of the ubiquitin ligase CUL4B and ADP-ribosyltransferase TiPARP in TCDD-induced nuclear export and proteasomal degradation of the transcription factor AHR, J. Biol. Chem. 297 (2) (2021), 100886.
[321] H. Clevers, R. Nusse, Wnt/beta-catenin signaling and disease, Cell 149 (6) (2012) 1192–1205.
[322] Z. Culig, F.R. Santer, Androgen receptor signaling in prostate cancer, Cancer Metastasis Rev. 33 (2–3) (2014) 413–427.
[323] M. Jia, K. Dahlman-Wright, J.A. Gustafsson, Estrogen receptor alpha and beta in health and disease, Best Pract. Res. Clin. Endocrinol. Metab. 29 (4) (2015) 557–568.
[324] M. Kono, T. Fujii, B. Lim, M.S. Karuturi, D. Tripathy, N.T. Ueno, Androgen Receptor Function and Androgen Receptor-Targeted Therapies in Breast Cancer: A Review, JAMA Oncol. 3 (9) (2017) 1266–1273.
[325] A. Kannt, I. Dikic, Expanding the arsenal of E3 ubiquitin ligases for proximity-induced protein degradation, Cell Chem. Biol. 28 (7) (2021) 1014–1031.
[326] C.M. Crews, Inducing Protein Degradation as a Therapeutic Strategy, J. Med. Chem. 61 (2) (2018) 403–404.
[327] M. Bekes, D.R. Langley, C.M. Crews, PROTAC targeted protein degraders: the past is prologue, Nat. Rev. Drug Discov. 21 (3) (2022) 181–200.
[328] D. Puppala, H. Lee, K.B. Kim, H.I. Swanson, Development of an aryl hydrocarbon receptor antagonist using the proteolysis-targeting chimeric molecules approach: a potential tool for chemoprevention, Mol. Pharmacol. 73 (4) (2008) 1064–1071.
[329] N. Ohoka, G. Tsuji, T. Shoda, T. Fujisato, M. Kurihara, Y. Demizu, M. Naito, Development of Small Molecule Chimeras That Recruit AhR E3 Ligase to Target Proteins, ACS Chem. Biol. 14 (12) (2019) 2822–2832.
[330] S. Wolff, P.A. Harper, J.M. Wong, V. Mostert, Y. Wang, J. Abel, Cell-specific regulation of human aryl hydrocarbon receptor expression by transforming growth factor-beta(1), Mol. Pharmacol. 59 (4) (2001) 716–724.
[331] S.A. Tischkau, Mechanisms of circadian clock interactions with aryl hydrocarbon receptor signalling, Eur. J. Neurosci. 51 (1) (2020) 379–395.
[332] H.A. Zablon, C.I. Ko, A. Puga, Converging Roles of the Aryl Hydrocarbon Receptor in Early Embryonic Development, Maintenance of Stemness, and Tissue Repair, Toxicol. Sci. 182 (1) (2021) 1–9.
[333] C. Rejano-Gordillo, A. Ordiales-Talavero, A. Nacarino-Palma, J.M. Merino, F. J. Gonzalez-Rico, P.M. Fernandez-Salguero, Aryl Hydrocarbon Receptor: From Homeostasis to Tumor Progression, Front. Cell Dev. Biol. 10 (2022), 884004.
[334] S. Akhtar, S. Hourani, L. Therachiyil, A. Al-Dhfyan, A. Agouni, A. Zeidan, S. Uddin, H.M. Korashy, Epigenetic Regulation of Cancer Stem Cells by the Aryl Hydrocarbon Receptor Pathway, Semin. Cancer Biol. 83 (2022) 177–196.

2.2 Unraveling the differential impact of PAHs and dioxin-like compounds on AKR1C3 reveals the EGFR extracellular domain as a critical determinant of the AHR response

Christian Vogeley, Natalie C. Sondermann, Selina Woeste, Afaque A. Momin, Viola Gilardino, Frederick Hartung, Markus Heinen, Sophia K. Maaß, Melina Mescher, Marius Pollet, Katharina M. Rolfes, Christoph F.A. Vogel, Andrea Rossi, Dieter Lang, Stefan T. Arold, Motoki Nakamura, Thomas Haarmann-Stemmann

PAKs und DLCs können zur Entstehung unterschiedlicher Krankheiten und Störungen beitragen, indem sie den AHR aktivieren und die zelluläre Antwort formen. Unsere Forschung zeigt, dass der EGFR die AHR-gesteuerten Reaktionen in humanen Keratinozyten maßgeblich formt. Dies geschieht einerseits über den komplexen Crosstalk zwischen AHR und EGFR, welcher zur Aktivierung des EGFR führen kann, und andererseits über die Bindung von DLCs an die ECD des EGFR, welche den Rezeptor inhibieren können. So induzieren beispielsweise sowohl BaP als auch PCB126 die Aktivierung des EGFR, jedoch führt nur BaP zur Expression von AKR1C3.

Journal:	Environment International
Impact Factor:	10,3 (2024)
Beitrag zur Veröffentlichung:	20 % Experimente für Abb. 4, 5, 6
Art der Autorenschaft:	Co-Autorenschaft
Status der Publikation:	Veröffentlicht am 20.11.2021

Environment International 158 (2022) 106989

Contents lists available at ScienceDirect

Environment International

journal homepage: www.elsevier.com/locate/envint

Unraveling the differential impact of PAHs and dioxin-like compounds on AKR1C3 reveals the EGFR extracellular domain as a critical determinant of the AHR response

Christian Vogeley [a], Natalie C. Sondermann [a], Selina Woeste [a], Afaque A. Momin [b], Viola Gilardino [a], Frederick Hartung [a], Markus Heinen [a], Sophia K. Maaß [a], Melina Mescher [a], Marius Pollet [a], Katharina M. Rolfes [a], Christoph F.A. Vogel [c], Andrea Rossi [a], Dieter Lang [d], Stefan T. Arold [b,e], Motoki Nakamura [a,f], Thomas Haarmann-Stemmann [a,*]

[a] IUF – Leibniz-Research Institute for Environmental Medicine, 40225 Düsseldorf, Germany
[b] King Abdullah University of Science and Technology (KAUST), Computational Bioscience Research Center (CBRC), Division of Biological and Environmental Sciences and Engineering (BESE), Thuwal 23955-6900, Saudi Arabia
[c] Department of Environmental Toxicology and Center for Health and the Environment, University of California, Davis, CA 95616, USA
[d] Bayer AG, Pharmaceuticals, Research Center, 42096 Wuppertal, Germany
[e] Centre de Biologie Structurale (CBS), INSERM, CNRS, Université de Montpellier, F-34090 Montpellier, France
[f] Department of Environmental and Geriatric Dermatology, Graduate School of Medical Sciences, Nagoya City University, Nagoya 467-8601, Japan

ARTICLE INFO

Handling Editor: Hefa Cheng

Keywords:
Aldo-keto reductase 1C3
Aryl hydrocarbon receptor
Environmental pollutants
Epidermal growth factor receptor
Dioxin-like compounds
Polycyclic aromatic hydrocarbons

ABSTRACT

Polycyclic aromatic hydrocarbons (PAHs), dioxin-like compounds (DLCs) and structurally-related environmental pollutants may contribute to the pathogenesis of various diseases and disorders, primarily by activating the aryl hydrocarbon receptor (AHR) and modulating downstream cellular responses. Accordingly, AHR is considered an attractive molecular target for preventive and therapeutic measures. However, toxicological risk assessment of AHR-modulating compounds as well as drug development is complicated by the fact that different ligands elicit remarkably different AHR responses. By elucidating the differential effects of PAHs and DLCs on aldo–keto reductase 1C3 expression and associated prostaglandin D_2 metabolism, we here provide evidence that the epidermal growth factor receptor (EGFR) substantially shapes AHR ligand-induced responses in human epithelial cells, i.e. primary and immortalized keratinocytes and breast cancer cells. Exposure to benzo[a]pyrene (B[a]P) and dioxin-like polychlorinated biphenyl (PCB) 126 resulted in a rapid c-Src-mediated phosphorylation of EGFR. Moreover, both AHR agonists stimulated protein kinase C activity and enhanced the ectodomain shedding of cell surface-bound EGFR ligands. However, only upon B[a]P treatment, this process resulted in an auto-/paracrine activation of EGFR and a subsequent induction of aldo–keto reductase 1C3 and 11-ketoreduction of prostaglandin D_2. Receptor binding and internalization assays, docking analyses and mutational amino acid exchange confirmed that DLCs, but not B[a]P, bind to the EGFR extracellular domain, thereby blocking EGFR activation by growth factors. Finally, nanopore long-read RNA-seq revealed hundreds of genes, whose expression is regulated by B[a]P, but not by PCB126, and sensitive towards pharmacological EGFR inhibition. Our data provide novel mechanistic insights into the ligand response of AHR signaling and identify EGFR as an effector of environmental chemicals.

1. Introduction

The aryl hydrocarbon receptor (AHR) is a transcription factor that modulates gene expression in response to a variety of small molecular weight compounds, including numerous environmental pollutants of emerging concern, such as dioxins, dioxin-like polychlorinated biphenyls (PCBs) and polycyclic aromatic hydrocarbons (PAHs) (Murray et al., 2014; Rothhammer and Quintana, 2019; Vogel et al., 2020). Whereas AHR signaling driven by endogenous and dietary ligands, such as tryptophan metabolites and indoles, contributes to proper organ

* Corresponding author at: IUF – Leibniz-Research Institute for Environmental Medicine, Auf`m Hennekamp 50, 40225 Düsseldorf, Germany.
E-mail address: thomas.haarmann-stemmann@IUF-duesseldorf.de (T. Haarmann-Stemmann).

https://doi.org/10.1016/j.envint.2021.106989
Received 24 August 2021; Received in revised form 14 October 2021; Accepted 16 November 2021
Available online 20 November 2021

development and maintains cell and tissue homeostasis, a long-lasting activation of AHR by environmental chemicals may contribute to a variety of adverse health effects, including autoimmune and allergic inflammatory diseases, endocrine disruption and cancer (Murray et al., 2014; Roman et al., 2018; Rothhammer and Quintana, 2019; Stockinger et al., 2021; Vogel et al., 2020). Accordingly, AHR is considered an attractive target for the development of novel preventive and therapeutic measures. However, drug development as well as the toxicological risk assessment of AHR-modulating compounds is considerably complicated by a remarkable ligand-specificity of AHR signaling and associated outcome. An illustrating example is the opposing impact of dioxin-like compounds (DLCs) and PAHs on T cell differentiation and the development and worsening of allergic inflammatory diseases, such as asthma and atopic dermatitis. Whereas a chronic exposure to 2,3,7,8-tetrachlorodibenzo-*p*-dioxin (TCDD) and related DLCs induces immunosuppressive regulatory T cells (Funatake et al., 2005; Quintana et al., 2008), exposure to PAHs and PAH-rich airborne particulate matter suppresses regulatory T cell differentiation (Nadeau et al., 2010; O'Driscoll et al., 2018) and promotes the expansion of Th2 and Th17 cells (Castañeda et al., 2018; Hidaka et al., 2017; Hong et al., 2016; O'Driscoll et al., 2018; Weng et al., 2018; Wong et al., 2018; Xia et al., 2015). Accordingly, an exposure to free and particle-bound PAHs is associated with an increased risk for asthma and atopic dermatitis (Dijkhoff et al., 2020; Lag et al., 2020), whereas elevated systemic levels of DLCs correlate with a decreased incidence of atopic diseases (Nakamoto et al., 2013; Ye et al., 2018). Furthermore, transcriptome analyses revealed that different AHR ligands induce a different pattern of gene expression even within the same tissue or cell-type (Kopec et al., 2010; Nault et al., 2013; Souza et al., 2016). The molecular mechanisms responsible for this ligand specificity of AHR signaling are not well understood.

Inactive AHR is part of a cytosolic multiprotein complex consisting of a heat-shock protein 90 dimer, AHR-interacting protein, the co-chaperone p23 and cytoplasmic tyrosine kinase c-Src. Upon ligand-binding, this complex dissociates and AHR translocates into the nucleus, dimerizes with AHR nuclear translocator (ARNT) and binds to xenobiotic-responsive elements (XRE) in the enhancer region of target genes, e.g. encoding cytochrome P450 (CYP) 1A1 and CYP1B1, to induce their transcription (Murray et al., 2014; Roman et al., 2018; Rothhammer and Quintana, 2019; Stockinger et al., 2021; Vogel et al., 2020). In addition, there are multiple non-canonical functions of AHR, for instance involving a modulation of epidermal growth factor receptor (EGFR) and NF-E2-related factor 2 (NRF2) signaling pathways, that may shape the outcome of AHR signaling (Roman et al., 2018; Vogel et al., 2020).

The expression of human aldo–keto reductase (AKR) 1C3 is differentially regulated by prototypical AHR ligands, i.e. upregulated in response to PAHs but unaffected by TCDD treatment (Burczynski et al., 1999). AKR1C3 is a cytosolic NADPH-dependent oxidoreductase that catalyzes the biosynthesis of 17β-estradiol and testosterone and the reduction of prostaglandin (PG) D_2 and PGH_2 to 9α,11β-PGF_2 and $PGF_2\alpha$, respectively (Liu et al., 2020; Penning, 2019). Accordingly, AKR1C3 contributes to the pathogenesis of various types of cancer, inflammatory diseases and endocrine disorders (Liu et al., 2020; Penning, 2019). Despite its clinical relevance, the regulation of AKR1C3, particularly in response to environmental factors, is not well understood.

Here, we elucidated the molecular mechanisms underlying the ligand-specific differences in the AHR response of human epithelial cells. We identified a complex AHR- and EGFR-dependent signaling pathway which is initiated by PAH treatment to modulate the expression of hundreds of genes. Although initially stimulating similar signaling events, dioxin-like compounds (DLCs) interrupted this pathway by binding to the extracellular domain (ECD) of EGFR and inhibiting its activation by growth factors.

2. Material and methods

2.1. Cell culture

Normal human epidermal keratinocytes (NHEKs) obtained from PromoCell (Heidelberg, Germany) were cultured in Keratinocyte Growth Medium 2 (PromoCell). HaCaT, HaCaT-AHR-KO, HaCaT-CYP1A1-KO and HaCaT-NRF2-KO keratinocytes were cultured in DMEM low glucose (1 g/l) medium (PAN Biotech, Aidenbach, Germany) and supplemented with 10% FBS and antibiotics/antimycotics (PAN Biotech). Stable AHR-knockdown HaCaT keratinocytes (HaCaT-shAHR) and respective empty vector control cells (HaCaT-EV) were cultured in regular HaCaT medium supplemented with 0.68 mg/ml G418 (Carl Roth, Karlsruhe, Germany). MCF-7 and MCF-7-AHR-KO cells were cultured in DMEM high glucose (4.5 g/l) medium (PAN Biotech) supplemented with 10% FBS and antibiotics/antimycotics. The generation and characterization of HaCaT-shAHR and HaCaT-EV cells (Fritsche et al., 2007) and MCF-7-AHR-KO cells (Vogel et al., 2021) has been previously described. HepG2 cells were cultured in RPMI 1640 containing 10% FBS and antibiotics/antimycotics (PAN Biotech). All cells were kept in a humidified atmosphere of 5% CO_2 at 37 °C.

2.2. Chemicals and treatment

Benzo[a]pyrene, benzo[k]fluoranthene, bosutinib, 1,2-dithiole-3-thione, flufenamic acid, MG132, PP2, Ro-31-8220 and hydrogen peroxide were purchased from Sigma-Aldrich (Taufkirchen, Germany), BPIQII, SR11302 and T-5224 from Cayman Chemicals (Ann Arbor, MI), and CH223191, cobimetinib and glutathione from Selleckchem (Houston, TX). Marimastat was purchased from Santa Cruz Biotechnology (Dallas, TX) and PD153035 from Absource Diagnostics (Munich, Germany). 3,3′,4,4′,5-Pentachlorobiphenyl (PCB126) and 2,3′,4,4′,5-pentachlorobiphenyl (PCB118) were bought from LGC Standards (Wesel, Germany) and 2,3,7,8-tetrachlorodibenzo-*p*-dioxin from Amchro (Hattersheim am Main, Germany). Prostaglandin D_2, AREG, TGFα and EGF were purchased from PeproTech (Rocky Hill, NY). Hydrogen peroxide, glutathione and the three EGFR ligands were dissolved or diluted in water, the other compounds in DMSO. Treatment time and applied concentrations of the chemicals and human recombinant proteins is indicated in the figure legends.

2.3. Quantitative real-time PCR

Total RNA was isolated and transcribed into cDNA by using the GenUP Total RNA Kit (Biotechrabbit, Hennigsdorf, Germany) and a M−MLV reverse transcriptase (Promega, Walldorf, Germany). Quantitative real-time PCR analyses were carried using the QuantiFast SYBR Green PCR Kit and a Corbett-Rotor Gene 300 light cycler (Qiagen, Hilden, Germany). Oligonucleotide sequences are listed in supplementary table 1a.

2.4. Transient transfection of siRNA and plasmid DNA

Transient transfection of HaCaT cells with ARNT-targeted and non-silencing siRNA (Santa Cruz Biotechnology, Dallas, TX) was done using the INTERFERin reagent (Polyplus Transfection, Illkirch, France). JetPEI DNA Transfection Reagent (Polyplus) was used for transient transfection with plasmid DNA.

2.5. SDS-PAGE/Western blot analysis

Cells were lysed in RIPA buffer on ice and subsequently centrifuged for 5 min at 4 °C at maximum speed. Protein samples were separated by 10% and 12% SDS-polyacrylamide gel electrophoresis and blotted onto PVDF membranes (GE Healthcare, Freiburg, Germany). Blots were blocked with 5% skim milk or bovine serum albumin in TBS-Tween-20

(0.1%) for 1 h at room temperature and subsequently incubated overnight at 4 °C with primary antibodies. Blots were washed and then incubated for 1 h with a 1:5000 dilution of HRP-conjugated secondary antibodies (Cell Signaling Technology, Leiden, The Netherlands) in 5% bovine serum albumin in TBS-Tween-20 (0.1%) at room temperature. Bands were visualized using WesternBright ECL HRP substrate (Advansta, San Jose, CA) and a C-DiGit Western Blot Scanner (LI-COR Biotechnology, Lincoln, NE). Primary antibodies are listed in supplementary table 1b.

2.6. Incubation of AKR isoforms with PGD_2

The incubation mixtures contained 50 mM phosphate buffer (pH 7.4) with 1 mM EDTA, 400 pmol/mL of recombinant AKRs and a NADPH generating system consisting of 1 mM NADP+, 5 mM glucose 6-phosphate, 0.5 IU of glucose 6-phosphate dehydrogenase and 2 μM PGD_2. After a preincubation of 2 min at 37 °C, the reaction was initiated by the addition of the NADPH generating system and was allowed to continue at 37 °C for up to 60 min. Incubations were terminated with the addition of 30% (v/v) acetonitrile. Protein was precipitated by centrifugation, and the supernatants were subjected to LC-MS analysis.

2.7. LC–MS analyses

Incubations were analyzed using reversed-phase HPLC with a Synergi Hydro-RP 4 μm, 150 × 2 mm column (Phenomenex, Aschaffenburg, Germany) and gradient elution using 10 mM ammonium formate and acetonitrile containing 0.1% formic acid as solvents. The HPLC was coupled to a high-resolution Orbitrap Fusion™ Tribride™ mass spectrometer (Thermo Fisher Scientific, Bremen, Germany) operated in full-scan mode. Selectivity of the analytes was gained by extracting a very narrow mass range in the order of 10–20 ppm of the exact mass of the analyte. 9α,11β-PGF_2 was identified using authentic standard.

2.8. Generation of CRISPR/Cas9 and CRISPR/Cas12 mutated cells

The generation of CYP1A1-KO and NRF2-KO HaCaT keratinocytes was carried out as described previously (Vogel et al., 2021). The respective gRNAs (Fig. S1) were designed using the CRISPR design tool CHOPCHOP (http://chopchop.cbu.uib.no/) and cloned into a modified version of the PX458 plasmid available at Addgene (#48138). The resulting bicistronic vectors each encoded the respective gRNA and the Cas9 nuclease. AHR-KO HaCaT keratinocytes were generated delivering a ribonucleoprotein consisting of a Cas12 protein (IDT) in complex with a targeting gRNA. Activity of the gRNAs and their efficiency were assessed *via* high resolution melt analysis. HaCaT cells were transfected with nuclease plasmids in antibiotic-free medium in a 12-well plate using FuGENE HD (Roche, Mannheim, Germany) or the NEON electroporation system (Thermo Fisher Scientific). After 48 h, cells were sorted (FACS or MACS) and plated as single cells in a 96-well plate and duplicated after a week. Clones were lysed in proteinase K and genotyped using high-resolution melt analysis, SANGER sequencing or deep sequencing using a MiSeq Illumina (San Diego, CA) (Ramachandran et al., 2021).

2.9. PKC activity assay

PKC activity was analyzed by using the PKC Kinase Activity Kit (Enzo Life Sciences, Loerrach, Germany). Treatment medium was removed from the cells were washed with PBS twice. Lysates were prepared using 100 μl MOPS lysis buffer and samples were analyzed according to manufacturer's instructions.

2.10. ELISA-based quantification of growth factors

The concentration of TGFα and AREG in cell culture supernatant was determined by using respective Quantikine ELISA Kits (Bio-Techne, Wiesbaden, Germany). Therefore, the supernatant from treated cells was transferred into microtubes and centrifuged at 5000 rcf at 4 °C for 5 min. The supernatant was analyzed according to manufacturer's instructions.

2.11. EGFR docking analyses

Crystal structures of the extracellular domain of EGFR in an inactive complex with EGF (PDB ID:1nql) and dimeric (2:2) complex of EGFR and EGF (PDB ID: 1ivo) were used to perform docking analyses. Ligand structures for TCDD (PubChem CID: 15625), PCB126 (PubChem CID: 63090), 1,2,3,7,8-pentachlorodibenzo-*p*-dioxin (PCDD; PubChem CID: 38439), 1,2,3,4,7,8-hexachlorodibenzo-*p*-dioxin (HCDD; PubChem CID: 38251), 2,3,7,8-tetrachlorodibenzofuran (TCDF; PubChem CID: 39929), 3,3′,4,4′-tetrachlorobiphenyl (PCB77; PubChem CID: 36187), PCB118 (PubChem CID: 35823), and B[a]P (PubChem CID:125144) were downloaded from PubChem database (Kim et al., 2016) in SD format. The EGF domain was removed from the protein structure using PyMol (www.pymol.org), and ligand structures were converted to PDB format using OpenBabel 2.3.1 (O'Boyle et al., 2011). Flexible docking was performed using AutoDock 4.2 (Goodsell et al., 1996) as previously described (Hawerkamp et al., 2019), except that the size for the grid box (x,y,z points) were set to 51 × 39 × 58, while centers for the grid were designated at X = 113.38, Y = 65.95, Z = 39.94 dimensions. The final docking poses were analyzed with PyMol (www.pymol.org).

2.12. EGFR internalization assay

Internalization of EGFR was investigated using a High-Content-Screening method adapted from Wang *et al.* (Wang and Xie, 2007). Cells were treated with 200 ng/ml EGF-AF555 (Thermo Fisher Scientific, Waltham, MA) for 2.5 min on ice. Afterwards the test compounds were added and incubated for another 2.5 min on ice. Internalization was enabled by incubating the cells at 37 °C and 5 % CO_2 for 25 min. The cells were fixed with 4 % paraformaldehyde. The membrane was stained with Wheat Germ Agglutinin, Oregon Green™ 488 Conjugate and the nuclei with Hoechst33342 (both Thermo Fisher Scientific). HCS analysis was performed using a Cellomics ArrayScan VTI (Thermo Fisher Scientific) and the images were analyzed with the HCS Studio Cellomics Scan software (version 6.6.0).

2.13. EGF-EGFR AlphaLISA binding assay

A potential disturbance of the binding of EGF to EGFR by the test compounds was analyzed by using the cell-free EGF/EGFR AlphaLISA Binding Kit (PerkinElmer, Waltham, MA).

2.14. Site-directed mutagenesis

For the generation of point-mutated EGFR variants, the pCMV3-$EGFR^{wt}$ plasmid (Sino Biological, Eschborn, Germany) was used as template. Briefly, a high fidelity Q5 polymerase (New England Biolabs, Ipswich, MA) was used to amplify the whole plasmid with complementary primer pairs, carrying the desired mutation in the form of mismatches to the original plasmid. PCR conditions were: 94 °C for 2 min, 21 cycles of 94 °C (30 sec), 55 °C (1 min) and 68 °C (30 sec/kb). After three cycles, the oligonucleotides for the introduction of the respective point-mutations were added; primer sequences are listed in supplementary table 1c. Afterwards, the PCR mix was treated with DpnI endonuclease (New England Biolabs) to remove parental DNA. The successful introduction of point-mutations was validated by Sanger Sequencing.

2.15. Measurement of DNA synthesis

DNA synthesis was assessed using a colorimetric BrdU incorporation

assay (Sigma-Aldrich, Taufkirchen, Germany). Briefly, HaCaT keratinocytes were seeded on 96-well-plates in quintuplicate ($2x10^4$ per well) and starved overnight. Approximately 12 h later, the cells were treated with the respective test substances and BrdU labeling solution for 4 h. Subsequently, the assay was carried out according to the manufacturers protocol. Finally, after 15 min incubation with substrate solution, absorbance was measured at 370 nm (reference wavelength 492 nm) using the Infinite 200 PRO plate-reader (Tecan, Maennedorf, Switzerland).

2.16. ROS measurement

Cells were incubated with 100 μM DCF-diacetate diluted in PBS *post* treatment for 30 min at 37 °C and 5 % CO_2. Afterwards, the DCF-diacetate dilution was removed and the fluorescence at $485_{ex}/535_{em}$ nm was measured using the Infinite 200 PRO plate-reader (Tecan).

2.17. CYP1A1 activity assay

Measurement of the deethylation of 7-ethoxyresorufin in living monolayer cultures was carried out as described previously (Frauenstein et al., 2015).

2.18. Library preparation and sample loading for long-read nanopore RNA-sequencing

Quality of isolated RNA was assessed using the High Sensitivity RNA Screen Tape System (Agilent Technologies, Santa Clara, CA). Reverse transcriptase and multiplexing of the samples were performed with the PCR cDNA Barcoding Kit (SQK-PCB109, Oxford Nanopore Technologies, Oxford, United Kingdom) using 50 ng total RNA. Quantity of amplified cDNA was determined with the Qubit™ 4 Fluorometer (Invitrogen, Carlsbad, CA) and the range of fragment size was examined using the Agilent D1000 SreenTape assay (Agilent Technologies). The Flowcell (FLO-MIN106) was prepared with the FlowCell Priming Kit (EXP FLP002, Oxford Nanopore Technologies) and equal amounts of barcoded cDNA was loaded. Sequencing was carried out with a MinION (MN33710) using the MinKNOW software (v.21.02.1) over a period of 72 h.

2.19. RNA-Seq data analysis

Raw fast5 reads were base-called and demultiplexed using Guppy (v4.5.4 + 66c1a7753). Reads were aligned to the reference genome (GRCh38.94) using Minimap2 (Li, 2018). Uniquely mapped reads were summarized with the featureCounts function of the R (v4.0.3) package Rsubread (v1.32.2) (Liao et al., 2019). Differential expression analysis was performed with DESeq2 (v1.22.1) (Love et al., 2014) and clusterProfiler (v4.0.0) (Yu et al., 2012) was used for gene set enrichment analysis.

2.20. Multiple sequence alignment

The multiple alignment of the N-terminal 420 amino acids of the EGFR protein (mature) from various mammalian species was carried out using Clustal Omega (v1.2.4) (Sievers et al., 2011) and the following NCBI Reference Sequences: *Homo sapiens*, NP_005219.2; *Macaca mulatta*, XP_014988922.2; *Callithrix jacchus*, XP_035109337.1; *Mus musculus*, NP_997538.1; *Rattus norvegicus*, AAF14008.1; *Oryctolagus cuniculus*, XP_008260065.1; *Sus scrofa*, NP_999172.1; *Ovis aries*, XP_014957685.2; *Felis catus*, XP_006929148.1; *Canis lupus dingo*, XP_025305356.1.

2.21. Statistical analysis

All data shown are mean (±standard deviation) from three or more independent experiments, if not indicated otherwise. Differences were considered significant at $p \leq 0.05$. A comparison of two groups was performed by unpaired, two-tailed Student's *t* test. A comparison of multiple groups was conducted with analysis of variance followed by a Tukey *post hoc* analysis to correct for multiple comparison.

3. Results

3.1. B[a]p but not PCB126 induces AKR1C3 expression in an AHR-dependent manner

Treatment of NHEKs with 2.5 μM of the PAH benzo[*a*]pyrene (B[a]P) and 1 μM of the DLC 3,3′,4,4′,5-pentachlorobiphenyl (PCB126) for 24 h increased *CYP1A1* copy numbers to a similar extent (Fig. 1a). In contrast, the *AKR1C3* transcript level was only induced by B[a]P but not by PCB126 treatment. Dose- and time course studies in immortalized human HaCaT keratinocytes confirmed a strict AHR ligand-dependent regulation of *AKR1C3* (Fig. 1b, S2a). Accordingly, exposure to benzo[*k*]fluoranthene (B[k]F) induced the expression of both *CYP1A1* and *AKR1C3*, whereas TCDD treatment only increased the copy numbers of *CYP1A1* (Fig. S2b). Gene and protein expression analyses of B[a]P- and PCB126-treated *AHR*-knockdown (HaCaT-shAHR) and CRISPR/Cas12-engineered *AHR*-knockout (HaCaT-AHR-KO) keratinocytes, *AHR*-knockout human MCF-7 breast cancer cells (MCF-7-AHR-KO) and respective AHR-proficient controls confirmed a ligand-specific and AHR-dependent upregulation of AKR1C3 (Fig. 1c,d, S2c,d). Further qPCR analyses revealed a similar expression pattern for other AKR1 isoforms, i.e. *AKR1C2* and *AKR1B10* (Fig. S2e). Hence, in contrast to PCB126, a treatment of human epithelial cells with B[a]P induces the expression of *AKR1C3* and related isoforms in an AHR-dependent manner.

3.2. B[a]p but not PCB126 stimulates PGD_2 metabolism

Next, we assessed potential alterations in AKR1C3 enzyme activity and analyzed the 11-ketoreduction of PGD_2. An incubation of 2 μM PGD_2 with microsomal preparations of heterologously expressed human AKR1C isoforms revealed an efficient and NADPH-dependent reduction of PGD_2 to 9α,11β-PGF_2 by AKR1C3 (Fig. S2f). AKR1C1 and AKR1C2 were roughly 10-times less effective in reducing PGD_2, whereas the liver-specific isoform AKR1C4 only had a minor impact. A pretreatment of AHR-proficient cells with B[a]P resulted in an enhanced formation of 9α,11β-PGF_2 as compared to solvent controls (Fig. 1e). This effect was neither observed in cells pretreated with PCB126 nor in B[a]P-exposed HaCaT-shAHR keratinocytes. AHR-dependency of the B[a]P-induced generation of 9α,11β-PGF_2 was confirmed in NHEKs cotreated with the AHR antagonist CH223191 (Fig. S2g). Moreover, a co-treatment of HaCaT cells and NHEKs with B[a]P and the AKR1C3 inhibitor flufenamic acid (FFA) blunted the B[a]P-stimulated reduction of PGD_2 to 9α,11β-PGF_2 (Fig. 1f, S2g). Taken together, these data provide evidence that in contrast to PCB126 an exposure of human primary and immortalized keratinocytes to B[a]P stimulates the AKR1C3-catalyzed metabolism of PGD_2 in an AHR-dependent manner.

3.3. B[a]p induces AKR1C3 expression independently from canonical AHR signaling

A transient RNAi-mediated knockdown of ARNT dampened the B[a]P-induced upregulation of CYP1A1 by approximately 40% but did not affect the B[a]P-mediated induction of AKR1C3 protein (Fig. 2a), indicating that AKR1C3 is not part of the AHR/XRE gene battery. Treatment of HaCaT cells with PP2, a pharmacological inhibitor of Src family kinases and potent AHR agonist (Frauenstein et al., 2015), elevated the transcript numbers of *CYP1A1* but not of *AKR1C3* (Fig. 2b), suggesting an upregulation of *AKR1C3* through the non-canonical c-Src- and EGFR-dependent signaling pathway (Dong et al., 2011; Fritsche et al., 2007).

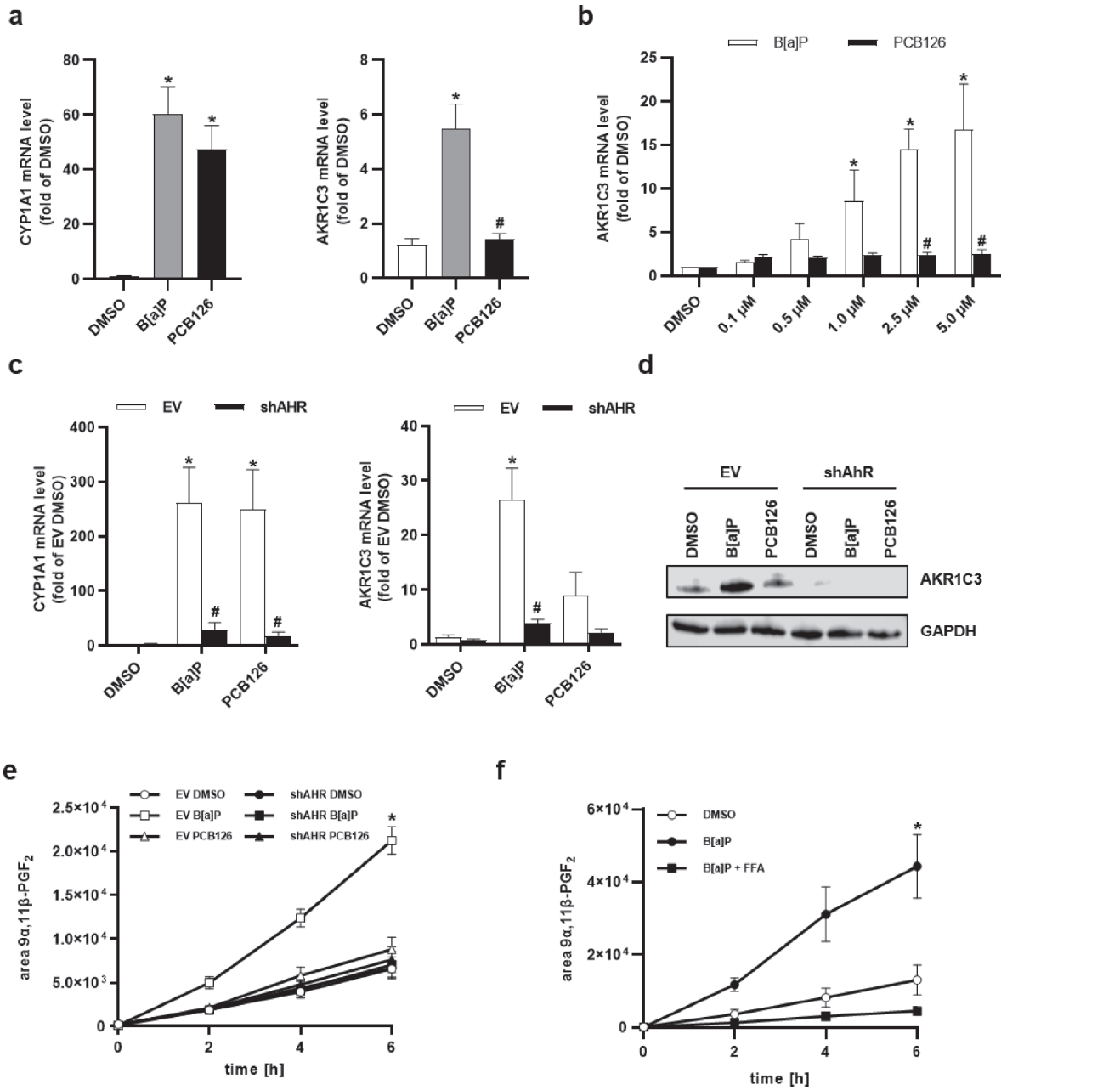

Fig. 1. B[a]P induces AKR1C3 expression in an AHR-dependent manner. **a** qRT-PCR analyses of *CYP1A1* and *AKR1C3* in NHEKs stimulated with B[a]P (2.5 µM), PCB126 (1 µM) or solvent (0.1 % DMSO) for 24 h. n = 9. *, p ≤ 0.05 compared to DMSO; #, p ≤ 0.05 compared to B[a]P. **b** qRT-PCR analysis of *AKR1C3* in HaCaT keratinocytes stimulated as indicated for 24 h. n = 6. *, p ≤ 0.05 compared to DMSO control, #, p ≤ 0.05, compared to B[a]P of the same concentration. **c** qRT-PCR analyses of *CYP1A1* and *AKR1C3* in HaCaT-shAHR and HaCaT-EV keratinocytes exposed to 2.5 µM B[a]P, 1 µM PCB126 or 0.1 % DMSO for 24 h. n = 4. *, p ≤ 0.05 compared to EV DMSO, #, p ≤ 0.05 compared to EV B[a]P. **d** Western blot analyses of AKR1C3 protein content in HaCaT-shAHR and HaCaT-EV keratinocytes stimulated as described in **c**. GAPDH level served as loading control. n = 3, representative picture. **e** LC-MS analyses of supernatants derived from HaCaT-shAHR and HaCaT-EV cells stimulated with 0.1 % DMSO, 1 µM PCB126 or 2.5 µM B[a]P for 24 h. Afterwards, cells were treated with 1 µM PGD_2 in conditioned medium and supernatants were collected at indicated time points. n = 3. *, p ≤ 0.05 compared to DMSO. **f** LC-MS analyses of the supernatants of HaCaT cells treated with 0.1 % DMSO and 2.5 µM B[a]P for 24 h. In addition, HaCaT cells pretreated for 23 h with 2.5 µM B[a]P were co-exposed for 1 h to 50 µM flufenamic acid (FFA) and B[a]P. Subsequently, cells were treated with 1 µM PGD2 in conditioned medium and the supernatant was collected at indicated time points. Supernatants were collected at indicated time points. n = 3. *, p ≤ 0.05 compared to DMSO.

This was supported by the observation that treatment with the EGFR ligand amphiregulin (AREG) increased *AKR1C3* copy numbers independently of AHR (Fig. 2c). An AREG-inducible expression of *AKR1C3* was also confirmed in NHEKs (Fig. 2d).

3.4. Treatment with B[a]P but not PCB126 results in a biphasic activation of EGFR

In line with earlier reports (Bessede et al., 2014; Dong et al., 2011), AHR activation by B[a]P and PCB126 resulted in a rapid phosphorylation of c-Src Y416 (Fig. 2e). This was accompanied by a phosphorylation of EGFR residue Y845, a substrate of c-Src (Chen et al., 2016), after 15 min of treatment with both AHR agonists (Fig. 2f). Upon B[a]P

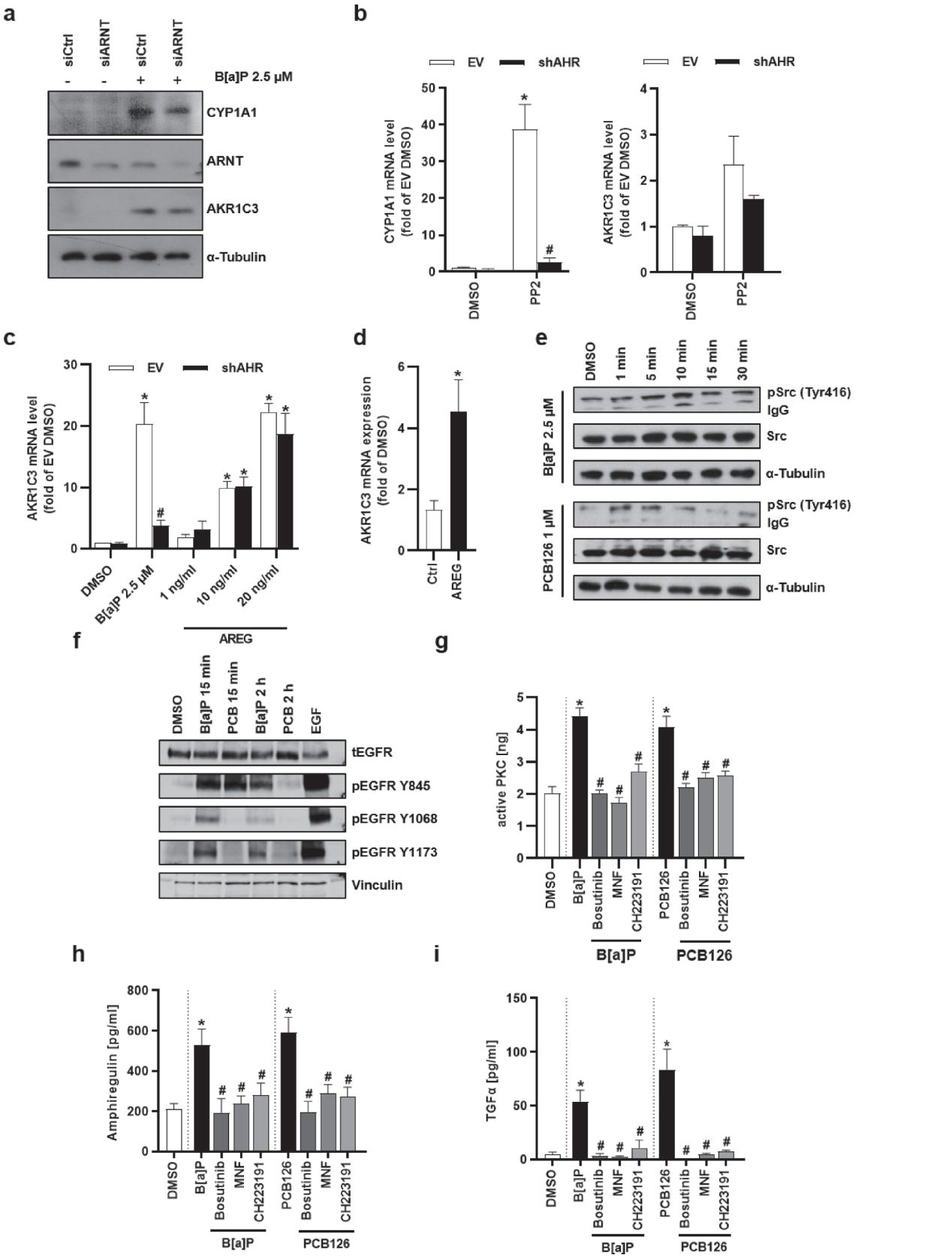

(caption on next page)

Fig. 2. B[a]P stimulates AKR1C3 expression in an EGFR-dependent manner. **a** HaCaT keratinocytes were transiently transfected with ARNT-targeted or non-silencing siRNA for 24 h. Next, cells were treated with 2.5 μM B[a]P or solvent for another 24 h. The protein level of CYP1A1, ARNT and AKR1C3 was detected by western blot analyses, α-tubulin was used as loading control. n = 2, representative pictures. **b** qRT-PCR analyses of *CYP1A1* and *AKR1C3* in HaCaT-shAHR and HaCaT-EV cells treated with 10 μM PP2 or 0.1 % DMSO for 24 h. n = 4. *, $p \leq 0.05$ compared to EV DMSO, #, $p \leq 0.05$ compared to EV B[a]P. **c** qRT-PCR analyses of *CYP1A1* and *AKR1C3* in HaCaT-shAHR and HaCaT-EV keratinocytes treated as indicated for 24 h. n = 4–7. *, $p \leq 0.05$ compared to EV DMSO, #, $p \leq 0.05$ compared to EV B[a]P. **d** NHEKs were treated with 20 ng/ml AREG for 24 h and *AKR1C3* transcript level were analyzed by qRT-PCR. **e** Western blot analyses of SRC and its phosphorylated form (Y416). HaCaT keratinocytes were treated with B[a]P (2.5 μM), PCB126 (1 μM) or 0.1 % DMSO for the indicated time. n = 3, representative pictures. **f** Phosphorylation of EGFR in HaCaT keratinocytes treated with B[a]P (2.5 μM) or PCB126 (1 μM) was examined by western blot analysis. Cells were treated for 15 min and 2 h. DMSO (0.1 %) served as solvent control, EGF (10 ng/ml) as positive control. n = 3, representative picture. **g** Levels of activated PKC were quantified using a non-radioactive protein kinase activity assay. HaCaT keratinocytes were pre-treated with Bosutinib (1 μM), MNF (20 μM), CH223191 (10 μM) or 0.1 % DMSO for 1 h. Afterwards, cells were stimulated with B[a]P (2.5 μM) or PCB126 (1 μM) and 0.1 % DMSO. After 2 h, cells were lysed and PKC activity was determined. ELISA-based quantification of **h** AREG and **i** TGFα in the cell culture supernatants. Cells were treated as described in **g.** Supernatants were collected 2 h after treatment. n = 4. *, $p \leq 0.05$ compared to DMSO, #, $p \leq 0.05$ compared to either B[a]P or PCB126 treated cells respectively.

treatment, an additional phosphorylation of EGFR at residues Y1068 and Y1173 was observed, indicating an EGFR ligand-mediated activation and subsequent autophosphorylation of the receptor tyrosine kinase (RTK) (Chen et al., 2016). After elongating the treatment time (2 h), these two residues were still phosphorylated in B[a]P-treated but not in PCB126-exposed cells (Fig. 2f). Importantly, c-Src may also activate PKC (Joseloff et al., 2002), which subsequently stimulates metalloproteases, such as A Disintegrin And Metalloprotease (ADAM) 17, to shed the ectodomain of cell-surface bound EGFR ligands, including AREG and transforming growth factor α (TGFα) (Chen et al., 2016; Seals and Courtneidge, 2003). Indeed, a 2 h exposure of HaCaT cells to B[a]P and PCB126 stimulated both PKC enzyme activity (Fig. 2g) and the release of AREG and TGFα in an AHR- and c-Src-dependent manner (Fig. 2h,i). Hence, although both AHR ligands stimulate the phosphorylation of c-Src and EGFR Y845 and activate PKC and associated shedding of EGFR ligands, only B[a]P mimicked an EGF-induced EGFR autophosphorylation (Y1068, Y1173). Accordingly, we noted AHR ligand-specific differences in the phosphorylation of EGFR downstream extracellular-regulated kinase 1/2 (ERK). B[a]P exposure of HaCaT cells caused a biphasic phosphorylation of ERK, with peaks observed after 5 and 120 min (Fig. 3a). On the contrary, PCB126 treatment only stimulated ERK phosphorylation at an early timepoint, i.e. after 15 min (Fig. 3b). Further experiments revealed that the early phosphorylation of EGFR residue Y845 induced by both B[a]P and PCB126 was sensitive towards AHR antagonists (MNF, CH223191), the Src kinase inhibitor bosutinib and the EGFR blocker PD153035, but not towards inhibition of PKC (Ro-31–8220) and metalloproteases (marimastat) (Fig. 3c,d). In contrast, the B[a]P-induced phosphorylation of EGFR residue Y1068 after 2 h of treatment was attenuated by all inhibitors tested (Fig. 3e). An analysis of B[k]F-treated HaCaT cells confirmed an enhanced phosphorylation of EGFR (Y1068) after 2 h, which was sensitive towards pharmacological inhibition of Src kinase and PKC (Fig. S3).

3.5. Inhibition of non-canonical AHR signaling abrogates the B[a]P-mediated AKR1C3 induction

So far, our data provide evidence that B[a]P and PCB126 have a differential impact on EGFR activation, with B[a]P causing a longer lasting activation through an extracellular stimulus. This was supported by co-treatment of HaCaT cells, NHEKs and MCF-7 cells with various pharmacological inhibitors, revealing that the B[a]P-induced upregulation of *AKR1C3* involved c-Src (bosutinib), PKC (RO-31–8220), metalloprotease activity (marimastat), EGFR (PD153035, BPIQII) and MEK (cobimetinib) (Fig. 3f–h, Fig. S4). Importantly, the B[a]P-triggered induction of *AKR1C3* was also reduced by the addition of an EGFR-blocking antibody in HaCaT cells (Fig. 3f) as well as by co-exposure to PCB126 in MCF-7 cells (Fig. S4). The latter observation indicates that although stimulating similar AHR-dependent signaling events as B[a]P, PCB126 may interfere with the growth factor-triggered autophosphorylation of EGFR and downstream signal transduction required for *AKR1C3* induction.

3.6. The AHR- and EGFR-dependent upregulation of AKR1C3 is mediated by NRF2

Transcription factors of the AP-1 family are well-known executors of the MEK/ERK axis, a co-exposure of HaCaT cells to two pharmacological AP-1 inhibitors, however, did not reduce the B[a]P-mediated upregulation of *AKR1C3* (Fig. S5a). Another transcription factor known to control *AKR1C3* expression by binding to antioxidant response elements in its promoter sequence is NRF2 (Tebay et al., 2015). In unstressed cells, NRF2 is rapidly degraded by the proteasome. Upon oxidative, metabolic or oncogenic stress, NRF2 accumulates in the cytosol and subsequently translocates into the nucleus (Tebay et al., 2015). Interestingly, AHR stimulates NRF2 activity in ketoconazole-treated NHEKs independently of oxidative stress (Tsuji et al., 2012), and it was suggested that this process involves EGFR and downstream MEK/ERK signal transduction (Haarmann-Stemmann et al., 2012). We found that treatment of HaCaT keratinocytes for 6 h with either B[a]P or a combination of 1,2-dithiole-3-thione (D3T), which activates NRF2 *via* ERK (Manandhar et al., 2007), and the proteasome inhibitor MG132 resulted in an accumulation of NRF2 protein, whereas exposure to PCB126 did not (Fig. 4a). Accompanying qPCR analyses revealed a slight increase after 6 h and a significant increase of the AKR1C3 transcript numbers after 12 h of B[a]P treatment (Fig. S5b). Co-exposure to EGFR and MEK inhibitors attenuated the B[a]P-triggered accumulation of NRF2 (Fig. 4a), suggesting that NRF2 may be involved in the PAH-specific upregulation of AKR1C3. To confirm this, we next engineered NRF2-knockout HaCaT (HaCaT-NRF2-KO) cells, which neither expressed detectable amounts of NRF2 protein nor responded to a treatment with D3T by upregulating heme oxygenase-1 (*HO-1*) expression (Fig. S5c,d). Exposure of HaCaT and HaCaT-NRF2-KO cells to B[a]P and PCB126 resulted in an upregulation of *CYP1A1* in both cell-lines, whereas *AKR1C3* expression was only inducible by B[a]P in the NRF2-proficient keratinocytes (Fig. 4b). Depending on parameters, such as the capacity of the conjugating and antioxidant enzyme systems, an exposure to PAHs may cause the generation of reactive oxygen species (ROS). Interestingly, AKR1C3 is known to convert the CYP1A1-derived B[a]P metabolite B[a]P-7,8-*trans*-hydrodiol to B[a]P-7,8-catechol, which then may undergo redox-cycling (Park et al., 2008). To exclude this potential source of ROS, we generated CYP1A1-knockout HaCaT cells (HaCaT-CYP1A1-KO), which exhibited neither basal nor B[a]P-inducible CYP1A1 enzyme activity (Fig. S5e). As expected, exposure studies revealed a B[a]P- and PCB126-inducible expression of *CYP1A1* in the control cells, but not in the HaCaT-CYP1A1-KO cells. However, B[a]P treatment increased *AKR1C3* expression in both cell-lines (Fig. S5f) and thus independently from CYP1A1 activity and potentially associated ROS and genotoxic metabolites. This was confirmed by ROS measurements in HaCaT cells, showing no signs of oxidative stress 6 h after treatment with B[a]P and PCB126 (Fig. 4c). Moreover, neither the B[a]P- nor the D3T-induced upregulation of *AKR1C3* was significantly affected by a co-treatment with glutathione (Fig. 4d), which, as expected, efficiently decreased H_2O_2-related oxidative stress (Fig. S5g). In case the B[a]P-induced upregulation of *AKR1C3* occurred *via* the AHR-EGFR-NRF2 axis, a

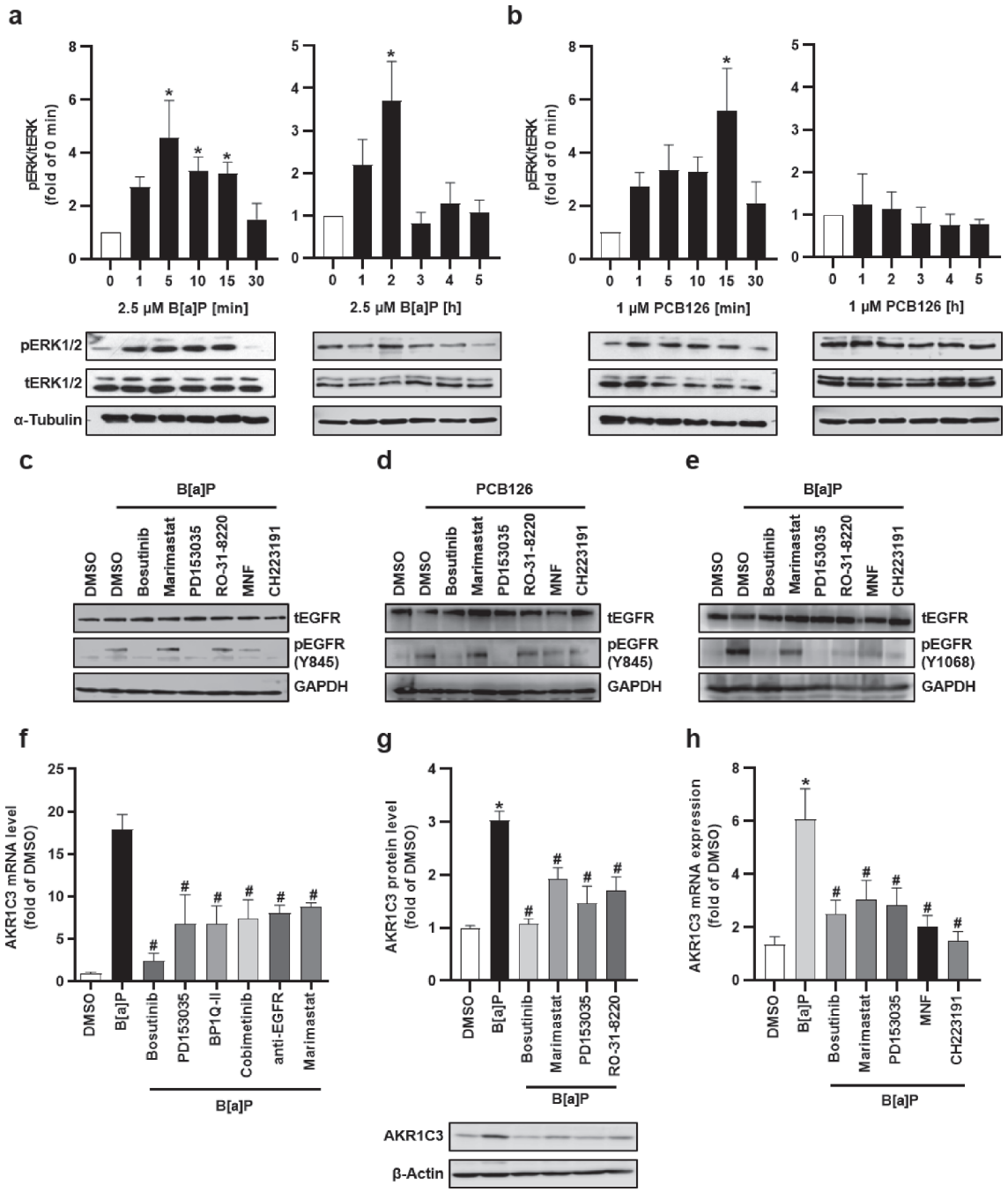

Fig. 3. B[a]P stimulates AKR1C3 expression through a non-canonical signaling pathway. Western blot analyses of ERK1/2 phosphorylation upon exposure to **a** B[a]P (2.5 µM) and **b** PCB126 (1 µM) for the indicated time points. In the upper panel the densitometric quantification, in the lower panel representative blots are shown. n = 3 – 5. *, p ≤ 0.05 compared to DMSO. Western blot analysis of HaCaT cells treated with **c** B[a]P (2.5 µM) and **d** PCB126 (1 µM) for 15 min or **e** B[a]P (2.5 µM) for 2 h. In parallel, cells were co-treated with bosutinib (1 µM), marimastat (1 µM), PD153035 (1 µM), RO-31–8220 (1 µM), MNF (20 µM), CH223191 (10 µM) or DMSO (0.1 %). In **c** and **d** EGFR phosphorylation at residue Y845 and in **e** EGFR phosphorylation at residue Y1068 was examined. All results were normalized to total EGFR, GAPDH was used as loading control. n = 3, representative pictures. **f** qRT-PCR analyses of *AKR1C3* in HaCaT keratinocytes. The cells were treated with B[a]P (2.5 µM) in the absence and presence of either Bosutinib (1 µM), PD153035 (1 µM), BP1-QII (1 µM), Cobimetinib (1 µM), EGFR-blocking antibody (4 µg/ml), Marimastat (1 µM) or DMSO (0.1 %) for 24 h. n = 3 – 6. *, p ≤ 0.05 compared to DMSO, #, p ≤ 0.05 compared to B[a]P. **g** Western blot analysis of AKR1C3 protein level in HaCaT keratinocytes. Cells were treated as indicated at the concentrations depicted in **f** for 24 h. In the lower panel a representative blot, in the upper panel the densitometric quantification is shown. n = 3. *, p ≤ 0.05 compared to DMSO, #, p ≤ 0.05 compared to B[a]P. **h** qRT-PCR analyses of *AKR1C3* in NHEKs treated for 24 h with B[a]P (2.5 µM) in the absence and presence of either Bosutinib (1 µM), PD153035 (1 µM), Marimastat (1 µM), MNF (20 µM), CH223191 (10 µM) or DMSO (0.1 %). Additional cells were treated with 20 ng/ml AREG. n = 7. *, p ≤ 0.05 compared to DMSO, #, p ≤ 0.05 compared to B[a]P.

stimulation of HaCaT-NRF2-KO cells with EGFR ligands should not affect *AKR1C3* copy numbers. Indeed, exposure to both EGF and AREG induced *AKR1C3* expression to a similar extent in NRF2-proficient but not in NRF2-KO cells (Fig. 4e). Although we will not exclude an occurrence of ROS during the 24 h treatment with the AHR agonists, the above data argue against a major contribution of oxidative stress to the PAH-stimulated upregulation of AKR1C3. Taken together, our results strongly indicate that PAHs induce AKR1C3 expression in an AHR-,

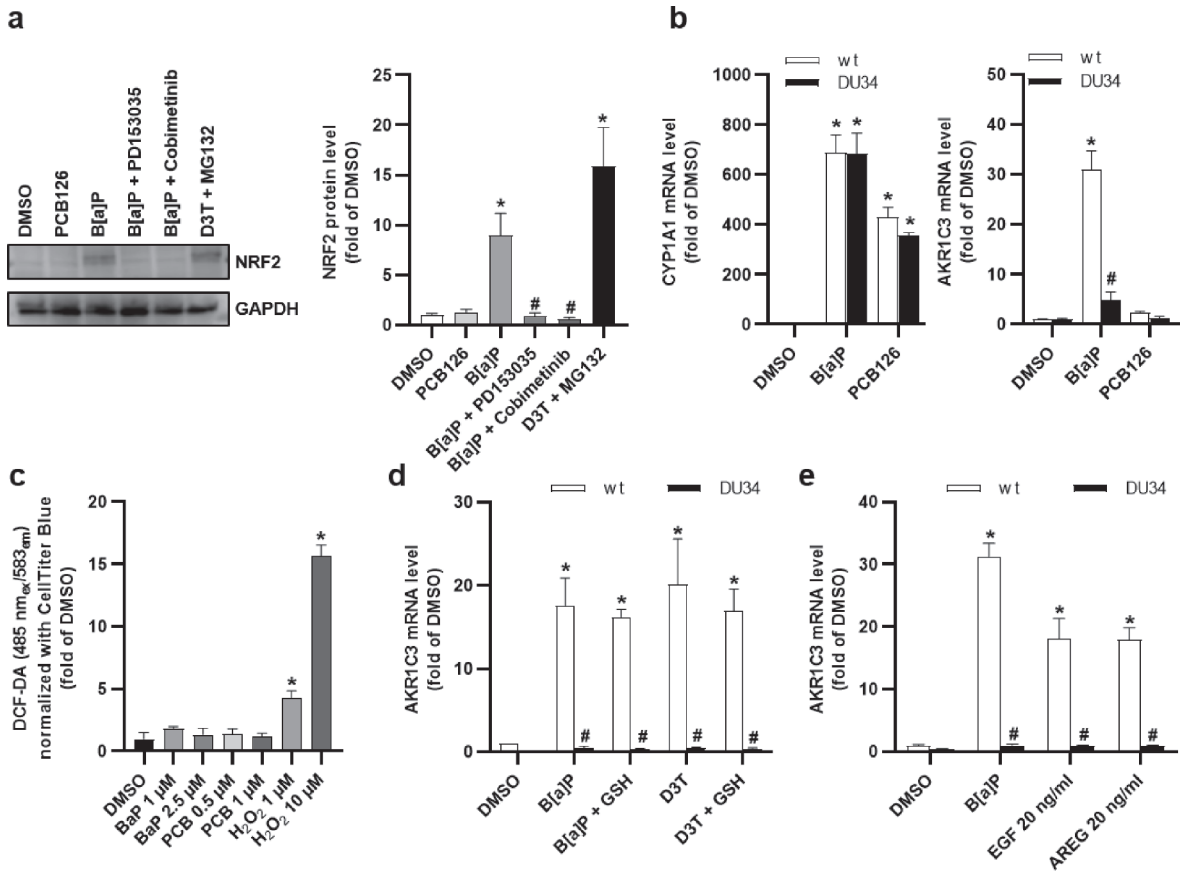

Fig. 4. Induction of AKR1C3 depends on NRF2 in HaCaT keratinocytes. **a** Western blot analyses of NRF2 protein stabilization. Cells were treated as indicated, the co-treatment with D3T (70 µM) and MG-132 (10 µM) served as positive control. Whole cell lysates were prepared 6 h post stimulation. GAPDH was used as loading control. On the left a representative western blot, on the right the densitometric quantification is shown. n = 4. *, p ≤ 0.05 compared to DMSO, #, p ≤ 0.05 compared to B[a]P. **b** qRT-PCR analyses of *CYP1A1* and *AKR1C3* in HaCaT and HaCaT-NRF2-KO (DU34) keratinocytes. Cells were treated with B[a]P (2.5 µM), PCB126 (1 µM) or DMSO (0.1 %) DMSO for 24 h. n = 3. *, p ≤ 0.05 compared to DMSO HaCaT control, #, p ≤ 0.05 compared to the respective proficient HaCaT control. **c** ROS formation was analyzed using the DCF-DA assay. HaCaT cells were treated as indicated for 6 h. As a positive control cells were treated with H_2O_2 30 min prior to staining. n = 3. *, p ≤ 0.05 compared to DMSO. **d** mRNA level of *AKR1C3* in HaCaT and HaCaT-NRF2-KO (DU34) cells treated for 24 h as indicated. Test compounds were used at the following concentrations: DMSO (0.1 %), B[a]P (2.5 µM), D3T (70 µM) and GSH (100 µM). n = 3. *, p ≤ 0.05 compared to DMSO, #, p ≤ 0.05 compared to the respective HaCaT control sample. **e** qRT-PCR analyses of *AKR1C3* in HaCaT and HaCaT-NRF2-KO (ΔNRF2) keratinocytes treated as indicated for 24 h. n = 4. *, p ≤ 0.05 compared to DMSO, #, p ≤ 0.05 compared to the respective HaCaT control sample.

EGFR-, MEK/ERK- and NRF2-dependent manner and that PCB126 and related DLCs may disturb this signaling pathway at the level of EGFR.

3.7. DLCs bind to EGFR and inhibit its growth factor-induced activation

The potential disturbance of the binding between EGFR and its ligands by DLCs was analyzed by using a cell-free AlphaLISA assay. The positive control, human recombinant EGF, reduced the binding of biotinylated EGF to antibody-captured EGFR by approximately 40% (Fig. 5a). As expected, the addition of B[a]P had no effect on ligand-receptor binding. PCB126, in contrast, inhibited the binding of biotinylated EGF to EGFR in a dose-dependent manner, and TCDD also slightly reduced ligand-receptor interaction (Fig. 5a). In addition, immunoblot analyses revealed that a 30 min co-treatment of HaCaT cells with PCB126, 2,3′,4,4′,5-pentachlorobiphenyl (PCB118), and TCDD nearly completely blunted the TGFα-induced phosphorylation of EGFR Y1068 and Y1173, while a treatment with B[a]P and B[k]F did not affect or even slightly increased it (Fig. 5b, Fig. S6a). We next performed high content analyses to monitor the effects of the DLCs on the internalization of the EGFR in HaCaT keratinocytes (Fig. 5c). A pretreatment of HaCaT cells with Alexa Fluor® 555-labeled EGF (AF-EGF) and a subsequent incubation with solvent (DMSO) led to an internalization of the AF-EGF-bound EGFR. An exposure of AF-EGF-pretreated cells with unlabeled EGF and increasing concentrations of PCB126 and TCDD dramatically reduced the internalization of EGFR, providing evidence that by binding to its ECD (Fig. 5c), DLCs interfere with the growth factor-induced activation of EGFR. To ensure that DLCs also inhibit functional endpoints of EGFR signaling, we assessed whether an exposure to PCB126 and TCDD affects EGFR ligand-stimulated DNA synthesis. Treatment of HaCaT keratinocytes with AREG induced DNA synthesis, which was inhibited by co-exposing the cells to either PCB126, TCDD or PD153035 (Fig. 5d). Subsequent dose response studies with TCDD, PCB118 and PCB126 in HaCaT-AHR-KO cells confirmed that DLCs inhibit AREG-induced DNA synthesis independently of AHR (Fig. 5e, Fig. S6b).

3.8. Docking analyses and mutational amino acid exchange identify EGFR residues required for DLC binding

To identify the molecular basis for the association between DLCs and EGFR, we conducted an *in silico* docking analysis for PCB126, TCDD and B[a]P with the ECD of human EGFR. In its inactive state the ECD adopts a “tethered” conformation that precludes EGFR dimerization. Binding of EGF or related growth factors stabilizes an extended ECD conformation, which can subsequently homo- or heterodimerize with another EGFR molecule or EGFR family member to build the active extended dimer (Chen et al., 2016). Our *in silico* docking analyses did not predict an

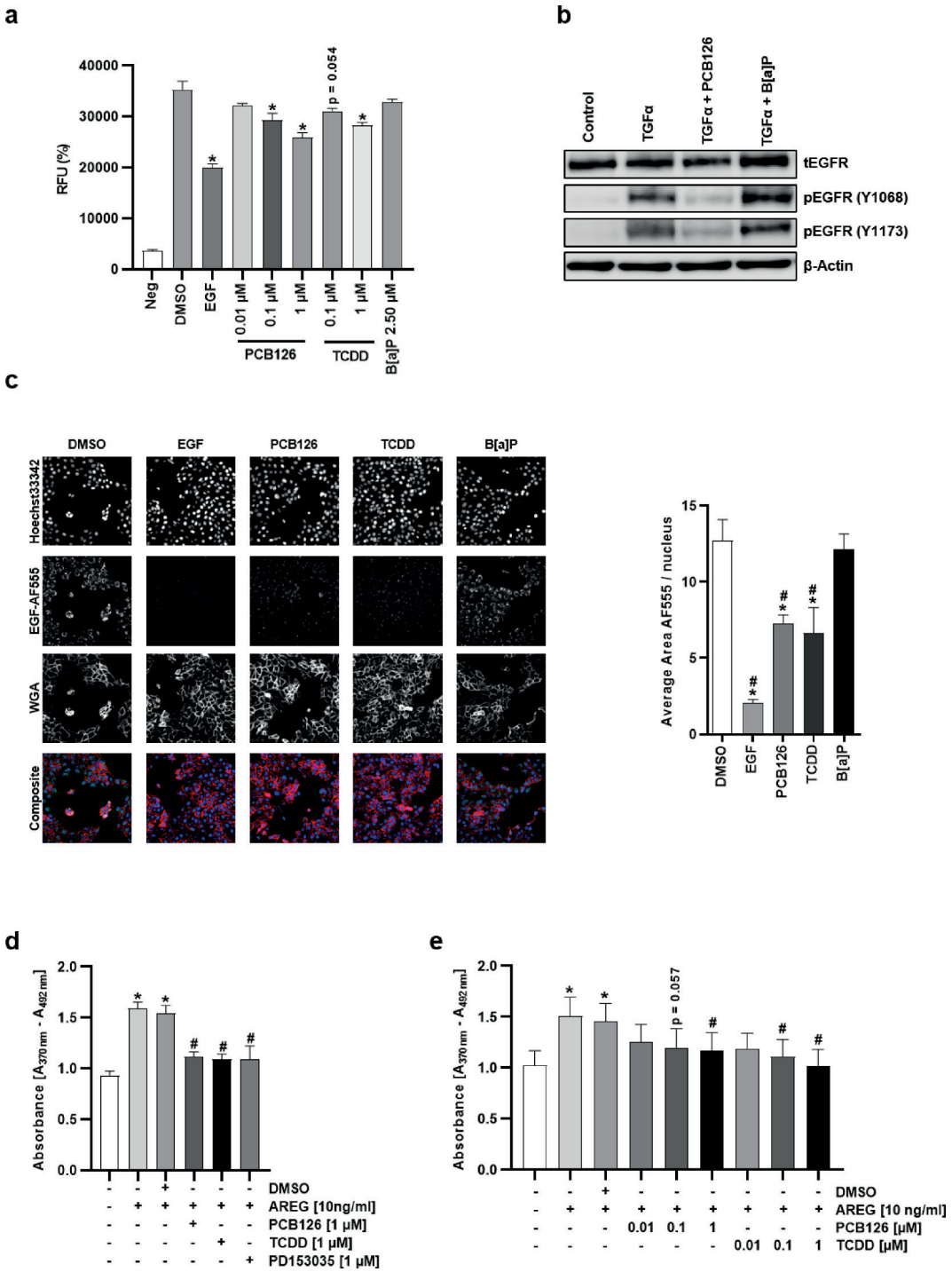

Fig. 5. TCDD and PCB126 interfere with the activation and internalization of EGFR. **a** The effect of the DLCs on the interaction of EGF with EGFR was analyzed by using a cell-free EGF/EGFR AlphaLISA binding kit. n = 3. *, $p \leq 0.05$ compared to DMSO. **b** Effect of B[a]P and PCB126 on EGFR activation upon TGFα stimulation was analyzed via western blot analyses. HaCaT keratinocytes were starved for 3 h and next stimulated with TGFα (20 ng/ml) for 2.5 min on ice. Afterwards, either DMSO (0.1 %), PCB126 (1 μM) or B[a]P (2.5 μM) was added and cells were incubated at 37 °C and 5 % CO_2 for 30 min. Levels of total and phosphorylated EGFR (Y1068, Y1137) were determined; β-Actin was used as loading control. n = 3. representative pictures. **c** Influence of PCB126 (1 μM), TCDD (0.1 μM) and B[a]P (2.5 μM) on EGFR internalization was investigated by EGFR internalization assay and subsequent high content screening microscopy. On the left representative pictures, on the right results from the automated quantification are shown. n = 4–7. *, $p \leq 0.05$ compared to DMSO. #, $p \leq 0.05$ compared to B[a]P. **d** Colorimetric BrdU incorporation assay to assess the influence of PCB126, TCDD and PD153035 on AREG-induced DNA synthesis. HaCaT keratinocytes were treated as indicated for 4 h. Absorption was measured at a wavelength of 370 nm (reference wavelength 492 nm). n = 3. *, $p \leq 0.05$ compared to DMSO. #, $p \leq 0.05$ compared to AREG/DMSO. **e** Colorimetric BrdU incorporation assay in HaCaT-AHR-KO (DU26) keratinocytes. Cells were treated as indicated and the experiment was performed as described in **e**. n = 7. *, $p \leq 0.05$ compared to DMSO. #, $p \leq 0.05$ compared to AREG/DMSO.

interaction of any of the tested AHR ligands with the tethered EGFR monomer. Conversely, docking analyses with the extended ECD conformation predicted that TCDD and PCB126, but not B[a]P, bind to the same region on the ECD (domain I and III) of EGFR (Fig. 6a-c). The estimated binding energy of −11.6 kcal/mol (TCDD) and −11.1 kcal/mol (PCB126) would correspond to dissociation constants of 55.7 nM and 59.3 nM, respectively (supplementary table 2). The site of interaction is next to the site where EGF intercalates to stabilize the extended ECD conformation (Fig. 6a). These analyses imply that binding of DLCs may stabilize the ECD in a slightly altered extended conformation that is incompatible with EGF binding and stable ECD dimerization. A further *in silico* docking analysis predicted that also other DLCs, namely PCB77, PCB118, PCDD, HCDD, and TCDF, are capable to interact with the EGFR ECD (Fig. S7a-f, supplementary table 2).

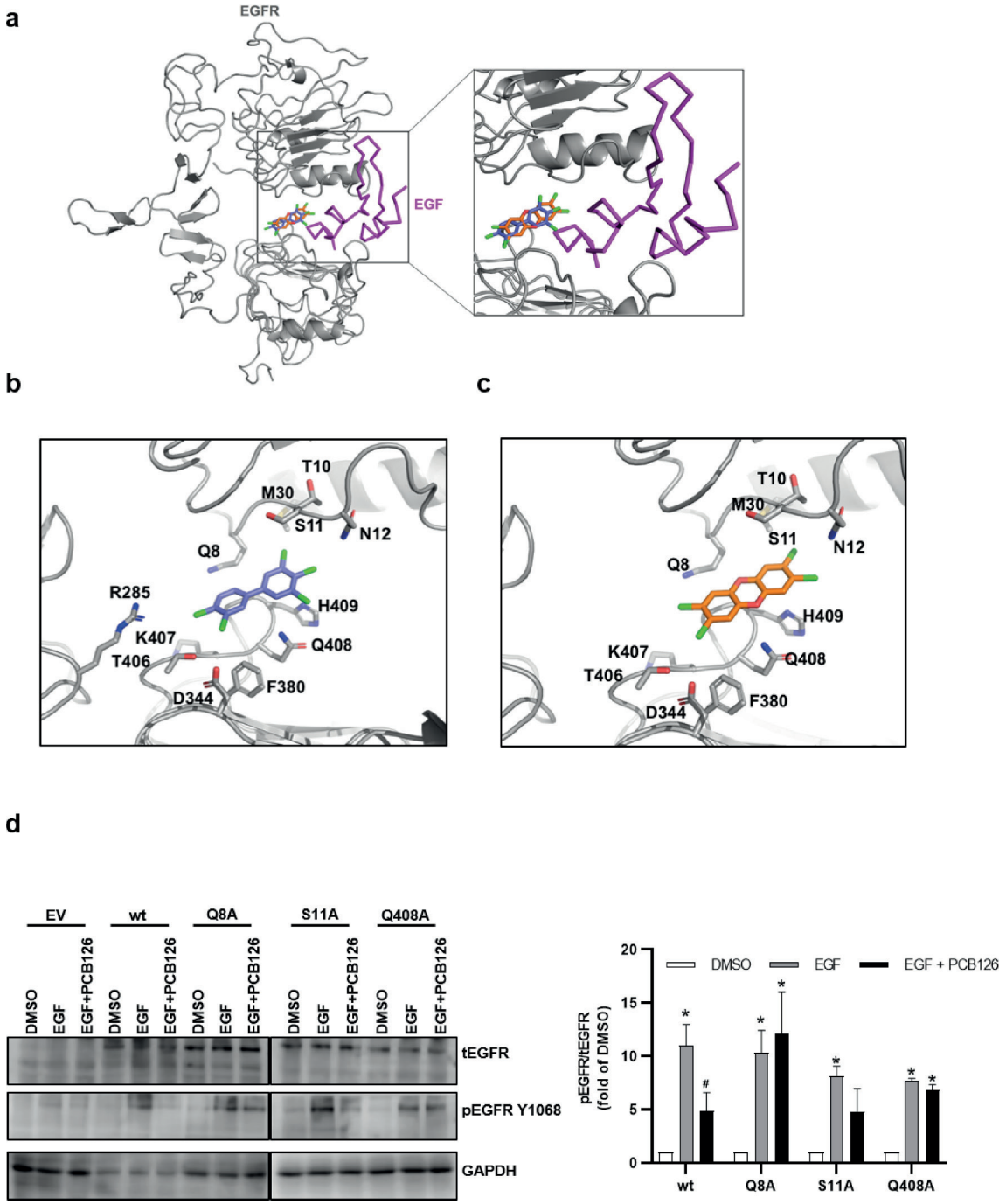

Fig. 6. PCB126 and TCDD bind to EGFR and inhibit its growth factor-induced activation. **a** *In silico* docking analyses predicting the binding of PCB126 (blue) and TCDD (orange) to the ECD of EGFR (grey). EGF (magenta; taken from PDB ID: 1ivo) is superimposed. Interacting amino acid residues of EGFR ECD for **b** PCB126 and **c** TCDD shown as stick models. **d** Potentially interacting residues were converted to alanine by site directed mutagenesis. HepG2 cells were either transfected with an empty vector (pCMV3), pCMV3-EGFR plasmid or a plasmid bearing one of the following point mutations: $EGFR^{Q8A}$, $EGFR^{S11A}$ or $EGFR^{Q408A}$. 24 h post transfection, cells were starved for 3 h and treated with EGF (10 ng/ml) alone and in combination with 1 μM PC126 for 15 min. Phosphorylation of EGFR residue Y1068 was assessed by western blotting and the results were normalized to total EGFR. GAPDH was used as loading control. Bar graph shows the densitometric quantification. Signals were compared with the respective DMSO control. n = 3. *, $p \leq 0.05$ compared to DMSO, #, ≤ 0.05 compared to EGF. (For interpretation of the references to colour in this figure legend, the reader is referred to the web version of this article.)

Moreover, a superimposition of the compound structure of PCB126, TCDD and B[a]P (Fig. S7g) illustrated that due to its larger size, B[a]P probably clashes with EGFR residue Q8 and thus is unable to occupy the same binding site than DLCs (Fig. S7h).

To confirm the functional relevance of the amino acid residues predicted to be involved in DLC-binding (Fig. 6b,c, Fig. S7b-f, supplementary table 2), we mutated a cDNA expression plasmid to replace the amino acids at position 8 (glutamine), 11 (serine) and 408 (glutamine) of the mature EGFR protein by alanine. Transient transfection experiments in low EGFR-expressing human HepG2 hepatoma cells (Fuchs et al., 2008) revealed that the mutated EGFR variants (Q8A, S11A and Q408A) are still responsive towards EGF treatment, as indicated by an enhanced phosphorylation of EGFR at Y1068 (Fig. 6d). In co-exposure experiments with transfected cells expressing wild-type EGFR, PCB126 reduced the EGF-induced phosphorylation of the RTK. However, when we repeated this experiment in cells overexpressing the Q8A and Q408A EGFR variants, PCB126 did not affect the EGF-induced phosphorylation of EGFR Y1068 (Fig. 6d). These data provide compelling evidence that DLCs can directly bind to the ECD of EGFR to replace bound growth factors. Moreover, our data identify the EGFR residues Q8 and Q408 as being critical for the binding of DLCs to EGFR ECD.

3.9. EGFR inhibition shapes B[a]P-induced gene expression

To identify genes that are specifically regulated in response to B[a]P treatment and sensitive towards EGFR inhibition, we performed Nanopore long-read RNA sequencing of HaCaT cells treated for 24 h with PCB126, B[a]P alone and in combination with PD153035, and solvent (Fig. 7a). Compared to solvent control and considering a cut-off of $|L2FC| \geq 1.5$, PCB126 and B[a]P treatment resulted in a differential expression of 910 and 1434 genes, respectively. A set of 370 genes was differentially regulated by both AHR agonists. In comparison to solvent control, the most molecular functions and pathways regulated by PCB126 or B[a]P treatment were related to xenobiotic metabolism, chemical carcinogenesis, steroid biosynthesis, and tryptophan metabolism (Fig. S8). Overall, suppression of gene expression, for instance related to cell adhesion and *O*-glycan biosynthesis, was more evident in response to B[a]P treatment (Fig. S8c,d). Moreover, 586 genes were solely regulated by B[a]P treatment. Given that these genes are not regulated in response to the combinatorial treatment, consisting of B[a]P and PD153035, they can be considered as being EGFR-dependent. In addition, the 478 genes representing the overlap between B[a]P- and B[a]P plus PD153035-treated samples, contains candidates whose expression is partially modulated in an EGFR-dependent manner (e.g. compared to DMSO, $|L2FC|$ of cotreatment $\geq$ 1.5 but $|L2FC|$ of cotreatment $< |L2FC|$ B[a]P treatment). A gene set enrichment analysis revealed that the B[a]P-specific induction of various metabolic processes as well as the inhibition of biosynthetic pathways and cell junctional organization was sensitive towards pharmacological EGFR inhibition (Fig. 7b). KEGG pathway analysis indicated a B[a]P-induced and EGFR-dependent regulation of genes related to steroidogenesis, chemical carcinogenesis, insulin signaling and adherence junctions (Fig. 7c). Amongst others, genes regulated in response to B[a]P exposure can be categorized in three subtypes: 'Type A' represents genes that are upregulated *via* the canonical AHR pathway. The expression of these genes was induced upon PCB126 and B[a]P treatment and, because EGFR signaling dampens AHR/XRE-dependent gene expression (Sutter et al., 2009), further increased in cells co-treated with B[a]P and PD153035; 'Type B' represents genes that are positively regulated by non-canonical AHR signaling pathways. The expression of these genes was inducible by B[a]P but not by PCB126 treatment and sensitive towards EGFR inhibition; 'Type C' represents genes that are negatively regulated by non-canonical AHR signaling pathways. The expression of these genes was downregulated by B[a]P but not by PCB126 treatment and this downregulation was attenuated in response to PD153035 co-exposure. The top 10 regulated genes in terms of highest variance of each subtype are shown in the heatmap (Fig. 7d). The expression level of representative genes of each subtype was validated by qPCR (Fig. 7e, S9). Taken together, these results provide evidence that a substantial part of the B[a]P-induced alterations of the transcriptome is mediated by EGFR-dependent non-canonical AHR signaling pathways.

4. Discussion

Ligand-specificity of AHR signaling is multifactorial and influenced by pharmacokinetic aspects, compound-specific conformational changes of AHR and other parameters (Denison and Faber, 2017; Safe et al., 2020). By unraveling the specific responses induced by PAHs and DLCs, two classes of ubiquitous environmental chemicals comprising of multiple prototypic ligands, we here identified EGFR as a chemical-binding cell-surface receptor and critical determinant of AHR ligand specificity.

We provide evidence that PAHs induce EGFR signal transduction *via* two pathways, both initiated by an AHR ligand-driven stimulation of c-Src. Active c-Src rapidly phosphorylated EGFR (Y845) resulting in a phosphorylation of ERK. In addition, c-Src stimulated PKC and downstream metalloprotease activity to induce ectodomain shedding of cell surface-bound AREG and TGFα. These growth factors activated EGFR (Y1068, Y1173) in an auto-/paracrine fashion, resulting in a second peak of ERK phosphorylation and a NRF2-dependent induction of *AKR1C3*. On the contrary, PCB126 exposure, although enforcing PKC activation and growth factor shedding, neither caused a second peak of ERK activation nor an induction of *AKR1C3*.

It has been repeatedly reported that an exposure to AHR agonists interferes with the binding of radiolabeled EGF to the plasma membrane (Hudson et al., 1985; Kärenlampi et al., 1983; Madhukar et al., 1984). The underlying molecular mechanism of this interaction, however, is still enigmatic. It may be due to an AHR ligand-mediated enforcement of EGFR internalization either by stimulating a phosphorylation of the RTK *via* c-Src or by inducing the release of growth factors that bind to EGFR ECD. However, in contrast to PAHs that, presumably due to recycling of EGFR, only cause a transient decline (Hudson et al., 1985; Kärenlampi et al., 1983), TCDD reduces the EGF-binding capacity of the plasma membrane for up to 4 days (human keratinocytes) and 40 days (rat liver), respectively (Hudson et al., 1985; Madhukar et al., 1984). In light of our data, it is likely that DLCs interact with EGFR ECD and thereby disturb a proper binding of (labeled) EGF. This scenario would still allow a rapid AHR- and c-Src-dependent endogenous activation of EGFR (Y845) and downstream signal transduction by DLCs, but would exclude an activation of the RTK through auto-/paracrine events. In contrast to B[a]P, the DLCs tested in this study bind to the ECD of EGFR in its extended conformation in close proximity to the binding site for EGF. Our results are compatible with a model where DLC binding distorts the ECD sufficiently to block EGF binding and ECD dimerization. This model is supported by previous studies reporting an inhibition of growth factor-stimulated EGFR internalization by halogenated pesticides, PCBs and bisphenol S (Hardesty et al., 2018; Ticiani et al., 2021). The same mechanism as described for DLCs may thus be extended to other structurally related chemicals, making the EGFR a novel direct effector of environmental pollutants. However, given that several endogenous EGFR ligands are under transcriptional control of AHR (John et al., 2014; Patel et al., 2006), an accumulation of these growth factors over time may overcome the inhibitory effect on EGFR internalization of the ECD-bound DLCs.

In contrast to PCB126 and other DLCs, exposure of keratinocytes to B[a]P stimulates the growth factor-mediated activation of EGFR, thereby modulating the expression of hundreds of genes involved in various metabolic processes, biosynthetic pathways and cell adherence. DLCs in turn may specifically affect cellular functions by blocking growth factor-induced EGFR activation.

As mentioned above, a chronic exposure to PAHs may foster the onset and worsening of atopic diseases, whereas an exposure to DLCs has

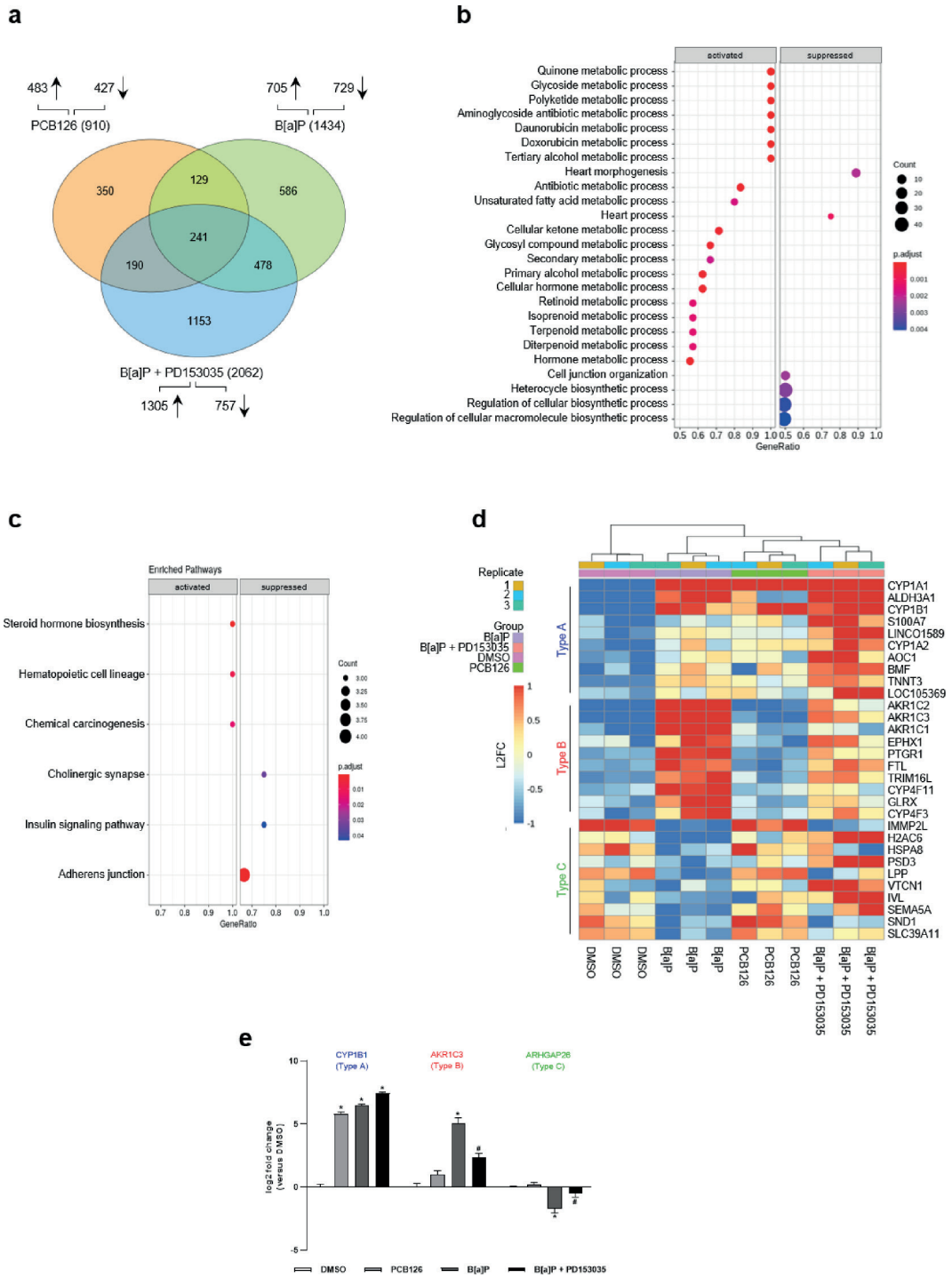

Fig. 7. RNA-Seq analysis reveals distinct expression patterns upon B[a]P treatment. RNA-Seq analyses of HaCaT keratinocytes using oxford nanopore long-read RNA sequencing technology. Cells were treated with DMSO (0.1 %), PCB126 (1 μM), B[a]P (2.5 μM) or B[a]P (2.5 μM) + PD153035 (1 μM) for 24 h. n = 3. **a** Differentially expressed genes compared to DMSO with a $|\log_2 \text{fold change}| \geq 1.5$ depicted in a venn diagram. **b** Gene set enrichment analysis of biological processes of a subset of filtered genes, which were solely regulated by B[a]P and where EGFR inhibition of EGFR signaling with PD153035 counteracted this regulation. Following filter strategy was applied: PCB126 vs. DMSO $|\log_2 \text{fold change}| \leq 1$ → B[a]P vs PCB126 $|\log_2 \text{fold change}| \geq 2$ → B[a]P vs B[a]P + PD153035 $|\log_2 \text{fold change}| \geq 1$. Data set of differentially expression analysis of PCB126 vs. B[a]P was filtered for the remaining genes. Regulation of biological processes was depicted in a dot plot. **c** Genes filtered for **b** were employed on a KEGG pathway analysis. Regulated pathways are shown in a dot plot. **d** Variance heatmap of predefined expression patterns. Shown are the top 10 genes with the highest variance of each gene expression type. Type A: PCB126 vs. DMSO $\log_2$ fold change > 1.5 → B[a]P vs. DMSO $\log_2$ fold change > 1.5 → B[a]P + PD153035 vs. B[a]P $\log_2$ fold change > 0. Type B: PCB126 vs. DMSO $\log_2$ fold change < 1 → B[a]P vs. DMSO $\log_2$ fold change > 1.5 → B[a]P vs. B[a]P + PD153035 $\log_2$ fold change > 0. Type C: PCB126 vs. DMSO $\log_2$ fold change > 0 → B[a]P vs. DMSO $\log_2$ fold change < –1 → B[a]P vs. B[a]P + PD153035 $\log_2$ fold change < 0. **e** qRT-PCR analysis of genes representing the different types of gene expression patterns. n = 4. *, p ≤ 0.05 compared to DMSO, #, ≤ 0.05 compared to B[a]P.

no or even the opposite effect on the pathogenesis of these Th2-driven diseases. The differential regulation of PGD_2 metabolism may partially contribute to this AHR ligand-specific difference. PGD_2 is mainly released by degranulating mast cells and contributes to the pathogenesis of allergic inflammatory diseases by binding to CRTH2 on Th2 cells and stimulating cytokine secretion (Pettipher et al., 2007). However, upon its release PGD_2 either spontaneously hydrolyzes to 15-deoxyΔ12–14 PGJ_2 or is reduced by AKR1C3 to 9α,11β-PGF_2. Whereas 15-deoxyΔ12–14 PGJ_2 acts as an anti-inflammatory (Pettipher et al., 2007), 9α,11β-PGF_2, which is less potent in activating CRTH2 than PGD_2 but metabolically stable, prolongs allergic inflammation and serves as systemic biomarker for allergen-induced mast cell activation (Bochenek et al., 2003; Seibert et al., 1987). In the skin, elevated expression levels of AKR1C3 and the associated formation of 9α,11β-PGF_2 may stimulate a Th2 cytokine-induced disturbance of keratinocyte differentiation (Mantel et al., 2012). In addition, by converting PAH diols to redox-cycling catechols, enhanced AKR1C3 levels may enforce mast cell activation and cause further oxidative tissue damage (Diaz-Sanchez et al., 2000; Park et al., 2008). A PAH-driven activation of AHR may thus contribute to allergic inflammatory diseases by perpetuating Th2 responses, impairing epithelial barrier function and enhancing the susceptibility towards inflammatory stimuli (Dijkhoff et al., 2020; Lag et al., 2020). For regulatory purposes, it should be considered that the mouse genome encodes neither AKR1C3 nor a functional homolog (Velica et al., 2009).

Regarding its important role in development and tissue homeostasis (Chen et al., 2016), an inhibition of growth factor-driven EGFR activation may be a critical mode of action of DLCs. In the skin, for instance, EGFR signaling contributes to epidermal homeostasis by tightly orchestrating keratinocyte fate and associated barrier functions (Chen et al., 2016). A systemic application of EGFR inhibitors, e.g. during lung cancer therapy, is frequently accompanied by cutaneous adverse effects, including an acceleration of keratinocyte differentiation and an impairment of the epidermal barrier (Lacouture, 2006; Lichtenberger et al., 2013). Accordingly, treatment of human keratinocytes with EGFR inhibitors switches the keratinocyte program from proliferation to differentiation (Lichtenberger et al., 2013; Peus et al., 1997). This program switch is also observed in human keratinocytes exposed to TCDD and may contribute to the pathogenesis of chloracne, the hallmark of an acute intoxication with DLCs in humans (Hudson et al., 1985; Sutter et al., 2019).

From a mechanistical point of view, a chemical inhibition of growth factor-driven proliferation and an induction of cellular differentiation may be of interest for the treatment of EGFR-positive cancers. In fact, results from rodent studies revealed an anti-carcinogenic effect of TCDD in certain tissues (DiGiovanni et al., 1980; Holcomb and Safe, 1994). However, whether DLCs may serve as a structural blueprint for the development of novel non-toxic EGFR ECD modulators for therapeutic purposes remains to be investigated. A limitation of this study is that we have not yet confirmed a direct interaction of DLCs with EGFR molecules from other species than human. However, a multiple alignment of the *N*-terminal 420 amino acids of the mature EGFR protein revealed a high conservation of the residues predicted and/or experimentally proven to be involved in DLC binding across several mammalian species (Fig. S10).

Taken together, we identified a PAH-specific non-canonical AHR signaling pathway responsible for the induction of AKR1C3 and the associated 11-ketoreduction of PGD_2 that provides a plausible link between PAH exposure and the pathogenesis of allergic inflammatory diseases. In addition, we revealed that DLCs interact with EGFR ECD, resulting in a displacement of bound growth factors and an inhibition of downstream events. This novel mode of action is probably relevant for various DLC-associated adverse health effects, in particular for those involving a dysbalance between cell proliferation and differentiation. We conclude that the expression level of EGFR and the presence of its ligands are critical parameters which have to be considered in order to optimize the prediction of the biological outcome in a given PAH- or DLC-exposed cell population or tissue.

CRediT authorship contribution statement

Christian Vogeley: Conceptualization, Formal analysis, Investigation, Visualization. **Natalie C. Sondermann:** Investigation. **Selina Woeste:** Investigation, Methodology. **Afaque A. Momin:** Investigation, Methodology. **Viola Gilardino:** Investigation. **Frederick Hartung:** Investigation. **Markus Heinen:** Investigation. **Sophia K. Maaß:** Investigation. **Melina Mescher:** Investigation. **Marius Pollet:** Investigation. **Katharina M. Rolfes:** Investigation. **Christoph F.A. Vogel:** Resources, Writing – review & editing. **Andrea Rossi:** Methodology, Resources, Writing – review & editing. **Dieter Lang:** Investigation, Methodology, Writing – review & editing. **Stefan T. Arold:** Methodology, Writing – review & editing. **Motoki Nakamura:** Conceptualization, Investigation, Writing – review & editing. **Thomas Haarmann-Stemmann:** Conceptualization, Methodology, Writing – original draft, Writing – review & editing, Supervision, Project administration, Funding acquisition.

Declaration of Competing Interest

The authors declare that they have no known competing financial interests or personal relationships that could have appeared to influence the work reported in this paper.

Acknowledgement

We thank Imke Meyer for kindly providing MNF, and Petra Boukamp and Ellen Fritsche for providing HaCaT and HaCaT-EV/HaCaT-shAHR cells, respectively. We thank Franziska Ickenroth, Melanie Scheinpflug, Ragnhild Wirth, Björn Hiller and Nadine Teichweyde for technical support.

NCS and KMR were supported by the Jürgen Manchot Foundation. VG was supported by the EU program Erasmus+. CFAV was supported by the National Institute of Environmental Health Sciences under award numbers R01ES029126 and R21ES030419. The scheme shown in the graphical abstract was created with BioRender software (www.biorender.com; agreement number UD232J5QDI).

Appendix A. Supplementary material

Supplementary data to this article can be found online at https://doi.org/10.1016/j.envint.2021.106989.

References

Bessede, A., Gargaro, M., Pallotta, M.T., Matino, D., Servillo, G., Brunacci, C., Bicciato, S., Mazza, E.M.C., Macchiarulo, A., Vacca, C., Iannitti, R., Tissi, L., Volpi, C., Belladonna, M.L., Orabona, C., Bianchi, R., Lanz, T.V., Platten, M., Della Fazia, M.A., Piobbico, D., Zelante, T., Funakoshi, H., Nakamura, T., Gilot, D., Denison, M.S., Guillemin, G.J., DuHadaway, J.B., Prendergast, G.C., Metz, R., Geffard, M., Boon, L., Pirro, M., Iorio, A., Veyret, B., Romani, L., Grohmann, U., Fallarino, F., Puccetti, P., 2014. Aryl hydrocarbon receptor control of a disease tolerance defence pathway. Nature 511 (7508), 184–190.

Bochenek, G., Nagraba, K., Nizankowska, E., Szczeklik, A., 2003. A controlled study of 9alpha,11beta-PGF2 (a prostaglandin D2 metabolite) in plasma and urine of patients with bronchial asthma and healthy controls after aspirin challenge. J. Allergy Clin. Immunol. 111, 743–749.

Burczynski, M.E., Lin, H.K., Penning, T.M., 1999. Isoform-specific induction of a human aldo-keto reductase by polycyclic aromatic hydrocarbons (PAHs), electrophiles, and oxidative stress: implications for the alternative pathway of PAH activation catalyzed by human dihydrodiol dehydrogenase. Cancer Res. 59, 607–614.

Castañeda, A.R., Vogel, C.F.A., Bein, K.J., Hughes, H.K., Smiley-Jewell, S., Pinkerton, K. E., 2018. Ambient particulate matter enhances the pulmonary allergic immune response to house dust mite in a BALB/c mouse model by augmenting Th2- and Th17-immune responses. Physiol. Rep. 6 (18), e13827. https://doi.org/10.14814/phy2.13827.

Chen, J., Zeng, F., Forrester, S.J., Eguchi, S., Zhang, M.-Z., Harris, R.C., 2016. Expression and Function of the Epidermal Growth Factor Receptor in Physiology and Disease. Physiol. Rev. 96 (3), 1025–1069.

Denison, M.S., Faber, S.C., 2017. And now for something completely different: diversity in ligand-dependent activation of Ah receptor responses. Curr. Opin. Toxicol. 2, 124–131.
Diaz-Sanchez, D., Penichet-Garcia, M., Saxon, A., 2000. Diesel exhaust particles directly induce activated mast cells to degranulate and increase histamine levels and symptom severity. J. Allergy Clin. Immunol. 106 (6), 1140–1146.
DiGiovanni, J., Berry, D.L., Gleason, G.L., Kishore, G.S., Slaga, T.J., 1980. Time-dependent inhibition by 2,3,7,8-tetrachlorodibenzo-p-dioxin of skin tumorigenesis with polycyclic hydrocarbons. Cancer Res. 40, 1580–1587.
Dijkhoff, I.M., Drasler, B., Karakocak, B.B., Petri-Fink, A., Valacchi, G., Eeman, M., Rothen-Rutishauser, B., 2020. Impact of airborne particulate matter on skin: a systematic review from epidemiology to in vitro studies. Part. Fibre Toxicol. 17, 35.
Dong, B., Cheng, W., Li, W., Zheng, J., Wu, D., Matsumura, F., Vogel, C.F.A., 2011. FRET analysis of protein tyrosine kinase c-Src activation mediated via aryl hydrocarbon receptor. BBA 1810 (4), 427–431.
Frauenstein, K., Tigges, J., Soshilov, A.A., Kado, S., Raab, N., Fritsche, E., Haendeler, J., Denison, M.S., Vogel, C.F.A., Haarmann-Stemmann, T., 2015. Activation of the aryl hydrocarbon receptor by the widely used Src family kinase inhibitor 4-amino-5-(4-chlorophenyl)-7-(dimethylethyl)pyrazolo[3,4-d]pyrimidine (PP2). Arch. Toxicol. 89 (8), 1329–1336.
Fritsche, E., Schafer, C., Calles, C., Bernsmann, T., Bernshausen, T., Wurm, M., Hubenthal, U., Cline, J.E., Hajimiragha, H., Schroeder, P., Klotz, L.-O., Rannug, A., Furst, P., Hanenberg, H., Abel, J., Krutmann, J., 2007. Lightening up the UV response by identification of the arylhydrocarbon receptor as a cytoplasmatic target for ultraviolet B radiation. PNAS 104 (21), 8851–8856.
Fuchs, B.C., Fujii, T., Dorfman, J.D., Goodwin, J.M., Zhu, A.X., Lanuti, M., Tanabe, K.K., 2008. Epithelial-to-mesenchymal transition and integrin-linked kinase mediate sensitivity to epidermal growth factor receptor inhibition in human hepatoma cells. Cancer Res. 68 (7), 2391–2399.
Funatake, C.J., Marshall, N.B., Steppan, L.B., Mourich, D.V., Kerkvliet, N.I., 2005. Cutting edge: activation of the aryl hydrocarbon receptor by 2,3,7,8-tetrachlorodibenzo-p-dioxin generates a population of CD4+ CD25+ cells with characteristics of regulatory T cells. J. Immunol. 175 (7), 4184–4188.
Goodsell, D.S., Morris, G.M., Olson, A.J., 1996. Automated docking of flexible ligands: applications of AutoDock. J. Mol. Recognit. 9 (1), 1–5.
Haarmann-Stemmann, T., Abel, J., Fritsche, E., Krutmann, J., 2012. The AhR-Nrf2 pathway in keratinocytes: on the road to chemoprevention? J, Invest. Dermatol. 132 (1), 7–9.
Hardesty, J.E., Al-Eryani, L., Wahlang, B., Falkner, K.C., Shi, H., Jin, J., Vivace, B.J., Ceresa, B.P., Prough, R.A., Cave, M.C., 2018. Epidermal Growth Factor Receptor Signaling Disruption by Endocrine and Metabolic Disrupting Chemicals. Toxicol. Sci. 162, 622–634.
Hawerkamp, H.C., Kislat, A., Gerber, P.A., Pollet, M., Rolfes, K.M., Soshilov, A.A., Denison, M.S., Momin, A.A., Arold, S.T., Datsi, A., Braun, S.A., Oláh, P., Lacouture, M.E., Krutmann, J., Haarmann-Stemmann, T., Homey, B., Meller, S., 2019. Vemurafenib acts as an aryl hydrocarbon receptor antagonist: Implications for inflammatory cutaneous adverse events. Allergy 74 (12), 2437–2448.
Hidaka, T., Ogawa, E., Kobayashi, E.H., Suzuki, T., Funayama, R., Nagashima, T., Fujimura, T., Aiba, S., Nakayama, K., Okuyama, R., Yamamoto, M., 2017. The aryl hydrocarbon receptor AhR links atopic dermatitis and air pollution via induction of the neurotrophic factor artemin. Nat. Immunol. 18 (1), 64–73.
Holcomb, M., Safe, S., 1994. Inhibition of 7,12-dimethylbenzanthracene-induced rat mammary tumor growth by 2,3,7,8-tetrachlorodibenzo-p-dioxin. Cancer Lett. 82 (1), 43–47.
Hong, C.-H., Lee, C.-H., Yu, H.-S., Huang, S.-K., 2016. Benzopyrene, a major polyaromatic hydrocarbon in smoke fume, mobilizes Langerhans cells and polarizes Th2/17 responses in epicutaneous protein sensitization through the aryl hydrocarbon receptor. Int. Immunopharmacol. 36, 111–117.
Hudson, L.G., Toscano, W.A., Greenlee, W.F., 1985. Regulation of epidermal growth factor binding in a human keratinocyte cell line by 2,3,7,8-tetrachlorodibenzo-p-dioxin. Toxicol. Appl. Pharmacol. 77 (2), 251–259.
John, K., Lahoti, T.S., Wagner, K., Hughes, J.M., Perdew, G.H., 2014. The Ah receptor regulates growth factor expression in head and neck squamous cell carcinoma cell lines. Mol. Carcinog. 53 (10), 765–776.
Joseloff, E., Cataisson, C., Aamodt, H., Ocheni, H., Blumberg, P., Kraker, A.J., Yuspa, S. H., 2002. Src family kinases phosphorylate protein kinase C delta on tyrosine residues and modify the neoplastic phenotype of skin keratinocytes. J. Biol. Chem. 277, 12318–12323.
Kärenlampi, S.O., Eisen, H.J., Hankinson, O., Nebert, D.W., 1983. Effects of cytochrome P1–450 inducers on the cell-surface receptors for epidermal growth factor, phorbol 12,13-dibutyrate, or insulin of cultured mouse hepatoma cells. J. Biol. Chem. 258 (17), 10378–10383.
Kim, S., Thiessen, P.A., Bolton, E.E., Chen, J., Fu, G., Gindulyte, A., Han, L., He, J., He, S., Shoemaker, B.A., Wang, J., Yu, B.o., Zhang, J., Bryant, S.H., 2016. PubChem Substance and Compound databases. Nucleic Acids Res. 44 (D1), D1202–D1213.
Kopec, A.K., Burgoon, L.D., Ibrahim-Aibo, D., Burg, A.R., Lee, A.W., Tashiro, C., Potter, D., Sharratt, B., Harkema, J.R., Rowlands, J.C., Budinsky, R.A., Zacharewski, T.R., 2010. Automated dose-response analysis and comparative toxicogenomic evaluation of the hepatic effects elicited by TCDD, TCDF, and PCB126 in C57BL/6 mice. Toxicol. Sci. 118, 286–297.
Lacouture, M.E., 2006. Mechanisms of cutaneous toxicities to EGFR inhibitors. Nat. Rev. Cancer 6 (10), 803–812.
Lag, M., Ovrevik, J., Refsnes, M., Holme, J.A., 2020. Potential role of polycyclic aromatic hydrocarbons in air pollution-induced non-malignant respiratory diseases. Respir. Res. 21, 299.
Li, H., 2018. Minimap2: pairwise alignment for nucleotide sequences. Bioinformatics 34, 3094–3100.
Liao, Y., Smyth, G.K., Shi, W., 2019. The R package Rsubread is easier, faster, cheaper and better for alignment and quantification of RNA sequencing reads. Nucleic Acids Res. 47 e47.
Lichtenberger, B.M., Gerber, P.A., Holcmann, M., Buhren, B.A., Amberg, N., Smolle, V., Schrumpf, H., Boelke, E., Ansari, P., Mackenzie, C., Wollenberg, A., Kislat, A., Fischer, J.W., Rock, K., Harder, J., Schroder, J.M., Homey, B., Sibilia, M., 2013. Epidermal EGFR controls cutaneous host defense and prevents inflammation. Sci. Transl. Med. 5, 199ra111.
Liu, Y., He, S., Chen, Y., Liu, Y., Feng, F., Liu, W., Guo, Q., Zhao, L.i., Sun, H., 2020. Overview of AKR1C3: Inhibitor Achievements and Disease Insights. J. Med. Chem. 63 (20), 11305–11329.
Love, M.I., Huber, W., Anders, S., 2014. Moderated estimation of fold change and dispersion for RNA-seq data with DESeq2. Genome Biol. 15, 550.
Madhukar, B.V., Brewster, D.W., Matsumura, F., 1984. Effects of in vivo-administered 2,3,7,8-tetrachlorodibenzo-p-dioxin on receptor binding of epidermal growth factor in the hepatic plasma membrane of rat, guinea pig, mouse, and hamster. PNAS 81 (23), 7407–7411.
Manandhar, S., Cho, J.-M., Kim, J.-A., Kensler, T.W., Kwak, M.-K., 2007. Induction of Nrf2-regulated genes by 3H–1, 2-dithiole-3-thione through the ERK signaling pathway in murine keratinocytes. Eur. J. Pharmacol. 577 (1-3), 17–27.
Mantel, A., Carpenter-Mendini, A.B., VanBuskirk, J.B., De Benedetto, A., Beck, L.A., Pentland, A.P., 2012. Aldo-keto reductase 1C3 is expressed in differentiated human epidermis, affects keratinocyte differentiation, and is upregulated in atopic dermatitis. J, Invest. Dermatol. 132 (4), 1103–1110.
Murray, I.A., Patterson, A.D., Perdew, G.H., 2014. Aryl hydrocarbon receptor ligands in cancer: friend and foe. Nat. Rev. Cancer 14 (12), 801–814.
Nadeau, K., McDonald-Hyman, C., Noth, E.M., Pratt, B., Hammond, S.K., Balmes, J., Tager, I., 2010. Ambient air pollution impairs regulatory T-cell function in asthma. J. Allergy Clin. Immunol. 126 (4), 845–852.e10.
Nakamoto, M., Arisawa, K., Uemura, H., Katsuura, S., Takami, H., Sawachika, F., Yamaguchi, M., Juta, T., Sakai, T., Toda, E., Mori, K., Hasegawa, M., Tanto, M., Shima, M., Sumiyoshi, Y., Morinaga, K., Kodama, K., Suzuki, T., Nagai, M., Satoh, H., 2013. Association between blood levels of PCDDs/PCDFs/dioxin-like PCBs and history of allergic and other diseases in the Japanese population. Int. Arch. Occup. Environ. Health 86 (8), 849–859.
Nault, R., Forgacs, A.L., Dere, E., Zacharewski, T.R., 2013. Comparisons of differential gene expression elicited by TCDD, PCB126, betaNF, or ICZ in mouse hepatoma Hepa1c1c7 cells and C57BL/6 mouse liver. Toxicol. Lett. 223, 52–59.
O'Boyle, N.M., Banck, M., James, C.A., Morley, C., Vandermeersch, T., Hutchison, G.R., 2011. Open Babel: An open chemical toolbox. J. Cheminform. 3, 33.
O'Driscoll, C.A., Owens, L.A., Gallo, M.E., Hoffmann, E.J., Afrazi, A., Han, M., Fechner, J. H., Schauer, J.J., Bradfield, C.A., Mezrich, J.D., 2018. Differential effects of diesel exhaust particles on T cell differentiation and autoimmune disease. Part. Fibre Toxicol. 15, 35.
Park, J.-H., Mangal, D., Tacka, K.A., Quinn, A.M., Harvey, R.G., Blair, I.A., Penning, T. M., 2008. Evidence for the aldo-keto reductase pathway of polycyclic aromatic trans-dihydrodiol activation in human lung A549 cells. Proc. Natl. Acad. Sci. USA 105 (19), 6846–6851.
Patel, R.D., Kim, D.J., Peters, J.M., Perdew, G.H., 2006. The aryl hydrocarbon receptor directly regulates expression of the potent mitogen epiregulin. Toxicol. Sci. 89, 75–82.
Penning, T.M., 2019. AKR1C3 (type 5 17beta-hydroxysteroid dehydrogenase/prostaglandin F synthase): Roles in malignancy and endocrine disorders. Mol. Cell. Endocrinol. 489, 82–91.
Pettipher, R., Hansel, T.T., Armer, R., 2007. Antagonism of the prostaglandin D2 receptors DP1 and CRTH2 as an approach to treat allergic diseases. Nat. Rev. Drug Discov. 6 (4), 313–325.
Peus, D., Hamacher, L., Pittelkow, M.R., 1997. EGF-receptor tyrosine kinase inhibition induces keratinocyte growth arrest and terminal differentiation. J. Invest. Dermatol. 109 (6), 751–756.
Quintana, F.J., Basso, A.S., Iglesias, A.H., Korn, T., Farez, M.F., Bettelli, E., Caccamo, M., Oukka, M., Weiner, H.L., 2008. Control of T(reg) and T(H)17 cell differentiation by the aryl hydrocarbon receptor. Nature 453 (7191), 65–71.
Ramachandran, H., Martins, S., Kontarakis, Z., Krutmann, J., Rossi, A., 2021. Fast but not furious: a streamlined selection method for genome-edited cells. Life Sci Alliance 4.
Roman, Á.C., Carvajal-Gonzalez, J.M., Merino, J.M., Mulero-Navarro, S., Fernández-Salguero, P.M., 2018. The aryl hydrocarbon receptor in the crossroad of signalling networks with therapeutic value. Pharmacol. Ther. 185, 50–63.
Rothhammer, V., Quintana, F.J., 2019. The aryl hydrocarbon receptor: an environmental sensor integrating immune responses in health and disease. Nat. Rev. Immunol. 19 (3), 184–197.
Safe, S., Jin, U.-h., Park, H., Chapkin, R.S., Jayaraman, A., 2020. Aryl Hydrocarbon Receptor (AHR) Ligands as Selective AHR Modulators (SAhRMs). Int. J. Mol. Sci. 21 (18), 6654. https://doi.org/10.3390/ijms21186654.
Seals, D.F., Courtneidge, S.A., 2003. The ADAMs family of metalloproteases: multidomain proteins with multiple functions. Genes Dev. 17 (1), 7–30.
Seibert, K., Sheller, J.R., Roberts, L.J., 1987. (5Z,13E)-(15S)-9 alpha,11 beta,15-trihydroxyprosta-5,13-dien-1-oic acid (9 alpha,11 beta-prostaglandin F2): formation and metabolism by human lung and contractile effects on human bronchial smooth muscle. PNAS 84 (1), 256–260.
Sievers, F., Wilm, A., Dineen, D., Gibson, T.J., Karplus, K., Li, W., Lopez, R., McWilliam, H., Remmert, M., Söding, J., Thompson, J.D., Higgins, D.G., 2011. Fast, scalable generation of high-quality protein multiple sequence alignments using Clustal Omega. Mol. Syst. Biol. 7 (1), 539. https://doi.org/10.1038/msb:2011.75.

Souza, T., Jennen, D., van Delft, J., van Herwijnen, M., Kyrtoupolos, S., Kleinjans, J., 2016. New insights into BaP-induced toxicity: role of major metabolites in transcriptomics and contribution to hepatocarcinogenesis. Arch. Toxicol. 90 (6), 1449–1458.

Stockinger, B., Shah, K., Wincent, E., 2021. AHR in the intestinal microenvironment: safeguarding barrier function. Nat. Rev. Gastroenterol. Hepatol. 18 (8), 559–570.

Sutter, C.H., Olesen, K.M., Bhuju, J., Guo, Z., Sutter, T.R., 2019. AHR Regulates Metabolic Reprogramming to Promote SIRT1-Dependent Keratinocyte Differentiation. J. Invest. Dermatol. 139 (4), 818–826.

Sutter, C.H., Yin, H., Li, Y., Mammen, J.S., Bodreddigari, S., Stevens, G., Cole, J.A., Sutter, T.R., 2009. EGF receptor signaling blocks aryl hydrocarbon receptor-mediated transcription and cell differentiation in human epidermal keratinocytes. Proc. Natl. Acad. Sci. USA 106 (11), 4266–4271.

Tebay, L.E., Robertson, H., Durant, S.T., Vitale, S.R., Penning, T.M., Dinkova-Kostova, A. T., Hayes, J.D., 2015. Mechanisms of activation of the transcription factor Nrf2 by redox stressors, nutrient cues, and energy status and the pathways through which it attenuates degenerative disease. Free Radic. Biol. Med. 88, 108–146.

Ticiani, E., Gingrich, J., Pu, Y., Vettathu, M., Davis, J., Martin, D., Petroff, M.G., Veiga-Lopez, A., 2021. Bisphenol S and Epidermal Growth Factor Receptor Signaling in Human Placental Cytotrophoblasts. Environ. Health Perspect. 129 (2), 027005. https://doi.org/10.1289/EHP7297.

Tsuji, G., Takahara, M., Uchi, H., Matsuda, T., Chiba, T., Takeuchi, S., Yasukawa, F., Moroi, Y., Furue, M., 2012. Identification of ketoconazole as an AhR-Nrf2 activator in cultured human keratinocytes: the basis of its anti-inflammatory effect. J, Invest. Dermatol. 132 (1), 59–68.

Velica, P., Davies, N.J., Rocha, P.P., Schrewe, H., Ride, J.P., Bunce, C.M., 2009. Lack of functional and expression homology between human and mouse aldo-keto reductase 1C enzymes: implications for modelling human cancers. Mol. Cancer 8, 121.

Vogel, C.F.A., Lazennec, G., Kado, S.Y., Dahlem, C., He, Y., Castaneda, A., Ishihara, Y., Vogeley, C., Rossi, A., Haarmann-Stemmann, T., Jugan, J., Mori, H., Borowsky, A.D., La Merrill, M.A., Sweeney, C., 2021. Targeting the Aryl Hydrocarbon Receptor Signaling Pathway in Breast Cancer Development. Front. Immunol. 12, 625346.

Vogel, C.F.A., Van Winkle, L.S., Esser, C., Haarmann-Stemmann, T., 2020. The aryl hydrocarbon receptor as a target of environmental stressors - Implications for pollution mediated stress and inflammatory responses. Redox Biol. 34, 101530. https://doi.org/10.1016/j.redox.2020.101530.

Wang, J., Xie, X., 2007. Development of a quantitative, cell-based, high-content screening assay for epidermal growth factor receptor modulators. Acta Pharmacol. Sin. 28 (10), 1698–1704.

Weng, C.-M., Wang, C.-H., Lee, M.-J., He, J.-R., Huang, H.-Y., Chao, M.-W., Chung, K.F., Kuo, H.-P., 2018. Aryl hydrocarbon receptor activation by diesel exhaust particles mediates epithelium-derived cytokines expression in severe allergic asthma. Allergy 73 (11), 2192–2204.

Wong, T.H., Lee, C.L., Su, H.H., Lee, C.L., Wu, C.C., Wang, C.C., Sheu, C.C., Lai, R.S., Leung, S.Y., Lin, C.C., Wei, Y.F., Wang, C.J., Lin, Y.C., Chen, H.L., Huang, M.S., Yen, J.H., Huang, S.K., Suen, J.L., 2018. A prominent air pollutant, Indeno[1,2,3-cd] pyrene, enhances allergic lung inflammation via aryl hydrocarbon receptor. Sci. Rep. 8, 5198.

Xia, M., Viera-Hutchins, L., Garcia-Lloret, M., Noval Rivas, M., Wise, P., McGhee, S.A., Chatila, Z.K., Daher, N., Sioutas, C., Chatila, T.A., 2015. Vehicular exhaust particles promote allergic airway inflammation through an aryl hydrocarbon receptor-notch signaling cascade. J. Allergy Clin. Immunol. 136 (2), 441–453.

Ye, M., Warner, M., Mocarelli, P., Brambilla, P., Eskenazi, B., 2018. Prenatal exposure to TCDD and atopic conditions in the Seveso second generation: a prospective cohort study. Environ. Health 17, 22.

Yu, G., Wang, L.-G., Han, Y., He, Q.-Y., 2012. clusterProfiler: an R package for comparing biological themes among gene clusters. OMICS 16 (5), 284–287.

Supplementary Information

Unraveling the differential impact of PAHs and dioxin-like compounds on AKR1C3 reveals the EGFR extracellular domain as a critical determinant of the AHR response

Christian Vogeley, Natalie C. Sondermann, Selina Woeste, Afaque A. Momin, Viola Gilardino, Frederick Hartung, Markus Heinen, Sophia K. Maaß, Melina Mescher, Marius Pollet, Katharina M. Rolfes, Christoph F.A. Vogel, Andrea Rossi, Dieter Lang, Stefan T. Arold, Motoki Nakamura, Thomas Haarmann-Stemmann

Correspondence to: Thomas.haarmann-stemmann@iuf-duesseldorf.de

This PDF file includes:

Supplementary Figures S1 – S10

Supplementary Table 1 – 2

AHR gene organization

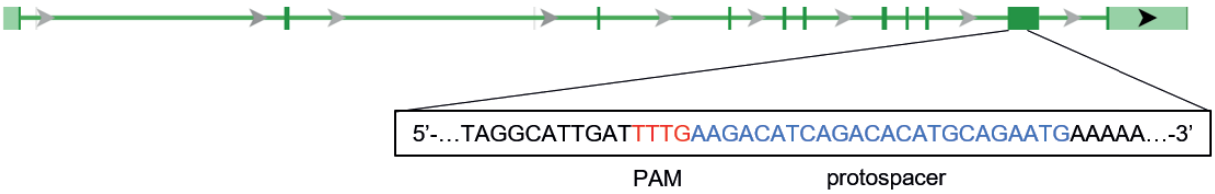

AHR DU26 indels

Δ2	5'-…TAGGCATTGATTTTGAAGACATCAGACACATG--GAATGAAAAA…-3'
Δ11	5'-…TAGGCATTGATTTTGAAGACATCAGA----------TGAAAAA…-3'
Δ4	5'-…TAGGCATTGATTTTGAAGACATCAGACACA----GAATGAAAAA…-3'

NFE2L2 gene organization

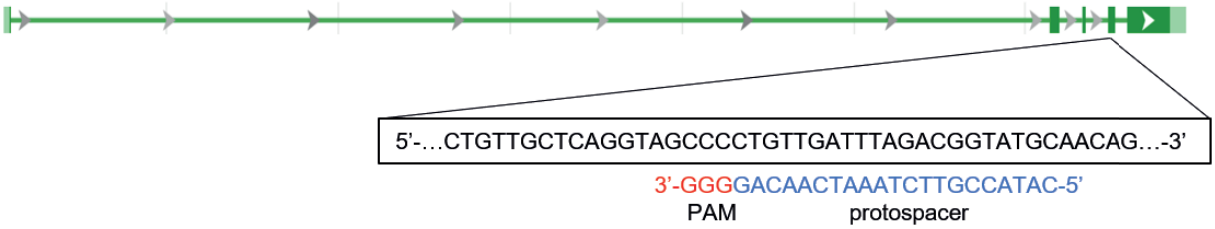

NFE2L2 DU34 indels

Δ1	5'-…CTGTTGCTCAGGTAGCCCCTGT-GATTTAGACGGTATGCAACAG…-3'
Δ4	5'-…CTGTTGCTCAGGTAGCCCCTGTT----TAGACGGTATGCAACAG…-3'

CYP1A1 gene organization

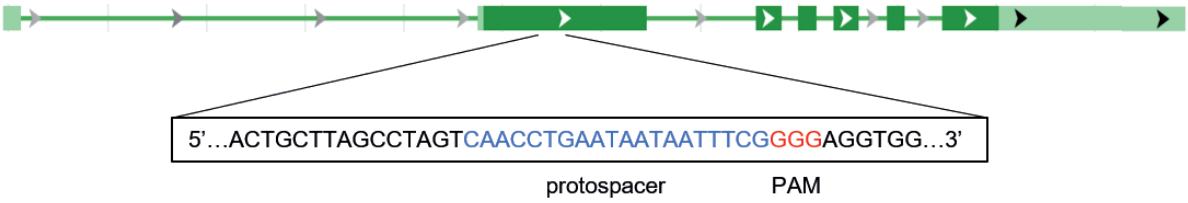

CYP1A1 DU46 indels

Δ1	5'…ACTGCTTAGCCTAGTCAACCTGAATA------TCGGGGAGGTGG…3'
Δ6	5'…ACTGCTTAGCCTAGTCAACCTGAATAATAATT-CGGGGAGGTGG…3'
Δ15	5'…ACTGCTTAGCCTAGTCAACC----------CAAAAGTGG…3'

Figure S1: Generation of AHR-, NRF2-, and CYP1A1-KO HaCaT keratinocytes

Shown is the organisation of the respective genes, as well as the sequence of the used gRNA with the protospacer adjacent motif depicted in red and the protospacer in blue. The clones were genotyped using high-resolution melt analysis, SANGER sequencing or deep sequencing. The induced indels are shown in the box below.

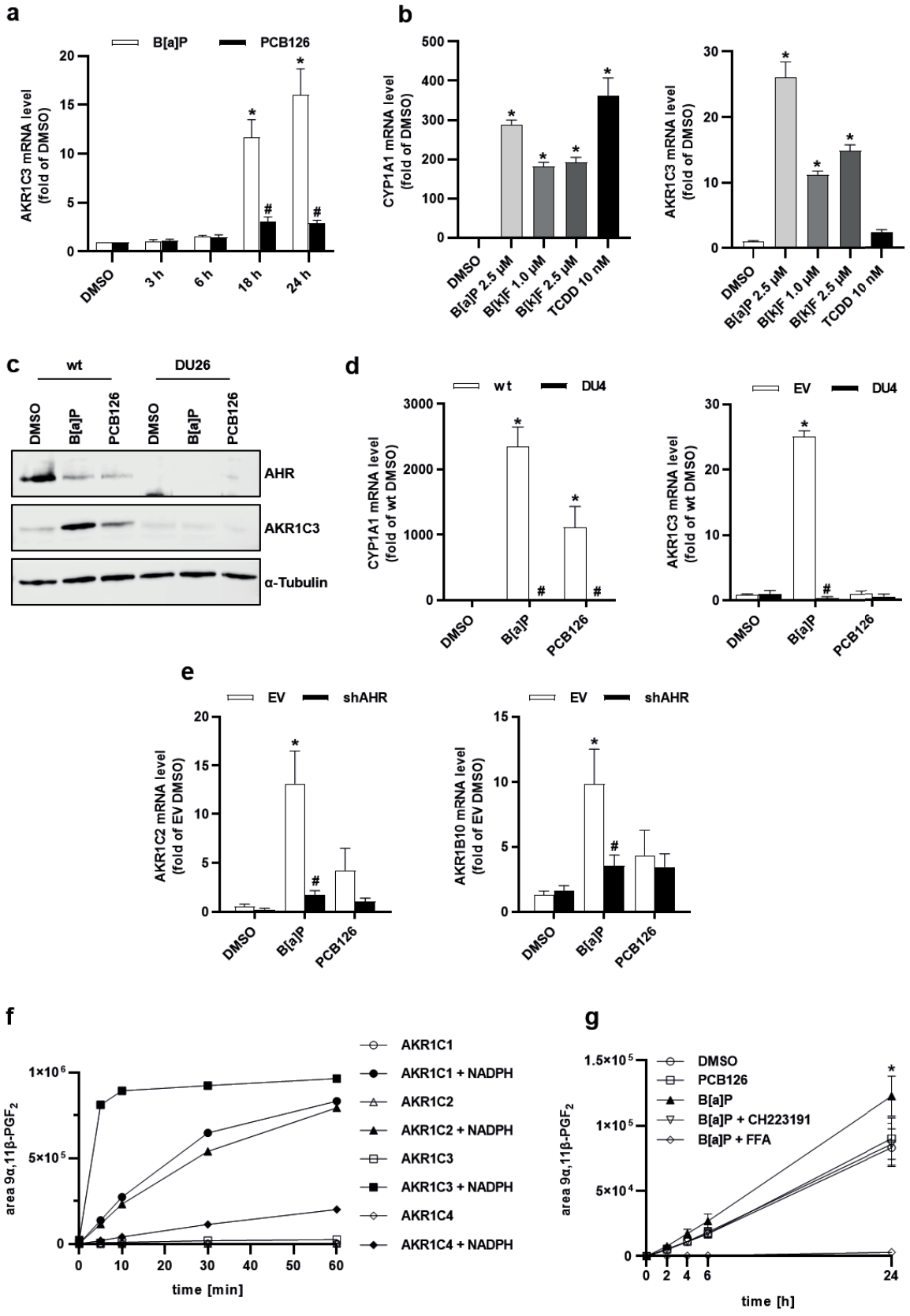
a
B[a]P
PCB126
AKR1C3 mRNA level (fold of DMSO)
DMSO
3 h
6 h
18 h
24 h
b
CYP1A1 mRNA level (fold of DMSO)
AKR1C3 mRNA level (fold of DMSO)
DMSO
B[a]P 2.5 µM
B[k]F 1.0 µM
B[k]F 2.5 µM
TCDD 10 nM
c
wt
DU26
DMSO
B[a]P
PCB126
AHR
AKR1C3
α-Tubulin
d
wt
DU4
CYP1A1 mRNA level (fold of wt DMSO)
EV
DU4
AKR1C3 mRNA level (fold of wt DMSO)
e
EV
shAHR
AKR1C2 mRNA level (fold of EV DMSO)
AKR1B10 mRNA level (fold of EV DMSO)
f
AKR1C1
AKR1C1 + NADPH
AKR1C2
AKR1C2 + NADPH
AKR1C3
AKR1C3 + NADPH
AKR1C4
AKR1C4 + NADPH
area 9α,11β-PGF2
time [min]
g
DMSO
PCB126
B[a]P
B[a]P + CH223191
B[a]P + FFA
area 9α,11β-PGF2
time [h]

Figure S2: PAHs but not DLCs induce AKR1C3 in an AHR-dependent manner

a qRT-PCR analyses of *AKR1C3* in HaCaT keratinocytes stimulated with 2.5 µM B[a]P or 1 µM PCB126 for the indicated time. n = 6. *, p ≤ 0.05 compared to the corresponding DMSO control, #, p ≤ 0.05, compared to B[a]P of the time point. **b** qRT-PCR analyses of *CYP1A1* and *AKR1C3* transcript level in HaCaT keratinocytes treated as indicated for 24 h. n = 3. *, p ≤ 0.05 compared to DMSO. **c** Western blot analyses of AHR and AKR1C3 levels in HaCaT-AHR-KO (DU26) and wild-type (wt) controls. Cells were stimulated either with 2.5 µM B[a]P, 1 µM PCB126 or 0.1 % DMSO. α-Tubulin was used as loading control. n = 3, representative picture. **d** qRT-PCR analyses of *CYP1A1* and *AKR1C3* transcript level in MCF-7-AHR-KO (DU4) and wildtype (wt) MCF-7 cells stimulated with 2.5 µM B[a]P, 1 µM PCB126 or 0.1 % DMSO for 24 h. n = 3. *, p ≤ 0.05 compared to EV DMSO, #, p ≤ 0.05 compared to EV B[a]P. **e** qRT-PCR analyses of *AKR1C2* and *AKR1B10* of HaCaT-shAHR and HaCaT-EV keratinocytes exposed to 0.1 % DMSO, 2.5 µM B[a]P or 1 µM PCB126 for 24 h. n = 4. *, p ≤ 0.05 compared to EV DMSO, #, p ≤ 0.05 compared to EV B[a]P. **f** Heterologously expressed AKR1C isoforms were incubated with to 2 µM PGD_2 in the presence or absence of NADPH. LC-MS was used to analyze metabolically formed 9α,11β-PGF_2 in the cell culture supernatants at the indicated time points. **g** LC-MS analyses of NHEK-derived culture supernatants. Cells were stimulated with 0.1 % DMSO, 1 µM PCB126, 2.5 µM B[a]P, 2.5 µM B[a]P plus 10 µM CH223191 for 24 h. In addition, keratinocytes pretreated for 23 h with 2.5 µM B[a]P were co-exposed for 1 h to 50 µM flufenamic acid (FFA) and B[a]P. Subsequently, cells were treated with 1 µM PGD_2 in conditioned medium and the supernatant was collected at indicated time points. n = 4. *, p ≤ 0.05 compared to DMSO.

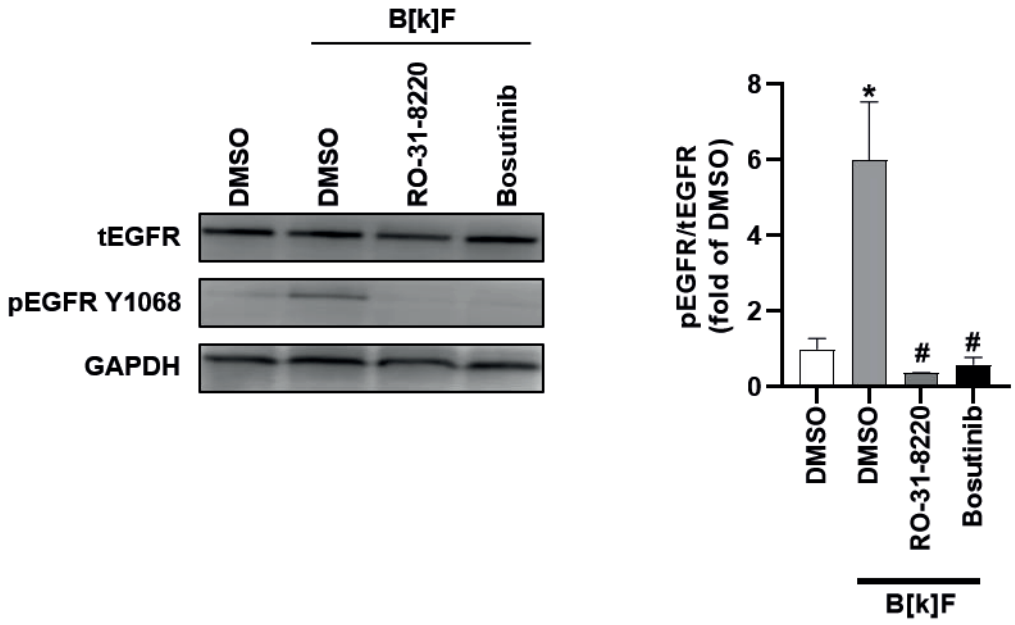

Figure S3: B[k]F induces phosphorylation of the EGFR

Western blot analysis of HaCaT cells treated with B[k]F (2.5 µM) for 2 h or control treated with DMSO (0.1 %). In parallel, cells were co-treated with RO-31-8220 (1 µM) or bosutinib (1 µM). Representative western blot of total EGFR and phosphorylated EGFR at residue Y1068. GAPDH was used as endogenous loading control. Densitometric quantification of the western blot analysis is shown in the right panel. n = 3. *, $p \leq 0.05$ compared to DMSO, #, $p \leq 0.05$ compared to DMSO/B[k]F.

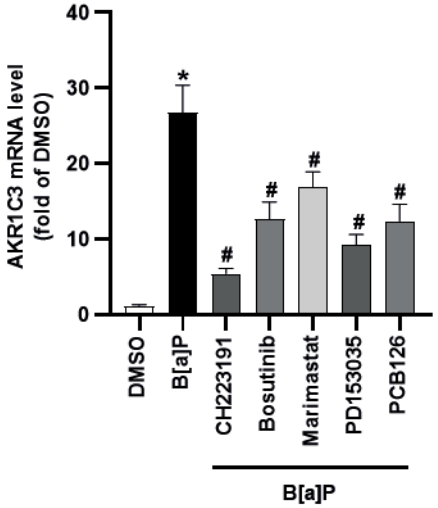

Figure S4: Induction of *AKR1C3 via* a non-canonical AHR signaling pathway is conserved in breast cancer cells

qRT-PCR analyses of *AKR1C3* in MCF-7 cells treated with B[a]P (2.5µM) in the absence or presence of CH223191 (10 µM), Bosutinib (1 µM), Marimastat (1 µM), PD153035 (1 µM), PCB126 (1 µM) or DMSO (0.1 %) for 24 h. n = 8. *, $p \leq 0.05$ compared to DMSO, #, $p \leq 0.05$ compared to B[a]P.

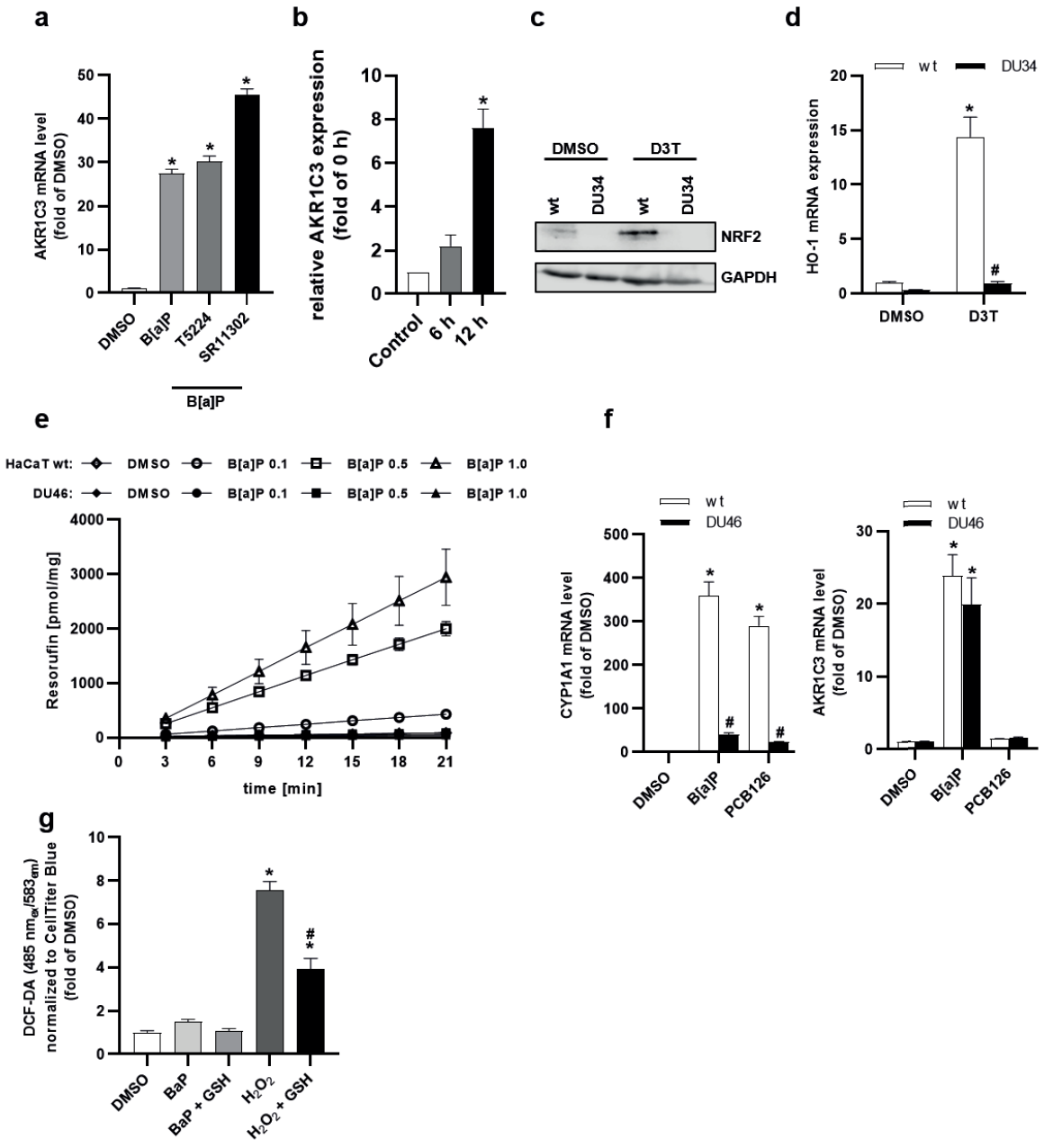

Figure S5: NRF2 regulates AKR1C3 expression in a ROS-independent manner

a Effect of AP-1 inhibition on AKR1C3 expression was analyzed via qRT-PCR. HaCaT keratinocytes were treated with DMSO (0.1 %), B[a]P (2.5 µM) alone or in combination with the AP-1 inhibitors T5224 or SR11302 (both 10 µM) for 24 h. n = 3. *, p ≤ 0.05 compared to DMSO**. b** qRT-PCR analysis of AKR1C3 in HaCaT keratinocytes. The cells were treated with 2.5 µM B[a]P or 0.1 % DMSO for 6 h and 12 h. n = 3. *, p ≤ 0.05 compared to DMSO **c** Western blot analyses of HaCaT and HaCaT-NRF2-KO (DU34) keratinocytes. Cells were treated for 24 h with DMSO (0.1 %) or D3T (70 µM). n = 1. **d** qRT-PCR analyses of *HO-1* in HaCaT and HaCaT-NRF2-KO (DU34) keratinocytes treated as described in **c.** n = 3. *, p ≤ 0.05 compared to DMSO wt, #, p ≤ 0.05 compared to the respective control sample. **e** HaCaT and HaCaT-CYP1A1-KO (DU46) cells were treated for 24 h with 0.1 µM, 0.5 µM and 1 µM B[a]P. Conversion of 7-ethoxyresorufin to resorufin was measured over 21 min and is shown in pmol/mg protein. **f** qRT-PCR analyses of CYP1A1 and AKR1C3 in HaCaT and HaCaT-CYP1A1-KO (DU46)

keratinocytes. Cells were treated with B[a]P (2.5 µM), PCB126 (1 µM) or DMSO (0.1 %) DMSO for 24 h. n = 3. *, $p \leq 0.05$ compared to DMSO HaCaT control, #, $p \leq 0.05$ compared to the respective proficient HaCaT control. **g** ROS formation was analyzed by DCF-DA assay. HaCaT cells were treated as indicated for 6 h. As a positive control cells were treated with H_2O_2 (10 µM) 30 min prior staining. n = 3. *, $p \leq 0.05$ compared to DMSO.

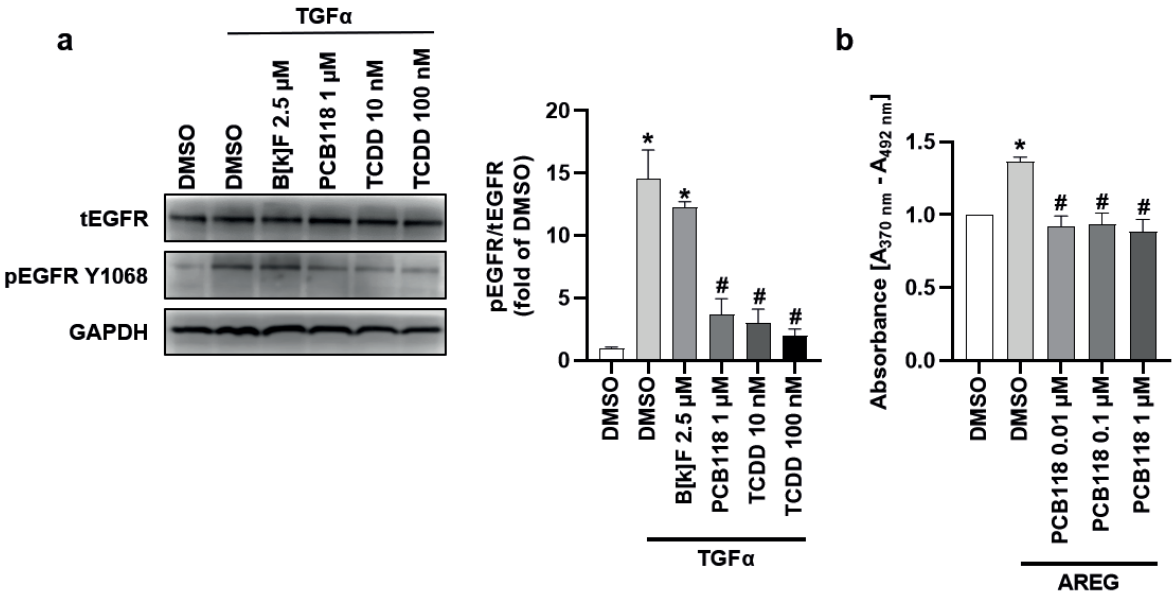

Fig. S6: Dioxin-like compounds interfere with EGFR ligand-induced EGFR activation

a Effect of B[k]F, PCB118 and TCDD on EGFR activation upon TGFα stimulation was analyzed via western blot analysis. HaCaT keratinocytes were starved for 3 h and next stimulated with TGFα (20 ng/ml) for 2.5 min on ice. Afterwards the cells were treated as indicated and the cells were incubated at 37 °C an 5 % CO2 for 30 min. Levels of total and phosphorylated EGFR (Y1068) were determined; GAPDH was used as endogenous loading control. n = 3. representative pictures are shown in the left panel. Densitometric quantification is depicted in the right panel. n = 3. *, p ≤ 0.05 compared to DMSO. #, p ≤ 0.05 compared to DMSO/AREG. **b** Colorimetric BrdU incorporation assay to assess the influence of PCB118 on AREG-induced DNA synthesis. HaCaT AHR-KO keratinocytes were treated as indicated for 4 h. Absorption was measured at a wavelength of 370 nm (reference wavelength 492 nm). n = 3. *, p ≤ 0.05 compared to DMSO. #, p ≤ 0.05 compared to AREG/DMSO.

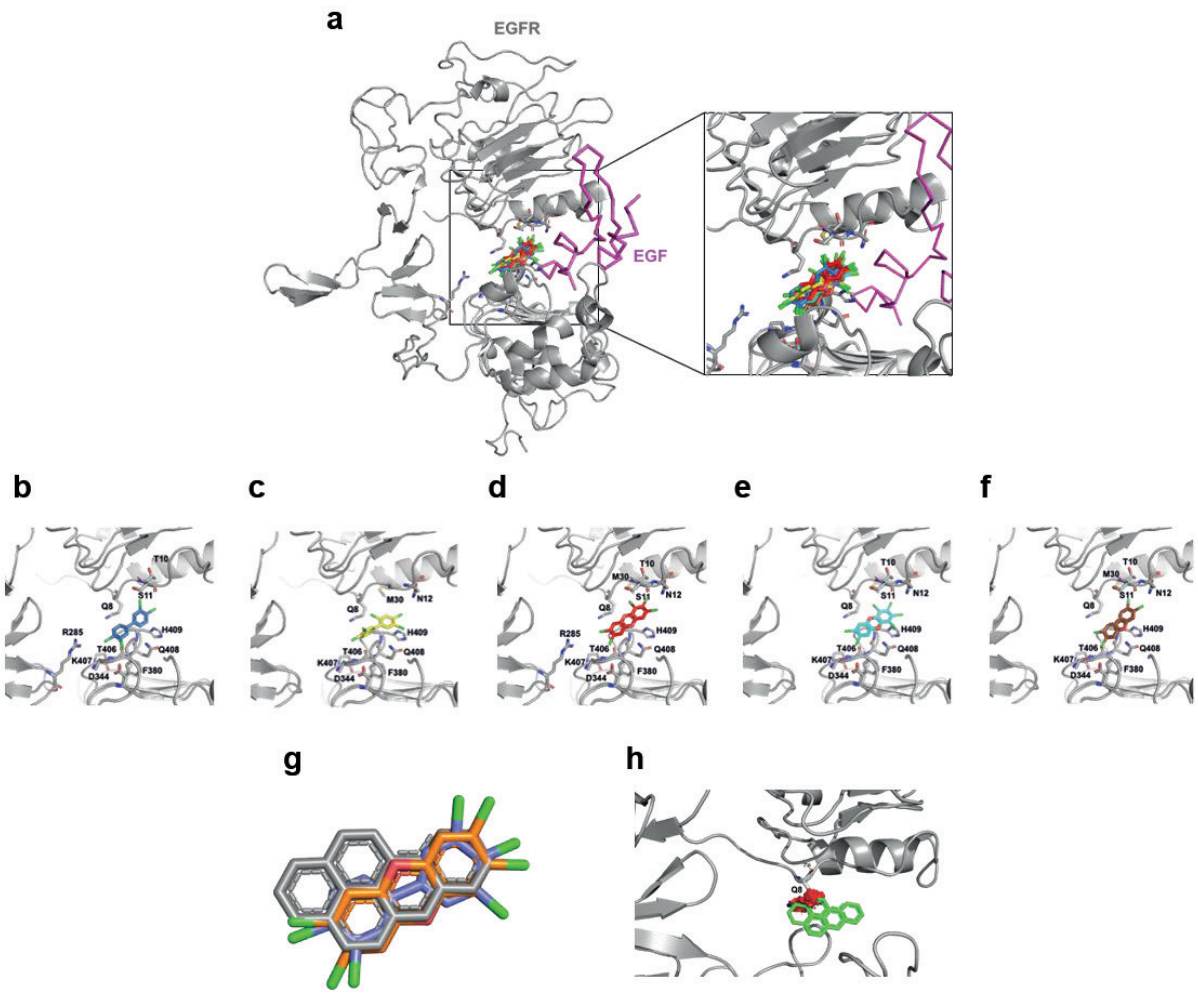

Fig. S7: Dioxin-like compounds bind to the extracellular domain of the EGFR.

a *In silico* docking analyses predicting the binding of PCB126 (slate blue), TCDD (orange), PCB77 (blue), PCB118 (yellow), PCDD (red), HCDD (cyan), and TCDF (brown) to the extracellular domain (ECD) of EGFR (grey). EGF (magenta; taken from PDB ID: 1ivo) is superimposed. Interacting residues for EGFR to the ligands are shown in stick representation. Interacting amino acid residues of EGFR ECD for **b** PCB77, **c** PCB118, **d** PCDD, **e** HCDD and **f** TCDF shows as stick models. **g** Superimposed compound structures of PCB126 (slate blue), TCDD (orange) and B[a]P (gray) shown as stick models. **h** B[a]P (green) would clash with EGFR Q8 in the same position as PCB126.

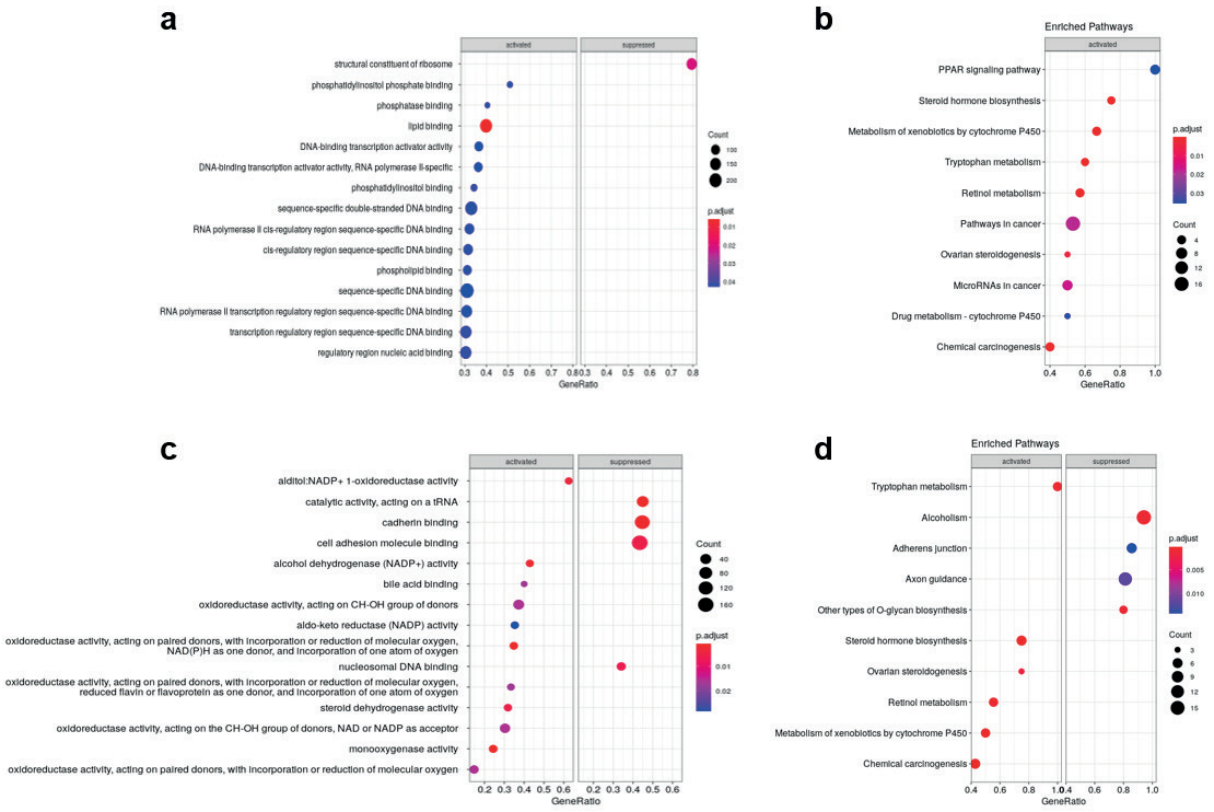

Figure S8: Gene set enrichment analyses of PCB126 and B[a]P treated HaCaT keratinocytes

Samples and data shown in Fig. 7 were used for these analyses. PCB126 treated HaCaT keratinocytes were compared to control treated cells (DMSO 0.1 %) and **a** gene set enrichment analysis of molecular functions and **b** KEGG pathway analysis were performed. **c** Gene set enrichment analysis of molecular functions and **d** KEGG pathway analysis of B[a]P treated samples compared to control treated cells (DMSO 0.1 %).

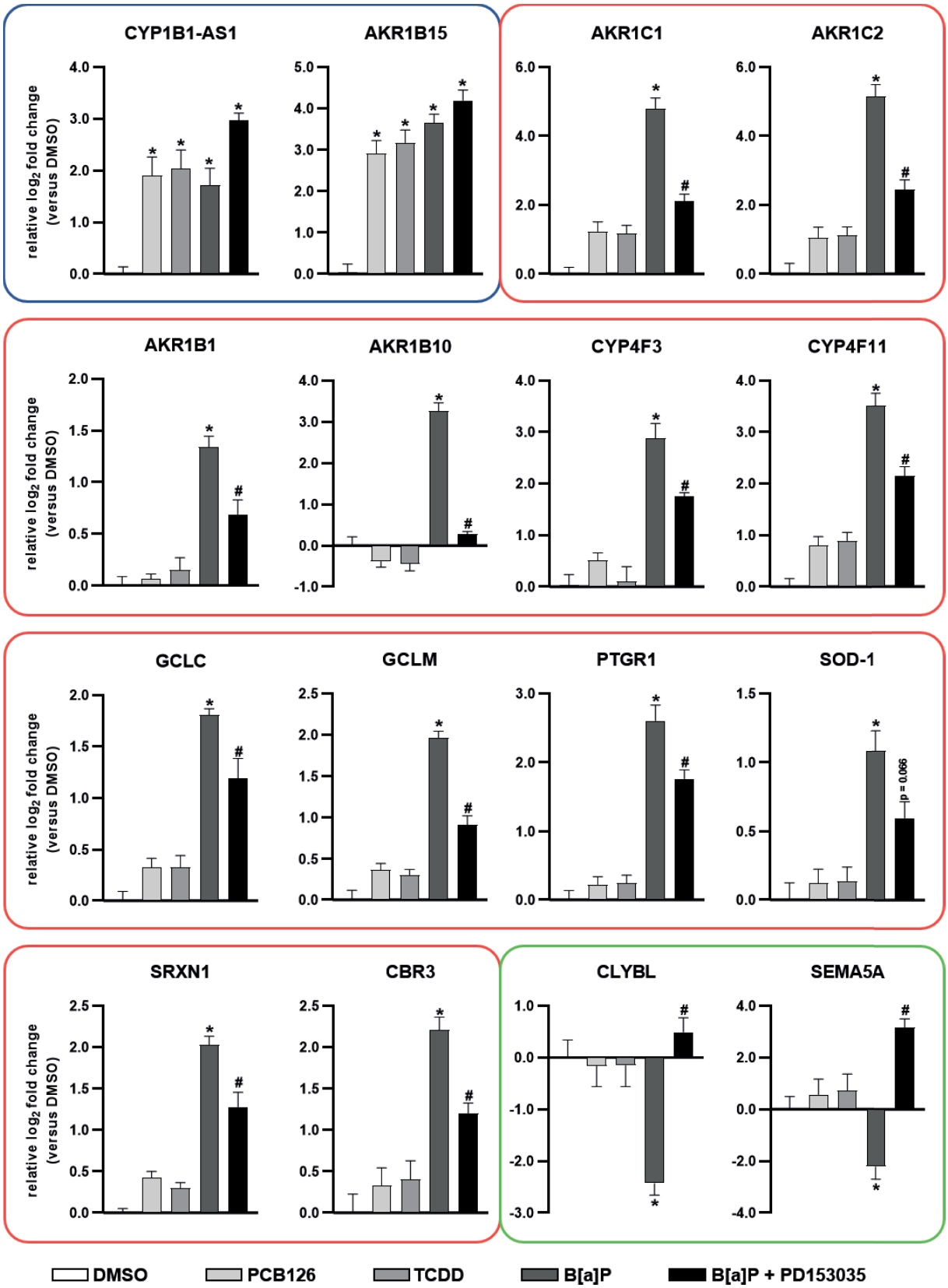

Figure S9: Ligand-specific gene expression pattern in HaCaT keratinocytes

qRT-PCR analyses of selected genes in HaCaT cells. Keratinocytes were treated for 24 h with either DMSO (0.1 %), PCB126 (1 µM), TCDD (10 nM), B[a]P (2.5 µM) or B[a]P (2.5 µM) + PD153035 (1 µM).

Results were normalized to DMSO-treated samples and log_2 transformed. n = 4. *, $p \leq 0.05$ compared to DMSO, #, $p \leq 0.05$ compared to B[a]P.

```
Human             LEEKKVCQGTSNKLTQLGTFEDHFLSLQRMFNNCEVVLGNLEITYVQRNYDLSFLKTIQE  60
Rhesus_monkey     LEEKKVCQGTSNKLTQLGTFEDHFLSLQRMFNNCEVVLGNLEITYVQRNYDLSFLKTIQE  60
Marmoset          LEEKKVCQGTSNKLTQLGTFEDHFLSLQRMFNNCEVVLGNLEITYVQRNYDLSFLKTIQE  60
Mouse             LEEKKVCQGTSNRLTQLGTFEDHFLSLQRMYNNCEVVLGNLEITYVQRNYDLSFLKTIQE  60
Rat               LEEKKVCQGTSNRLTQLGTFEDHFLSLQRMFNNCEVVLGNLEITYVQRNYDLSFLKTIQE  60
Rabbit            LEEKRVCQGTSNKLTQLGPFEDHFLSLQRMFNSCEVVLGNLEITYVQRNHDLSFLKTIQE  60
Pig               LEEKKVCQGTSNKLTQLGTFEDHFLSLQRMFNNCEVVLGNLEITYMQNSYNLSFLKTIQE  60
Sheep             LEEKKVCQGTSNKLTQLGTFEDHFLSLQRMFNNCEVVLGNLEITYMQSGYNLSFLKTIQE  60
Cat               LEEKKVCQGTSNRLTQLGTFEDHFLSLQRMFNNCEVVLGNLEITYMQRNYDLSFLKTIQE  60
Dog               LEEKRVCQGTSNRLTQLGTFEDHFLSLQRMFNNCEVVLGNLEITYMQRNYDLSFLKTIQE  60
                  ****:*******:***** ***********:*.************:* .::*********

Human             VAGYVLIALNTVERIPLENLQIIRGNMYYENSYALAVLSNYDANKTGLKELPMRNLQEIL  120
Rhesus_monkey     VAGYVLIALNTVERIPLENLQIIRGNMYYENSYALAVLSNYDANKTGLKELPMRNLQEIL  120
Marmoset          VAGYVLIALNTVERIPLENLQIIRGNMFYENSYALAVLSNYDANKTGLKELPMRNLQEIL  120
Mouse             VAGYVLIALNTVERIPLENLQIIRGNALYENTYALAILSNYGTNRTGLRELPMRNLQEIL  120
Rat               VAGYVLIALNTVERIPLENLQIIRGNALYENTYALAVLSNYGTNKTGLRELPMRNLQEIL  120
Rabbit            VAGYVLIALNTVESIPLESLQIIRGNVLYENTYALAVLSNYGANKTGLRELPMRNLQEIL  120
Pig               VAGYVLIALNTVEKIPLENLQIIRGNVLYENTHALAVLSNYGANKTGLRELPMRNLQEIL  120
Sheep             VAGYVLIALNTVEKIPLENLQIIRGNVLYENTHALAVLSNYGANKTGLRELPLRNLQEIL  120
Cat               VAGYVLIALNTVEKIPLENLQIIRGNVLYENTHALSVLSNYGTNKTGLRELPMRNLHEIL  120
Dog               VAGYVLIALNTVEKIPLENLQIIRGNVLYENTHALSVLSNYGSNKTGLQELPLRNLHEIL  120
                  ************* ****.*******  ***::**::****.:*:***:***:***:***

Human             HGAVRFSNNPALCNVESIQWRDIVSSDFLSNMSMDFQNHLGSCQKCDPSCPNGSCWGAGE  180
Rhesus_monkey     HGAVRFSNNPALCNVESIQWRDIVSSEFLSNMSMDFQNHLGSCQKCDPSCPNGSCWGAGE  180
Marmoset          HGAVRFSNNPTLCNVDSIQWRDIVSNDFLSNMSMDFQNHVAGCQKCDPSCPNGSCWGAGE  180
Mouse             IGAVRFSNNPILCNMDTIQWRDIVQNVFMSNMSMDLQSHPSSCPKCDPSCPNGSCWGGGE  180
Rat               IGAVRFSNNPILCNMETIQWRDIVQDVFLSNMSMDVQRHLTGCPKCDPSCPNGSCWGRGE  180
Rabbit            HGAVRFSNNPVLCNVETIQWRDIVHGDFLSNMSLDMQNPLGSCQKCDPSCPNGSCWGAGG  180
Pig               QGAVRFSNNPALCHAESIQWRDIVNSDFLSNMSMDFQSQLGSCPKCDPGCLNGSCWGAGK  180
Sheep             QGAVRFSNNPVLCNMETIQWRDIINTDFLSNVTGDFQNQQGNCSKCDPGCLNRSCWGAGE  180
Cat               QGAVRFSNNPVLCNVETIQWRDIVDNDFISNMSMDFQNHVGNCQKCDPGCPNGSCWGPGK  180
Dog               QGAVRFSNNPVLCNVETIQWRDIVDNDFISNMSMDIQNQAGRCQKCDPSCPNGSCWGPGK  180
                  ********* **: ::*******:   *:**:: *.*     * ****.* * **** *

Human             ENCQKLTKIICAQQCSGRCRGKSPSDCCHNQCAAGCTGPRESDCLVCRKFRDEATCKDTC  240
Rhesus_monkey     ENCQKLTKIICAQQCSGRCRGKSPSDCCHNQCAAGCTGPRESDCLVCRKFRDEATCKDTC  240
Marmoset          ENCQKLTKIICAQQCSGRCRGKSPSDCCHNQCAAGCTGPRESDCLVCRKFRDEATCKDTC  240
Mouse             ENCQKLTKIICAQQCSHRCRGRSPSDCCHNQCAAGCTGPRESDCLVCQKFQDEATCKDTC  240
Rat               ENCQKLTKIICAQQCSRRCRGRSPSDCCHNQCAAGCTGPRESDCLVCHRFRDEATCKDTC  240
Rabbit            ENCQRLTKIICAQQCSGRCRGKSPSDCCHNQCAAGCTGPRESDCLVCRKFRDEATCKDTC  240
Pig               ENCQKLTKVICAQQCSGRCRGRSPSDCCHNQCAAGCTGPRESDCLVCRRFRDEATCKDTC  240
Sheep             ENCQKLTKIICAQQCSGRCRGRSPSDCCHNQCAAGCTGPRESDCLVCRRFRDEATCKDTC  240
Cat               ENCQKLTKIICAQQCSGRCRGRSPSDCCHNQCAAGCTGPRESDCLVCRKFRDEATCKDTC  240
Dog               ENCQKLTKIICAQQCSGRCRGRSPSDCCHNQCAAGCTGPRESDCLVCRKFRDEATCKDTC  240
                  ****:***:******* ****:*************************::*:*********

Human             PPLMLYNPTTYQMDVNPEGKYSFGATCVKKCPRNYVVTDHGSCVRACGADSYEMEEDGVR  300
Rhesus_monkey     PPLMLYNPTTYQMDVNPEGKYSFGATCVKKCPRNYVVTDHGSCVRACGADSYEMEEDGVR  300
Marmoset          PPLMLYNPTTYQMDVNPEGKYSFGATCVKKCPRNYVVTDHGSCVRACGADSYEVEEDGVR  300
Mouse             PPLMLYNPTTYQMDVNPEGKYSFGATCVKKCPRNYVVTDHGSCVRACGPDYYEVEEDGIR  300
Rat               PPLMLYNPTTYQMDVNPEGKYSFGATCVKKCPRNYVVTDHGSCVRACGPDYYEVEEDGVS  300
Rabbit            PPLMLYNPTTYQMDVNPEGKYSFGATCVKKCPRNYVVTDHGSCVRACGPDSYEVEEDGVR  300
Pig               PPLMLYNPTTYQMDVNPLGKYSFGATCVKKCPRNYVVTDHGSCVRACSSDSYEVEEDGVR  300
Sheep             PPLMLYDPTTYEMKVNPLGKYSFGATCVKKCPRNYVVTDHGSCVRACSSDSQEVEEDGVR  300
Cat               PPLMLYNPTTYQMDVNPEGKYSFGATCVKKCPRNYVVTDHGSCVRACSSDSYEVEEDGVR  300
Dog               PPLMLYNPTTYQMDVNPEGKYSFGATCVKKCPRNYVVTDHGSCVRACSSDSYEVEEDGVR  300
                  ******:****:*.*** ****************************. *  *:****:

Human             KCKKCEGPCRKVCNGIGIGEFKDSLSINATNIKHFKNCTSISGDLHILPVAFRGDSFTHT  360
Rhesus_monkey     KCKKCEGPCRKVCNGIGIGEFKDTLSINATNIKHFKNCTSISGDLHILPVAFRGDSFTHT  360
Marmoset          KCKKCEGPCRKVCNGIGIGKFKDTLSINATNIKHFKNCTSISGDLHILPVAFRGDSFTHT  360
Mouse             KCKKCDGPCRKVCNGIGIGEFKDTLSINATNIKHFKYCTAISGDLHILPVAFKGDSFTRT  360
Rat               KCKKCDGPCRKVCNGIGIGEFKDTLSINATNIKHFKYCTAISGDLHILPVAFKGDSFTRT  360
Rabbit            KCKKCEGPCRKVCNGIGIGEFKDTLSINATNIKHFKNCTSISGDLHILPVAFRGDSFTRT  360
Pig               KCKKCDGPCGKVCNGIGIGEFKDTLSINATNIKHFRNCTSISGDLHILPVAFRGDSFTRT  360
Sheep             KCKKCDGPCAKVCNGIGIGEFKDTLSINATNIKHFRNCTSISGDLHILPVAFRGDSFTRT  360
```

```
Cat                 KCKKCEGPCRKVCNGIGIGEFKDTLSINATNIKHFKNCTSISGDLHILPVAFRGDSFTHT  360
Dog                 KCKKCEGPCRKVCNGIGIGEFKDTLSINATNIKHFKNCTSISGDLHILPVAFRGDSFTHT  360
                    *****:*** *********:***:***********: **:************:*****:*

Human               PPLDPQELDILKTVKEITGFLLIQAWPENRTDLHAFENLEIIRGRTKQHGQFSLAVVSLN  420
Rhesus_monkey       PPLDPQELDILKTVKEITGFLLIQAWPENRTDLHAFENLEIIRGRTKQHGQFSLAVVSLN  420
Marmoset            PPLDPKELDILKTVKEITGFLLIQAWPENRTDLHAFENLEIIRGRTKQHGQFSLAVVSLN  420
Mouse               PPLDPRELEILKTVKEITGFLLIQAWPDNWTDLHAFENLEIIRGRTKQHGQFSLAVVGLN  420
Rat                 PPLDPRELEILKTVKEITGFLLIQAWPENWTDLHAFENLEIIRGRTKQHGQFSLAVVGLN  420
Rabbit              PPLDPEELDILKTVREITGFLLIQAWPENKTDLHAFENLEIIRGRTKQHGQFSLAVVGLD  420
Pig                 PPLDPKELDILKTVKEITGFLLIQAWPENRTGLHAFENLEIIRGRTKQHGQFSLAVVGLD  420
Sheep               APLDPKELDILKTVKEITGFLLIQAWPENRTDLHAFENLEIIRGRTKQHGQFSLAVVGLD  420
Cat                 PPLDPKELDILKTVKEITGFLLIQAWPENRTDLHAFENLEIIRGRTKQHGQFSLAVVGLD  420
Dog                 LPLDPKELDILKTVKEITGFLLIQAWPENRTDLHAFENLEIIRGRTKQHGQFSLAVVGLN  420
                    ****.**:*****:************:* *.************************.*:
```

Supplementary figure S10: Multiple alignment of mammalian EGFR protein sequences.

A multiple alignment of the N-terminal 420 amino acids of the mammalian EGFR protein (mature) was carried out using the Clustal Omega online tool and the NCBI References Sequences given in the Material and Methods section. Bold letters in blue stand for amino acid residues predicted to be involved in the binding of all tested DLCs. Bold letter in purple stand for amino acid residues predicted to be involved in the binding of some of the test compounds. Bold letters in green stand for predicted amino acid residues that were experimentally proven to be required for binding of PCB126. Bold letters in red stand for predicted amino acids that were experimentally excluded being critically required for DLC binding. “*” = fully conserved residue, “:” = conservation between groups of strongly similar properties, “.” = conservation between groups of weakly similar properties.

Supplementary table 1

A) qPCR oligonucleotides

Gene symbol	Gene	Direction	Sequence (5' > 3')
ACTB	β-Actin	F	CCCCAGGCACCAGGGCGTGAT
		R	GGTCATCTTCTCGCGGTTGGCCTTGGGGT
AKR1B1	Aldo-keto reductase 1B1	F	TACCATGAGAAGGGCCTGGTGAAA
		R	TCCAGAATGTTGGTGTCACTGGGA
AKR1B10	Aldo-keto reductase 1B10	F	TTCTTTGAGAGACCCCTTGTGAGG
		R	TCCAAGAACGTTGCTTTTCCACCG
AKR1B15	Aldo-keto reductase 1B15	F	ACTGGCCTAAAGAGTTCCCTTC
		R	GCATCAATGGCCACCTTCAC
AKR1C1	Aldo-keto reductase 1C1	F	CAATTGAAGCTGGCTTCCGC
		R	TCACTTCCTCACCTGGCTTT
AKR1C2	Aldo-keto reductase 1C2	F	TCTAGAGGCCGTCAAATTGGCA
		R	TGGTCGATGGGAATTGCTCCAA
AKR1C3	Aldo-keto reductase 1C3	F	AAGCTGGGTTCCGCCATATAGA
		R	CAGTGAGTTTTCCAAGGCTGG
ARHGAP26	Rho GTPase activating protein 26	F	TAAGAATGCTTCCAGGACCACTC
		R	GCTGTAACATCTGCCGATTTTTC
CBR3	Carbonyl reductase 3	F	AGTTCTCTGGGGATGTGGTG
		R	GTTGACCAGTACGTTGAGCC
CLYBL	Citrate lyase beta like	F	TCGACTGTGAGGATGGAGTG
		R	ATCAGGCTGGAAGGAAGGAC
CYP1A1	Cytochrome P450 1A1	F	TTCATGCAGAAGATGGTC
		R	TCTCCTGACAGTGCTCAATC
CYP1B1	Cytochrome P450 1B1	F	CGGCTGGATTTGGAGAACGTA
		R	TGATCCAATTCTGCCTGCACT
CYP1B1-AS1	CYP1B1-antisense RNA 1	F	GTGCAGTTGTGAAGTCAGCA
		R	ATGAGCATGGAGAAGGGAGG
CYP4F3	Cytochrome P450 4F3	F	GAGGAGGTTGTGTGGGACAAGG
		R	GTGGAAGATGCGGACGATTGCG
CYP4F11	Cytochrome P450 4F11	F	CGAAACAGAACTGGTTTTGGG
		R	GGTCAATGTCTTCATGCCCTC
GAPDH	Glyceraldehyde 3-phosphate	F	AGGTGAAGGTCGGAGTCA
	dehydrogenase	R	GGTCATTGATGGCAACAA
GCLC	Glutamate-cysteine ligase	F	GGCACAAGGACGTTCTCAAGT
	catalytic subunit	R	CAGACAGGACCAACCGGAC
GCLM	Glutamate-cysteine ligase	F	CATTTACAGCCTTACTGGGAGG
	modifier subunit	R	ATGCAGTCAAATCTGGTGGCA
HO-1	Heme oxygenase 1	F	GCCATGAACTTTGTCCGGTG
		R	GGATGTGCTTTTCGTTGGGG
PTGR1	Prostaglandin reductase 1	F	TGGCCAGACACAATACCACT

		R	CAGACCCTACTGCTCCAACA
SEMA5A	Semaphorin 5a	F	GTCTATACTTACTGCCAGCG
		R	GTTAAATGCCTTGATGGCCTC
SOD1	Superoxide dismutase 1	F	GGCCGATGTGTCTATTGAAGA
		R	GGGCCTCAGACTACATCCAA
SRXN1	Sulfiredoxin 1	F	CAAGGTGCAGAGCCTCGT
		R	CAGCCCCCAAAGGAGTAGAA

B) Primary antibodies

Antibody	Supplier	Catalog No.
β-Actin	Cell Signaling Technology, Frankfurt a.M., Germany	3700
AHR	Cell Signaling Technology, Frankfurt a.M., Germany	83200
AKR1C3	R&D Systems, Minneapolis, MI, USA	MAB7678
ARNT	Santa Cruz Biotechnology, Dallas, TX, USA	sc-55526
CYP1A1	Santa Cruz Biotechnology, Dallas, TX, USA	sc-20772
EGFR	Cell Signaling Technology, Frankfurt a.M., Germany	2232
pEGFR Y845	Cell Signaling Technology, Frankfurt a.M., Germany	2231
pEGFR Y1068	Cell Signaling Technology, Frankfurt a.M., Germany	3777
pEGFR Y1173	Cell Signaling Technology, Frankfurt a.M., Germany	4407
ERK1/2	Cell Signaling Technology, Frankfurt a.M., Germany	9102
pERK1/2 T202/Y204	Cell Signaling Technology, Frankfurt a.M., Germany	9101
GAPDH	Cell Signaling Technology, Frankfurt a.M., Germany	2118
NRF2	GeneTex, Irvine, CA, USA	GTX103322
Src	Upstate, Lake Placid, NY, USA	05-184
pSrc Y416	Cell Signaling Technology, Frankfurt a.M., Germany	6943
α-Tubulin	ExBio, Vestec, Czech Republic	11-250-C025
Vinculin	Cell Signaling Technology, Frankfurt a.M., Germany	13901

C) Mutagenesis oligonucleotides

AA exchange	Direction	Sequence (5' > 3')
Q8A	F	GAAAAGAAAGTTTGCGCAGGCACGAGTAACAAG
	R	CTTTTCTTTCAAACGCGTCCGTGCTCATTGTTC
S11A	F	GTTTGCCAAGGCACGGCTAACAAGCTCACGCAG
	R	CAAACGGTTCCGTGCCGATTGTTCGAGTGCGTC
Q408A	F	CGCGGCAGGACCAAGGCACATGGTCAGTTTTCT
	R	GCGCCTGGTTCCGTGTACCAGTAAAAGA

Supplementary table 2: Docking score, calculated affinity and residues involved for all AHR ligands tested with the ECD of EGFR.

Ligand name	Docking Score (kcal/mol)	Calculated affinity (nM)	Residues involved
TCDD	-11.6	55.7	Q8, T10, S11, N12, M30, D344, F380, T406, K407, Q408, H409
PCB126	-11.1	59.3	Q8, T10, S11, N12, M30, R285, D344, F380, T406, K407, Q408, H409
PCB77	-10.1	67.9	Q8, T10, S11, R285, D344, F380, T406, K407, Q408, H409
PCB118	-9.3	78.6	Q8, N12, M30, D344, F380, T406, K407, Q408, H409
PCDD	-11.5	56.4	Q8, T10, S11, N12, M30, R285, D344, F380, T406, K407, Q408, H409
HCDD	-11.9	51.2	Q8, T10, S11, N12, M30, D344, F380, T406, K407, Q408, H409
TCDF	-11.5	55.9	Q8, T10, S11, N12, M30, D344, F380, T406, K407, Q408, H409
B[a]P	-	-	No interaction at binding site

2.3 Benzotriazole UV stabilizers disrupt epidermal growth factor receptor signaling in human cells

Natalie C. Sondermann, Afaque A. Momin, Stefan T. Arold, Thomas Haarmann-Stemmann

BUVs sind weit verbreitete Zusatzstoffe in synthetischen Polymeren, die in die Umwelt freigesetzt werden und persistent sind. Sie können sich in Organismen, einschließlich Menschen, anreichern und wurden in Fischen, Vögeln, Meeressäugern und Muttermilch nachgewiesen. Behörden wie die Europäische Chemikalienagentur stufen einige BUVs als besonders besorgniserregend ein und fordern weitere Untersuchungen. In dieser Studie zeigen wir, dass BUVs, insbesondere chlorierte Varianten, an die ECD des EGFR binden und somit die Aktivierung durch Wachstumsfaktoren blockieren. Dadurch hemmen sie auch das Downstream-Signaling des EGFR, wie die ERK1/2-Phosphorylierung und DNA-Synthese in menschlichen Keratinozyten, was neue mechanistische Einblicke bietet.

Journal:	Environment International
Impact Factor:	10,3 (2024)
Beitrag zur Veröffentlichung:	90 % Konzept, Literaturrecherche, Schreiben, Editieren, Visualisierung, Experimente für Abb. 2, 3, 4, 5, 6, 7
Art der Autorenschaft:	Erstautorenschaft
Status der Publikation:	Veröffentlicht am 17.07.2024

Environment International 190 (2024) 108886

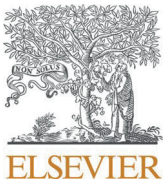

Contents lists available at ScienceDirect

Environment International

journal homepage: www.elsevier.com/locate/envint

Full length article

Benzotriazole UV stabilizers disrupt epidermal growth factor receptor signaling in human cells

Natalie C. Sondermann [a], Afaque A. Momin [b], Stefan T. Arold [b], Thomas Haarmann-Stemmann [a,*]

[a] IUF – Leibniz-Research Institute for Environmental Medicine, 40225 Düsseldorf, Germany
[b] Biological and Environmental Science and Engineering Division, Center of Excellence on Smart Health, King Abdullah University of Science and Technology (KAUST), Thuwal 23955-6900, Kingdom of Saudi Arabia

ARTICLE INFO

Keywords:
Benzotriazoles
Epidermal growth factor receptor
Human epithelial cells
Persistent organic pollutants
Tyrosine kinase inhibitors
UV absorber

ABSTRACT

Phenolic benzotriazole UV stabilizers (BUV) are commonly used additives in synthetic polymeric products, which constantly leak into the environment. They are persistent and bioaccumulative, and have been detected not only in fish, birds, and sea mammals, but also in humans, including breast milk samples. Several authorities including the European Chemical Agency already consider some BUVs as Substances of Very High Concern in need of further information, e.g. mechanistical studies and biomonitoring. In this study, we are addressing this need by investigating the effect of several BUVs on the activity of the human epidermal growth factor receptor (EGFR), an important regulator of cellular processes that has recently been identified as a cell-surface receptor for environmental organic chemicals. By combining *in silico* docking, mutant analyses, receptor binding and internalization assays, we demonstrate that BUVs, particularly the chlorinated variants, bind to the extracellular domain of EGFR and thereby prevent the binding of growth factors. Accordingly, BUVs can inhibit EGFR downstream events, such as ERK1/2 phosphorylation and DNA synthesis, in human keratinocytes. Our data establish EGFR as a plasma membrane receptor for BUVs, offering novel mechanistic insights into the biological effects induced by these widespread and persistent chemicals. The findings of this study may not only improve hazard assessment for BUVs, but also contribute to the development of novel EGFR-targeting drugs.

1. Introduction

Benzotriazole UV stabilizers (BUVs), also referred to as phenolic benzotriazoles, are a class of industrial chemicals that are considered to be one of the most important UV absorbers. Due to their ability to absorb damaging ultraviolet (UV) radiation and rapidly convert it into heat (Köhler et al., 2010), they are commonly used as additives in synthetic polymeric industrial or household products and plastic packages, as well as paints, coatings, and adhesives. Because of their chemical properties, BUVs consistently leak into the environment during production, application, and disposal stages of plastics (Khare et al., 2023). The environmental occurrence of these anthropogenic compounds was first described in 1978 by Jungclaus *et al.* following analysis of water and sediment samples (Jungclaus et al., 1978). BUVs tend to accumulate in biological tissues of aquatic invertebrates (Nakata et al., 2012), fish (Lu et al., 2019), seabirds (Tanaka et al., 2020), and marine mammals (Nakata and Shinohara, 2010). Thus, humans are commonly exposed to BUVs through their diet. BUVs have also been detected in a variety of sunscreens and isolation cosmetics, from where they can easily penetrate into the human skin due to their lipophilic nature (Bai et al., 2024). Moreover, BUVs are present in outdoor and indoor particulate air pollution, and thus may be inhaled or ingested upon mucociliary clearance (An et al., 2022; Kim et al., 2012; Maceira et al., 2019).

In 2023, the BUV UV-328 was added to Annex A of the Stockholm Convention on Persistent Organic Pollutants (POPs) with the aim to eliminate its production and use (Stockholm Convention on POPs, 2023). The internal exposure to UV-328 and potentially associated health effects will be monitored in a recently launched European Union-wide human biomonitoring program (Ougier et al., 2021). Also, German authorities and industry associations joined forces to promote the development of analytical methods for monitoring serval chemicals of high concern, including UV-327, UV-328 and other UV filters, in human

Abbreviations: AREG, Amphiregulin; BUV, Benzotriazole UV Stabilizers; ECD, Extracellular Domain; ECHA, European Chemical Agency; EGF, Epidermal Growth Factor; EGFR, Epidermal Growth Factor Receptor; PCB, Polychlorinated biphenyl; POP, Persistent Organic Pollutant; UV, Ultraviolet.

* Corresponding author at: IUF – Leibniz-Research Institute for Environmental Medicine, Auf˙m Hennekamp 50, 40225 Düsseldorf, Germany.
E-mail address: thomas.haarmann-stemmann@IUF-duesseldorf.de (T. Haarmann-Stemmann).

https://doi.org/10.1016/j.envint.2024.108886
Received 23 May 2024; Received in revised form 3 July 2024; Accepted 12 July 2024
Available online 14 July 2024

blood and urine (Kolossa-Gehring et al., 2017). Similar concerns were risen by Japan in 2007, when they declared UV-320 a "Class I Specified Chemical Substance", indicating that it was comparable to well-known POPs concerning its nature and toxicity. This chemical was approximately used in 70 % of plastics in Japan at that time, specifically in long-life products such a car parts and construction materials (Watanabe and Noma, 2010). UV-326, UV-327 and UV-350 are currently on the European Chemical Agency's (ECHA) candidate list of Substances of Very High Concern and are being investigated as subjects for informal risk assessment and risk management (ECHA, 2023). However, despite their ubiquitous distribution and persistence in the environment, and the resulting exposure of wildlife and humans, our current understanding of the biological effects induced by BUVs, in particular in mammals, remains limited (Khare et al., 2023). In fact, besides a few studies reporting that several BUVs activate the aryl hydrocarbon receptor (Nagayoshi et al., 2015) and induce the expansion of immunosuppressive regulatory T cells in mice (Kubota et al., 2022), the majority of mechanistic studies focusses on the potential interference of BUVs with sex steroid hormone receptors (Zhuang et al., 2017; Feng et al., 2020; He et al., 2022; Sakuragi et al., 2021).

Regardless of the eco-/toxicological concerns of its phenolic derivatives, benzotriazole is widely used as a scaffold for the synthesis of novel bioactive compounds. Many benzotriazole derivatives exhibit antiproliferative properties and thus are of interest for the development of drugs against cancer and other hyperproliferative diseases (Kassab, 2023). An important regulator of cell proliferation and differentiation in development, physiology and disease, is the epidermal growth factor receptor (EGFR) (Gschwind et al., 2004; Chen et al., 2016). This receptor tyrosine kinase belongs to the ErbB family and is activated upon binding of polypeptide growth factors, such as the epidermal growth factor (EGF) and amphiregulin (AREG), to its extracellular domain (ECD). Subsequently, the ECD undergoes conformational changes that facilitate homodimerization or heterodimerization with another ErbB protein. Dimerization stimulates the intrinsic tyrosine kinase activity of EGFR resulting in its autophosphorylation and the subsequent recruitment of adapter proteins and activation of downstream signal transduction (Chen et al., 2016). Neutralizing EGFR antibodies and small molecules that block the ATP-binding site of the receptor tyrosine kinase have been utilized as therapeutic agents for decades (Gschwind et al., 2004; Chen et al., 2016). However, there is accumulating evidence for the existence of small molecules that bind directly to the EGFR ECD, thereby avoiding growth factor-binding and the subsequent activation of EGFR. To the best of our knowledge, phenobarbital was the first compound identified to interact with the EGFR ECD and to reduce EGF binding (Mutoh et al., 2013). Meanwhile, we and others have shown that dioxins and structurally-related polychlorinated biphenyls (PCBs) can bind to the EGFR ECD and inhibit its activation by growth factors (Hardesty et al., 2018; Vogeley et al., 2022). In the current study, we therefore tested if the ECD of the human EGFR serves as a cell-surface receptor for BUVs. To this aim, we investigated whether BUVs bind to the EGFR ECD, interfere with growth factor-induced EGFR activation, and affect downstream signaling events and biological functions in human cell cultures.

2. Material & methods

2.1. Cell culture

HaCaT keratinocytes were kindly provided by Petra Boukamp (DKFZ, Heidelberg, Germany) and cultured in DMEM low glucose (1 g/l) medium (PAN Biotech, Aidenbach, Germany) and supplemented with 10 % FBS and 1 % antibiotics/antimycotics (PAN Biotech). HepG2 cells were cultured in RPMI 1640 containing 10 % FBS and 1 % antibiotics/antimycotics (PAN Biotech). All cells were kept in a humidified atmosphere of 5 % CO2 at 37 °C. Cells were cultured in T175 flasks (#83.3912.002, Sarstedt, Nümbrecht, Germany) and seeded in transparent polystyrene 6-well plates (#83.3920, Sarstedt) or 96-well plates (#655180, Greiner Bio One, Frickenhausen, Germany).

2.2. Chemicals and treatment

UV-326 (2-*tert*-Butyl-6-(5-chlor-2H-benzotriazol-2-yl)-4-methylphenol), UV-327 (2,4-di-*tert*-butyl-6-(5-chlorobenzotriazol-2-yl) phenol), UV-350 (2-(2H-benzotriazol-2-yl)-4-(*tert*-butyl)-6-(*sec*-butyl) phenol) and UV-PS (2-(5-*tert*-Butyl-2-hydroxyphenyl)benzotriazole) were purchased from Sigma-Aldrich (Taufkirchen, Germany). UV-320 (2-benzotriazol-2-yl-4,6-di-*tert*-butylphenol) was purchased from Santa Cruz Biotechnology (Dallas, TX). PD153035 and PD98059 were purchased from Absource Diagnostics (Munich, Germany). 3,3′,4,4′,5-Pentachlorobiphenyl (PCB126) and 2,3′,4,4′,5-pentachlorobiphenyl (PCB118) were bought from LGC Standards (Wesel, Germany). Recombinant human amphiregulin (AREG) and recombinant human EGF were purchased from PeproTech (Rocky Hill, NY). AREG and EGF were dissolved and diluted in water, the other compounds in DMSO. Treatment time and applied concentrations of the chemicals and recombinant human proteins are indicated in the figure legends.

2.3. In silico analyses of interactions between EGFR and ligands

Computational molecular flexible docking was performed as previously described (Vogeley et al., 2022). Briefly, EGFR ECD (residues 25–527) from the crystal structure of the EGFR:EGF complex (PDB 1ivo) was used to perform docking analyses. Ligand structures for UV-320 (PubChem CID 77455), UV-326 (PubChem CID 62531), UV-327 (PubChem CID 77470), UV-350 (PubChem CID 118327) and UV-PS (PubChem CID 76605) were downloaded from PubChem database in SD format (Kim et al., 2016). The ligands were converted to PDB format using OpenBabel 2.3.1 (O'Boyle et al., 2011). Flexible docking was performed using AutoDock 4.2 (Goodsell et al., 1996) as described (Hawerkamp et al., 2019), except that the size for the grid box (x,y,z points) was set to 51 × 39 × 58. The centers of the protein grid were set at X = 113.38, Y = 65.95, Z = 39.94 dimensions.

The binding affinity of the protein–ligand interaction was estimated values calculated directly by AutoDock 4 (Eberhardt et al., 2021). The algorithm uses the binding energy which approximates the free energy change for the protein-inhibitor interaction (ΔG) and different types of interactions such as H-bond formation, electrostatics, and orientation in the active site to calculate the binding affinity (K) as:

$K = \exp(\Delta G \times 1000)/(Rcal \times TK)$

where ΔG is the docking energy, Rcal is 1.98719, and TK is 298. The final docking poses were analyzed manually using PyMOL (www.pymol.org).

The complex structure between the ECD of EGFR (residues 25–527; UniProt ID P00533) and AREG (residues 141–200; UniProt ID P15514) was predicted with Alphafold3 (Abramson et al., 2024). The confidence of the complex model was evaluated based on the predicted aligned error (PAE), the interface predicted template modeling (ipTM), and predicted template modeling (pTM) scores output by Alphafold3.

2.4. EGF-EGFR AlphaLISA binding assay

A potential disturbance of the binding of EGF to EGFR by the test compounds was analyzed by using the cell-free EGF-EGFR AlphaLISA Binding Kit (PerkinElmer, Waltham, MA).

2.5. Site-directed mutagenesis

Point-mutated EGFR variants were generated as described previously (Vogeley et al., 2022). HepG2 cells were seeded in 6-well plates as duplicates ($5x10^5$ per well). Transient transfection of HepG2 cells with plasmid DNA was performed with JetPEI DNA Transfection Reagent (Polyplus) according to manual. Treatment of the cells was performed

24 h after transfection.

2.6. EGFR internalization assay

Internalization of EGFR was investigated using a High-Content-Screening method adapted from Wang et al. (2007) (Wang and Xie, 2007). HaCaT keratinocytes were seeded 24 h previously, then washed twice with PBS and serum-starved in DMEM low glucose (1 g/l) without additional FBS for 3 h. Cells were treated with 200 ng/ml EGF-AF555 (Thermo Fisher Scientific, Waltham, MA) for 2.5 min on ice. Afterwards the test compounds were added and incubated for another 2.5 min on ice. Internalization was enabled by incubating the cells at 37 °C and 5 % CO2 for 25 min. The cells were fixed with 4 % paraformaldehyde. The membrane was stained with Wheat Germ Agglutinin, Oregon Green™ 488 Conjugate and the nuclei with Hoechst33342 (both Thermo Fisher Scientific). HCS analysis was performed using the CellInsight CX7 LZR Pro platform (Thermo Fisher Scientific) and the images were analyzed with the HCS Studio Cellomics Scan software (version 6.6.0). For the automated evaluation by the software, a short script was prepared. Briefly, only cells with a Hoechst33342-stained nucleus were considered and the WGA-staining of the membranes was converted into a 'circle' mask. Then, the average fluorescence intensity and number of AF555-EGF 'spots' inside each WGA 'circle' was determined and automatically evaluated by the software.

2.7. SDS-PAGE/Western blot analysis

Cells were lysed in RIPA buffer on ice and subsequently centrifuged for 15 min at 4 °C at maximum speed. Protein samples were separated by 10 % and 12 % SDS-polyacrylamide gel electrophoresis and blotted onto PVDF membrane (GE Healthcare, Freiburg, Germany). Blots were blocked with 5 % skim bovine serum albumin in TBS-Tween-20 (0.1 %) for 1 h at room temperature and subsequently incubated overnight at 4 °C with primary antibodies (tEGFR #4267, pEGFR Y1068 #3777, tERK1/2 #9102, pERK1/2 T202 #9101, GAPDH #2118) diluted 1:1000 in 5 % bovine serum albumin. Blots were washed and then incubated for 2 h with a 1:5000 dilution of HRP-conjugated secondary antibodies (Anti-rabbit IgG HRP-linked #7074) in 5 % bovine serum albumin in TBS-Tween-20 (0.1 %) at room temperature. All antibodies were purchased from Cell Signaling Technology (Leiden, The Netherlands). Bands were visualized using WesternBright ECL HRP substrate (Advansta, San Jose, CA) and a C-DiGit Western Blot Scanner (LI-COR Biotechnology, Lincoln, NE).

2.8. Measurement of DNA synthesis

DNA synthesis was assessed using a colorimetric BrdU incorporation assay (Sigma-Aldrich, Taufkirchen, Germany). Briefly, HaCaT keratinocytes were seeded on 96-well-plates in quintuplicates ($2x10^4$ per well) and starved overnight. Approximately 12 h later, the cells were treated with the respective test substances and BrdU labeling solution for 4 h. Subsequently, the assay was carried out according to the manufacturers protocol. Finally, after 15 min incubation with substrate solution, absorbance was measured at 370 nm (reference wavelength 492 nm) using the Infinite 200 PRO plate-reader (Tecan, Maennedorf, Switzerland).

2.9. Multiple sequence alignment

The multiple alignment of the 417——420 N-terminal amino acids of the EGFR protein (mature) from various animal species was carried out using Clustal Omega (v1.2.4) (Sievers et al., 2011) and the following NCBI Reference Sequences: *Homo sapiens*, NP_005219.2; *Neomonachus schauinslandi*, XP_021559426.1 (Hawaiian monk seal); *Lontra canadensis*, XP_032730878.1 (North American river otter); *Delphinapterus leucas*, XP_022448878.1 (Beluga whale); *Chroicocephalus ridibundus*, XP_063181702.1 (Black-headed gull); *Anas platyrhynchos*, XP_027307116.2 (Mallard); *Acipenser oxyrinchus oxyrinchus*, KAK1172474.1 (Atlantic sturgeon); *Amblyraja radiata*, XP_032906398.1 (Thorny skate).

2.10. Statistical analysis

All data shown are mean (±standard deviation) from three or more independent experiments, if not indicated otherwise. Differences were considered significant at $p \leq 0.05$. If not stated otherwise, a comparison of two groups was performed by unpaired, two-tailed Student's *t* test and a comparison of multiple groups was conducted with analysis of variance followed by a Tukey post hoc analysis to correct for multiple comparison.

3. Results

3.1. Computational docking analyses predict BUVs to bind the ECD of EGFR

We first performed *in silico* docking analyses to investigate whether BUVs could bind to the EGFR ECD. For this, we chose three BUVs currently listed as Substances of Very High Concern by ECHA (UV-326, UV-327, UV-350) as well as UV-320 and UV-PS which are structurally similar to UV-327 and UV-350 respectively (Fig. 1A). Because the EGF binding site (situated between ECD domains I and III) has previously been shown to interact with other organic pollutants (Vogeley et al., 2022), we focused on this region. The calculated binding poses and energies supported that all tested BUVs are capable of associating with the EGF binding site of the ECD (Fig. 1B-G). Of the five BUVs tested, UV-326 and UV-327 were calculated to have the strongest binding energy ($\Delta G_{binding}$) (Eberhardt et al., 2021), with −11.6 kcal/mol for UV-326 and −11.3 kcal/mol for UV-327, corresponding to dissociation constants (K_ds) of 55.7 nM and 57.6 nM, respectively. However, also the other three compounds produced similarly strong binding energies *in silico* (UV-320: −9.9 kcal/mol, $K_d = 70.3$ nM; UV-350: −9.5 kcal/mol $K_d = 77.9$ nM; UV-PS: −9.2 kcal/mol, $K_d = 83.7$ nM). All binding poses would lead to clashes with an EGF binding to this site (Fig. 1A). The two strongest binding BUVs have an additional chlorine group which may contribute to their stronger *in silico* binding (Fig. 1D, E).

3.2. Buvs UV-320 and UV-327 compete with EGFR ligands for EGFR binding site

To confirm the computational docking data, a cell-free AlphaLISA assay was conducted. Recombinant human EGF and the EGFR monoclonal antibody Cetuximab were used as positive controls that would reduce the binding of biotinylated EGF to antibody-captured EGFR by approximately 32 % and 20 % (Fig. 2). We chose to conduct this assay with UV-320, the non-halogenated BUV with the strongest predicted binding affinity, and UV-327 since both BUVs have a similar structure and are only distinguished by a chlorine group on the benzene ring of UV-327. While UV-320 did not induce significant effects, UV-327 achieved significant reduction of EGF:EGFR complex formation of about 17 %. This effect strength is comparable to the one achieved by the EGFR-blocking antibody Cetuximab (Supplementary Table S1). Since the beads-coupled EGFR utilized in this assay might not resemble the conformation and flexibility of the plasma membrane-bound EGFR, we next confirmed the interaction of the test compounds with the receptor tyrosine kinase using a respective internalization assay.

3.3. Buvs interfere with ligand-driven EGFR internalization

We next conducted EGFR internalization assays in HaCaT keratinocytes, an immortalized non-transformed human keratinocyte cell line that expresses wildtype EGFR and responds to growth factor treatment

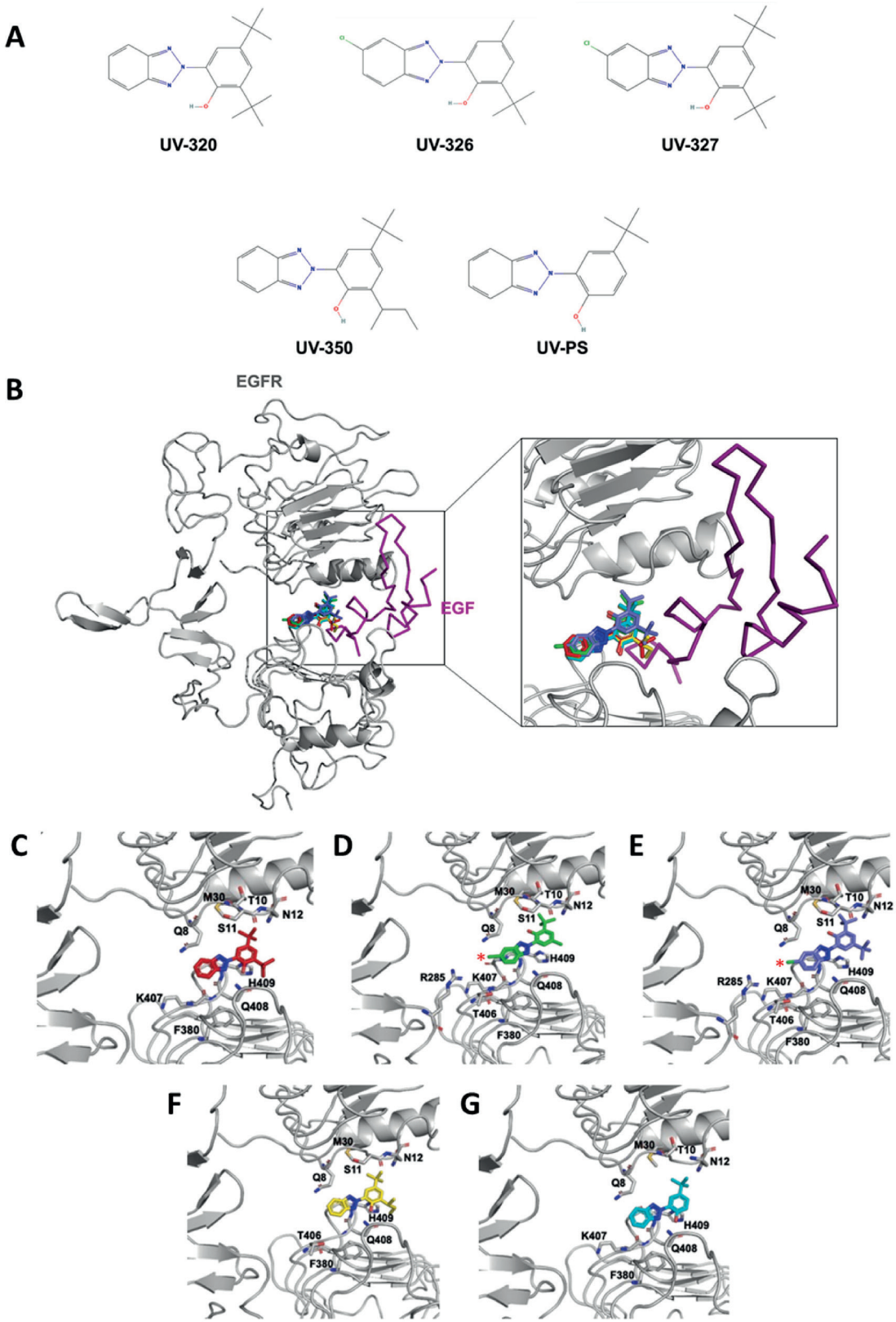

Fig. 1. In silico docking predicts that BUVs interfere with the binding of EGF to the EGFR extracellular domain. **A** 2D representations of the tested BUVs shown as sticks, taken from the PubChem website (https://pubchem.ncbi.nlm.nih.gov/). PubChem IDs are given. **F** *In* silico docking of EGFR and BUVs. **B** The EGFR protein structure is shown as gray cartoon. EGF is represented as magenta backbone trace. BUVs, shown in stick representation, are superimposed. Side chain and BUV atoms are colored according to: blue, nitrogen; light green, chlorine; yellow, sulfur; red, oxygen. EGFR carbons are colored gray, and BUV carbons are colored as in panels **C-G**: **C** UV-320 (red), **D** UV-326 (green), **E** UV-327 (slate blue), **F** UV-350 (yellow) and **G** UV-PS (cyan). The chlorine groups in UV-326 and UV-327 are labelled with a red asterisk. (For interpretation of the references to colour in this figure legend, the reader is referred to the web version of this article.)

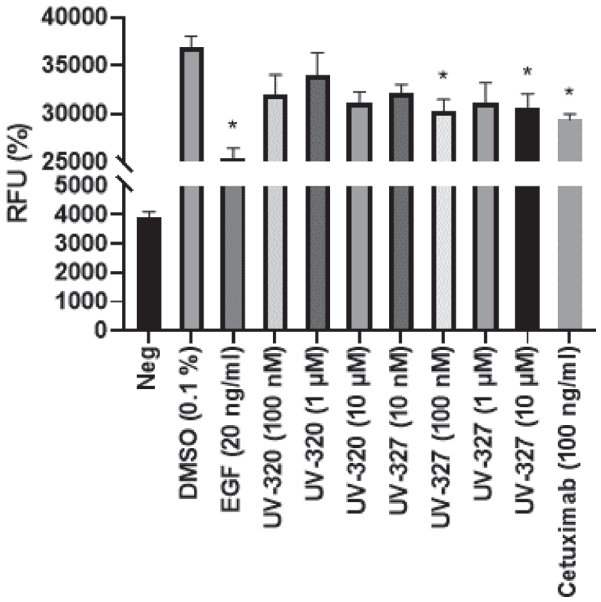

Fig. 2. BUVs UV-320 and UV-327 compete with EGF for binding of the EGFR extracellular domain. The effect of the BUVs on the interaction of EGF with EGFR was analyzed by using a cell-free EGF/EGFR AlphaLISA binding kit. n = 3. *, $p \leq 0.05$ compared to DMSO.

(Boukamp et al., 1988; Marques et al., 1999). Cells were first treated with an Alexa Fluor555-labeled EGF (EGF-AF555) and subsequently incubated with the solvent DMSO, resulting in the internalization of the EGF-AF555-bound EGFR (Fig. 3). Unlabeled EGF in a 20-fold concentration compared to AF555-EGF and the EGFR inhibitor PD153035 were used as positive controls, both leading to a significant decrease of intracellular EGF-AF555 fluorescent signal. A similar effect was observed for UV-326 and UV-327, depleting EGFR internalization to approx. 30 % resp. 40 %. UV-350 also reduced EGFR internalization to ca. 70 %. However, UV-320 and UV-PS did not show any significant effect on EGFR internalization in the tested concentrations.

3.4. *Buvs affect growth factor-induced EGFR activity and downstream signaling*

Having observed that UV-326, UV-327 and UV-350 inhibited EGF-induced EGFR internalization, we next investigated EGFR activation and downstream signaling. The phosphorylation of EGFR and ERK1/2 upon treatment with EGF and BUVs alone and in combination was investigated by SDS-PAGE/Western blot analysis in HaCaT cells (Fig. 4). At concentrations of 0.1 µM and 1 µM, UV-320 did not inhibit EGF-induced EGFR and ERK1/2 phosphorylation (Fig. 4A). Conversely, UV-327 inhibited EGF-induced phosphorylation of EGFR and ERK1/2 in a dose-dependent manner (Fig. 4B). Similar dose-dependent inhibitory effects were observed concerning UV-326 (Fig. 4C). UV-350 significantly inhibited EGFR and ERK1/2 phosphorylation only at a concentration of 10 µM (Fig. 4D). No effects on EGF-induced phosphorylation of EGFR or ERK1/2 was observed for UV-PS (Fig. 4E). Additionally, none of the tested BUVs showed any significant effects on basal EGFR or ERK1/2 phosphorylation.

3.5. *EGFR residue Q408 is essential for the inhibitory effect of UV-327*

After confirming that several BUVs competed with EGF for the EGFR ECD, we wanted to further investigate the binding site predicted by *in silico* docking analysis (Fig. 1). For this, we first transiently transfected low EGFR-expressing HepG2 cells (Fuchs et al., 2008) with either with wild type EGFR, point-mutated $EGFR^{Q408A}$ or the respective empty vector (EV) plasmid as a control. $EGFR^{Q408}$ was chosen for mutational analysis because it was predicted to establish important hydrogen bonds to the ligands in our *in silico* docking analysis (Fig. 1) and moreover is not essential for EGF-binding (Vogeley et al., 2022). The successful integration of the plasmids was confirmed by western blot analysis, showing a significant induction of EGFR phosphorylation after 15 min treatment with EGF in the EGFR- and $EGFR^{Q408A}$-transfected cells (Fig. 5). The previously observed interference of UV-327 with EGF-EGFR binding could be confirmed via western blot analysis, showing a significant inhibition of EGF-induced phosphorylation by UV-327 in the cells transfected with EGFR. Conversely, UV-327 did not interfere with EGF-induced phosphorylation in the cells that were transfected with $EGFR^{Q408A}$. Hence, we conclude that, at least for UV-327, the EGFR ECD residue Q408 is critical for the inhibition of EGF-induced EGFR activation.

Notably, a multiple alignment of animal N-terminal EGFR protein sequences revealed that Q408 as well as most of the other amino acid residues of the EGFR ECD predicted be involved in BUV binding (Fig. 1) are highly conserved across fish, birds, and mammals (Fig. S2).

3.6. *Buvs attenuate AREG-induced DNA synthesis*

Since EGFR is involved in several regulatory processes, we tested for the influence of BUVs on proliferation, through monitoring DNA synthesis induced by an EGFR ligand via colorimetric BrdU incorporation assay. The probably most important growth factor driving keratinocyte proliferation in an EGFR-dependent manner is AREG (Billings et al., 2003; Stoll et al., 2016). AREG contains a ~ 50 residue segment with homology to the EGFR-interacting region of EGF (34 % sequence identity). Accordingly, AlphaFold3 predicted that this segment adopts an EGF-like structure and associates with the subdomain I and III of EGFR ECD similarly to EGF (ipTM and pTM scores were 0.85 and 0.88, respectively; Fig. S1). AREG treatment led to a significant increase of incorporated BrdU as compared to solvent-treated HaCaT keratinocytes (Fig. 6). The EGFR inhibitor PD153035 and MEK inhibitor PD98059 were used as positive controls as they are both known to inhibit AREG-induced DNA synthesis (Berasain et al., 2005). Indeed, both inhibitors significantly reduced AREG-driven DNA synthesis. Again, UV-320 only interfered with AREG-induced activation of EGFR in the highest tested concentration of 10 µM. UV-326 on the other hand led a dose-dependent significant reduction of BrdU incorporation at 1 µM and 10 µM. For UV-327, a dose-dependent significant depletion of AREG-triggered DNA synthesis was observed for treatment with concentrations of 100 nM, 1 µM and 10 µM. For UV-350 and UV-PS none of the tested concentrations had a depleting effect on AREG-induced DNA synthesis.

3.7. *UV-320 and UV-327 interfere with EGFR activation in a ligand-specific manner*

We observed an interference of UV-320 with AREG-induced DNA synthesis at a concentration of 10 µM (Fig. 6B), but no inhibitory effects on EGF-induced EGFR or ERK1/2 phosphorylation at concentrations of 0.1 µM or 1 µM (Fig. 4A). To further investigate whether the inhibitory effect of UV-320 is concentration- or ligand-dependent, we performed SDS PAGE/Western blot analysis with regard to the phosphorylation of EGFR upon ligand treatment of HaCaT cells. In addition, we also tested UV-327 (10 µM), again due to both BUVs only distinguishing by a chlorine group on the benzene ring of UV-327. For this experiment, the HaCaT cells were serum-starved and then treated with either the EGFR ligand EGF or AREG, both resulting in a significant EGFR phosphorylation compared to the solvent control (Fig. 7). Further, PCB126 and PCB118 served as positive controls since they have been previously shown to inhibit EGF-induced EGFR phosphorylation (Vogeley et al., 2022). UV-327 led to a significant decrease of EGFR phosphorylation induced by EGF as well as AREG. Interestingly, in the co-treatment 10 µM of UV-320 did not affect EGF-induced receptor phosphorylation, but decreased the induction with AREG, possibly due to differences in the

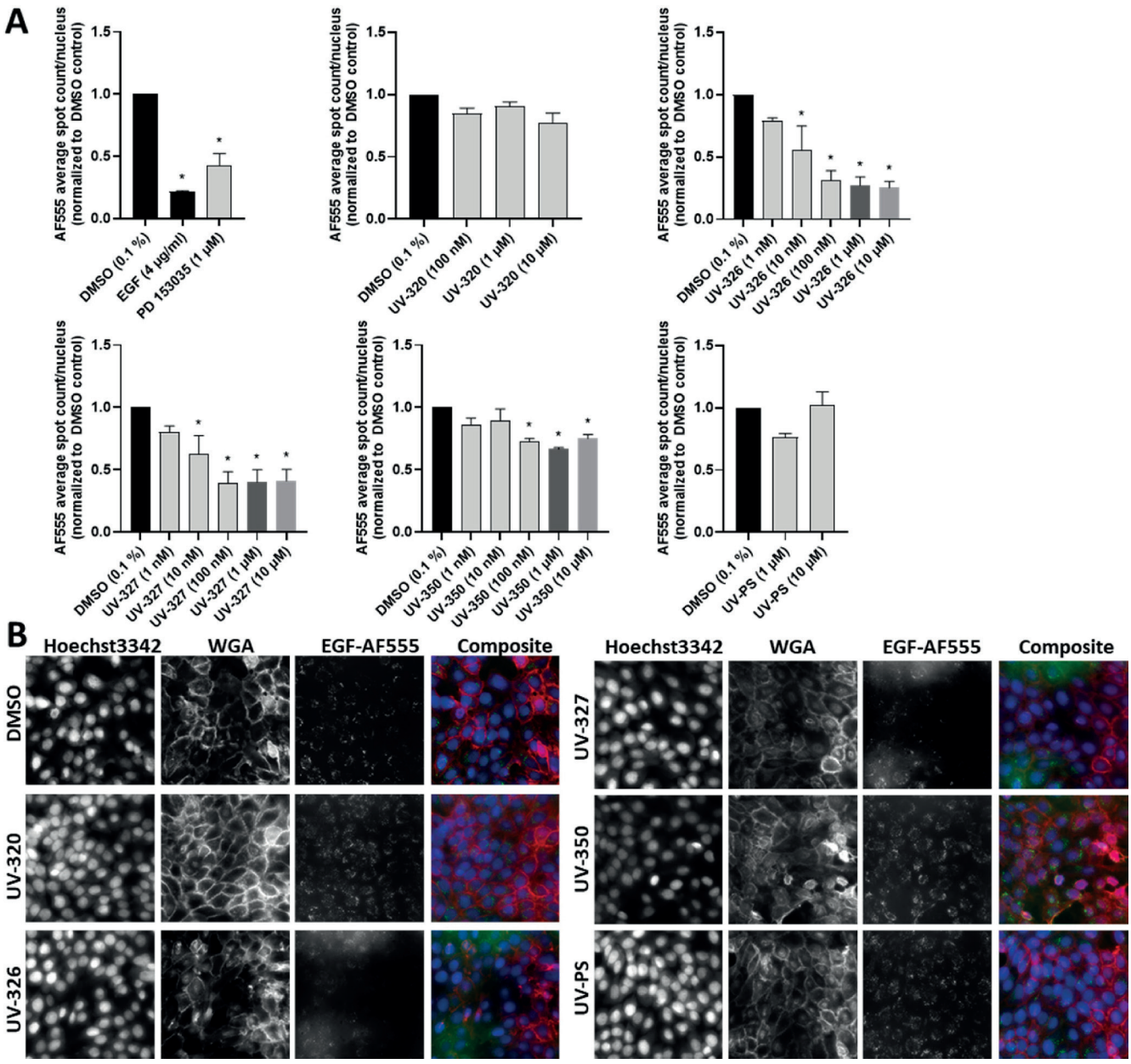

Fig. 3. Some BUVs inhibit the EGF-induced EGFR internalization. Influence of BUVs on EGFR internalization was investigated by EGFR internalization assay and subsequent high content screening microscopy. HaCaT keratinocytes were serum-starved for 3 h and subsequently treated with fluorescently labeled EGF-AF555 (200 ng/µl) on ice for 2.5 min, followed by addition of the respective BUV and another 2.5 min on ice. Then the cells were incubated at 37 °C for 25 min. **A** DMSO (0.1 %) served as solvent control. Unlabeled EGF (4 µg/ml) and PD153035 (1 µM) served as positive control. Treatment with UV-320, UV-326, UV-327, UV-350 and UV-PS at stated concentrations. Results from the automated quantification (n = 4), **B** Representative pictures for the respective treatment (BUVs all shown at 1 µM concentration). *, $p \leq 0.05$ compared to DMSO.

EGFR binding affinity and/or binding positions of EGF and AREG (Shoyab et al., 1989).

4. Discussion

In this study, we demonstrated that all tested BUVs except UV-PS were capable to interfere with EGFR activation or downstream signaling. UV-326 and UV-327, which are in distinction from the other tested BUVs both chlorinated, had the most consistent inhibitory effects on EGFR, and were the only compounds to achieve effects in concentrations below 1 µM. A relatively stronger binding was also predicted for UV-326 and UV-327 by our *in silico* docking analyses, even though the absolute affinity values differed from the experimental ones due to approximations in the calculations (Nassar et al., 2023; Goettig et al., 2024; Toprakci and Yelekci, 2005). However, *in silico* docking also supported that all BUVs bind in the same manner to the same ECD region, between domain I and III and in close proximity to the EGF-binding site. The same ECD region has already been shown to accommodate dioxin-like chemicals (Vogeley et al., 2022), suggesting it to be a hotspot for interference from different environmental pollutants. Indeed, mutational exchange of glutamine at position 408, which is not only critical for the inhibitory effect of dioxin-like chemicals (Vogeley et al., 2022) but also for the binding of the clinically applied EGFR antibody Cetuximab (Li et al., 2005), abrogated the BUV-mediated inhibition of EGF-induced EGFR phosphorylation in transfected HepG2 cells.

From literature it is known that in contrast to most of the other tested BUVs, the two halogenated compounds UV-326 and UV-327 do neither show agonistic nor antagonistic activity against human estrogen and

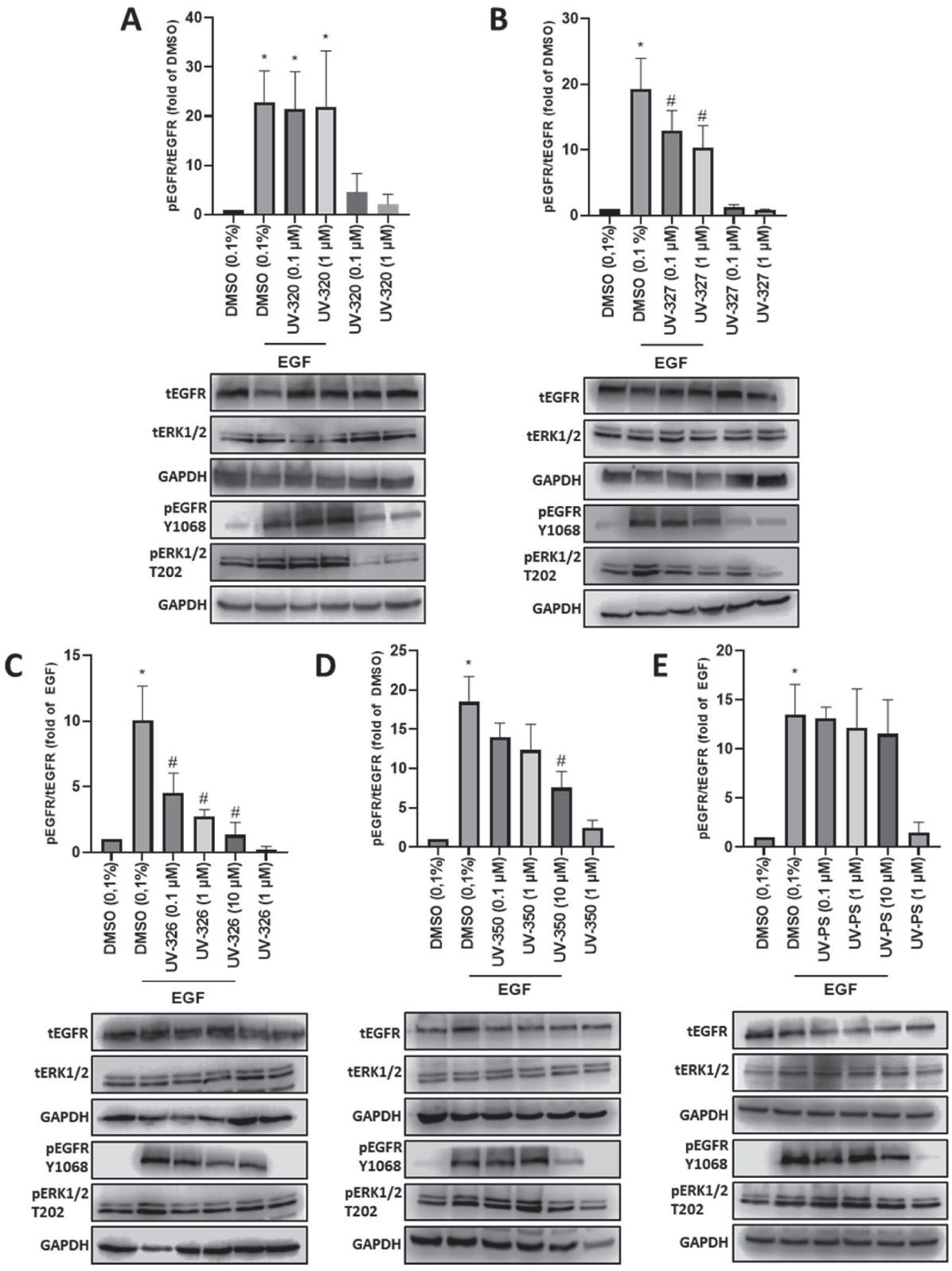

Fig. 4. Some BUVs interfere with the EGF-induced phosphorylation of EGFR and downstream signaling. Phosphorylation of EGFR and ERK1/2 in HaCaT keratinocytes with GAPDH as loading control. Cells were serum-starved for 3 h and subsequently treated for 15 min with solvent control DMSO (0.1 %), EGF (20 ng/ml) alone, EGF in combination with the respective BUV (0.1 μm, 1 μM, 10 μM) and the BUV (0.1 μM, 1 μM) alone. **A** Treatment with UV-320 (n = 3). Representative western blot for EGFR and ERK1/2 (n = 2). **B** Treatment with UV-327 (n = 4). Representative western blot for EGFR and ERK1/2 (n = 2). **C** Treatment with UV-326 (n = 3). Representative western blot for EGFR and ERK1/2 (n = 2). **D** Treatment with UV-350 (n = 4). Representative western blot for EGFR and ERK1/2 (n = 2). **E** Treatment with UV-PS (n = 3). Representative western blot for EGFR and ERK1/2 (n = 2). *, $p \leq 0.05$ compared to DMSO. #, $p \leq 0.05$ compared to EGF single treatment.

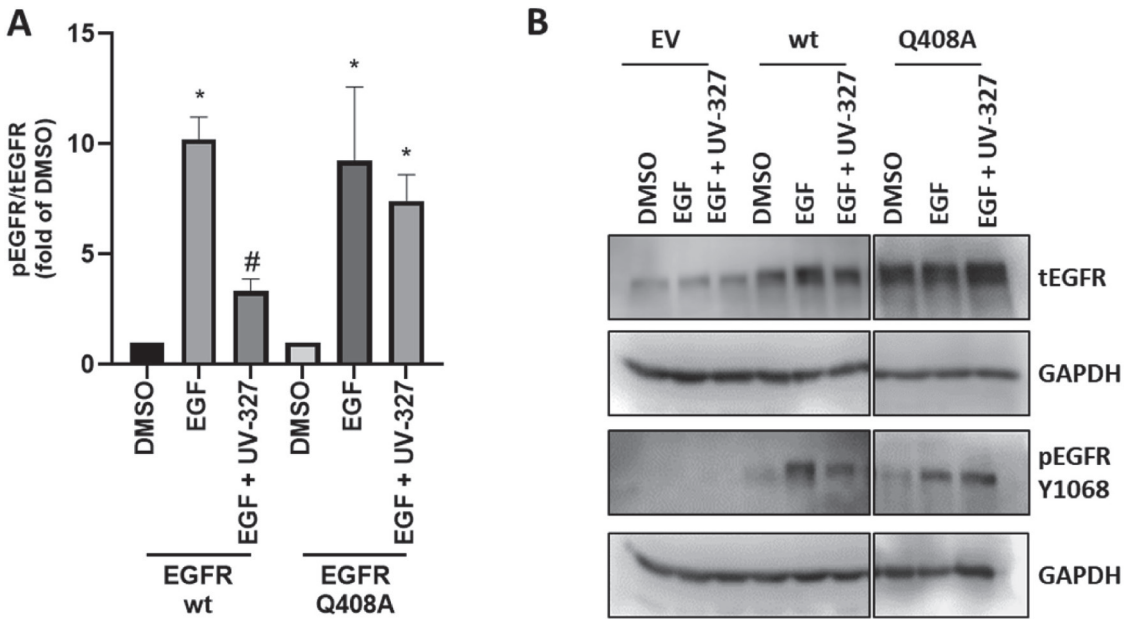

Fig. 5. Amino acid residue Q408 on the EGFR ECD seems to be vital for inhibition of EGF-induced phosphorylation via UV-327. Phosphorylation of EGFR in HepG2 cells overexpressing EGFR wt or EGFR with point mutation Q408A. GAPDH as loading control. **A** Cells were transiently transfected 24 h prior to serum-starvation for 3 h and subsequent treatment for 15 min with solvent control DMSO (0.1 %), EGF (20 ng/ml) alone and in combination with UV-327 (n = 3). **B** Representative Western blot for EGFR, also presenting EV (empty vector plasmid control) (see A). *, $p \leq 0.05$ compared to DMSO. #, $p \leq 0.05$ compared to EGF.

androgen receptors (Sakuragi et al., 2021). According to Sakuragi and co-workers, the latter may be due to the chlorine at position 5 which may hinder the compounds from binding to the steroid hormone receptors (Sakuragi et al., 2021). In addition, BUVs, including UV-326 and UV-327, do not seem to interact with human thyroid hormone receptors (Nagayoshi et al., 2015). Hence, UV-326 and UV-327 may interfere with cellular pathways and functions rather by dampening growth factor-triggered EGFR activity than by acting on steroid hormone receptors.

Human exposure to BUVs is evident. In fact, BUVs have been found in human adipose tissue samples from Japan, South Korea, Poland, India and the USA (ECHA, 2015). Even more alarming, relatively high concentrations of BUVs have been detected in breast milk samples (Liu et al., 2022; Kim et al., 2019; Molins-Delgado et al., 2018; Lee et al., 2015), pointing to an enhanced exposure risk for infants. A study assessing the concentrations of UV filters in a South Korean population, for instance, detected a peak concentration of UV-328 of 46 ng/g lipid weight (Lee et al., 2015). In a population cohort of the Philippines, a peak concentration of UV-326 of 64 ng/g lipid weight was measured (Kim et al., 2019). Assuming a fat content of 4 %, this roughly corresponds to peak concentrations of 5.2 nM (UV-328) and 8.1 nM (UV-326) in breast milk from the East and Southeast Asian women, respectively. Hence, especially with regards to potential additive effects, breastfed infants may be exposed to BUVs in a concentration range that is close to the one being effective in our *in vitro* experiments. Importantly, in the South Korean study (Lee et al., 2015), the total BUV concentration measured in breast milk negatively correlated with the gestational age at delivery. Of course, not necessarily caused by the same pathomechanism, it is still interesting that similar correlations between *in utero* exposure and gestational age have been reported for dioxin-like chemicals (Fein et al., 1984; Vafeiadi et al., 2014) and bisphenols (Huang et al., 2019; Aung et al., 2019), all of which are POPs that have been shown to bind to the human EGFR ECD (Hardesty et al., 2018; Vogeley et al., 2022; Ticiani et al., 2021; Ticiani et al., 2023).

Studies on EGFR-deficient mice, which die early after birth due to epithelial immaturity and multiorgan failure, have demonstrated the utmost relevance of EGFR for proper embryonic development (Miettinen et al., 1995; Sibilia and Wagner, 1995; Miettinen et al., 1999). Interestingly, EGFR is also critical for the postnatal differentiation of the neurogenic niche (Abdi et al., 2019) as well as for proper astrocyte proliferation and differentiation (Sibilia et al., 1998), indicating that a disturbance of EGFR in neonates, for instance by EGFR-inhibiting chemicals contained in breast milk, might have neurodevelopmental consequences. Of note, exposure to BUVs is known to cause neurotoxicity in bony fish (Li et al., 2024). A potential involvement of EGFR in mediating these neurotoxic effects has not been investigated yet, but the high evolutionary conservation of EGFR, especially of its N-terminal half (Bogdan and Klambt, 2001), supports this notion. In fact, most of the amino acid residues predicted and/or experimentally proven by us to be required for the binding of BUVs as well as of dioxin-like compounds (Vogeley et al., 2022) to the EGFR ECD, are highly conserved in species frequently exposed to BUVs, such as fish, sea birds, seals and whales (Lu et al., 2019; Tanaka et al., 2020; Nakata and Shinohara, 2010). In case BUVs indeed inhibit proper EGFR signal transduction in wildlife, other adverse effects, such as an inappropriate differentiation of epithelia and associated barrier defects (Miettinen et al., 1995; Sibilia and Wagner, 1995; Lacouture, 2006), may be expected. Hence, it is likely that the findings of our study are not only relevant with regards to human exposure, but may also help to explain and predict toxic effects in wildlife exposed to BUVs.

Importantly, the 23-hydroxybetulinic acid derivative DBPA was recently found to induce the degradation of EGFR and suppress the growth of EGFR-driven non-small cell lung cancers (Yao et al., 2020). The initiating event for these effects was the direct interaction of DBPA with the EGFR ECD and the associated abrogation of its activation by growth factors (Yao et al., 2020). Since this class of chemicals does not exhibit pronounced acute toxicity (Khare et al., 2023), the BUVs analyzed in this study may serve as a structural blueprint for the development of small molecules for clinical purpose.

A caveat of this study is the use of plastic cell culture flasks and plates. To some extent, which has not been assessed in this study, the test compounds will stick to cell culture plastics and proteins present in the culture media, effects which reduce the free fraction of the test compounds and thus may make effective concentrations appear higher than they actually are. On the other hand, the plastic material itself may contain BUVs and related UV stabilizers, which may migrate into the culture medium and possibly affect the biology in the control samples

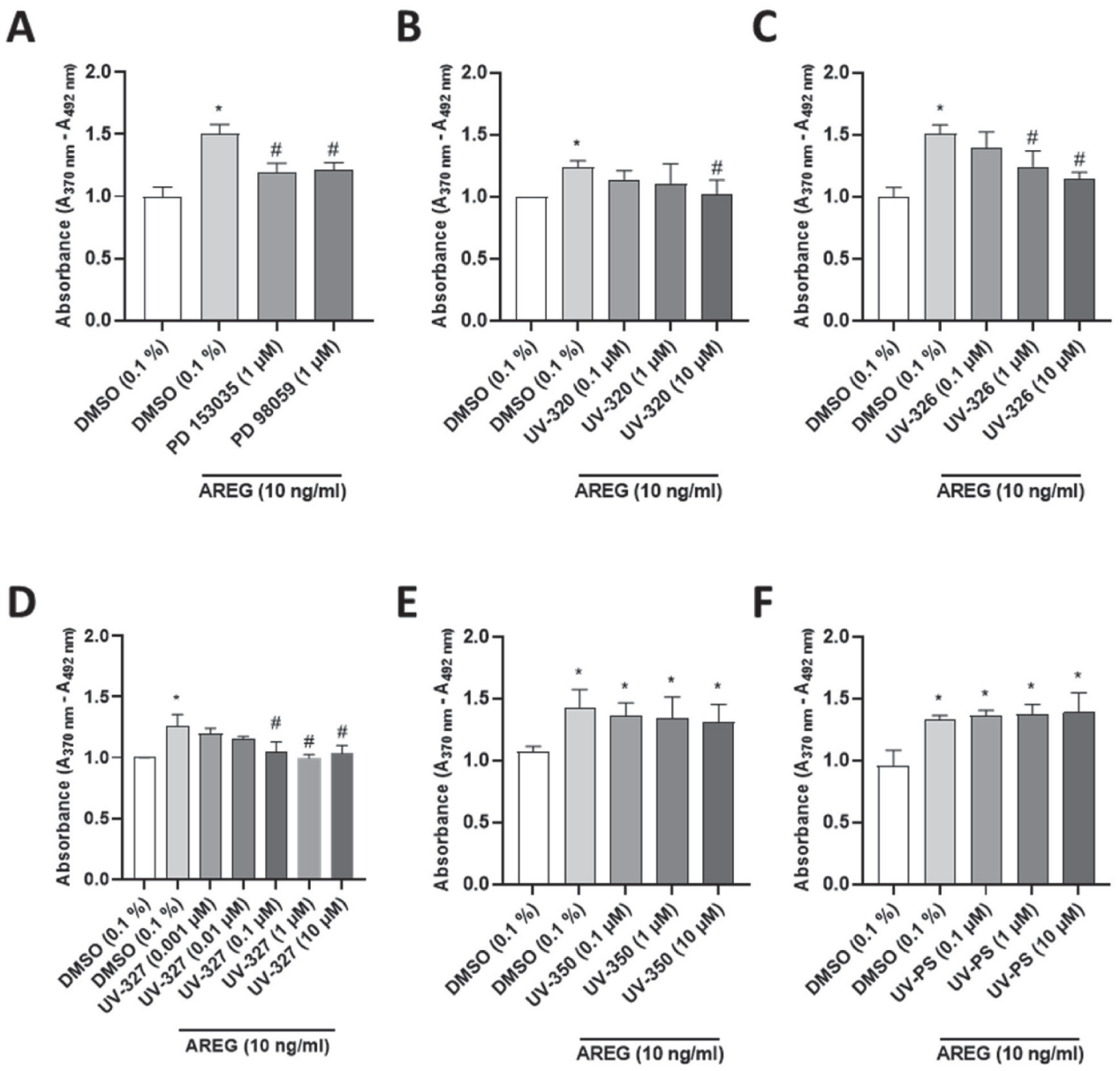

Fig. 6. UV-320, UV-326 and UV-327 can interfere with EGFR ligand AREG-induced DNA synthesis. A-F Colorimetric BrdU incorporation assay to assess the influence of PD153035, PD98059, UV-320, UV-326, UV-327, UV-350 and UV-PS on AREG-induced DNA synthesis. HaCaT keratinocytes were treated as indicated for 4 h. Absorption was measured at a wavelength of 370 nm (reference wavelength 492 nm). n = 4–8. *, $p \leq 0.05$ compared to DMSO, #, $p \leq 0.05$ compared to AREG.3.7 UV-320 and UV-327 interfere with EGFR activation in a ligand-specific manner.

and thereby the effect strength in the treated cells associated therewith.

Taken together, our data identify environmentally ubiquitous BUVs, especially the halogenated members UV-326 and UV-327, to bind to the EGFR ECD and inhibit downstream signal transduction and biological functions in human cells *in vitro*. Human exposure to these BUVs may therefore disturb proper EGFR signaling and associated biological functions. By showing that several BUVs affect the EGFR in the same way as dioxin-like chemicals and bisphenols rises the possibility for mixture effects, i.e. additive effects of otherwise sub-effective concentrations of chemicals sharing the same mode of action (Chatterjee and Roy, 2022). These findings underscore the urgent need for a better understanding of the molecular and cellular consequences of human BUV exposure to improve the hazard assessment for widespread and persistent POPs.

CRediT authorship contribution statement

Natalie C. Sondermann: Writing – original draft, Visualization, Investigation, Conceptualization. **Afaque A. Momin:** Writing – review & editing, Methodology, Investigation. **Stefan T. Arold:** Writing – review & editing, Supervision, Methodology. **Thomas Haarmann-Stemmann:** Writing – review & editing, Writing – original draft, Supervision, Project administration, Conceptualization.

Declaration of competing interest

The authors declare that they have no known competing financial interests or personal relationships that could have appeared to influence the work reported in this paper.

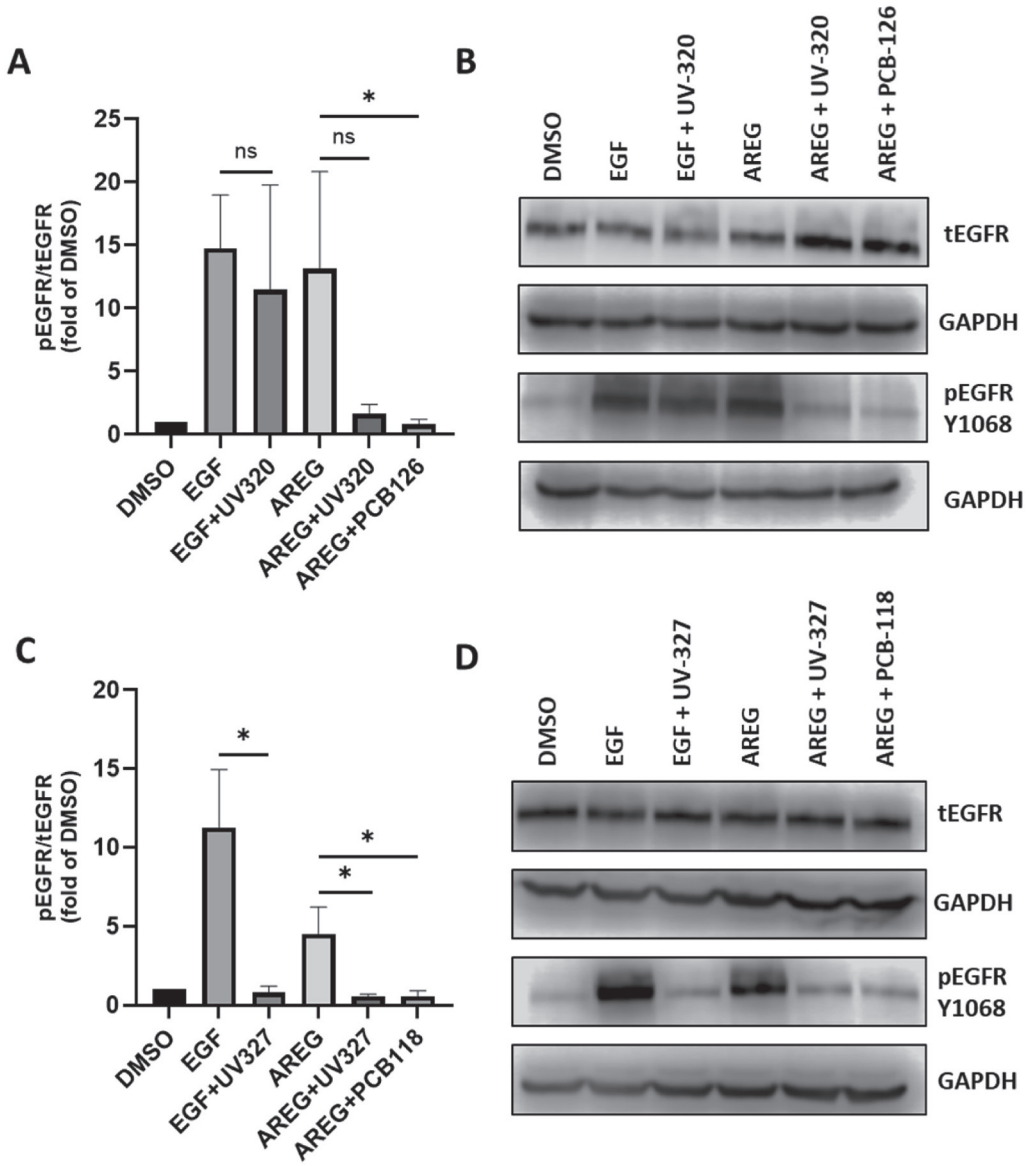

Fig. 7. UV-320 and UV-327 inhibit phosphorylation of EGFR in a ligand-specific manner. Phosphorylation of EGFR in HaCaT keratinocytes with GAPDH as loading control. **A** Cells were serum-starved for 3 h and subsequently treated for 15 min with solvent control DMSO (0.1 %), EGF (20 ng/ml) alone and in combination with UV-320, AREG (10 ng/ml) alone and in combination with UV-320 and AREG in combination with PCB-126 (1 μM) serving as positive control (n = 4). **B** Representative western blot for EGFR (see A). **C** Cells were serum-starved for 3 h and subsequently treated for 15 min with solvent control DMSO (0.1 %), EGF (20 ng/ml) alone and in combination with UV-327, AREG (10 ng/ml) alone and in combination with UV-327 and AREG in combination with PCB-118 (1 μM) serving as positive control (n = 4). **D** Representative western blot for EGFR (see C). Kruskal-Wallis test was performed to compare the mean rank of preselected pairs. *, $p \leq 0.05$ compared to EGF/AREG single treatment.

Data availability

Data will be made available on request.

Acknowledgement

We thank Petra Boukamp for providing HaCaT cells, and Etta Zühr and Inken Hacheney for excellent technical support. We are grateful to Claudia Wigmann for statistical advice. NCS was supported by the Jürgen Manchot Foundation. The research conducted by AAM and STA was supported by the King Abdullah University of Science and Technology (KAUST) through the baseline fund and the Award No. FCC/1/1976-33 and REI/1/4446-01 from the Office of Sponsored Research (OSR). For computer time, this research used the resources of the KAUST Supercomputing Laboratory (KSL). We thank N. Kathiresan and G. Wickham from the KSL for their support.

The scheme shown in the graphical abstract was created with BioRender software (www.biorender.com; agreement number AZ270KVGDA).

Appendix A. Supplementary data

Supplementary data to this article can be found online at https://doi.org/10.1016/j.envint.2024.108886.

References

Abdi, K., Neves, G., Pyun, J., Kiziltug, E., Ahrens, A., Kuo, C.T., 2019. EGFR Signaling Termination via Numb Trafficking in Ependymal Progenitors Controls Postnatal Neurogenic Niche Differentiation. Cell Rep. 28(8), 2012-2022.

Abramson, J., Adler, J., Dunger, J., Evans, R., Green, T., Pritzel, A., Ronneberger, O., Willmore, L., Ballard, A.J., Bambrick, J., Bodenstein, S.W., Evans, D.A., Hung, C.C.,

O'Neill, M., Reiman, D., Tunyasuvunakool, K., Wu, Z., Zemgulyte, A., Arvaniti, E., Beattie, C., Bertolli, O., Bridgland, A., Cherepanov, A., Congreve, M., Cowen-Rivers, A.I., Cowie, A., Figurnov, M., Fuchs, F.B., Gladman, H., Jain, R., Khan, Y.A., Low, C.M.R., Perlin, K., Potapenko, A., Savy, P., Singh, S., Stecula, A., Thillaisundaram, A., Tong, C., Yakneen, S., Zhong, E.D., Zielinski, M., Zidek, A., Bapst, V., Kohli, P., Jaderberg, M., Hassabis, D., Jumper, J.M., 2024. Accurate structure prediction of biomolecular interactions with AlphaFold 3. Nature.

An, D., Xing, X., Tang, Z., Li, Y., Sun, J., 2022. Concentrations, distribution and potential health risks of organic ultraviolet absorbents in street dust from Tianjin, a megacity in northern China. Environ Res 204 (Pt B), 112130.

Aung, M.T., Ferguson, K.K., Cantonwine, D.E., McElrath, T.F., Meeker, J.D., 2019. Preterm birth in relation to the bisphenol A replacement, bisphenol S, and other phenols and parabens. Environ Res 169, 131–138.

Bai, L., Li, J., Guo, B., Cai, R., Zhao, C., Guo, Y., Wang, Y., Jiang, G., 2024. Percutaneous Penetration and Dermal Exposure Risk Assessment of UV Absorbents in Sunscreens and Isolation Cosmetics. Environ. Health.

Berasain, C., Garcia-Trevijano, E.R., Castillo, J., Erroba, E., Lee, D.C., Prieto, J., Avila, M. A., 2005. Amphiregulin: an early trigger of liver regeneration in mice. Gastroenterology 128 (2), 424–432.

Billings, S.D., Southall, M.D., Li, T., Cook, P.W., Baldridge, L., Moores, W.B., Spandau, D. F., Foley, J.G., Travers, J.B., 2003. Amphiregulin overexpression results in rapidly growing keratinocytic tumors: an in vivo xenograft model of keratoacanthoma. Am J Pathol 163 (6), 2451–2458.

Bogdan, S., Klambt, C., 2001. Epidermal growth factor receptor signaling. Curr Biol 11 (8), R292–R295.

Boukamp, P., Petrussevska, R.T., Breitkreutz, D., Hornung, J., Markham, A., Fusenig, N. E., 1988. Normal keratinization in a spontaneously immortalized aneuploid human keratinocyte cell line. J Cell Biol 106 (3), 761–771.

Chatterjee, M., Roy, K., 2022. Recent Advances on Modelling the Toxicity of Environmental Pollutants for Risk Assessment: from Single Pollutants to Mixtures. Current Pollution Reports 8 (2), 81–97.

Chen, J., Zeng, F., Forrester, S.J., Eguchi, S., Zhang, M.Z., Harris, R.C., 2016. Expression and Function of the Epidermal Growth Factor Receptor in Physiology and Disease. Physiol Rev 96 (3), 1025–1069.

Eberhardt, J., Santos-Martins, D., Tillack, A.F., Forli, S., 2021. AutoDock Vina 1.2.0: New Docking Methods, Expanded Force Field, and Python Bindings. J Chem Inf Model 61 (8), 3891–3898.

ECHA, Candidate List of substances of very high concern for Authorisation, 2023. https://echa.europa.eu/candidate-list-table. (Accessed 05 April 2024).

ECHA, Annex XV report: Proposal for Identification of a Substance of Very High Concern on the Basis of the Criteria Set out in REACH Article 57, annex XV - Identification of UV-327 as SVCH (2015).

Fein, G.G., Jacobson, J.L., Jacobson, S.W., Schwartz, P.M., Dowler, J.K., 1984. Prenatal exposure to polychlorinated biphenyls: effects on birth size and gestational age. J Pediatr 105 (2), 315–320.

Feng, H., Cao, H., Li, J., Zhang, H., Xue, Q., Liu, X., Zhang, A., Fu, J., 2020. Estrogenic activity of benzotriazole UV stabilizers evaluated through in vitro assays and computational studies. Sci Total Environ 727, 138549.

Fuchs, B.C., Fujii, T., Dorfman, J.D., Goodwin, J.M., Zhu, A.X., Lanuti, M., Tanabe, K.K., 2008. Epithelial-to-mesenchymal transition and integrin-linked kinase mediate sensitivity to epidermal growth factor receptor inhibition in human hepatoma cells. Cancer Res 68 (7), 2391–2399.

Goettig, P., Chen, X., Harris, J.M., 2024. Correlation of Experimental and Calculated Inhibition Constants of Protease Inhibitor Complexes. Int J Mol Sci 25 (4).

Goodsell, D.S., Morris, G.M., Olson, A.J., 1996. Automated docking of flexible ligands: applications of AutoDock. J Mol Recognit 9 (1), 1–5.

Gschwind, A., Fischer, O.M., Ullrich, A., 2004. The discovery of receptor tyrosine kinases: targets for cancer therapy. Nat Rev Cancer 4 (5), 361–370.

Hardesty, J.E., Al-Eryani, L., Wahlang, B., Falkner, K.C., Shi, H., Jin, J., Vivace, B.J., Ceresa, B.P., Prough, R.A., Cave, M.C., 2018. Epidermal Growth Factor Receptor Signaling Disruption by Endocrine and Metabolic Disrupting Chemicals. Toxicol Sci 162 (2), 622–634.

Hawerkamp, H.C., Kislat, A., Gerber, P.A., Pollet, M., Rolfes, K.M., Soshilov, A.A., Denison, M.S., Momin, A.A., Arold, S.T., Datsi, A., Braun, S.A., Olah, P., Lacouture, M.E., Krutmann, J., Haarmann-Stemmann, T., Homey, B., Meller, S., 2019. Vemurafenib acts as an aryl hydrocarbon receptor antagonist: Implications for inflammatory cutaneous adverse events. Allergy 74 (12), 2437–2448.

He, S., Xiao, H., Luo, S., Li, X., Zhang, J.D., Ren, X.M., Yang, Y., Xie, X.D., Zhou, Y.Y., Yin, Y.L., Luo, L., Cao, L.Y., 2022. Benzotriazole Ultraviolet Stabilizers Promote Breast Cancer Cell Proliferation via Activating Estrogen-Related Receptors alpha and gamma at Human-Relevant Levels. Environ Sci Technol 56 (4), 2466–2475.

Huang, S., Li, J., Xu, S., Zhao, H., Li, Y., Zhou, Y., Fang, J., Liao, J., Cai, Z., Xia, W., 2019. Bisphenol A and bisphenol S exposures during pregnancy and gestational age - A longitudinal study in China. Chemosphere 237, 124426.

Jungclaus, G., Avila, V., Hites, R., 1978. Organic compounds in an industrial Wastewater: a case study of their environmental impact. Environ. Sci. Tech. 12 (1), 88–96.

Kassab, A.E., 2023. Benzotriazole scaffold: An overview of antiproliferative potential, mechanisms of action, and structure-activity relationships. Arch Pharm (weinheim) 356 (8), e2300102.

Khare, A., Jadhao, P., Vaidya, A.N., Kumar, A.R., 2023. Benzotriazole UV stabilizers (BUVs) as an emerging contaminant of concern: a review. Environ Sci Pollut Res Int 30 (58), 121370–121392.

Kim, J.-W., Chang, K.-H., Prudente, M., Viet, P.H., Takahashi, S., Tanabe, S., Kunisue, T., Isobe, T., 2019. Occurrence of benzotriazole ultraviolet stabilizers (BUVSs) in human breast milk from three Asian countries. Sci. Total Environ. 655, 1081–1088.

Kim, J.W., Isobe, T., Malarvannan, G., Sudaryanto, A., Chang, K.H., Prudente, M., Tanabe, S., 2012. Contamination of benzotriazole ultraviolet stabilizers in house dust from the Philippines: implications on human exposure. Sci. Total Environ. 424, 174-181.

Kim, S., Thiessen, P.A., Bolton, E.E., Chen, J., Fu, G., Gindulyte, A., Han, L., He, J., He, S., Shoemaker, B.A., Wang, J., Yu, B., Zhang, J., Bryant, S.H., 2016. PubChem Substance and Compound databases. Nucleic Acids Res 44 (D1), D1202–D1213.

Köhler, K., Simmendinger, P., Roelle, W., Scholz, W., Valet, A., Slongo, M., 2010. Paints and Coatings, 4. Extenders, and Additives, Ullmann's Encyclopedia of Industrial Chemistry, Pigments.

Kolossa-Gehring, M., Fiddicke, U., Leng, G., Angerer, J., Wolz, B., 2017. New human biomonitoring methods for chemicals of concern-the German approach to enhance relevance. Int J Hyg Environ Health 220 (2 Pt A), 103–112.

Kubota, A., Terasaki, M., Sakuragi, Y., Muromoto, R., Ikeda-Araki, A., Takada, H., Kojima, H., 2022. Effects of benzotriazole UV stabilizers, UV-PS and UV-P, on the differentiation of splenic regulatory T cells via aryl hydrocarbon receptor. Ecotoxicol Environ Saf 238, 113549.

Lacouture, M.E., 2006. Mechanisms of cutaneous toxicities to EGFR inhibitors. Nat Rev Cancer 6 (10), 803–812.

Lee, S., Kim, S., Park, J., Kim, H.J., Lee, J.J., Choi, G., Choi, S., Kim, S., Kim, S.Y., Choi, K., Kim, S., Moon, H.B., 2015. Synthetic musk compounds and benzotriazole ultraviolet stabilizers in breast milk: Occurrence, time-course variation and infant health risk. Environ Res 140, 466–473.

Li, M., Ivantsova, E., Liang, X., Martyniuk, C.J., 2024. Neurotoxicity of Benzotriazole Ultraviolet Stabilizers in Teleost Fishes: A Review. Toxics 12 (2).

Li, S., Schmitz, K.R., Jeffrey, P.D., Wiltzius, J.J., Kussie, P., Ferguson, K.M., 2005. Structural basis for inhibition of the epidermal growth factor receptor by cetuximab. Cancer Cell 7 (4), 301–311.

Liu, Y., Gao, L., Qiao, L., Huang, D., Lyu, B., Li, J., Wu, Y., Zheng, M., 2022. Concentrations, Compound Profiles, and Possible Sources of Organic UV Filters in Human Milk in China. Environ. Sci. Tech. 56 (22), 15930–15940.

Lu, Z., De Silva, A.O., Provencher, J.F., Mallory, M.L., Kirk, J.L., Houde, M., Stewart, C., Braune, B.M., Avery-Gomm, S., Muir, D.C.G., 2019. Occurrence of substituted diphenylamine antioxidants and benzotriazole UV stabilizers in Arctic seabirds and seals. Sci. Total Environ. 663, 950–957.

Maceira, A., Borrull, F., Marce, R.M., 2019. Occurrence of plastic additives in outdoor air particulate matters from two industrial parks of Tarragona, Spain: Human inhalation intake risk assessment. J Hazard Mater 373, 649–659.

Marques, M.M., Martinez, N., Rodriguez-Garcia, I., Alonso, A., 1999. EGFR family-mediated signal transduction in the human keratinocyte cell line HaCaT. Exp Cell Res 252 (2), 432–438.

Miettinen, P.J., Berger, J.E., Meneses, J., Phung, Y., Pedersen, R.A., Werb, Z., Derynck, R., 1995. Epithelial immaturity and multiorgan failure in mice lacking epidermal growth factor receptor. Nature 376 (6538), 337–341.

Miettinen, P.J., Chin, J.R., Shum, L., Slavkin, H.C., Shuler, C.F., Derynck, R., Werb, Z., 1999. Epidermal growth factor receptor function is necessary for normal craniofacial development and palate closure. Nat Genet 22 (1), 69–73.

Molins-Delgado, D., Olmo-Campos, M.D.M., Valeta-Juan, G., Pleguezuelos-Hernandez, V., Barcelo, D., Diaz-Cruz, M.S., 2018. Determination of UV filters in human breast milk using turbulent flow chromatography and babies' daily intake estimation. Environ Res 161, 532–539.

Mutoh, S., Sobhany, M., Moore, R., Perera, L., Pedersen, L., Sueyoshi, T., Negishi, M., 2013. Phenobarbital indirectly activates the constitutive active androstane receptor (CAR) by inhibition of epidermal growth factor receptor signaling. Sci Signal 6 (274), ra31.

Nagayoshi, H., Kakimoto, K., Takagi, S., Konishi, Y., Kajimura, K., Matsuda, T., 2015. Benzotriazole ultraviolet stabilizers show potent activities as human aryl hydrocarbon receptor ligands. Environ Sci Technol 49 (1), 578–587.

Nakata, H., Shinohara, R.-I., 2010. Concentrations of Benzotriazole UV Stabilizers and Polycyclic Musks in Wastewater Treatment Plant Samples in Japan, Interdisciplinary Studies on Environmental Chemistry —. Environmental Specimen Bank 4, 51–59.

Nakata, H., Shinohara, R.-I., Nakazawa, Y., Isobe, T., Sudaryanto, A., Subramanian, A., Tanabe, S., Zakaria, M.P., Zheng, G.J., Lam, P.K.S., Kim, E.Y., Min, B.-Y., We, S.-U., Viet, P.H., Tana, T.S., Prudente, M., Frank, D., Lauenstein, G., Kannan, K., 2012. Asia-Pacific mussel watch for emerging pollutants: Distribution of synthetic musks and benzotriazole UV stabilizers in Asian and US coastal waters. Mar. Pollut. Bull. 64 (10), 2211–2218.

Nassar, H., Sippl, W., Dahab, R.A., Taha, M., 2023. Molecular docking, molecular dynamics simulations and in vitro screening reveal cefixime and ceftriaxone as GSK3beta covalent inhibitors. RSC Adv 13 (17), 11278–11290.

O'Boyle, N.M., Banck, M., James, C.A., Morley, C., Vandermeersch, T., Hutchison, G.R., 2011. Open Babel: An open chemical toolbox. J Cheminform 3, 33.

Ougier, E., Ganzleben, C., Lecoq, P., Bessems, J., David, M., Schoeters, G., Lange, R., Meslin, M., Uhl, M., Kolossa-Gehring, M., Rousselle, C., Vicente, J.L., 2021. Chemical prioritisation strategy in the European Human Biomonitoring Initiative (HBM4EU) - Development and results. Int J Hyg Environ Health 236, 113778.

Sakuragi, Y., Takada, H., Sato, H., Kubota, A., Terasaki, M., Takeuchi, S., Ikeda-Araki, A., Watanabe, Y., Kitamura, S., Kojima, H., 2021. An analytical survey of benzotriazole UV stabilizers in plastic products and their endocrine-disrupting potential via human estrogen and androgen receptors. Sci Total Environ 800, 149374.

Shoyab, M., Plowman, G.D., McDonald, V.L., Bradley, J.G., Todaro, G.J., 1989. Structure and function of human amphiregulin: a member of the epidermal growth factor family. Science 243 (4894 Pt 1), 1074–1076.

Sibilia, M., Steinbach, J.P., Stingl, L., Aguzzi, A., Wagner, E.F., 1998. A strain-independent postnatal neurodegeneration in mice lacking the EGF receptor. EMBO J 17 (3), 719–731.

Sibilia, M., Wagner, E.F., 1995. Strain-dependent epithelial defects in mice lacking the EGF receptor. Science 269 (5221), 234–238.
Stoll, S.W., Stuart, P.E., Lambert, S., Gandarillas, A., Rittie, L., Johnston, A., Elder, J.T., 2016. Membrane-Tethered Intracellular Domain of Amphiregulin Promotes Keratinocyte Proliferation. J Invest Dermatol 136 (2), 444–452.
Tanaka, K., Watanuki, Y., Takada, H., Ishizuka, M., Yamashita, R., Kazama, M., Hiki, N., Kashiwada, F., Mizukawa, K., Mizukawa, H., Hyrenbach, D., Hester, M., Ikenaka, Y., Nakayama, S.M.M., 2020. Nakayama, In Vivo Accumulation of Plastic-Derived Chemicals into Seabird Tissues. Curr. Biol. 30(4), 723-728.
Ticiani, E., Gingrich, J., Pu, Y., Vettathu, M., Davis, J., Martin, D., Petroff, M.G., Veiga-Lopez, A., 2021. Bisphenol S and Epidermal Growth Factor Receptor Signaling in Human Placental Cytotrophoblasts. Environ Health Perspect 129 (2), 27005.
Ticiani, E., Villegas, J.A., Murga-Zamalloa, C., Veiga-Lopez, A., 2023. Binding sites in the epidermal growth factor receptor are responsible for bisphenol S effects on trophoblast cell invasion. Chemosphere 318, 137960.
Toprakci, M., Yelekci, K., 2005. Docking studies on monoamine oxidase-B inhibitors: estimation of inhibition constants (K(i)) of a series of experimentally tested compounds. Bioorg Med Chem Lett 15 (20), 4438–4446.
Vafeiadi, M., Agramunt, S., Pedersen, M., Besselink, H., Chatzi, L., Fthenou, E., Fleming, S., Hardie, L.J., Wright, J., Knudsen, L.E., Nielsen, J.K., Sunyer, J., Carreras, R., Brunborg, G., Gutzkow, K.B., Nygaard, U.C., Lovik, M., Kyrtopoulos, S. A., Segerback, D., Merlo, D.F., Kleinjans, J.C., Vrijheid, M., Kogevinas, M., NewGeneris, C., 2014. In utero exposure to compounds with dioxin-like activity and birth outcomes. Epidemiology 25 (2), 215–224.
Vogeley, C., Sondermann, N.C., Woeste, S., Momin, A.A., Gilardino, V., Hartung, F., Heinen, M., Maass, S.K., Mescher, M., Pollet, M., Rolfes, K.M., Vogel, C.F.A., Rossi, A., Lang, D., Arold, S.T., Nakamura, M., Haarmann-Stemmann, T., 2022. Unraveling the differential impact of PAHs and dioxin-like compounds on AKR1C3 reveals the EGFR extracellular domain as a critical determinant of the AHR response. Environ Int 158, 106989.
Wang, J., Xie, X., 2007. Development of a quantitative, cell-based, high-content screening assay for epidermal growth factor receptor modulators. Acta Pharmacol Sin 28 (10), 1698–1704.
Watanabe, M., Noma, Y., 2010. Behavior of 2-(3,5-di-tert-butyl-2-hydroxyphenyl) benzotriazole (DBHPBT) and 2-(3,5-di-tert-butyl-2-hydroxyphenyl)-5-chlorobenzotriazole during incineration of solid waste contaminated with thousand mg/kg levels of DBHPBT. J. Hazard. Mater. 178 (1), 1065–1069.
Yao, N., Wang, C.R., Liu, M.Q., Li, Y.J., Chen, W.M., Li, Z.Q., Qi, Q., Lu, J.J., Fan, C.L., Chen, M.F., Qi, M., Li, X.B., Hong, J., Zhang, D.M., Ye, W.C., 2020. Discovery of a novel EGFR ligand DPBA that degrades EGFR and suppresses EGFR-positive NSCLC growth. Signal Transduct Target Ther 5 (1), 214.
Zhuang, S., Lv, X., Pan, L., Lu, L., Ge, Z., Wang, J., Wang, J., Liu, J., Liu, W., Zhang, C., 2017. Benzotriazole UV 328 and UV-P showed distinct antiandrogenic activity upon human CYP3A4-mediated biotransformation. Environ Pollut 220 (Pt A), 616–624.
Stockholm Convention on POPs. Eleventh meeting of the Conference of the Parties to the Stockholm Convention, 2023. https://chm.pops.int/TheConvention/ConferenceoftheParties/Meetings/COP11/tabid/9310/Default.aspx. (Accessed 03 April 2024).

Supplementary Information

Benzotriazole UV stabilizers disrupt epidermal growth factor receptor signaling in human cells

Natalie C. Sondermann, Afaque A. Momin, Stefan T. Arold, Thomas Haarmann-Stemmann

Correspondence to: Thomas.haarmann-stemmann@iuf-duesseldorf.de

This PDF file includes:

Supplementary Table 1

Supplementary Figures S1 – S2

Supplementary table 1: UV-327 interferes with EGF:EGFR complex formation resulting in an effect strength comparable to that of Cetuximab. Effect strength of test compounds in relation to the maximal effect achieved (100 %) by EGFR blocking positive control Cetuximab (n = 3, mean).

Compound (concentration)	Effect strength [%]
Cetuximab (100 ng/ml)	100
UV-320 (100 nM)	61
UV-320 (1 µM)	35
UV-320 (10 µM)	73
UV-327 (10 nM)	61
UV-327 (100 nM)	83
UV-327 (1 µM)	77
UV-327 (10 µM)	86

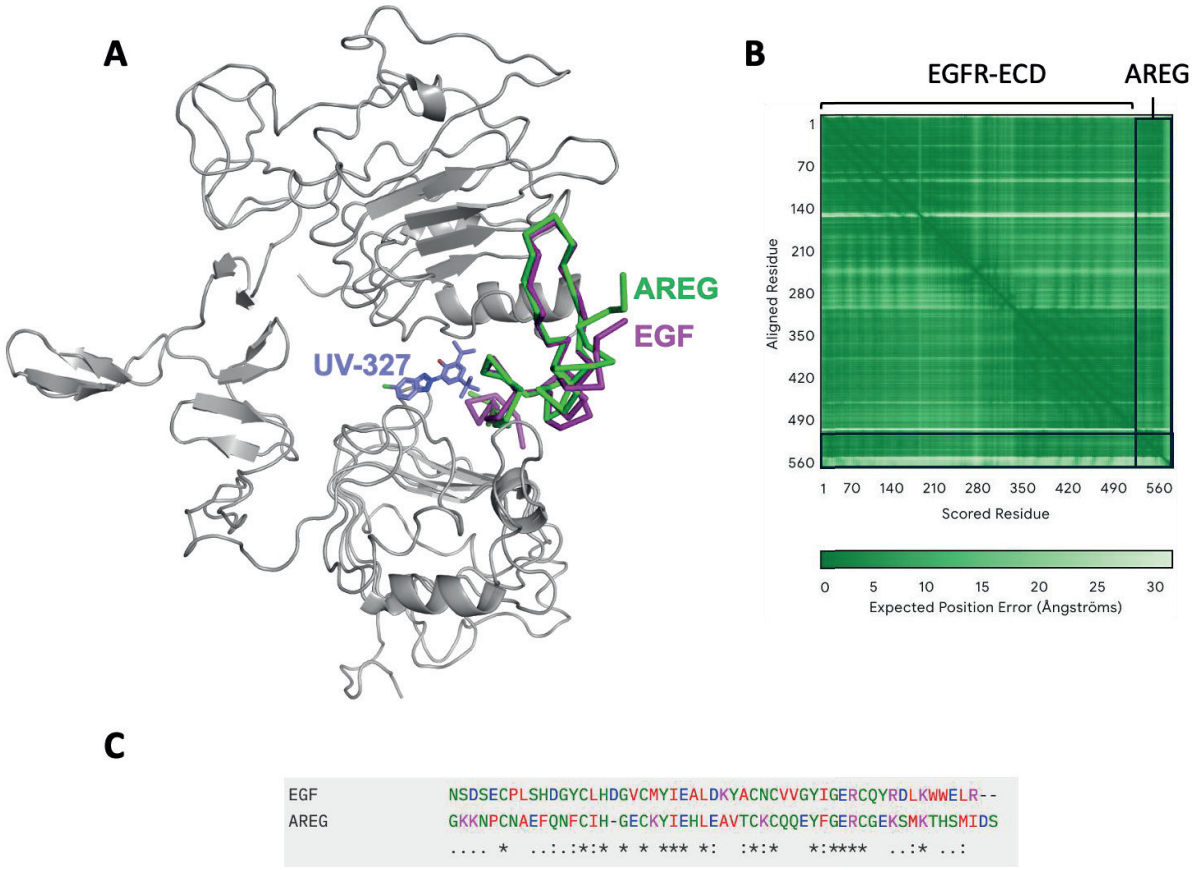

Figure S1: AlphaFold3 predicts that AREG and EGF bind to the same site on the EGFR extracellular domain. **A** The EGFR protein structure (gray cartoon) in complex was taken from PDB id 1ivo. EGF (taken from PDB ivo) is shown as magenta backbone trace, and AREG (AlphaFold3 model in complex with EGFR; EGFR omitted for clarity) is shown in green. UV-327 (slate blue; our docking result) is shown as stick figure **B** The Predicted Aligned error (PAE) plot showing the expected position error per residue pair. The region corresponding to the EGFR-ECD and the EGF binding region of AREG (residues 1-502, 503-561, boxed) are indicated. **C** Sequence alignment of the EGFR-binding regions of EGF and AREG, showing sequence conservation (produced by Muscle 3.8).

```
Ray          SLSREVCSGSENKLTILSNVKDHYHNLRKTYNACEVVMGNLEITFLEPHHDVSFLQSIQE  60
Sturgeon     LQDKKVCQGISNKLTRLGTHEDHYNNLVRMYRNCTVVLENLEITYVEENRDLSFLKTIQE  60
Mallard      VEEKKVCQGTNNKLTQLGHVEDHFTSLQRMYNNCEVVLSNLEITYVEHNRDLSFLKTIQE  60
Gull         VEEKKVCQGTNNKLTQLGHVEDHFTSLQRMYNNCEVVLSNLEITYVEHNRDLSFLKTIQE  60
Beluga       LEEKKVCQGTSNKLTQLGTFEDHFLSLQRMFNNCEVVLGNLEITYMQSSYNLSFLKTIQE  60
Otter        LEEKKVCQGTSNRLTQLGTFEDHFLSLQRMFNNCEVVLGNLEITYMQKNYDLSFLKTIQE  60
Seal         LEEKKVCQGTSNRLTQLGTFEDHFLSLQRMFNNCEVVLGNLEITYMQRNYDLSFLKTIQE  60
Human        LEEKKVCQGTSNKLTQLGTFEDHFLSLQRMFNNCEVVLGNLEITYVQRNYDLSFLKTIQE  60
               .::**.* .*:** *.  :**: .* : :. * **: *****:::   ::***::***

Ray          VSGYVLIALNNISRIPLQNLRIIRGHRLYEDKFALVILSNYKRKR-IGLTELHLQNLTEI  119
Sturgeon     VGGYVLIALNNIAKLHLENLQIIRGHTLYDNKYALAVLSNYDKNSTVGVTELALRSLTEI  120
Mallard      VAGYVLIALNMVDVIPLENLQIIRGNVLYDNSFALAVLSNYHMNKTQGLRELPMKRLSEI  120
Gull         VAGYVLIALNMVDVIPLENLQIIRGNVLYDNSYALAVLSNYHMNKTQGLQQLPMKRLSEI  120
Beluga       VAGYVLIALNTVEKIPLEKLQIIRGNVLYENTHALAVLSNYGANK-TGLRELPMRNLQEI  119
Otter        VAGYVLIALNTVEKIPLENLQIIRGNVLYENTHALSVLSNYGANK-TGLQELPLRNLHEI  119
Seal         VAGYVLIALNTVQRIPLENLQIIRGNVLYENTHALSVLSNYGTNK-TGLQELPLRNLHEI  119
Human        VAGYVLIALNTVERIPLENLQIIRGNMYYENSYALAVLSNYDANK-TGLKELPMRNLQEI  119
             *.******** :  : *::*:****:  *::..** :****  :   *: :* :: * **

Ray          LSGTVKIMSNPQLCYLQTIHWDDILDNASASNMATHFTE--KICPKCHLKCQNEACWGPG  177
Sturgeon     IKGGVKFTNNMLLCNLDTIQWNDIVDFKANPEMVLPSVNNKPHCQKCDPGCSNGSCWAPG  180
Mallard      LNGGVKISNNPKLCNMDTVLWNDIIDTSRKPLTVLDFASNLSTCPKCHPNCTEDHCWGAG  180
Gull         LNGGVKISNNPKLCNMDTVLWNDIIDTSKQPLKVLEFASNLSSCPKCHPNCTEDHCWGPG  180
Beluga       LQGAVRFSNNPILCNMDTVQWRDIVNTDFLSNMSIEFQSQLSRCPKCDPVCLNGSCWGAG  179
Otter        LQGAVRFSNNPVLCNVDSIKWQDIVDDSFVSNMSMDFQNHAGNCQKCDPSCPNGSCWGPG  179
Seal         LQGAVRFSNNPVLCNVETIQWRDIVDSDFISNMSMDFQNQAGSCQKCDPDCPDGSCWGPG  179
Human        LHGAVRFSNNPALCNVESIQWRDIVSSDFLSNMSMDFQNHLGSCQKCDPSCPNGSCWGAG  179
             : * *:: .*  ** :::: * **:.           .    * **.  * :  **. *

Ray          VVNCQKFTKKICADQCSGRCMGPQPSDCCHIQCAAGCTGPREHDCLACRKFSDGDTCKES  237
Sturgeon     PDNCQTLTRSICADQCSGRCKGPKPSDCCNDHCAAGCTGPRPTDCLACRAFQDDGTCKDA  240
Mallard      EQNCQTLTKVICAQQCSGRCRGKVPSDCCHNQCAAGCTGPRESDCLACRKFRDDATCKDT  240
Gull         EQNCQTLTKVICAQQCSGRCRGKVPSDCCHNQCAAGCTGPRESDCLACRKFRDDATCKDT  240
Beluga       KENCQKLTKVICAQQCSGRCRGRSPSDCCHSQCAAGCTGPRESDCLVCRRFRDGATCKDT  239
Otter        KENCQKLTKIICAQQCSGRCRGRSPSDCCHNQCAAGCTGPRESDCLVCRKFRDETTCKDT  239
Seal         KENCQKLTKTICAQQCSGRCRGRSPSDCCHNQCAAGCTGPRESDCLVCRRFRDEATCKDT  239
Human        EENCQKLTKIICAQQCSGRCRGKSPSDCCHNQCAAGCTGPRESDCLVCRKFRDEATCKDT  239
               ***.:*: ***:****** *  *****: :*********  ***.** * *  ***::

Ray          CPHLFVYNTIKFQMERNPNGKYSFGSSCVEKCPHNYAVTDHGSCVRACSPGTYEVDEDKI  297
Sturgeon     CPQLMLYNPNTHQLEVNPKGKYNFGATCVKNCPHNYVVTDHGSCVRTCSSKTYEVDENGL  300
Mallard      CPPLVLYNPTTYQMDVNPDGKYSFGATCVRECPHNYVVTDHGSCVRSCNTDTYEVEENGV  300
Gull         CPPLVLYNPTTYQMDVNPDGKYSFGATCVRECPHNYVVTDHGSCVRSCNTDTYEVEENGV  300
Beluga       CPPLMLYDPTTYEMKVNPLGKYSFGATCVRKCPRNYVVTDHGSCVRACSSESQEVEEDGV  299
Otter        CPPLMLYNPTTYQMDVNPEGKYSFGATCVKKCPRNYVVTDHGSCVRACSSDSYEVEEDGV  299
Seal         CPPLMLYNPTTYQMDVNPEGKYSFGATCVKKCPRNYVVTDHGSCVRACSSDSYEVEEDGV  299
Human        CPPLMLYNPTTYQMDVNPEGKYSFGATCVKKCPRNYVVTDHGSCVRACGADSYEMEEDGV  299
             ** *.:*:  ..::. ** ***.**::**.:**:**.**********:*.  : *::*: :

Ray          RKCKRCEGPCPKDCSGLGVPPLKDVMSINSTNIDSFKNCTKINGNVVILEVTFNGDSYSK  357
Sturgeon     RKCKKCEGPCPKACNGLGMGNLKDVLSINATNIDSFRDCTTINGDVSILPVTFTGDKFTN  360
Mallard      RKCKKCDGLCSKVCNGIGIGELKGILSINATNIDSFKNCTKINGDVSILPVAFLGDAFTK  360
Gull         RKCKKCDGLCSKVCNGIGIGELKGILSINATNIDSFKNCTKINGDVSILPVAFLGDAFTK  360
Beluga       RKCKKCDGPCGKVCNGIGIGEFKDTLSINATNIKHFRNCTSISGDLHILPVAFKGDSFTR  359
Otter        RKCKKCEGPCRKVCNGIGIGEFKDTLSINATNIKHFKNCTSISGDLHILPVAFRGDSFTR  359
Seal         RKCKKCEGPCRKVCNGIGIGEFKDTLSINATNIKHFKNCTSISGDLHILPVAFRGDSFTR  359
Human        RKCKKCEGPCRKVCNGIGIGEFKDSLSINATNIKHFKNCTSISGDLHILPVAFRGDSFTH  359
             ****:*:* * * *.*:*:  :*. :***:***. *::**.*.*:: ** *:* ** ::.

Ray          AAPLLLEKLEVFRTVREITGYFLIQSWPANYTDLQVFENLEIIRGRTLHHSHVSFAVVNL  417
Sturgeon     TAALDPAELNVFKTVKEITGFLLVQHWPANLTDLNPFENLEIIRGRTKQHGTVSLAVVNI  420
Mallard      TLPLDPKKLDVFKTVKEISGFLLIQAWPDNATDLYAFENLEIIRGRTKQHGQYSLAVVNL  420
Gull         TLPLDPKKLDVFKTVKEISGFLLIQAWPDNATDLYAFENLEIIRGRTKQHGQYSLAVVNL  420
Beluga       TPPLDPKELDILKTVKEITGFLLIQAWPANRTGLHAFENLEIIRGRTKQHGQFSLAVVGL  419
Otter        TLPLDPKELDILKTVKEITGFLLIQAWPENRTDLHAFENLEIIRGRTKQHGQFSLAVVGL  419
Seal         TLPLDPKELDILKTVREITGFLLIQAWPENRTDLHAFENLEIIRGRTKQHGQFSLAVVGL  419
Human        TPPLDPQELDILKTVKEITGFLLIQAWPENRTDLHAFENLEIIRGRTKQHGQFSLAVVSL  419
             :  *   :*:::::**:**:*::*:* ** * *.*  *********** :*.  *:***.:
```

Figure S2: Multiple alignment of EGFR protein sequences. A multiple alignment of the 417 - 420 N-terminal amino acids of the animal EGFR protein (mature) was carried out using the Clustal Omega online tool and the NCBI References Sequences given in the Material and Methods section. Bold letter in red stands for the amino acid residue that was predicted and experimentally proven to be required for the binding of BUVs as well as of dioxin-like compounds. Bold letters in blue stand for amino acid residues that were predicted to be required for BUV binding. Bold letter in purple stands for an amino acid residue that was predicted to be required for BUV binding and previously identified being critical for the binding of dioxin-like compounds. "*" = fully conserved residue, ":" = conservation between groups of strongly similar properties, "." = conservation between groups of weakly similar properties.

2.4 Polybrominated diphenyl ether flame retardants inhibit growth factor-induced activation of EGFR by binding to its extracellular domain

Natalie C. Sondermann, Afaque A. Momin, Stefan T. Arold, Thomas Haarmann-Stemmann

PBDEs wurden lange Zeit als Flammschutzmittel in Konsumgütern verwendet. Trotz internationaler Verbote gelangen diese persistenten und bioakkumulierbaren Chemikalien weiterhin in die Umwelt und können in Tieren und Menschen nachgewiesen werden. Studien zeigen eine Verbindung zwischen PBDE-Exposition und gesundheitlichen Problemen, was ein besseres Verständnis ihrer Wirkungsweise erforderlich macht. Unsere Untersuchungen zeigen, dass die PBDEs BDE-47 und BDE-99 die Aktivierung des EGFR durch Bindung an dessen ECD hemmen. Dies beeinträchtigt z.B. die DNA-Synthese in Keratinozyten. EGFR wird als Zelloberflächenrezeptor für PBDEs identifiziert, was neue Einblicke in deren Wirkmechanismus bietet.

Journal:	Archives of Toxicology
Impact Factor:	4,8 (2024)
Beitrag zur Veröffentlichung:	90 % Konzept, Literaturrecherche, Schreiben, Editieren, Visualisierung, Experimente für Abb. 1, 2, 3, 4
Art der Autorenschaft:	Erstautorenschaft
Status der Publikation:	Seit 17.10.24 in Begutachtung

Archives of Toxicology

Polybrominated diphenyl ether flame retardants inhibit growth factor-induced activation of EGFR by binding to its extracellular domain

--Manuscript Draft--

Manuscript Number:	
Full Title:	Polybrominated diphenyl ether flame retardants inhibit growth factor-induced activation of EGFR by binding to its extracellular domain
Article Type:	Original Article
Corresponding Author:	Thomas Haarmann-Stemmann IUF - Leibniz Research Institute for Environmental Medicine Düsseldorf, NRW GERMANY
Corresponding Author Secondary Information:	
Corresponding Author's Institution:	IUF - Leibniz Research Institute for Environmental Medicine
Corresponding Author's Secondary Institution:	
First Author:	Natalie C. Sondermann
First Author Secondary Information:	
Order of Authors:	Natalie C. Sondermann
	Afaque A. Momin
	Stefan T. Arold
	Thomas Haarmann-Stemmann
Order of Authors Secondary Information:	
Funding Information:	Office of Sponsored Research, KAUST (FCC/1/1976-33) — Dr. Stefan T. Arold
	Office of Sponsored Research, KAUST (REI/1/4446-01) — Dr. Stefan T. Arold
	Jürgen Manchot Stiftung (NCS) — M.Sc. Natalie C. Sondermann
Abstract:	For many years, polybrominated diphenyl ethers (PBDEs) were used as flame retardants in a large number of consumer products. Even though international law meanwhile prohibits the production and usage of PBDEs, these persistent and bioaccumulative chemicals still leak into the environment, and are frequently detected in wildlife and humans. Population-based studies reveal positive correlations between human PBDE exposure and various adverse health effects, emphasizing that a better understanding of the mode of action of these polybrominated chemicals is urgently needed. Therefore, we investigated the effect of two widespread PBDEs, namely BDE-47 and BDE-99, on epidermal growth factor receptor (EGFR) activity in human cells. Recent studies showed that the EGFR is not only orchestrating cellular functions, but also serves as a cell-surface receptor for dioxins, phenolic benzotriazoles and related organic pollutants. Results form in silico docking analyses, AlphaLISA-based receptor binding studies and SDS-PAGE/Western blot analyses revealed that BDE-47 and BDE-99 inhibit the growth factor-triggered activation of EGFR by binding to its extracellular domain. In keratinocytes, PBDEs also inhibit amphiregulin-induced and EGFR-mediated DNA synthesis as well as the EGFR-triggered trans-repression of the aryl hydrocarbon receptor signaling pathway. Our data identify EGFR as a cell-surface receptor for PBDEs and shed light on a novel mode of action of these ubiquitous and persistent chemicals. This finding may contribute to an improved hazard assessment of PBDEs and structurally related flame retardants.
Suggested Reviewers:	Zdenek Dvorak Palacky University Olomouc: Univerzita Palackeho v Olomouci moulin@email.cz
	Markus Wahl BASF markus.wahl@basf.com

	Dalei Wu Shandong University, Jinan, China dlwu@sdu.edu.cn
	Jamie J Bernard Michigan State University, Department of Pharmacology and Toxicology jbernard@msu.edu

Polybrominated diphenyl ether flame retardants inhibit growth factor-induced activation of EGFR by binding to its extracellular domain

Natalie C. Sondermann[1], Afaque A. Momin[2], Stefan T. Arold[2], Thomas Haarmann-Stemmann[1,*]

[1]IUF – Leibniz-Research Institute for Environmental Medicine, 40225 Düsseldorf, Germany

[2]Biological and Environmental Science and Engineering Division, Center of Excellence on Smart Health, King Abdullah University of Science and Technology (KAUST), Thuwal 23955-6900, Kingdom of Saudi Arabia

*Corresponding author:

Thomas Haarmann-Stemmann

IUF – Leibniz-Research Institute for Environmental Medicine

Auf'm Hennekamp 50, 40225 Düsseldorf, Germany

Office: +492113389204

E-mail: thomas.haarmann-stemmann@IUF-duesseldorf.de

Abstract

For many years, polybrominated diphenyl ethers (PBDEs) were used as flame retardants in a large number of consumer products. Even though international law meanwhile prohibits the production and usage of PBDEs, these persistent and bioaccumulative chemicals still leak into the environment, and are frequently detected in wildlife and humans. Population-based studies reveal positive correlations between human PBDE exposure and various adverse health effects, emphasizing that a better understanding of the mode of action of these polybrominated chemicals is urgently needed. Therefore, we investigated the effect of two widespread PBDEs, namely BDE-47 and BDE-99, on epidermal growth factor receptor (EGFR) activity in human cells. Recent studies showed that the EGFR is not only orchestrating cellular functions, but also serves as a cell-surface receptor for dioxins, phenolic benzotriazoles and related organic pollutants. Results form *in silico* docking analyses, AlphaLISA-based receptor binding studies and SDS-PAGE/Western blot analyses revealed that BDE-47 and BDE-99 inhibit the growth factor-triggered activation of EGFR by binding to its extracellular domain. In keratinocytes, PBDEs also inhibit amphiregulin-induced and EGFR-mediated DNA synthesis as well as the EGFR-triggered trans-repression of the aryl hydrocarbon receptor signaling pathway. Our data identify EGFR as a cell-surface receptor for PBDEs and shed light on a novel mode of action of these ubiquitous and persistent chemicals. This finding may contribute to an improved hazard assessment of PBDEs and structurally related flame retardants.

Keywords: AHR, BDE-47, BDE-99, EGFR, flame retardants, persistent organic pollutants

Introduction

For several decades, polybrominated diphenyl ethers (PBDEs) were used as flame retardants in a variety of consumer products, including textiles, furniture, and electronic devices. Due to their toxicity, their ubiquitous distribution in the environment, and their tendency to bioaccumulate in food chains (Chain et al. 2024; Wu et al. 2020), the production and use of PBDEs is nowadays entirely prohibited by the Stockholm Convention, i.e. a multilateral treaty regulating selected persistent organic pollutants (POPs) of very high concern (Sharkey et al. 2020). Humans can be exposed to PBDEs through inhaling contaminated air, ingesting contaminated food or dust, and skin contact with dust or soil (Wu et al. 2020). In fact, a large body of population-based studies, identifying different PBDE congeners in fetal and adult tissues, blood, urine, hair, and breast milk (Bjermo et al. 2017; Kim et al. 2011; Lin et al. 2023; Zota et al. 2018), provides ample evidence for extensive human exposure to these flame retardants. PBDEs disturb various physiological and developmental processes and even facilitate carcinogenesis (Wu et al. 2020), for instance by disrupting proper steroid hormone receptor signaling (Meerts et al. 2001; Schreiber et al. 2010) and inducing oxidative stress (Ji et al. 2011; Montalbano et al. 2020). Moreover, results from several studies suggest a role of the aryl hydrocarbon receptor (AHR) in mediating PBDE toxicity (Chen and Bunce 2003; Doan et al. 2019; Peters et al. 2006; Yang et al. 2016).

The AHR is a transcription factor that is activated upon binding of dioxins, polycyclic aromatic hydrocarbons and other small molecular weight molecules and, amongst others, regulates xenobiotic metabolism and immune responses (Rothhammer and Quintana 2019; Vogel et al. 2020). In its resting state, AHR is part of a cytosolic multiprotein complex consisting of two heat-shock protein 90 molecules, AHR-interacting protein, the cochaperone p23 and tyrosine kinase c-Src. Upon ligand-binding, AHR experiences conformational changes leading to the dissociation of the cytosolic multiprotein complex and the subsequent nuclear translocation of AHR. Nuclear AHR dimerizes with AHR nuclear translocator (ARNT) and binds to xenobiotic-responsive elements (XRE) in the regulatory region of target genes, for instance encoding

cytochrome P450 (CYP) 1A1 and CYP1B1, to enforce their expression (Rothhammer and Quintana 2019; Vogel et al. 2020). In addition to this so-called canonical AHR signaling pathway, active AHR cross-talks with numerous other cellular signaling pathways and molecules, such as the epidermal growth factor receptor (EGFR) (Sondermann et al. 2023). Specifically, the soluble tyrosine kinase c-Src, which is released from the cytosolic multiprotein complex upon ligand-binding of AHR, activates EGFR and downstream signal transduction pathways (Vogeley et al. 2022). Interestingly, it was shown that active EGFR in turn attenuates the transcriptional activity of AHR (Joiakim et al. 2016; Sutter et al. 2009).

Noteworthy, the reported effects of PBDEs on AHR activity are rather weak and partially controversial (e.g., agonistic vs. antagonistic effects) (Chen and Bunce 2003; Doan et al. 2019; Peters et al. 2006; Yang et al. 2016), which might be due to the fact that some commercially available PBDE mixtures are impurified with traces of highly AHR-reactive polyhalogenated dibenzo-*p*-dioxins and dibenzofurans (Hanari et al. 2006; Ren et al. 2011; Wahl et al. 2008). Moreover, we and others have identified several dioxins and dioxin-like compounds, including 2,3,7,8-tetrachlorodibenzo-*p*-dioxin and polychlorinated biphenyl (PCB) congener 126, to directly bind to the extracellular domain (ECD) of human EGFR and inhibit its activation by growth factors (Hardesty et al. 2018; Vogeley et al. 2022). By conducting AHR/XRE-dependent reporter gene assays, *in silico* docking simulations, AlphaLISA EGF:EGFR binding assays, SDS-PAGE/Western blot analyses, and other experimental approaches, we here tested the hypothesis that PBDE congeners, in particular BDE-47 and BDE-99, inhibit growth factor-induced EGFR activation and affect downstream biological functions, including DNA synthesis and the transcriptional activity of AHR, in human HaCaT keratinocytes and HepG2 hepatoma cells.

Material and Methods

Cell culture

The CRISPR/Cas9-based generation and validation of HaCaT-AHR-KO keratinocytes was described previously (Vogeley et al. 2022). Both HaCaT keratinocytes and HaCaT-AHR-KO keratinocytes were cultured in DMEM low glucose (1 g/l) medium and supplemented with 10 % FBS (v/v) and 1 % (v/v) antibiotics/antimycotics. The XRE-HepG2 reporter cell-line was cultured in RPMI 1640 medium containing 3.7 % $NaHCO_3$ (w/v), 10 % FBS (v/v), 1 % (v/v) antibiotic/antimycotic solution, and 0.8 mg/ml G418. All culture media and supplements were purchased from PAN Biotech (Aidenbach, Germany). All cells were cultivated in a humidified atmosphere of 5 % CO_2 at 37 °C.

Chemicals and treatment

BDE-47 (2,2′,4,4′-Tetrabromdiphenyl ether), BDE-99 (2,2',4,4',5-Pentabromodiphenyl ether) and B[a]P (benzo[a]pyrene) were purchased from Sigma-Aldrich (Taufkirchen, Germany). Cetuximab (anti-EGFR, #A2000) was ordered from Selleckchem (Houston, TX, USA).

Recombinant human amphiregulin (AREG) and epidermal growth factor (EGF) were bought from PeproTech (Rocky Hill, NY) and dissolved in water, all other compounds were dissolved in DMSO. Information about the time and dose of the applied compounds is given in the figures and/or figure legends.

Reporter gene assay

AHR/XRE-dependent reporter gene activation was determined as described previously (Frauenstein et al. 2015). Luciferase activity was normalized to the respective protein concentration of each sample.

***In silico* docking analyses of PBDEs with EGFR**

Potential docking poses and binding affinities were obtained by molecular flexible docking simulations as outlined in detail in previous work (Sondermann et al. 2024). BDE-47 (PubChem CID 95170), BDE-99 (PubChem CID 36159) and BDE-209 (PubChem CID 14410) ligand structures were downloaded (SD format) from PubChem database (Kim et al. 2016).

EGF-EGFR AlphaLISA binding assay

In order to analyze a potential interaction of the test compounds with the EGFR ECD, the cell-free EGF:EGFR AlphaLISA Binding Kit (PerkinElmer, Waltham, MA) was used according to the manufacturer's instructions.

SDS-PAGE/Western blot analysis

SDS-PAGE/Western blot analyses was performed as described earlier (Sondermann et al. 2024). All primary and secondary antibodies used in this study (tEGFR #4267, pEGFR Y1068 #3777, GAPDH #2118, and anti-rabbit IgG HRP-linked #7074) are from Cell Signaling Technology (Leiden, Netherlands). Bands were visualized using WesternBright ECL HRP substrate (Advansta, San Jose, CA) and a C-DiGit Western Blot Scanner (LI-COR Biotechnology, Lincoln, NE).

BrdU incorporation assay

Potential effects of PBDEs on DNA synthesis in HaCaT-AHR-KO keratinocytes were examined using a colorimetric BrdU incorporation assay (Sigma-Aldrich, Taufkirchen, Germany) as previously described (Sondermann et al. 2024).

Statistical analysis

Unless otherwise stated, all data are mean values (± standard deviation) from three or more independent experiments. Comparison between two groups was performed using an unpaired, two-tailed Student's t test, while comparison among multiple groups was conducted using analysis of variance (ANOVA) followed by a Tukey post hoc test to correct for multiple comparison. Differences were considered significant at $p \leq 0.05$.

Results

BDE-47 and BDE-99 do not affect basal but AHR ligand-induced XRE-driven reporter gene activity

According to the literature, it is quite controversial whether BDE-47 and BDE-99 may serve as agonistic or antagonistic ligands of AHR. Therefore, we first tested this using an established luciferase-based XRE reporter gene assay (Fig. 1A). We found that the two PBDEs did not cause an AHR-/XRE-driven induction of reporter gene activity, whereas exposure to the positive control, i.e. the known AHR agonist B[a]P, led to a significant induction. To further evaluate the potential effects of PBDEs on the transcriptional activity of AHR, we continued with a co-treatment of 1 µM B[a]P and the respective PBDE (1 µM, 10 µM; Fig. 1B). The higher concentration of both PBDEs significantly increased the B[a]P-mediated effect.

As activation of EGFR is known to decrease AHR agonist-induced expression of XRE-harboring genes (Sutter et al. 2009), we added EGFR ligand epidermal growth factor (EGF) as a control. As expected, this led to a significant decrease of the B[a]P-driven reporter gene activity. Previously it was shown that inhibition of EGFR also shapes B[a]P-induced gene expression, leading to an increase in XRE-driven reporter gene activity (Joiakim et al. 2016). Therefore, we next co-treated the cells with B[a]P and the EGFR-blocking monoclonal antibody Cetuximab as a positive control for the enhancing effect of EGFR inhibition (Vogeley et al. 2022). Based on these results, we conclude that, at least in our test model, BDE-47 and BDE-99 do not serve as AHR agonists or antagonists, but may have an inhibitory effect on EGFR.

PBDEs seem to directly bind to the EGFR ECD

Next, we performed *in silico* docking analyses investigating the potential binding of PBDEs to the ECD of EGFR (Fig. 2). Here, we focused on the EGF binding site, situated between EGFR ECD domains I and III, since interactions of this binding site with other organic pollutants have been described previously (Vogeley et al. 2022). The predicted binding poses and binding energies indicated that both tested PBDEs can associate with the EGF binding site (Fig. 2C, D)D). The calculated binding energy ($\Delta G_{binding}$) (Eberhardt et al. 2021) and interacting residues for both PBDEs were similar. For BDE-47 it was -8.6 kcal/mol and for BDE-99 it was -8.1 kcal/mol, corresponding to dissociation constants ($K_d s$) of 95.1 nM and 99.3 nM, respectively. Similar results were also achieved for another environmentally relevant PBDE (BDE-209, Fig. S1). Its calculated binding affinity corresponding to a $K_d s$ of 132.9 nM was -7.7 kcal/mol.

To validate the computational docking data, we performed a cell-free EGF-EGFR AlphaLISA binding assay (Fig. 2E). For this, recombinant human EGF and the EGFR monoclonal antibody Cetuximab were used as positive controls that should reduce the binding of biotinylated EGF to antibody-captured EGFR by occupying its binding site on the ECD. Indeed, both substances significantly reduced the fluorescence measured upon formation of the EGF:EGFR complex. We tested both BDE-47 and BDE-99 in three concentrations (0.1 µM, 1 µM, 10 µM) and all of them significantly reduced EGF:EGFR complex formation.

EGFR ligand-induced receptor phosphorylation is inhibited by BDE-47 and BDE-99

Knowing that BDE-47 and BDE-99 bind the EGFR ECD and even compete with EGF, we next investigated their potential effect on EGFR phosphorylation via SDS PAGE/western blot analysis (Fig. 3). For this, we treated HaCaT cells for 15 min with either EGFR agonist EGF or amphiregulin (AREG), each alone and in combination with 1 µM BDE-47 (Fig. 3A) or 1 µM BDE-99 (Fig. 3B). Both PBDEs did not affect total EGFR protein levels but reduced the EGF-

as well as the AREG-induced phosphorylation of EGFR at tyrosine (Y) residue 1068 in a significant manner.

BDE-47 and BDE-99 interfere with AREG-induced DNA synthesis

After observing that BDE-47 and BDE-99 inhibit the ligand-induced phosphorylation of EGFR, we wanted to investigate a functional endpoint further downstream in the EGFR signaling pathway. Since EGFR is involved in several regulatory processes, we chose to investigate PBDE's influence on cell proliferation since this is a prominently EGFR-driven and AREG-induced regulatory process in human keratinocytes (Stoll et al. 2016). For this, we conducted a colorimetric BrdU incorporation assay measuring the AREG-induced DNA synthesis in HaCaT-AHR-KO keratinocytes. As shown in figure 4, both PBDEs attenuated the AREG-induced DNA synthesis in a dose-dependent and AHR-independent manner. For both test compounds, a statistically significant inhibition of the growth factor-induced DNA synthesis was achieved at a concentration of 1 µM.

Discussion

Due to their lingering presence in the environment as well as their bioaccumulative and toxic potential, regulatory authorities regard the sustained exposure of the general population to PBDEs as a major health threat (Chain et al. 2024). In this study, we reported for the first time that two exposure-relevant PBDEs, namely BDE-47 and BDE-99, directly interact with EGFR and inhibit its growth factor-triggered activation as well as downstream processes, such as DNA synthesis or crosstalk with the AHR signaling pathway. In addition, results from *in silico* docking analyses strongly indicate that BDE-209, another ubiquitously distributed flame retardant, is capable of interfering with EGFR activation in a similar manner.

Zhang et al. observed an influence of BDE-47 on EGFR signaling where it increased receptor phosphorylation and promoted cell growth and migration in endometrial carcinoma cells

(Zhang et al. 2019). Similar tumor-promoting effects were observed for BDE-99 in colorectal cancer cells involving the PI3K/AKT/Snail signaling pathway downstream of EGFR (Wang et al. 2015). In human bronchial epithelial cells, BDE-71 promoted EGFR phosphorylation and induced proinflammatory responses (Koike et al. 2014). In contrast to our findings, these studies observed an activation of EGFR upon PBDE exposure. Considering the difference in cell type and cell environment, this not only indicates that PBDEs directly interact with EGFR and interfere with its downstream signaling, but also that the outcome of these interactions is probably shaped by cell-specificity and might be the result of complex interplays with other signaling pathways. Another contributing factor to these EGFR-activating effects of some PBDEs might be that many of them are contaminated with dioxins (Hanari et al. 2006; Ren et al. 2011; Wahl et al. 2008). Whereas dioxin-like chemicals also bind to the EGFR ECD and inhibit its activation by growth factors (Hardesty et al. 2018; Vogeley et al. 2022), these compounds can also stimulate EGFR activation early upon exposure by binding to AHR in the cytoplasm and enforcing the release of the EGFR-phosphorylating tyrosine kinase c-Src (Vogeley et al. 2022).

EGFR-deficient mice die early after birth due to epithelial immaturity and multiorgan failure, thus underscoring the critical relevance of EGFR for proper embryonic development (Miettinen et al. 1995). EGFR is expressed in the central and peripheral nervous system and, for instance, contributes to proper brain development by controlling the migration of neural stem cells as well as the proliferation and migration of neural progenitor cells (NPC) (Koch et al. 2022). Interestingly, an administration of the EGFR inhibitor PD153035 was found to reduce the migration of human NPCs (Masjosthusmann et al. 2018), while a treatment with BDE-47 as well as BDE-99 also decreased migration distance in human NPCs (Schreiber et al. 2010). Blood concentration of PBDEs in total is within the nanomolar range (Costa and Giordano 2007). However, infants may be exposed via breast milk to 4,000 ng/kg of PBDEs per day, leading to a significantly higher body burden (Jones-Otazo et al. 2005). According to Schreiber and colleagues, who considered bioaccumulation rates derived from PBDE-treated human neurospheres (60-fold), rat neocortical cells (100-fold) (Mundy et al. 2004) and mice (140-fold)

(Viberg et al. 2003), this PBDE exposure level of infants may lead to brain concentrations ranging from 0.5 µM to 1.1 µM (Schreiber et al. 2010). Given that BDE-47 and BDE-99 at a concentration of 1 µM inhibited the ligand-induced phosphorylation of EGFR and downstream DNA synthesis, and considering potential additive effects, internal PBDE exposure is likely to affect EGFR activity in humans.

Results from another study in primary human hepatocytes also point towards an interaction of the polybrominated flame retardants with the EGFR ECD. Specifically, BDE-47 treatment of the hepatocytes resulted in an enhanced transcription of *CYP2B10* via the constitutive androstane receptor (CAR), a finding that was confirmed by using CAR KO mice (Sueyoshi et al. 2014). An earlier study has shown that phenobarbital activates CAR by binding to the EGFR ECD, thereby inhibiting the receptor tyrosine kinase (Mutoh et al. 2013), leading the authors to conclude that the BDE-47-mediated CAR activation might function in a similarly EGFR-directed manner.

Work by Sutter and colleagues demonstrated that activation as well as inhibition of EGFR significantly shapes the outcome of ligand-activated AHR signaling in normal human epidermal keratinocytes, i.e. induction of xenobiotic-metabolizing enzymes and stimulation of cell differentiation (Sutter et al. 2009). They found that EGFR activation decreases dioxin-induced binding of the histone acetyltransferase p300 to the *CYP1A1* XRE region, pointing to a competition for the common transcriptional co-activator. Another study revealed that EGFR inhibition, on the other hand, increases the dioxin-induced expression of *CYP1A1* and *CYP1A2* in a human breast epithelial cell-line (Joiakim et al. 2016). Thus, modulation of EGFR activity can influence xenobiotic metabolism in an AHR-dependent manner. Whether under a given co-exposure this is of any functional relevance, for instance with regards to the metabolic activation of polycyclic aromatic hydrocarbons and the subsequent formation of highly mutagenic DNA adducts (Vogel et al. 2020), remains to be elucidated. Nevertheless, mixture effects, not only among compounds that bind to EGFR ECD, but also with chemicals that activate AHR, should be taken into consideration when assessing the risk of environmental or occupational exposure situations.

Although the toxicity of PBDEs has been studied over the past decades, the underlying pathomechanisms are not fully understood yet. This study further establishes the EGFR ECD as a prominent interaction site for PBDEs and other environmental pollutants of global concern, such as dioxin-like chemicals (Hardesty et al. 2018; Vogeley et al. 2022), bisphenols (Ticiani et al. 2021) and benzotriazole UV stabilizers (Sondermann et al. 2024), which should be considered as a new mode of action of organic chemicals.

Supplementary information

The online version of this article contains supplementary information available at….

Authorship contribution statement

Natalie C. Sondermann: Performed research, Analyzed data, Wrote the paper. Afaque A. Momin: Performed research, Analyzed data. Stefan T. Arold: Analyzed data, Contributed new methods or models. Thomas Haarmann-Stemmann: Conceived of or designed study, Analyzed data, Wrote the paper.

Declaration of Competing Interest

The authors declare that they have no competing interests.

Acknowledgement

We thank Petra Boukamp for providing HaCaT cells, and Katharina Gradin and Lorenz Poellinger for providing the HepG2 XRE reporter cell-line. We thank Inken Hacheney for excellent technical support. NCS was supported by the Jürgen Manchot Foundation. The research conducted by AAM and STA was supported by the King Abdullah University of Science and Technology (KAUST) through the baseline fund and the Award No. FCC/1/1976-33 and REI/1/4446-01 from the Office of Sponsored Research (OSR). For computer time, this

research used the resources of the KAUST Supercomputing Laboratory (KSL). We thank N. Kathiresan and G. Wickham from the KSL for their support

References

Bjermo H, Aune M, Cantillana T, et al. (2017) Serum levels of brominated flame retardants (BFRs: PBDE, HBCD) and influence of dietary factors in a population-based study on Swedish adults. Chemosphere 167:485-491 doi:10.1016/j.chemosphere.2016.10.008

Chain EPoCitF, Schrenk D, Bignami M, et al. (2024) Update of the risk assessment of polybrominated diphenyl ethers (PBDEs) in food. EFSA J 22(1):e8497 doi:10.2903/j.efsa.2024.8497

Chen G, Bunce NJ (2003) Polybrominated diphenyl ethers as Ah receptor agonists and antagonists. Toxicol Sci 76(2):310-20 doi:10.1093/toxsci/kfg236

Costa LG, Giordano G (2007) Developmental neurotoxicity of polybrominated diphenyl ether (PBDE) flame retardants. Neurotoxicology 28(6):1047-67 doi:10.1016/j.neuro.2007.08.007

Doan TQ, Berntsen HF, Verhaegen S, et al. (2019) A mixture of persistent organic pollutants relevant for human exposure inhibits the transactivation activity of the aryl hydrocarbon receptor in vitro. Environ Pollut 254(Pt B):113098 doi:10.1016/j.envpol.2019.113098

Eberhardt J, Santos-Martins D, Tillack AF, Forli S (2021) AutoDock Vina 1.2.0: New Docking Methods, Expanded Force Field, and Python Bindings. J Chem Inf Model 61(8):3891-3898 doi:10.1021/acs.jcim.1c00203

Frauenstein K, Tigges J, Soshilov AA, et al. (2015) Activation of the aryl hydrocarbon receptor by the widely used Src family kinase inhibitor 4-amino-5-(4-chlorophenyl)-7-(dimethylethyl)pyrazolo[3,4-d]pyrimidine (PP2). Arch Toxicol 89(8):1329-36 doi:10.1007/s00204-014-1321-8

Hanari N, Kannan K, Miyake Y, et al. (2006) Occurrence of polybrominated biphenyls, polybrominated dibenzo-p-dioxins, and polybrominated dibenzofurans as impurities in commercial polybrominated diphenyl ether mixtures. Environ Sci Technol 40(14):4400-5 doi:10.1021/es060559k

Hardesty JE, Al-Eryani L, Wahlang B, et al. (2018) Epidermal Growth Factor Receptor Signaling Disruption by Endocrine and Metabolic Disrupting Chemicals. Toxicol Sci 162(2):622-634 doi:10.1093/toxsci/kfy004

Ji K, Choi K, Giesy JP, Musarrat J, Takeda S (2011) Genotoxicity of several polybrominated diphenyl ethers (PBDEs) and hydroxylated PBDEs, and their mechanisms of toxicity. Environ Sci Technol 45(11):5003-8 doi:10.1021/es104344e

Joiakim A, Mathieu PA, Shelp C, Boerner J, Reiners JJ, Jr. (2016) Epidermal Growth Factor Receptor Kinase Inhibitors Synergize with TCDD to Induce CYP1A1/1A2 in Human Breast Epithelial MCF10A Cells. Drug Metab Dispos 44(5):665-71 doi:10.1124/dmd.115.066274

Jones-Otazo HA, Clarke JP, Diamond ML, et al. (2005) Is house dust the missing exposure pathway for PBDEs? An analysis of the urban fate and human exposure to PBDEs. Environ Sci Technol 39(14):5121-30 doi:10.1021/es048267b

Kim S, Thiessen PA, Bolton EE, et al. (2016) PubChem Substance and Compound databases. Nucleic Acids Res 44(D1):D1202-13 doi:10.1093/nar/gkv951

Kim UJ, Lee IS, Kim HS, Oh JE (2011) Monitoring of PBDEs concentration in umbilical cord blood and breast milk from Korean population and estimating the effects of various parameters on accumulation in humans. Chemosphere 85(3):487-93 doi:10.1016/j.chemosphere.2011.08.008

Koch K, Bartmann K, Hartmann J, et al. (2022) Scientific Validation of Human Neurosphere Assays for Developmental Neurotoxicity Evaluation. Front Toxicol 4:816370 doi:10.3389/ftox.2022.816370

Koike E, Yanagisawa R, Takigami H, Takano H (2014) Penta- and octa-bromodiphenyl ethers promote proinflammatory protein expression in human bronchial epithelial cells in vitro. Toxicol In Vitro 28(2):327-33 doi:10.1016/j.tiv.2013.10.014

Lin M, Ma S, Tang J, et al. (2023) Polybrominated diphenyl ethers and bromophenols in paired serum, hair, and urine samples of e-waste dismantlers: Insights into hair as an indicator

of endogenous exposure. Sci Total Environ 871:161980 doi:10.1016/j.scitotenv.2023.161980

Masjosthusmann S, Becker D, Petzuch B, et al. (2018) A transcriptome comparison of time-matched developing human, mouse and rat neural progenitor cells reveals human uniqueness. Toxicol Appl Pharmacol 354:40-55 doi:10.1016/j.taap.2018.05.009

Meerts IA, Letcher RJ, Hoving S, et al. (2001) In vitro estrogenicity of polybrominated diphenyl ethers, hydroxylated PDBEs, and polybrominated bisphenol A compounds. Environ Health Perspect 109(4):399-407 doi:10.1289/ehp.01109399

Miettinen PJ, Berger JE, Meneses J, et al. (1995) Epithelial immaturity and multiorgan failure in mice lacking epidermal growth factor receptor. Nature 376(6538):337-41 doi:10.1038/376337a0

Montalbano AM, Albano GD, Anzalone G, et al. (2020) Cytotoxic and genotoxic effects of the flame retardants (PBDE-47, PBDE-99 and PBDE-209) in human bronchial epithelial cells. Chemosphere 245:125600 doi:10.1016/j.chemosphere.2019.125600

Mundy WR, Freudenrich TM, Crofton KM, DeVito MJ (2004) Accumulation of PBDE-47 in primary cultures of rat neocortical cells. Toxicol Sci 82(1):164-9 doi:10.1093/toxsci/kfh239

Mutoh S, Sobhany M, Moore R, et al. (2013) Phenobarbital indirectly activates the constitutive active androstane receptor (CAR) by inhibition of epidermal growth factor receptor signaling. Sci Signal 6(274):ra31 doi:10.1126/scisignal.2003705

Peters AK, Nijmeijer S, Gradin K, et al. (2006) Interactions of polybrominated diphenyl ethers with the aryl hydrocarbon receptor pathway. Toxicol Sci 92(1):133-42 doi:10.1093/toxsci/kfj186

Ren M, Peng P, Cai Y, et al. (2011) PBDD/F impurities in some commercial deca-BDE. Environ Pollut 159(5):1375-80 doi:10.1016/j.envpol.2011.01.004

Rothhammer V, Quintana FJ (2019) The aryl hydrocarbon receptor: an environmental sensor integrating immune responses in health and disease. Nat Rev Immunol 19(3):184-197 doi:10.1038/s41577-019-0125-8

Schreiber T, Gassmann K, Gotz C, et al. (2010) Polybrominated diphenyl ethers induce developmental neurotoxicity in a human in vitro model: evidence for endocrine disruption. Environ Health Perspect 118(4):572-8 doi:10.1289/ehp.0901435

Sharkey M, Harrad S, Abou-Elwafa Abdallah M, Drage DS, Berresheim H (2020) Phasing-out of legacy brominated flame retardants: The UNEP Stockholm Convention and other legislative action worldwide. Environ Int 144:106041 doi:10.1016/j.envint.2020.106041

Sondermann NC, Fassbender S, Hartung F, et al. (2023) Functions of the aryl hydrocarbon receptor (AHR) beyond the canonical AHR/ARNT signaling pathway. Biochem Pharmacol 208:115371 doi:10.1016/j.bcp.2022.115371

Sondermann NC, Momin AA, Arold ST, Haarmann-Stemmann T (2024) Benzotriazole UV stabilizers disrupt epidermal growth factor receptor signaling in human cells. Environ Int 190:108886 doi:10.1016/j.envint.2024.108886

Stoll SW, Stuart PE, Lambert S, et al. (2016) Membrane-Tethered Intracellular Domain of Amphiregulin Promotes Keratinocyte Proliferation. J Invest Dermatol 136(2):444-452 doi:10.1016/j.jid.2015.10.061

Sueyoshi T, Li L, Wang H, et al. (2014) Flame retardant BDE-47 effectively activates nuclear receptor CAR in human primary hepatocytes. Toxicol Sci 137(2):292-302 doi:10.1093/toxsci/kft243

Sutter CH, Yin H, Li Y, et al. (2009) EGF receptor signaling blocks aryl hydrocarbon receptor-mediated transcription and cell differentiation in human epidermal keratinocytes. Proc Natl Acad Sci U S A 106(11):4266-71 doi:10.1073/pnas.0900874106

Ticiani E, Gingrich J, Pu Y, et al. (2021) Bisphenol S and Epidermal Growth Factor Receptor Signaling in Human Placental Cytotrophoblasts. Environ Health Perspect 129(2):27005 doi:10.1289/EHP7297

Viberg H, Fredriksson A, Jakobsson E, Orn U, Eriksson P (2003) Neurobehavioral derangements in adult mice receiving decabrominated diphenyl ether (PBDE 209) during a defined period of neonatal brain development. Toxicol Sci 76(1):112-20 doi:10.1093/toxsci/kfg210

Vogel CFA, Van Winkle LS, Esser C, Haarmann-Stemmann T (2020) The aryl hydrocarbon receptor as a target of environmental stressors - Implications for pollution mediated stress and inflammatory responses. Redox Biol 34:101530 doi:10.1016/j.redox.2020.101530

Vogeley C, Sondermann NC, Woeste S, et al. (2022) Unraveling the differential impact of PAHs and dioxin-like compounds on AKR1C3 reveals the EGFR extracellular domain as a critical determinant of the AHR response. Environ Int 158:106989 doi:10.1016/j.envint.2021.106989

Wahl M, Lahni B, Guenther R, et al. (2008) A technical mixture of 2,2',4,4'-tetrabromo diphenyl ether (BDE47) and brominated furans triggers aryl hydrocarbon receptor (AhR) mediated gene expression and toxicity. Chemosphere 73(2):209-15 doi:10.1016/j.chemosphere.2008.05.025

Wang F, Ruan XJ, Zhang HY (2015) BDE-99 (2,2',4,4',5-pentabromodiphenyl ether) triggers epithelial-mesenchymal transition in colorectal cancer cells via PI3K/Akt/Snail signaling pathway. Tumori 101(2):238-45 doi:10.5301/tj.5000229

Wu Z, He C, Han W, et al. (2020) Exposure pathways, levels and toxicity of polybrominated diphenyl ethers in humans: A review. Environ Res 187:109531 doi:10.1016/j.envres.2020.109531

Yang J, Zhu J, Chan KM (2016) BDE-99, but not BDE-47, is a transient aryl hydrocarbon receptor agonist in zebrafish liver cells. Toxicol Appl Pharmacol 305:203-215 doi:10.1016/j.taap.2016.06.023

Zhang F, Peng L, Huang Y, Lin X, Zhou L, Chen J (2019) Chronic BDE-47 Exposure Aggravates Malignant Phenotypes and Chemoresistance by Activating ERK Through ERalpha and GPR30 in Endometrial Carcinoma. Front Oncol 9:1079 doi:10.3389/fonc.2019.01079

Zota AR, Mitro SD, Robinson JF, et al. (2018) Polybrominated diphenyl ethers (PBDEs) and hydroxylated PBDE metabolites (OH-PBDEs) in maternal and fetal tissues, and

associations with fetal cytochrome P450 gene expression. Environ Int 112:269-278 doi:10.1016/j.envint.2017.12.030

Figure legends

Fig. 1: BDE-47 and BDE-99 do not induce XRE-dependent reporter gene activity, but increase AHR ligand-induced activation similar to EGFR-blocking antibody. A XRE-HepG2 cells were treated with 0.2 % DMSO, 1 µM B[a]P, BDE-47 or BDE-99 (1 µM and 10 µM). **B** Additionally, XRE-HepG2 cells were co-treated with 1 µM B[a]P and each PBDE (1 µM and 10 µM). Further, the cells were co-treated with 1 µM B[a]P and the EGFR ligand EGF (20 ng/ml) as well as the EGFR-blocking monoclonal antibody Cetuximab (10 µg/ml). AHR/XRE-dependent luciferase activity was determined after 24 h. n = 4. *, $p \leq 0.05$ compared to DMSO, #, $p \leq 0.05$ compared to B[a]P.

Fig. 2: Computational flexible docking analysis and assay validation predict that PBDEs interfere with the binding of EGF to the EGFR extracellular domain. A 2D representations of the tested PBDEs shown as sticks, taken from the PubChem website (https://pubchem.ncbi.nlm.nih.gov/). **B** *In silico* docking of EGFR and PBDEs. EGFR is shown as gray cartoon, while EGF is visualized as magenta backbone trace. PBDEs, shown in stick representation, are superimposed. Side chain and PBDE atoms are colored according to: blue, nitrogen; light red, oxygen; dark red, bromine. EGFR carbons are gray, BUV carbons are colored as following. **C** BDE-47 (orange). **D** BDE-99 (magenta). **E** BDE-47 and BDE-99 compete with EGF for binding of the EGFR extracellular domain. PBDEs influence on interaction of EGF with EGFR was examined with a cell-free EGF/EGFR AlphaLISA. n = 3. *, $p \leq 0.05$ compared to DMSO.

Fig. 3: BDE-47 and BDE-99 interfere with the ligand-induced phosphorylation of EGFR. HaCaT keratinocytes were serum-starved for 3 h and subsequently treated for 15 min with DMSO (0.1 %), EGF (20 ng/ml) alone, EGF in combination with the respective PBDE (1 µM), AREG (10 ng/ml)) alone and AREG in combination with the respective PBDE and the PBDE (1 µM) alone. GAPDH as loading control. **A** Treatment with BDE-47 (n = 3). Representative western blot. **B** Treatment with BDE-99 (n = 3). Representative western blot. *, $p \leq 0.05$ compared to EGF treatment. #, $p \leq 0.05$ compared to AREG treatment.

Fig. 4: BDE-47 and BDE-99 can interfere with AREG-induced DNA synthesis. Colorimetric BrdU incorporation assay to assess the influence of **A** BDE-47 and **B** BDE-99 on AREG-induced DNA synthesis in HaCaT-AHR-KO cells after 4 h treatment. n = 4-8. *, $p \leq 0.05$ compared to DMSO, #, $p \leq 0.05$ compared to AREG.

Figure 1

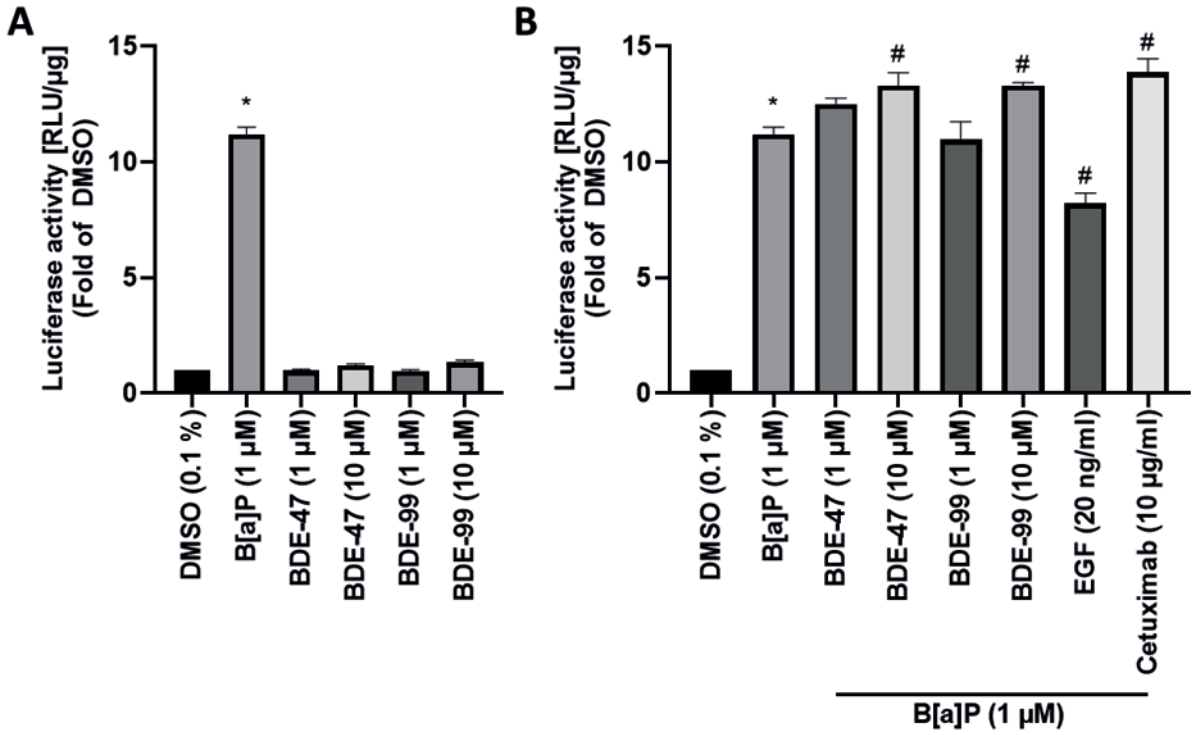
A
Luciferase activity [RLU/µg]
(Fold of DMSO)
15
10
5
0
*
DMSO (0.1 %)
B[a]P (1 µM)
BDE-47 (1 µM)
BDE-47 (10 µM)
BDE-99 (1 µM)
BDE-99 (10 µM)
B
Luciferase activity [RLU/µg]
(Fold of DMSO)
15
10
5
0
*
#
#
#
#
DMSO (0.1 %)
B[a]P (1 µM)
BDE-47 (1 µM)
BDE-47 (10 µM)
BDE-99 (1 µM)
BDE-99 (10 µM)
EGF (20 ng/ml)
Cetuximab (10 µg/ml)
B[a]P (1 µM)

Figure 2

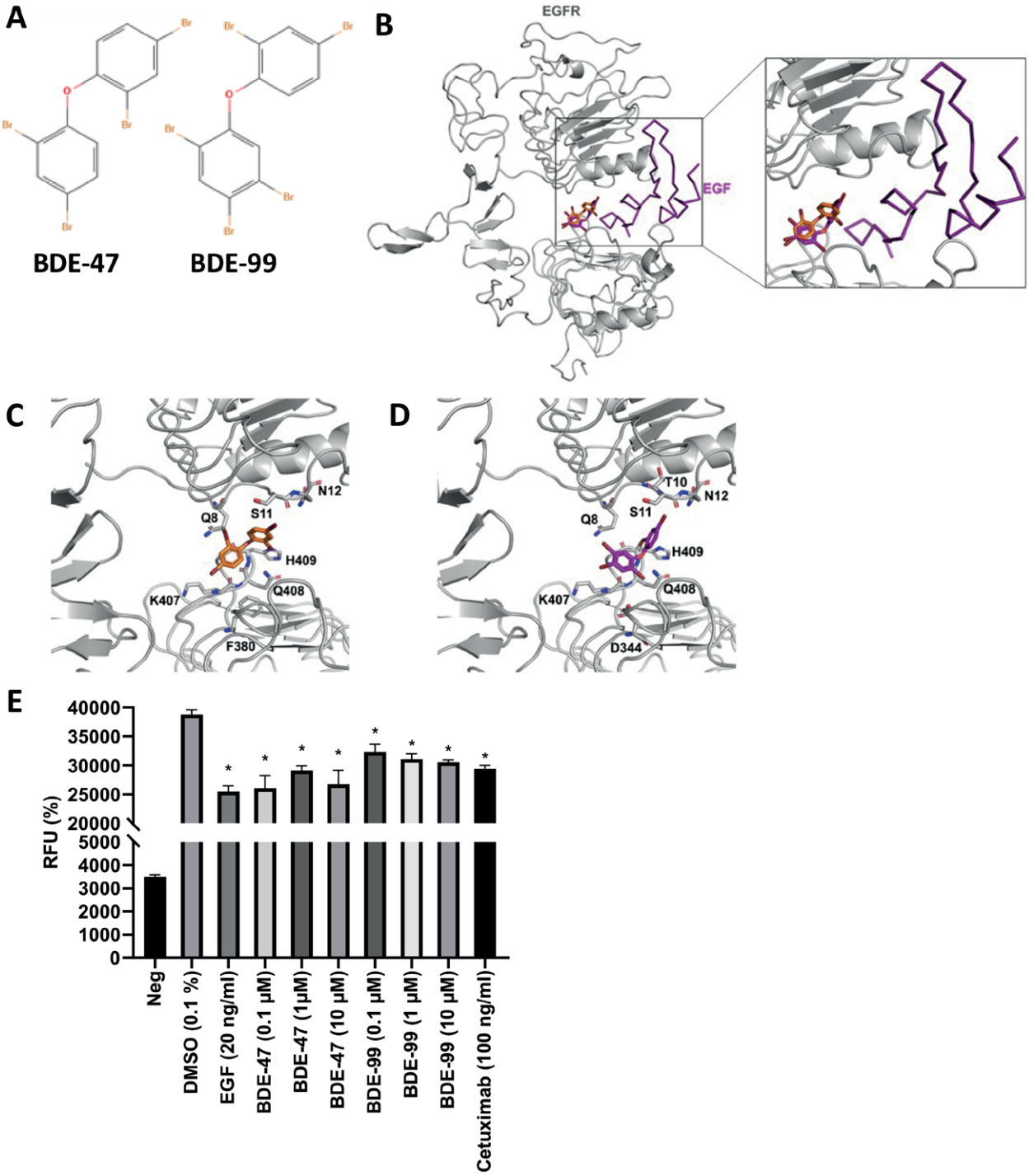
A
BDE-47
BDE-99
B
EGFR
EGF
C
N12
Q8
S11
H409
K407
Q408
F380
D
T10
N12
Q8
S11
H409
K407
Q408
D344
E
RFU (%)
40000
35000
30000
25000
20000
5000
4000
3000
2000
1000
0
Neg
DMSO (0.1 %)
EGF (20 ng/ml)
BDE-47 (0.1 µM)
BDE-47 (1µM)
BDE-47 (10 µM)
BDE-99 (0.1 µM)
BDE-99 (1 µM)
BDE-99 (10 µM)
Cetuximab (100 ng/ml)

Figure 3

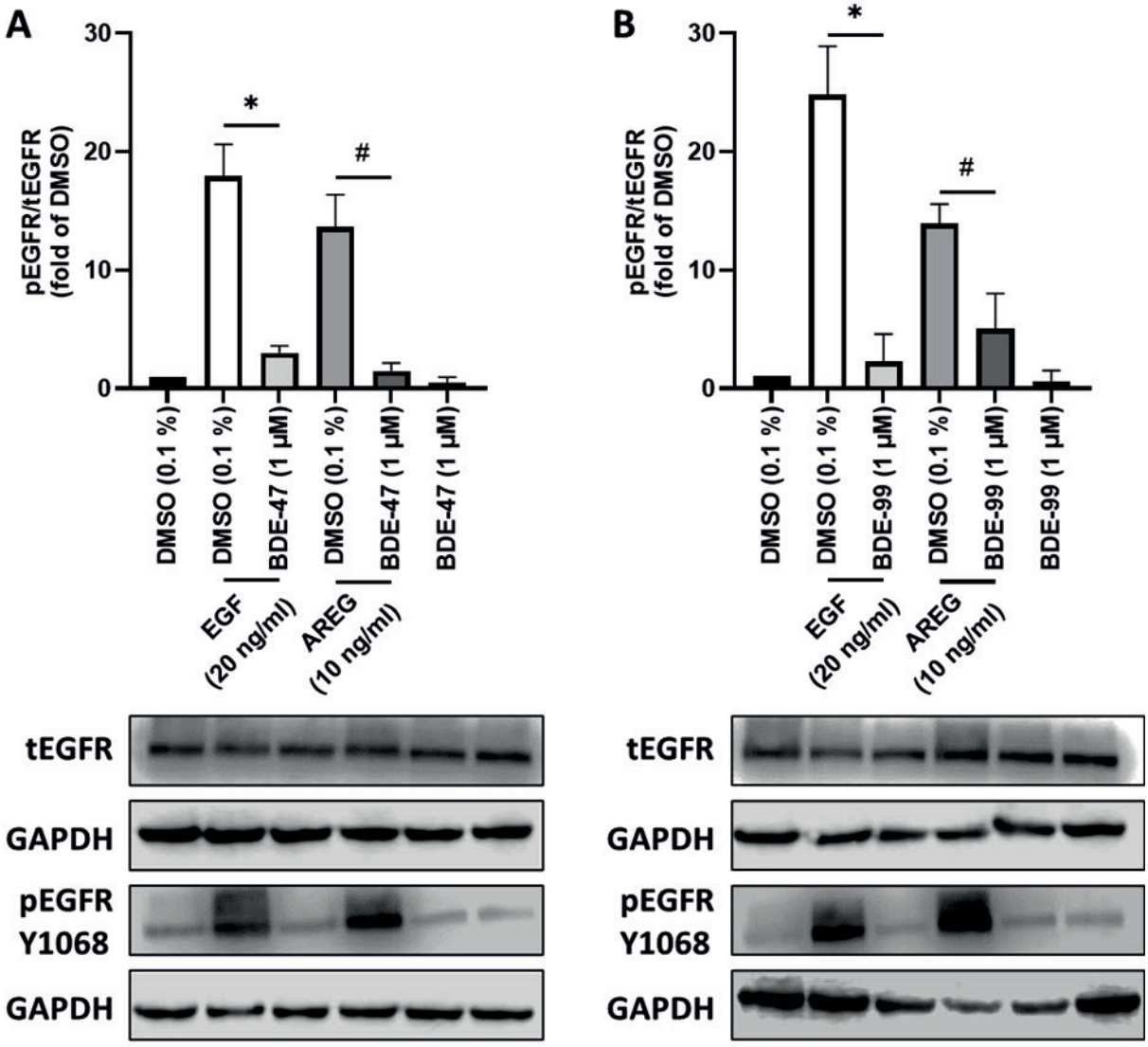
A
pEGFR/tEGFR (fold of DMSO)
30
20
10
0
*
#
DMSO (0.1 %)
DMSO (0.1 %)
BDE-47 (1 µM)
DMSO (0.1 %)
BDE-47 (1 µM)
BDE-47 (1 µM)
EGF (20 ng/ml)
AREG (10 ng/ml)
tEGFR
GAPDH
pEGFR Y1068
GAPDH
B
pEGFR/tEGFR (fold of DMSO)
30
20
10
0
*
#
DMSO (0.1 %)
DMSO (0.1 %)
BDE-99 (1 µM)
DMSO (0.1 %)
BDE-99 (1 µM)
BDE-99 (1 µM)
EGF (20 ng/ml)
AREG (10 ng/ml)
tEGFR
GAPDH
pEGFR Y1068
GAPDH

Figure 4

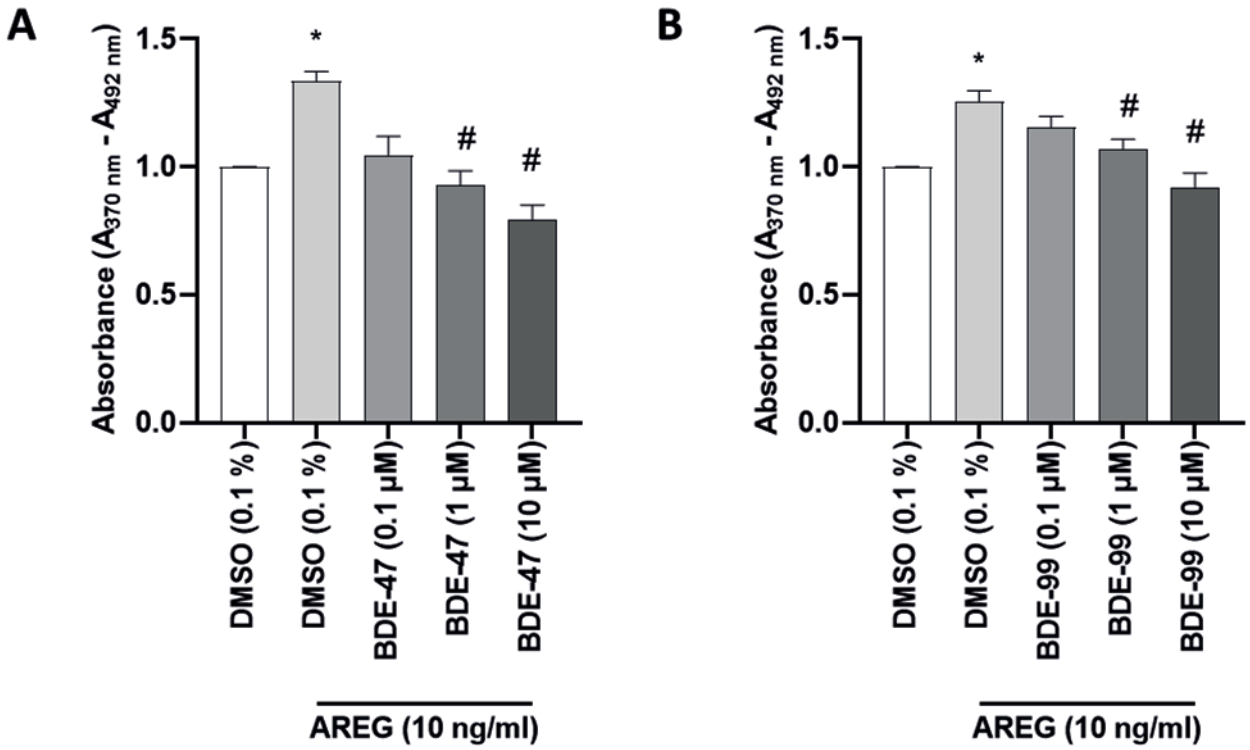
A
B
Absorbance (A370 nm - A492 nm)
1.5
1.0
0.5
0.0
*
#
#
DMSO (0.1 %)
DMSO (0.1 %)
BDE-47 (0.1 µM)
BDE-47 (1 µM)
BDE-47 (10 µM)
AREG (10 ng/ml)
DMSO (0.1 %)
DMSO (0.1 %)
BDE-99 (0.1 µM)
BDE-99 (1 µM)
BDE-99 (10 µM)
AREG (10 ng/ml)

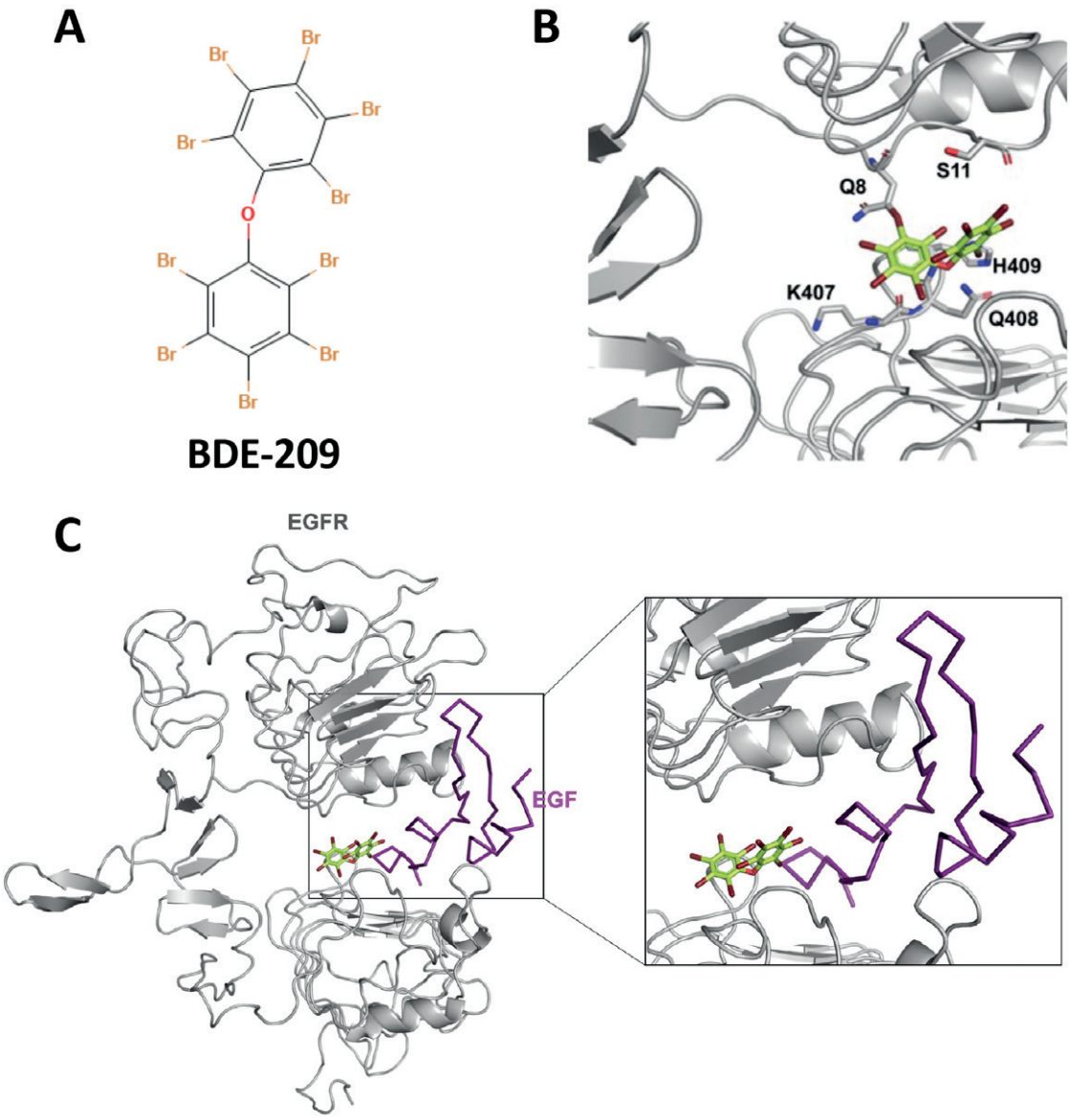

Supplementary figure 1: *In silico* docking analysis predicts that BDE-209 interferes with the binding of EGF to the EGFR extracellular domain. A 2D representation of BDE-209 shown as sticks, taken from the PubChem website (https://pubchem.ncbi.nlm.nih.gov/). PubChem ID is given. **B** The EGFR protein structure is shown as gray cartoon. Side chain and BDE-209 atoms are colored according to: blue, nitrogen; light red, oxygen; dark red, bromine. EGFR carbons are colored gray, and BUV carbons are colored as in panels. **C** *In silico* docking of EGFR and BDE-209. The EGFR protein structure is shown as gray cartoon. EGF is represented as magenta backbone trace. BDE-209, shown in stick representation, is superimposed.

3 Generelle Diskussion

3.1 Unterschiedliche Funktionsweise von PAKs und DLCs hinsichtlich des AHR-EGFR-Crosstalks

Umweltschadstoffe stellen einen großen Risikofaktor hinsichtlich der Entstehung und Entwicklung von Krankheiten dar. Als Rezeptor, der für die Interaktion mit Umweltschadstoffen verantwortlich ist, trägt der AHR einen maßgeblichen Anteil zur Entstehung und Entwicklung verschiedener Krankheiten und Störungen bei (Murray et al. 2014, Rothhammer und Quintana 2019). So ist beispielsweise bekannt, dass TCDD-induzierte gesundheitsschädliche Effekte über den AHR gesteuert werden, jedoch scheinen auch andere Signalwege hierbei eine Rolle zu spielen (Mimura und Fujii-Kuriyama 2003, Sorg 2014). Im Rahmen dieser kumulativen Dissertation konnte erstmals aufgezeigt werden, dass die direkte Bindung von AHR-Liganden und anderen POPs an den EGFR über Inhibition zu ebendiesen Effekten beitragen könnten. Die Mechanismen, welche zu diesen AHR- und EGFR-mediierten Unterschieden führen, hat unsere Arbeitsgruppe 2022 in einer Studie genauer untersucht (Vogeley et al. 2022). Dort haben wir herausgefunden, dass PAKs in humanen Keratinozyten eine biphasische EGFR-Aktivierung sowie Induktion des MAPK-Signalweges bewirken. Nach etwa 15 Minuten wurde dabei eine Phosphorylierung an der intrazellulären Phosphorylierungsstelle Y845 des EGFR festgestellt, welche vermutlich über das aus dem AHR-Komplex freigewordene Src reguliert wird. Eine weitere Phosphorylierung von EGFR und MEK/ERK wurde nach ca. 2 Stunden festgestellt, wobei hier das sogenannten *Ectodomain-Shedding* eine Rolle spielte, also die Freisetzung von membrangebundenen EGFR-Liganden über die Src-abhängige Aktivierung von PKC und Metalloproteinasen. Während PAKs nun EGFR-Phosphorylierung nach beiden Zeitpunkten induzierten, bewirkten DLCs diese lediglich nach 2 Stunden. Des Weiteren

konnten wir in dieser Studie zeigen, dass TCDD, PCB126 und weitere DLCs eine inhibierende Wirkung auf den EGFR und nachgeschaltete Signalwege haben, während *in silico*-Dockinganalysen eine direkte Bindung verschiedener DLCs an die EGFR ECD vorhersagten. Für die PAKs BaP und Benzo[k]fluoranthen hingegen konnten diese inhibierenden Effekte nicht beobachtet werden, wobei auch *in silico*-Dockinganalysen keine Bindung von BaP an die EGFR ECD voraussagten, da es vermutlich aufgrund seiner weniger flexiblen Struktur und Größe keine passende Position einnehmen kann (Vogeley et al. 2022).

Während der AHR bereits seit Jahrzehnten als Rezeptor für Umweltschadstoffe bekannt ist, wurde die mögliche Rolle des EGFR als direkte Zielstruktur für verschiedene Umweltschadstoffe an der Zelloberfläche erst in den letzten Jahren aufgedeckt (Hardesty et al. 2018, Ticiani et al. 2021, Vogeley et al. 2022, Ticiani et al. 2023, Sondermann et al. 2024). Unter diesen Umweltschadstoffen sind auch TCDD und PCB126, welche sowohl AHR-Agonist als auch allosterischer Inhibitor des EGFR zu sein scheinen. RNA-Sequenzierungen konnten zeigen, dass eine Behandlung mit BaP oder PCB126 in humanen Keratinozyten zu unterschiedlichen Genexpressionsmustern führte. Zudem wurde beobachtet, dass eine Behandlung mit PCB126 und eine Co-Behandlung von BaP plus EGFR-Inhibitor PD153035 mehr Übereinstimmungen in den von ihnen regulierten Genen aufwiesen (190 Gene), als PCB126 vs. BaP allein (129 Gene) (Vogeley et al. 2022). Dies spricht nicht nur für die Rolle von PCB126 als AHR-Agonist mit inhibitorischem Effekt auf den EGFR, sondern rückt auch die Bedeutung der EGFR-Expression in liganden- und zelltypspezifischen Auswirkungen von Dioxinen und DLCs (Safe et al. 2020) in den Fokus.

Zwar sind Dioxine und PCBs durch ihre anhaltende AHR-Aktivierung als Karzinogene und Tumorpromotoren anerkannt, doch diese Effekte sind nicht auf jeden Zelltyp

übertragbar (Murray et al. 2014). Es gibt Studien, die darauf hinweisen, dass TCDD einen Tumor-inhibierenden Effekt haben kann. So zeigten Holocomb und Safe, dass eine zweijährige tägliche orale Aufnahme nicht-toxischer Dosen TCDD (10 µg/kg; entspricht ca. 31,1 nM) in Ratten mit Brustkarzinom zu einer signifikanten Verminderung des Tumorvolumens führte (Holcomb und Safe 1994). Hinzu kommen Studien in humanen Keratinozyten, die zeigten, dass TCDD die Bindung von EGF an den EGFR unterdrücken konnte, wobei auch die EGF-induzierte DNA-Synthese inhibiert wurde (Hudson et al. 1985). Bei Versuchen in der Rattenleber wurde durch einmalige TCDD-Gabe (intraperitoneal, 115 µg/kg, entspricht ca. 357 nM) eine über 40 Tage andauernde Unterdrückung der Bindung von EGF and den EGFR beobachtet (Madhukar et al. 1984). Weitere Rattenstudien konnten eine durch TCDD vermittelte Abnahme der Bindung von EGF an den EGFR beobachten (Astroff et al. 1990, Dickerson et al. 1992). Im Rahmen dieser Arbeit wurde bei einmaliger TCDD-Behandlung von humanen AHR-defizienten HaCaT Keratinozyten bei 100 nM bereits ein signifikant inhibierender Effekt auf die AREG-induzierte DNA-Synthese sowie eine Verminderung der EGF-induzierten EGFR-Internalisierung, zwei für die Zellproliferation relevante Ereignisse, beobachtet (Vogeley et al. 2022).

Darüber hinaus beschrieben Kerkvliet und Kimeldorf, dass sowohl eine Vor- als auch eine Nachbehandlung von Ratten, denen Rattenbrustkarzinomzellen (Walker 256) transplantiert wurden, mit dem PCB-Gemisch Aroclor 1254 das Tumorwachstum verlangsamte und die Überlebenszeit der Tiere verlängerte. Während alle Kontrolltiere eine fortlaufende Tumorprogression aufwiesen, erlebten 25 % der PCB-behandelten Tiere sogar eine vollständige Tumorregression (Kerkvliet und Kimeldorf 1977). Im Rahmen der vorliegenden Dissertation wurde auch die Auswirkung von Aroclor 1254 auf die EGFR-Liganden-aktivierte DNA-Synthese in einer Co-Behandlung von AHR-

defizienten HaCaT Keratinozyten untersucht, wobei eine inhibierende Wirkung bei Konzentrationen ab 10 nM festgestellt wurde (nicht publizierte Daten, Anhang I). Ebenfalls wurde im Rahmen dieser Arbeit ein signifikant inhibierender Effekt auf die Liganden-induzierte Phosphorylierung und Internalisierung des EGFR sowie die Liganden-induzierte DNA-Synthese bei Behandlung von HaCaT Keratinozyten mit PCB 126 festgestellt. Des Weiteren konnte in dieser Arbeit eine signifikante Inhibierung auf die Liganden-vermittelte EGFR-Phosphorylierung sowie DNA-Synthese durch eine Behandlung von HaCaT Keratinozyten mit PCB 118 festgestellt werden. Darüber hinaus ergaben *in silico* Dockinganalysen eine Bindung von PCB 126, PCB 118, PCB 77 und dem nicht-dioxinähnlichen PCB 47 an die EGFR ECD, wobei alle Moleküle eine ähnliche Position einnahmen. Diese Bindestelle wurde mithilfe von punktmutierten Plasmiden und Western Blot Analysen experimentell überprüft, wobei sich die Aminosäuren Q8 und Q408 als essentiell für die inhibierenden Effekte von PCB 126 auf die EGF-induzierte EGFR-Phosphorylierung erwiesen (Vogeley et al. 2022).

In Versuchen mit einer Brustkrebszelllinie inhibierte TCDD das Zellwachstum, wobei eine Behandlung mit einem EGFR-Antikörper diesen Effekt aufheben konnte (Wang et al. 1997). Kociba und Kollegen stellten in einer zweijährigen chronischen TCDD-Belastungsstudie in Ratten fest, dass manche Organe gehäuft Tumore aufwiesen, darunter Leber und Lunge. Andere Tumortypen traten hingegen signifikant seltener als in der Kontrollgruppe auf, z.B. in weiblichen Ratten Tumore des endokrinen Systems und in männlichen Ratten Tumore des Pankreas (Kociba et al. 1978). Pankreastumore weisen häufig eine Überexpression des EGFR und seiner Liganden EGF und TGFA auf (Korc et al. 1992), deren Bindung an den EGFR über eine TCDD-Behandlung vermindert werden kann (Vogeley et al. 2022). Versuche in Brustkrebszellen zeigten,

dass TCDD und verschiedene PCBs deren Liganden-induzierte Proliferation hemmten (Oenga et al. 2004). Eine mögliche Erklärung für diese Beobachtungen könnte die EGFR-inhibierende Wirkung von Dioxinen und DLCs sein, welche das Binden bekannter Wachstumsfaktoren an den Rezeptor verhindern, wie es in dieser kumulativen Dissertation erstmals mechanistisch über eine Punktmutation in der EGFR ECD *in vitro* nachgewiesen wurde (Vogeley et al. 2022). Interessanterweise ist bekannt, dass der EGFR zumindest in Glioblastomen nicht nur als Onkogen, sondern als Tumorsuppressor wirken kann, indem das invasive Wachstum inhibiert wird. Dies wird dadurch erklärt, dass der konstitutiv aktivierte EGFR und der Liganden-aktivierte EGFR unterschiedliche Effekte haben. Während der konstitutiv aktivierte EGFR im Glioblastom zu einer vermehrten Invasion über *Epithelial Membrane Protein 1* führt, resultiert die Aktivierung des EGFR durch Liganden in einer vermehrten Proliferation über ERK1/2. Als Resultat liegt ein hyperproliferierender Tumor vor, der nicht weiter invasiv wächst, wodurch die Überlebenschance von Patienten gesteigert wird (Beytagh und Weiss 2022, Guo et al. 2022). Somit könnte der paradoxe Effekt von TCDD in der Tumorprogression je nach Gewebe auch damit zusammenhängen, dass der EGFR einerseits über AHR-gesteuerte Wege intrazellulär über Src aktiviert wird (Sondermann et al. 2023), andererseits jedoch auch das extrazelluläre Binden seiner Liganden durch TCDD allosterisch gehemmt wird (Hardesty et al. 2018, Vogeley et al. 2022). Des Weiteren könnte es eine Rolle spielen, wie stark der EGFR und seine Dimerisierungspartner im jeweiligen Zelltyp vertreten sind und welche weiteren Faktoren die Expression seiner Liganden regulieren. Wie komplex das spezifische Anvisieren des EGFR als therapeutisches Ziel ist, zeigen beispielsweise die Nebenwirkungen oder auch die Resistenz, welche noch während der Therapie gegen ein Medikament entstehen kann (Uribe et al. 2021). Cetuximab, einer der

monoklonalen EGFR-Antikörper aus der Krebstherapie, führt häufig zu kutanen Nebenwirkungen, darunter trockene juckende Haut (Xerose) und ein papulopustulöser Ausschlag, welcher das Gesicht und den Oberkörper betrifft (Lacouture 2006). Interessanterweise kann eine akute oder chronische TCDD-Intoxikation zu ähnlichen Symptomen in der Haut führen wie eine EGFR-Inhibierung. So wird ein von Dioxinen und DLCs verursachter papulopustulöser Ausschlag, welcher vornehmlich im Gesicht und am Oberkörper auftritt, Chlorakne genannt (Passarini et al. 2010). Es steht zumindest die Vermutung im Raum, dass diese Dioxin-induzierter Hauttoxizität über den EGFR gesteuert werden könnte, da einige Dioxin-Effekte denen von EGF in der murinen Entwicklung ähneln, wie z.B. ein verfrühtes Öffnen der Augen, der Verlust von Körpergewicht oder epitheliale Hyperplasie (Moore et al. 1986, Gray et al. 1997, Panteleyev und Bickers 2006). Doch neben der AHR-initiierten EGFR-Aktivierung könnte auch eine EGFR-Inhibierung ursächlich für die kutanen Symptome sein, da sie denen einer EGFR-Inhibitor-Therapie ähneln. EGFR-Inhibition nimmt direkten Einfluss auf das Signaling in Keratinozyten, in welchen dann eine Abnahme der Proliferation und eine Zunahme der Differenzierung beobachtet werden kann (Joly-Tonetti et al. 2021). Studien in humanen Keratinozyten-basierten Hautmodellen zeigten, dass auch eine Behandlung mit TCDD zu einem verfrühten Einsatz der Differenzierung führt (Loertscher et al. 2001, Forrester et al. 2014). Dass die Entwicklung von Chlorakne oder Veränderungen im Differenzierungsprofil von Keratinozyten nicht durch andere prominente AHR-Liganden, wie PAKs, induziert wird (Forrester et al. 2014), spricht zudem dafür, dass dieser Mechanismus nicht ausschließlich über den AHR reguliert wird. Das weitere Aufschlüsseln des komplexen und teilweise paradox erscheinenden Mechanismus, über welchen z.B. TCDD seine scheinbar AHR- sowie EGFR-

abhängigen Auswirkungen im Organismus steuert, ist auch für andere strukturell verwandte organische Umweltschadstoffe von Interesse.

In einer französischen Kohortenstudie mit knapp 64.000 Frauen, welche den Zeitraum von 1993 bis 2008 untersucht, wurde der Zusammenhang von nahrungsbedingter Dioxinexposition und dem Auftreten von Brustkrebs untersucht. Tatsächlich stellten sie fest, dass bei erhöhter Dioxinexposition unter post-menopausalen Frauen eine Abnahme der Fälle von Östrogenrezeptor (*estrogen receptor*, ER)- und Progesteronrezeptor (PR)-negativem Brustkrebs auftrat (Danjou et al. 2015). In einer dänischen Studie mit ca. 30.000 Teilnehmerinnen fand man heraus, dass ein höherer Anteil von diversen Organochlorverbindungen im Fettgewebe post-menopausaler Frauen mit einem niedrigeren Risiko für ER-negativen Brustkrebs in Zusammenhang stand (Raaschou-Nielsen et al. 2005). Ebenfalls beobachteten Gammon et al. ein niedrigeres Risiko für ER- und PR-negativen Brustkrebs bei höherer Konzentration von PCBs im Blutserum von Frauen (Gammon et al. 2002). In ER- und PR-negativem Brustkrebs ist häufig eine Überexpression von EGFR und ErbB2 zu beobachten (Vranic et al. 2010). Somit könnte die negative Korrelation zwischen erhöhter Aufnahme von Dioxinen und DLCs zum Auftreten von ER/PR-negativem Brustkrebs möglicherweise zum Teil über eine Inhibierung des EGFR zu erklären sein.

Ayotte et al. führten Untersuchungen von 40 Anwohnern, welche regelmäßig lokal gefangenen Fisch aßen, entlang der Küstenregion von Québec durch. Unter anderem bestimmten sie die Plasmakonzentration verschiedener PCBs, wobei der durchschnittliche gesamte PCB-Gehalt bei 18 µg/l (ca. 50 nM) lag und der höchste Messwert 61 µg/l (ca. 169 nM) betrug. Zudem konnten sie auch weitere chlorierte Pestizide im Blutserum nachweisen, darunter auch DLCs (Ayotte et al. 2005). Die PCB-Konzentration im Blut von Arbeitern, die aufgrund der Exposition am Arbeitsplatz

Chlorakne entwickelt haben, lag bei 88 µg/l (ca. 244 nM) bis hin zu 1359 µg/l (ca. 3,77 µM) (Maroni et al. 1984). Diese besonders exponierten Menschen, sei es über bestimmte Nahrung oder den Arbeitsplatz, erreichen somit in ihrem Blutserum Konzentrationen, welche signifikant inhibierende Auswirkungen auf den EGFR und die AREG-induzierte DNA-Synthese haben. Im Rahmen dieser Arbeit führte eine Konzentration von 100 nM PCB 126 bei einmaliger Behandlung von HaCaT Keratinozyten bereits zu einer signifikanten EGF-induzierten EGFR-Internalisierung. Darüber hinaus erzielten 1 µM eine signifikante Inhibierung auf mehrere Liganden-induzierte EGFR-Prozesse, wie die Phosphorylierung des Rezeptors und der DNA-Synthese (Vogeley et al. 2022). Die in dieser Arbeit gewonnenen Erkenntnisse könnten somit auch zum Verständnis der Entwicklung bestimmter Krankheiten beitragen oder neue präventive Ansätze liefern.

3.2 Interaktion von BUVs mit der EGFR ECD sowie deren Auswirkungen auf nachgeschaltete Signalwege

Im weiteren Verlauf dieser Arbeit konnte gezeigt werden, dass nicht nur Dioxine und DLCs als organische Umweltschadstoffe eine direkte Bindung an die EGFR ECD vornehmen, sondern auch einige BUVs (Sondermann et al. 2024). Dabei schienen besonders die getesteten chlorierten BUVs, UV-326 und UV-327, stärkere inhibierende Effekte auf den Rezeptor und EGFR-abhängige zelluläre Prozesse auszuwirken. Weitere im Rahmen dieser Arbeit getestete Umweltkontaminanten, wie z.B. die Pestizide DTT, Atrazin und Bifenox, zeigten keine oder nur in hohen, im Hinblick auf die Allgemeinbevölkerung nicht expositionsrelevanten Konzentrationen, inhibitorische Effekte auf EGFR-abhängige Prozesse, und wurden daher im weiteren Verlauf nicht näher untersucht (nicht publizierte Daten, Anhang I).

Für UV-326 und UV-327 ist bekannt, dass sie weder agonistische noch antagonistische Effekte auf den humanen Östrogen-, Androgen- oder Schilddrüsenhormonrezeptor haben (Nagayoshi et al. 2015, Sakuragi et al. 2021). Da sie keine Auswirkungen auf Steroidhormonrezeptoren zu haben scheinen, ist es auf Basis der in dieser Arbeit vorgestellten Ergebnisse naheliegend, dass sie ihre Wirkung stattdessen über Beeinflussung der zellulären Wachstumsfaktoren-gesteuerten EGFR-Signalwege erzielen. Dadurch, dass keine akut toxischen Effekte von BUVs im Menschen bekannt sind (Khare et al. 2023), könnten die hier getesteten Substanzen womöglich als strukturelle Vorlagen für die Entwicklung neuer niedermolekularer allosterischer EGFR-Inhibitoren dienen. Beispielsweise entdeckte erst 2020 die Gruppe um Yao herum mit DPBA einen neuartigen EGFR-Liganden, der an die EGFR ECD bindet, die Degradierung des Rezeptors initiiert und das Tumorwachstum in nicht-kleinzelligem Lungenkrebs sowohl *in vitro* in humanen Zellen als auch *in vivo* in Mäusen inhibiert (Yao et al. 2020). Im Rahmen dieser Arbeit erzielten die BUVs UV-326, UV-327 und UV-350 in verschiedenen Konzentrationen inhibierende Wirkungen auf die Liganden-induzierten Prozesse der EGFR- und ERK1/2-Phosphorylierung, EGFR-Internalisierung sowie DNA-Synthese. Darüber hinaus ergaben *in* silico Dockinganalysen eine mögliche Bindung aller BUVs in ähnlicher Position. Für UV-327 wurde diese Bindestelle experimentell mithilfe eines punktmutierten Plasmids und Western Blot Analyse in humanen HepG2 Zellen untersucht. Dabei konnte Aminosäure Q8 der EGFR ECD als essentiell für die inhibierende Wirkung von UV-327 auf die EGF-induzierte EGFR-Phosphorylierung bestätigt werden (Sondermann et al. 2024).

Eine Belastung des Menschen mit BUVs konnte bereits über Proben aus menschlichem Fettgewebe (ECHA 2015) und Muttermilch (Kim et al. 2019, Liu et al.

2022) nachgewiesen werden. Eine Studie aus Südkorea zeigte außerdem einen Zusammenhang zwischen der BUV-Konzentration in Muttermilch, welche auf eine bereits während der Schwangerschaft bestehende BUV-Exposition hindeuten kann, und einem niedrigeren Gestationsalter bei Entbindung (Lee et al. 2015), wie es bereits für DLCs (Fein et al. 1984, Vafeiadi et al. 2014) und Bisphenole (Aung et al. 2019, Huang et al. 2019) bekannt ist – eben jene POPs, welche auch mit der ECD EGFR interagieren (Hardesty et al. 2018, Ticiani et al. 2021, Vogeley et al. 2022, Ticiani et al. 2023). Darüber hinaus erfolgt auch nach der Geburt womöglich eine Weitergabe von BUVs durch die Mutter an den Säugling. Geht man davon aus, dass Muttermilch einen Fettgehalt von 4 % hat, so wären die höchsten gemessenen Werte in Muttermilch für UV-328 (5,2 nM) und UV-326 (8,1 nM) (Lee et al. 2015) nah an den Konzentrationen, welche im Rahmen der hier vorliegenden Arbeit bereits Effekte auf die EGFR-Aktivität hatten. So erzielten bereits 10 nM UV-326 sowie 10 nM UV-327 eine signifikante Reduktion der EGF-induzierten EGFR-Internalisierung in humanen HaCaT Keratinozyten (Sondermann et al. 2024), was sich auf nachgeschaltete zelluläre Prozesse bzw. die Gewebshomöostase auswirken könnte.

Zudem ist der EGFR essentiell für die embryonale Entwicklung (Miettinen et al. 1999, Butte und Heinzow 2002) sowie die postnatale Proliferation und Differenzierung neuronaler Zellen (Sibilia et al. 1998, Abdi et al. 2019). Demnach könnten BUVs womöglich auch im Menschen und Wildtieren neurotoxische Effekte über den stark evolutionär konservierten EGFR (Bogdan und Klambt 2001) hervorrufen, wie es bereits in Knochenfischen beobachtet wurde (Li et al. 2024).

3.3 Auswirkungen von PBDEs auf die Liganden-induzierte EGFR-Aktivierung sowie die EGFR-gesteuerte transkriptionelle Aktivität des AHR

Auch die im großen Maßstab als Flammschutzmittel eingesetzten PBDEs wurden in zahlreichen menschlichen Proben gefunden, darunter sowohl fetale als auch adulte Gewebe, Blut, Urin, Haare und Muttermilch (Kim et al. 2011, Bjermo et al. 2017, Zota et al. 2018, Lin et al. 2023). Eine direkte Interaktion der PBDEs BDE-47 und BDE-99 mit der EGFR ECD konnte sowohl *in silico* als auch in einem zellfreien AlphaLISA-Assay erstmalig beobachtet werden. Darüber hinaus bewirkten beide PBDEs eine signifikante Inhibierung der durch AREG oder EGF induzierten EGFR-Phosphorylierung sowie der AREG-induzierten DNA-Synthese. Außerdem konnte im Rahmen dieser Arbeit zum ersten Mal mithilfe eines Luziferase-basierten XRE-Reportergen-Assays eine verstärkende Wirkung beider PBDEs auf die BaP-induzierte transkriptionelle Aktivität des AHR beobachtet werden. So führte eine Co-Behandlung der Reportergen-Zelllinie mit BDE-47 und BaP oder BDE-99 und BaP zu einer signifikant stärkeren transkriptionellen AHR-Aktivität als eine Einzelbehandlung mit BaP. Dieser verstärkende Effekt wurde ebenso für eine Co-Behandlung der Zellen mit BaP und dem EGFR-Inhibitor PD 153035 beobachtet. Zudem konnte durch eine Einzelbehandlung der Reportergen-Zelllinie mit BDE-47 und BDE-99 die Kontamination der verwendeten PBDEs mit AHR-Agonisten ausgeschlossen werden, da sie keine transkriptionelle AHR-Aktivität induzierten (Manuskript 2.4). Bisher ist die Studienlage zu den Auswirkungen von PBDEs auf den EGFR und seine Signalwege überschaubar. So zeigten Zhang et al., dass BDE-47 in Gebärmutterkrebszellen zur Phosphorylierung des ER-α, EGFR sowie ERK führt und so die Tumorprogression fördert (Zhang et al. 2019). In kolorektalen Krebszellen führte BDE-99 über eine Aktivierung des PI3K/AKT-Signalweges zur Epithelial-mesenchymale Transition, wobei die EGFR-Phosphorylierung hier nicht untersucht wurde (Wang et al. 2015).

Neben einer direkten Aktivierung des EGFR oder dem Rezeptor nachgeschalteten Signalmolekülen könnte auch der AHR hier eine Rolle spielen. So gibt es einige wenige Publikationen, die agonistische Effekte von manchen PBDEs auf den AHR beschreiben (Chen und Bunce 2003, Peters et al. 2006, Yang et al. 2016). Eine Erklärung dafür könnte jedoch auch die häufig auffindbare Dioxin-Kontamination in PBDEs sein (Hanari et al. 2006, Wahl et al. 2008, Ren et al. 2011). Diese Kontamination mit AHR-Liganden könnten zudem über den nicht-kanonischen AHR-Signalweg zu einer EGFR-Aktivierung führen (Sondermann et al. 2023). Insbesondere in Krebsarten, bei denen der EGFR konstitutiv aktiv oder überproliferiert vorliegt, ist es vorstellbar, dass die EGFR-inhibierenden Effekte von Dioxinen womöglich den AHR-vermittelten EGFR-aktivierenden Effekten unterliegen. In neuronalen Vorläuferzellen wurde z.B. beobachtet, dass der EGFR-Inhibitor PD153035 deren Migration reduziert (Masjosthusmann et al. 2018). Untersuchungen derselben Arbeitsgruppe zeigten auch, dass BDE-47 und BDE-99 die Migration dieser Zellen vermindert (Schreiber et al. 2010). Dies lässt in Zusammenhang mit den hier gezeigten Daten (Manuskript 2.4) vermuten, dass die PBDE-induzierte Reduktion der Migration über eine Bindung und Inhibierung des EGFR zu erklären sein könnte.

Eine Behandlung humaner Hepatozyten mit BDE-47 induzierte eine C*onstitutive Androstane Receptor* (CAR)-gesteuerte Zunahme der CYP2B10-Expression (Sueyoshi et al. 2014). Das Sedativum Phenobarbital kann über eine Inhibierung des EGFR durch direkte Bindung an dessen ECD ebenfalls zu einer Aktivierung von CAR führen (Mutoh et al. 2013), was vermuten lässt, dass auch die BDE-47-induzierte CAR-Aktivierung über eine EGFR-Inhibierung läuft. Ebenso zeigten Sutter et al., dass eine EGFR-Aktivierung die Dioxin-induzierte CYP1-Expression vermindert. Dieser Mechanismus soll über die Histon-Acetyltransferase p300, einen Co-Aktivator der

CYP1A1-Enhancer-Region, gesteuert werden. Die Aktivierung des EGFR über Liganden inhibiert die Rekrutierung von p300 als Co-Aktivator und die CYP1A1-Expression wird so vermindert. Dementsprechend führte eine Überexpression von p300 weitestgehend zur Aufhebung des EGF-induzierten Effekts (Sutter et al. 2009). Eine weitere EGFR-gesteuerte Modulation des AHR-Signalweges wurde in einer humanen Brustepithelzelllinie beobachtet, in der eine EGFR-Inhibierung die Dioxin-induzierte CYP1-Expression steigerte (Joiakim et al. 2016). So ist es vorstellbar, dass auch die in dieser Arbeit beobachteten verstärkenden Effekte von BDE-47 und BDE-99 auf die Liganden-induzierte transkriptionelle Aktivität des AHR (Manuskript 2.4) über deren Bindung an den EGFR und die darauffolgende Aktivierung von CAR gesteuert sind.

Erst Anfang 2024 hat die Europäische Behörde für Lebensmittelsicherheit eine umfängliche Risikobewertung zu PBDEs veröffentlicht, wobei sie aufgrund vieler Unsicherheiten zu dem Entschluss kam, dass die aktuelle ernährungsbedingte Exposition der Bevölkerung Europas gegenüber PBDEs gesundheitlich bedenklich sein könnte. Ein TDI-Wert, also eine lebenslang duldbare tägliche Aufnahme, wurde für PBDEs bisher noch nicht bestimmt. Die Französische Agentur für Nahrungssicherheit nutzte bei ihrer Risikobewertung den TDI-Wert, welcher für nicht-doxinähnliche PCBs festgelegt wurde und bei 10 ng/kg liegt (EFSA et al. 2024). Nun kann ein Säugling über die Muttermilch täglich bis zu 4 µg/kg PBDEs aufnehmen, was ca. einer Exposition von 8 nM entspricht (Jones-Otazo et al. 2005). Da diese Substanzen sich *in vivo* im Menschen in Abhängigkeit vom Gewebe anreichern können, ist es möglich, dass sie sich in ihrer Konzentration nochmal um ein Vielfaches steigern. Dabei könnten menschliche Säuglinge beispielsweise im Gehirn Konzentrationen von 0,5 – 1,1 µM PBDEs erreichen (Viberg et al. 2003, Schreiber et

al. 2010). Diese Konzentrationen bewegen sich bereits in dem Bereich, in welchem auch im Rahmen dieser Dissertation bereits bei 1 µM BDE-47 und 1 µM BDE-99 eine signifikante Inhibierung der EGFR-Phosphorylierung und AREG-induzierter DNA-Synthese beobachtet wurde (Manuskript 2.4).

3.4 Fazit und Ausblick

Die im Rahmen meiner kumulativen Dissertation vorgestellten und diskutierten Ergebnisse unterstreichen das komplexe Zusammenspiel zwischen AHR- und EGFR-abhängigen Signalwegen und deren Relevanz für patho-/physiologische Vorgänge. Dabei kann die jeweilige Aktivierung oder Inhibierung eines der beiden Moleküle die Signalantwort des anderen beeinflussen. Insbesondere bei Mischungsexpositionen mit Umweltschadstoffen, die einerseits AHR-aktivierende und andererseits EGFR-inhibierende Wirkung zeigen, sollte diese komplexe Interaktion von Signalwegen bedacht werden, um die daraus hervorgehenden Risiken, z.B. am Arbeitsplatz, besser einzuschätzen.

Zusammenfassend wurde die EGFR ECD in dieser Arbeit erstmalig *in vitro* als direkter Interaktionspartner für verschiedene organische Umweltschadstoffe nachgewiesen, die für die Allgemeinbevölkerung von hoher Expositionsrelevanz sind. Die vorliegende Arbeit konnte darüber hinaus zum besseren mechanistischem Verständnis AHR Liganden-spezifischer Effekte beitragen, indem die unterschiedlichen Wirkungen von PAKs und Dioxinen sowie DLCs auf den EGFR aufgedeckt wurden. So könnte nicht nur die AHR-vermittelte Aktivierung des EGFR über Src oder Transkription von EGFR-Liganden eine Rolle in der Signalantwort spielen, sondern auch die inhibierende Wirkung von DLCs auf den EGFR. Darüber hinaus wurden weitere Umweltschadstoffe identifiziert, die den AHR zwar nicht aktivieren, jedoch die transkriptionelle Aktivität des

AHR, vermutlich über EGFR-Inhibierung, zusätzlich verstärken können. Die Substanzen, welche hier ihre inhibierende Wirkung auf den EGFR zeigten, könnten als strukturelle Vorlagen für die Entwicklung weiterer niedermolekularer EGFR-Inhibitoren dienen. Dies wäre in erster Linie für Tumore mit einer Überexpression von EGFR und/oder EGFR-Liganden von Interesse. Darüber hinaus kann das hier erlangte Wissen über BUVs und PBDEs nicht nur in die Risikobewertung der einzelnen Substanzen, sondern insbesondere auch bei Mischungseffekten von Umweltschadstoffen, einfließen. Ebenso könnten die im Rahmen dieser Arbeit aus *in silico* Dockinganalysen gewonnenen Daten, welche zum Teil über anschließende Experimente mit PCB 126 und UV-327 *in vitro* validiert wurden, zur Entwicklung eines Tools zur Chemikalientestung beitragen. So wäre es einerseits eine große Ersparnis von Zeit und Rechenleistung, wenn man sich bei *in silico* Analysen auf die hier an der EGFR ECD identifizierte Region fokussieren würde, anstatt die gesamte Struktur des Rezeptors miteinzubeziehen. Andererseits könnte eine erfolgreiche *in silico* Positionierung von Substanzen an dieser Bindestelle bzw. Interaktion mit den in dieser Arbeit beschriebenen Aminosäuren erste Hinweise auf eine womöglich EGFR-inhibierende Wirkung der jeweiligen Testchemikalie liefern. Ein solches Tool könnte für prädikative Zwecke sowohl in der Entwicklung niedermolekularer EGFR-Inhibitoren als auch der Risikobewertung organischer Umweltschadstoffe im Hinblick auf deren Auswirkung auf EGFR-gesteuerte Prozesse, sowohl prä- als auch postnatal, von Nutzen sein.

4 Abkürzungsverzeichnis

AHR	Arylhydrocarbon-Rezeptor
AREG	Amphiregulin
ARNT	AHR-nuclear translocator
BaP	Benzo(a)pyren
BUV	Benzotriazole-UV-Stabilisator
CAR	C*onstitutive Androstane Receptor*
CYP	Cytochrom P450
DDT	Dichlordiphenyltrichlorethan
DLC	Dioxinähnliche Substanzen (D*ixoin-like Compounds*)
ECD	Extrazelluläre Domäne (E*xtracellular Domain*)
EGF	Epidermaler Wachstumsfaktor (*epidermal growth factor*)
EGFR	Epidermaler Wachstumsfaktor-Rezeptor
ER	Östrogenrezeptor (*estrogen receptor*)
EREG	Epiregulin
ERK	*Extracellular-signal Regulated Kinase*
MAPK	*Mitogen-activated Protein Kinase*
NF-κB	*Nuclear factor 'kappa-light-chain-enhancer' of activated B-cells*
PAK	Polyzyklischer aromatischer Kohlenwasserstoff
PAS	Per-Arnt-Sim

PBDE	Polybromierter Diphenylether
PCB	Polychloriertes Biphenyl
PCDD	Polychloriertes Dibenzodioxin
PCDF	Polychloriertes Dibenzofuran
POP	Persistenter organischer Schadstoff (*Persistent Organic Pollutant*)
PR	Progesteronrezeptor
ROS	Reaktive Sauerstoffspezies
RTK	Rezeptortyrosinkinase
TCDD	2,3,7,8-Tetrachlordibenzodioxin
TEQ	Toxizitätsäquivalenz
TGFA	*Transforming Growth Factor-α*
VEGFR	*Vascular Endothelial Growth Factor Receptor*
XRE	Xenobiotisch-responsives Element

5 Literaturverzeichnis

Abafe, O. A. und B. S. Martincigh (2015). "An assessment of polybrominated diphenyl ethers and polychlorinated biphenyls in the indoor dust of e-waste recycling facilities in South Africa: implications for occupational exposure." Environ Sci Pollut Res Int **22**(18): 14078-14086.

Abdi, K., G. Neves, J. Pyun, E. Kiziltug, A. Ahrens und C. T. Kuo (2019). "EGFR Signaling Termination via Numb Trafficking in Ependymal Progenitors Controls Postnatal Neurogenic Niche Differentiation." Cell Rep **28**(8): 2012-2022 e2014.

Alaee, M., P. Arias, A. Sjodin und A. Bergman (2003). "An overview of commercially used brominated flame retardants, their applications, their use patterns in different countries/regions and possible modes of release." Environ Int **29**(6): 683-689.

Albertolle, M. E. und F. Peter Guengerich (2018). "The relationships between cytochromes P450 and H(2)O(2): Production, reaction, and inhibition." J Inorg Biochem **186**: 228-234.

Andl, C. D., T. Mizushima, K. Oyama, M. Bowser, H. Nakagawa und A. K. Rustgi (2004). "EGFR-induced cell migration is mediated predominantly by the JAK-STAT pathway in primary esophageal keratinocytes." Am J Physiol Gastrointest Liver Physiol **287**(6): G1227-1237.

Astroff, B., C. Rowlands, R. Dickerson und S. Safe (1990). "2,3,7,8-Tetrachlorodibenzo-p-dioxin inhibition of 17 beta-estradiol-induced increases in rat uterine epidermal growth factor receptor binding activity and gene expression." Mol Cell Endocrinol **72**(3): 247-252.

Aung, M. T., K. K. Ferguson, D. E. Cantonwine, T. F. McElrath und J. D. Meeker (2019). "Preterm birth in relation to the bisphenol A replacement, bisphenol S, and other phenols and parabens." Environ Res **169**: 131-138.

Avilla, M. N., K. M. C. Malecki, M. E. Hahn, R. H. Wilson und C. A. Bradfield (2020). "The Ah Receptor: Adaptive Metabolism, Ligand Diversity, and the Xenokine Model." Chem Res Toxicol **33**(4): 860-879.

Ayotte, P., E. Dewailly, G. H. Lambert, S. L. Perkins, R. Poon, M. Feeley, C. Larochelle und D. Pereg (2005). "Biomarker measurements in a coastal fish-eating population environmentally exposed to organochlorines." Environ Health Perspect **113**(10): 1318-1324.

Beyett, T. S., C. To, D. E. Heppner, J. K. Rana, A. M. Schmoker, J. Jang, D. J. H. De Clercq, G. Gomez, D. A. Scott, N. S. Gray, P. A. Janne und M. J. Eck (2022). "Molecular basis for cooperative binding and synergy of ATP-site and allosteric EGFR inhibitors." Nat Commun **13**(1): 2530.

Beytagh, M. C. und W. A. Weiss (2022). "EGFR ligands dictate tumour suppression." Nat Cell Biol **24**(8): 1189-1191.

Birnbaum, L. S. (1994). "The mechanism of dioxin toxicity: relationship to risk assessment." Environ Health Perspect **102 Suppl 9**(Suppl 9): 157-167.

Bjermo, H., M. Aune, T. Cantillana, A. Glynn, P. M. Lind, P. Ridefelt und P. O. Darnerud (2017). "Serum levels of brominated flame retardants (BFRs: PBDE, HBCD) and influence of dietary factors in a population-based study on Swedish adults." Chemosphere **167**: 485-491.

Bogdan, S. und C. Klambt (2001). "Epidermal growth factor receptor signaling." Curr Biol **11**(8): R292-295.

Bull, S. und C. Collins (2013). "Promoting the use of BaP as a marker for PAH exposure in UK soils." Environ Geochem Health **35**(1): 101-109.

Burgess, A. W. (2008). "EGFR family: structure physiology signalling and therapeutic targets." Growth Factors **26**(5): 263-274.
Butte, W. und B. Heinzow (2002). "Pollutants in house dust as indicators of indoor contamination." Rev Environ Contam Toxicol **175**: 1-46.
Chen, G. und N. J. Bunce (2003). "Polybrominated diphenyl ethers as Ah receptor agonists and antagonists." Toxicol Sci **76**(2): 310-320.
Consonni, D., M. Rognoni, L. Cavalieri d'Oro und A. C. Pesatori (2024). "Mortality and cancer incidence in a population exposed to TCDD after the Seveso, Italy, accident (1976-2013)." Occup Environ Med **81**(7): 349-358.
Dai, Q., X. Min und M. Weng (2016). "A review of polychlorinated biphenyls (PCBs) pollution in indoor air environment." J Air Waste Manag Assoc **66**(10): 941-950.
Danjou, A. M., B. Fervers, M. C. Boutron-Ruault, T. Philip, F. Clavel-Chapelon und L. Dossus (2015). "Estimated dietary dioxin exposure and breast cancer risk among women from the French E3N prospective cohort." Breast Cancer Res **17**: 39.
Dawson, J. P., M. B. Berger, C. C. Lin, J. Schlessinger, M. A. Lemmon und K. M. Ferguson (2005). "Epidermal growth factor receptor dimerization and activation require ligand-induced conformational changes in the dimer interface." Mol Cell Biol **25**(17): 7734-7742.
Dickerson, R., L. Howie und S. Safe (1992). "The effect of 6-nitro-1,3,8-trichlorodibenzofuran as a partial estrogen in the female rat uterus." Toxicol Appl Pharmacol **113**(1): 55-63.
Dopico, M. und A. Gomez (2015). "Review of the current state and main sources of dioxins around the world." J Air Waste Manag Assoc **65**(9): 1033-1049.
Du, B., N. K. Altorki, L. Kopelovich, K. Subbaramaiah und A. J. Dannenberg (2005). "Tobacco smoke stimulates the transcription of amphiregulin in human oral epithelial cells: evidence of a cyclic AMP-responsive element binding protein-dependent mechanism." Cancer Res **65**(13): 5982-5988.
Eaton, D. L., T. W. Simon, N. E. Kaminski, G. H. Perdew und D. W. Nebert (2024). "The 2022 revised WHO TEFs for dioxins and dioxin-like chemicals: The importance of considering the use of species-specific information to determine relative effective potency for human-based risk assessment." Regul Toxicol Pharmacol **149**: 105599.
ECHA (2015). Annex XV report: Proposal for Identification of a Substance of Very High Concern on the Basis of the Criteria Set out in REACH Article 57, annex XV - Identification of UV-327 as SVCH.
ECHA. (2023). "Candidate List of substances of very high concern for Authorisation, 2023.", from https://echa.europa.eu/de/candidate-list-table.
EFSA, P. o. C. i. t. F. Chain, D. Schrenk, M. Bignami, L. Bodin, J. K. Chipman, J. Del Mazo, B. Grasl-Kraupp, C. Hogstrand, L. Ron Hoogenboom, J. C. Leblanc, C. S. Nebbia, E. Nielsen, E. Ntzani, A. Petersen, S. Sand, T. Schwerdtle, H. Wallace, D. Benford, P. Furst, A. Hart, M. Rose, H. Schroeder, M. Vrijheid, S. Ioannidou, M. Nikolic, L. R. Bordajandi und C. Vleminckx (2024). "Update of the risk assessment of polybrominated diphenyl ethers (PBDEs) in food." EFSA J **22**(1): e8497.
Eskenazi, B., M. Warner, P. Brambilla, S. Signorini, J. Ames und P. Mocarelli (2018). "The Seveso accident: A look at 40 years of health research and beyond." Environ Int **121**(Pt 1): 71-84.
Fazakas, E., I. A. Neamtiu und E. S. Gurzau (2024). "Health effects of air pollutant mixtures (volatile organic compounds, particulate matter, sulfur and nitrogen oxides) - a review of the literature." Rev Environ Health **39**(3): 459-478.

Fein, G. G., J. L. Jacobson, S. W. Jacobson, P. M. Schwartz und J. K. Dowler (1984). "Prenatal exposure to polychlorinated biphenyls: effects on birth size and gestational age." J Pediatr **105**(2): 315-320.
Feng, H., H. Cao, J. Li, H. Zhang, Q. Xue, X. Liu, A. Zhang und J. Fu (2020). "Estrogenic activity of benzotriazole UV stabilizers evaluated through in vitro assays and computational studies." Sci Total Environ **727**: 138549.
Ferguson, K. M. (2008). "Structure-based view of epidermal growth factor receptor regulation." Annu Rev Biophys **37**: 353-373.
Fernandez-Martinez, N. F., A. Ching-Lopez, A. Olry de Labry Lima, E. Salamanca-Fernandez, B. Perez-Gomez, J. J. Jimenez-Moleon, M. J. Sanchez und M. Rodriguez-Barranco (2020). "Relationship between exposure to mixtures of persistent, bioaccumulative, and toxic chemicals and cancer risk: A systematic review." Environ Res **188**: 109787.
Forrester, A. R., M. S. Elias, E. L. Woodward, M. Graham, F. M. Williams und N. J. Reynolds (2014). "Induction of a chloracne phenotype in an epidermal equivalent model by 2,3,7,8-tetrachlorodibenzo-p-dioxin (TCDD) is dependent on aryl hydrocarbon receptor activation and is not reproduced by aryl hydrocarbon receptor knock down." J Dermatol Sci **73**(1): 10-22.
Fowler, K. J., F. Walker, W. Alexander, M. L. Hibbs, E. C. Nice, R. M. Bohmer, G. B. Mann, C. Thumwood, R. Maglitto, J. A. Danks und et al. (1995). "A mutation in the epidermal growth factor receptor in waved-2 mice has a profound effect on receptor biochemistry that results in impaired lactation." Proc Natl Acad Sci U S A **92**(5): 1465-1469.
Freudlsperger, C., J. R. Burnett, J. A. Friedman, V. R. Kannabiran, Z. Chen und C. Van Waes (2011). "EGFR-PI3K-AKT-mTOR signaling in head and neck squamous cell carcinomas: attractive targets for molecular-oriented therapy." Expert Opin Ther Targets **15**(1): 63-74.
Fromme, H., G. Becher, B. Hilger und W. Volkel (2016). "Brominated flame retardants - Exposure and risk assessment for the general population." Int J Hyg Environ Health **219**(1): 1-23.
Fuller, R., P. J. Landrigan, K. Balakrishnan, G. Bathan, S. Bose-O'Reilly, M. Brauer, J. Caravanos, T. Chiles, A. Cohen, L. Corra, M. Cropper, G. Ferraro, J. Hanna, D. Hanrahan, H. Hu, D. Hunter, G. Janata, R. Kupka, B. Lanphear, M. Lichtveld, K. Martin, A. Mustapha, E. Sanchez-Triana, K. Sandilya, L. Schaefli, J. Shaw, J. Seddon, W. Suk, M. M. Tellez-Rojo und C. Yan (2022). "Pollution and health: a progress update." Lancet Planet Health **6**(6): e535-e547.
Gammon, M. D., M. S. Wolff, A. I. Neugut, S. M. Eng, S. L. Teitelbaum, J. A. Britton, M. B. Terry, B. Levin, S. D. Stellman, G. C. Kabat, M. Hatch, R. Senie, G. Berkowitz, H. L. Bradlow, G. Garbowski, C. Maffeo, P. Montalvan, M. Kemeny, M. Citron, F. Schnabel, A. Schuss, S. Hajdu, V. Vinceguerra, N. Niguidula, K. Ireland und R. M. Santella (2002). "Environmental toxins and breast cancer on Long Island. II. Organochlorine compound levels in blood." Cancer Epidemiol Biomarkers Prev **11**(8): 686-697.
Gomes, J., M. Begum und P. Kumarathasan (2024). "Polybrominated diphenyl ether (PBDE) exposure and adverse maternal and infant health outcomes: Systematic review." Chemosphere **347**: 140367.
Gray, L. E., J. S. Ostby und W. R. Kelce (1997). "A dose-response analysis of the reproductive effects of a single gestational dose of 2,3,7,8-tetrachlorodibenzo-p-dioxin in male Long Evans Hooded rat offspring." Toxicol Appl Pharmacol **146**(1): 11-20.

Gschwind, A., O. M. Fischer und A. Ullrich (2004). "The discovery of receptor tyrosine kinases: targets for cancer therapy." Nat Rev Cancer **4**(5): 361-370.
Guardans, R. (2024). "Global monitoring of persistent organic pollutants (POPs) in biota, water and sediments: its role in screening for unregulated POPs, in compiling time trends of regulated POPs under the Stockholm Convention (SC) and their relevance for biodiversity in a changing climate." Environmental Science: Advances(3): 1111-1123.
Guo, G., K. Gong, N. Beckley, Y. Zhang, X. Yang, R. Chkheidze, K. J. Hatanpaa, T. Garzon-Muvdi, P. Koduru, A. Nayab, J. Jenks, A. A. Sathe, Y. Liu, C. Xing, S. Y. Wu, C. M. Chiang, B. Mukherjee, S. Burma, B. Wohlfeld, T. Patel, B. Mickey, K. Abdullah, M. Youssef, E. Pan, D. E. Gerber, S. Tian, J. N. Sarkaria, S. K. McBrayer, D. Zhao und A. A. Habib (2022). "EGFR ligand shifts the role of EGFR from oncogene to tumour suppressor in EGFR-amplified glioblastoma by suppressing invasion through BIN3 upregulation." Nat Cell Biol **24**(8): 1291-1305.
Guo, G., K. Gong, B. Wohlfeld, K. J. Hatanpaa, D. Zhao und A. A. Habib (2015). "Ligand-Independent EGFR Signaling." Cancer Res **75**(17): 3436-3441.
Han, S. C., G. Z. Wang und G. B. Zhou (2023). "Air pollution, EGFR mutation, and cancer initiation." Cell Rep Med **4**(5): 101046.
Hanari, N., K. Kannan, Y. Miyake, T. Okazawa, P. R. Kodavanti, K. M. Aldous und N. Yamashita (2006). "Occurrence of polybrominated biphenyls, polybrominated dibenzo-p-dioxins, and polybrominated dibenzofurans as impurities in commercial polybrominated diphenyl ether mixtures." Environ Sci Technol **40**(14): 4400-4405.
Hardesty, J. E., L. Al-Eryani, B. Wahlang, K. C. Falkner, H. Shi, J. Jin, B. J. Vivace, B. P. Ceresa, R. A. Prough und M. C. Cave (2018). "Epidermal Growth Factor Receptor Signaling Disruption by Endocrine and Metabolic Disrupting Chemicals." Toxicol Sci **162**(2): 622-634.
Harding, J. und B. Burtness (2005). "Cetuximab: an epidermal growth factor receptor chemeric human-murine monoclonal antibody." Drugs Today (Barc) **41**(2): 107-127.
He, S., H. Xiao, S. Luo, X. Li, J. D. Zhang, X. M. Ren, Y. Yang, X. D. Xie, Y. Y. Zhou, Y. L. Yin, L. Luo und L. Y. Cao (2022). "Benzotriazole Ultraviolet Stabilizers Promote Breast Cancer Cell Proliferation via Activating Estrogen-Related Receptors alpha and gamma at Human-Relevant Levels." Environ Sci Technol **56**(4): 2466-2475.
Henriksen, L., M. V. Grandal, S. L. Knudsen, B. van Deurs und L. M. Grovdal (2013). "Internalization mechanisms of the epidermal growth factor receptor after activation with different ligands." PLoS One **8**(3): e58148.
Holbro, T. und N. E. Hynes (2004). "ErbB receptors: directing key signaling networks throughout life." Annu Rev Pharmacol Toxicol **44**: 195-217.
Holcomb, M. und S. Safe (1994). "Inhibition of 7,12-dimethylbenzanthracene-induced rat mammary tumor growth by 2,3,7,8-tetrachlorodibenzo-p-dioxin." Cancer Lett **82**(1): 43-47.
Honda, M. und N. Suzuki (2020). "Toxicities of Polycyclic Aromatic Hydrocarbons for Aquatic Animals." Int J Environ Res Public Health **17**(4).
Huang, S., J. Li, S. Xu, H. Zhao, Y. Li, Y. Zhou, J. Fang, J. Liao, Z. Cai und W. Xia (2019). "Bisphenol A and bisphenol S exposures during pregnancy and gestational age - A longitudinal study in China." Chemosphere **237**: 124426.
Hudson, L. G., W. A. Toscano, Jr. und W. F. Greenlee (1985). "Regulation of epidermal growth factor binding in a human keratinocyte cell line by 2,3,7,8-tetrachlorodibenzo-p-dioxin." Toxicol Appl Pharmacol **77**(2): 251-259.

Ivanovic, V. und I. B. Weinstein (1982). "Benzo[a]pyrene and other inducers of cytochrome P1-450 inhibit binding of epidermal growth factor to cell surface receptors." Carcinogenesis **3**(5): 505-510.
Jia, Y., Y. Tao, C. Lv, Y. Xia, Z. Wei und Y. Dai (2019). "Tetrandrine enhances the ubiquitination and degradation of Syk through an AhR-c-src-c-Cbl pathway and consequently inhibits osteoclastogenesis and bone destruction in arthritis." Cell Death Dis **10**(2): 38.
John, K., T. S. Lahoti, K. Wagner, J. M. Hughes und G. H. Perdew (2014). "The Ah receptor regulates growth factor expression in head and neck squamous cell carcinoma cell lines." Mol Carcinog **53**(10): 765-776.
Joiakim, A., P. A. Mathieu, C. Shelp, J. Boerner und J. J. Reiners, Jr. (2016). "Epidermal Growth Factor Receptor Kinase Inhibitors Synergize with TCDD to Induce CYP1A1/1A2 in Human Breast Epithelial MCF10A Cells." Drug Metab Dispos **44**(5): 665-671.
Joly-Tonetti, N., T. Ondet, M. Monshouwer und G. N. Stamatas (2021). "EGFR inhibitors switch keratinocytes from a proliferative to a differentiative phenotype affecting epidermal development and barrier function." BMC Cancer **21**(1): 5.
Jones-Otazo, H. A., J. P. Clarke, M. L. Diamond, J. A. Archbold, G. Ferguson, T. Harner, G. M. Richardson, J. J. Ryan und B. Wilford (2005). "Is house dust the missing exposure pathway for PBDEs? An analysis of the urban fate and human exposure to PBDEs." Environ Sci Technol **39**(14): 5121-5130.
Kafafi, S. A., H. Y. Afeefy, A. H. Ali, H. K. Said und A. G. Kafafi (1993). "Binding of polychlorinated biphenyls to the aryl hydrocarbon receptor." Environ Health Perspect **101**(5): 422-428.
Karenlampi, S. O., H. J. Eisen, O. Hankinson und D. W. Nebert (1983). "Effects of cytochrome P1-450 inducers on the cell-surface receptors for epidermal growth factor, phorbol 12,13-dibutyrate, or insulin of cultured mouse hepatoma cells." J Biol Chem **258**(17): 10378-10383.
Keil, A. P. und K. M. O'Brien (2024). "Considerations and targeted approaches to identifying bad actors in exposure mixtures." Stat Biosci **16**(2): 459-481.
Kerkvliet, N. I. und D. J. Kimeldorf (1977). "Antitumor activity of a polychlorinated biphenyl mixture, Aroclor 1254, in rats inoculated with Walker 256 carcinosarcoma cells." J Natl Cancer Inst **59**(3): 951-955.
Khare, A., P. Jadhao, A. N. Vaidya und A. R. Kumar (2023). "Benzotriazole UV stabilizers (BUVs) as an emerging contaminant of concern: a review." Environ Sci Pollut Res Int **30**(58): 121370-121392.
Kim, J. W., K. H. Chang, M. Prudente, P. H. Viet, S. Takahashi, S. Tanabe, T. Kunisue und T. Isobe (2019). "Occurrence of benzotriazole ultraviolet stabilizers (BUVSs) in human breast milk from three Asian countries." Sci Total Environ **655**: 1081-1088.
Kim, U. J., I. S. Lee, H. S. Kim und J. E. Oh (2011). "Monitoring of PBDEs concentration in umbilical cord blood and breast milk from Korean population and estimating the effects of various parameters on accumulation in humans." Chemosphere **85**(3): 487-493.
Knerr, S., J. Schaefer, S. Both, A. Mally, W. Dekant und D. Schrenk (2006). "2,3,7,8-Tetrachlorodibenzo-p-dioxin induced cytochrome P450s alter the formation of reactive oxygen species in liver cells." Mol Nutr Food Res **50**(4-5): 378-384.
Kociba, R. J., D. G. Keyes, J. E. Beyer, R. M. Carreon, C. E. Wade, D. A. Dittenber, R. P. Kalnins, L. E. Frauson, C. N. Park, S. D. Barnard, R. A. Hummel und C. G. Humiston (1978). "Results of a two-year chronic toxicity and oncogenicity study of 2,3,7,8-tetrachlorodibenzo-p-dioxin in rats." Toxicol Appl Pharmacol **46**(2): 279-303.

Köhler, K., P. Simmendinger, W. Roelle, W. Scholz, A. Valet und M. Slongo (2010). "Paints and Coatings, 4." Extenders, and Additives, Ullmann's Encyclopedia of Industrial Chemistry, Pigments.
Kohler, M., J. Tremp, M. Zennegg, C. Seiler, S. Minder-Kohler, M. Beck, P. Lienemann, L. Wegmann und P. Schmid (2005). "Joint sealants: an overlooked diffuse source of polychlorinated biphenyls in buildings." Environ Sci Technol **39**(7): 1967-1973.
Korc, M., B. Chandrasekar, Y. Yamanaka, H. Friess, M. Buchier und H. G. Beger (1992). "Overexpression of the epidermal growth factor receptor in human pancreatic cancer is associated with concomitant increases in the levels of epidermal growth factor and transforming growth factor alpha." J Clin Invest **90**(4): 1352-1360.
Kozer, N., J. Rothacker, A. W. Burgess, E. C. Nice und A. H. Clayton (2011). "Conformational dynamics in a truncated epidermal growth factor receptor ectodomain." Biochemistry **50**(23): 5130-5139.
Kubota, A., M. Terasaki, Y. Sakuragi, R. Muromoto, A. Ikeda-Araki, H. Takada und H. Kojima (2022). "Effects of benzotriazole UV stabilizers, UV-PS and UV-P, on the differentiation of splenic regulatory T cells via aryl hydrocarbon receptor." Ecotoxicol Environ Saf **238**: 113549.
Kulkarni, P. S., J. G. Crespo und C. A. Afonso (2008). "Dioxins sources and current remediation technologies--a review." Environ Int **34**(1): 139-153.
Lacouture, M. E. (2006). "Mechanisms of cutaneous toxicities to EGFR inhibitors." Nat Rev Cancer **6**(10): 803-812.
Larsen, A. K., D. Ouaret, K. El Ouadrani und A. Petitprez (2011). "Targeting EGFR and VEGF(R) pathway cross-talk in tumor survival and angiogenesis." Pharmacol Ther **131**(1): 80-90.
Lee, S., S. Kim, J. Park, H. J. Kim, J. J. Lee, G. Choi, S. Choi, S. Kim, S. Y. Kim, K. Choi, S. Kim und H. B. Moon (2015). "Synthetic musk compounds and benzotriazole ultraviolet stabilizers in breast milk: Occurrence, time-course variation and infant health risk." Environ Res **140**: 466-473.
Lee, T. C. und D. W. Threadgill (2009). "Generation and validation of mice carrying a conditional allele of the epidermal growth factor receptor." Genesis **47**(2): 85-92.
Li, M., E. Ivantsova, X. Liang und C. J. Martyniuk (2024). "Neurotoxicity of Benzotriazole Ultraviolet Stabilizers in Teleost Fishes: A Review." Toxics **12**(2).
Li, Q. Q., A. Loganath, Y. S. Chong, J. Tan und J. P. Obbard (2006). "Persistent organic pollutants and adverse health effects in humans." J Toxicol Environ Health A **69**(21): 1987-2005.
Lin, M., S. Ma, J. Tang, Y. Yu, G. Li, R. Fan, G. Zhang, B. Mai und T. An (2023). "Polybrominated diphenyl ethers and bromophenols in paired serum, hair, and urine samples of e-waste dismantlers: Insights into hair as an indicator of endogenous exposure." Sci Total Environ **871**: 161980.
Linares, V., M. Belles und J. L. Domingo (2015). "Human exposure to PBDE and critical evaluation of health hazards." Arch Toxicol **89**(3): 335-356.
Liu, Y., L. Gao, L. Qiao, D. Huang, B. Lyu, J. Li, Y. Wu und M. Zheng (2022). "Concentrations, Compound Profiles, and Possible Sources of Organic UV Filters in Human Milk in China." Environ Sci Technol **56**(22): 15930-15940.
Loertscher, J. A., C. A. Sattler und B. L. Allen-Hoffmann (2001). "2,3,7,8-Tetrachlorodibenzo-p-dioxin alters the differentiation pattern of human keratinocytes in organotypic culture." Toxicol Appl Pharmacol **175**(2): 121-129.
Madhukar, B. V., D. W. Brewster und F. Matsumura (1984). "Effects of in vivo-administered 2,3,7,8-tetrachlorodibenzo-p-dioxin on receptor binding of epidermal

growth factor in the hepatic plasma membrane of rat, guinea pig, mouse, and hamster." Proc Natl Acad Sci U S A **81**(23): 7407-7411.
Mallah, M. A., L. Changxing, M. A. Mallah, S. Noreen, Y. Liu, M. Saeed, H. Xi, B. Ahmed, F. Feng, A. A. Mirjat, W. Wang, A. Jabar, M. Naveed, J. H. Li und Q. Zhang (2022). "Polycyclic aromatic hydrocarbon and its effects on human health: An overeview." Chemosphere **296**: 133948.
Manisalidis, I., E. Stavropoulou, A. Stavropoulos und E. Bezirtzoglou (2020). "Environmental and Health Impacts of Air Pollution: A Review." Front Public Health **8**: 14.
Marinkovic, N., D. Pasalic, G. Ferencak, B. Grskovic und A. Stavljenic Rukavina (2010). "Dioxins and human toxicity." Arh Hig Rada Toksikol **61**(4): 445-453.
Maroni, M., A. Colombi, A. Ferioli und V. Foa (1984). "Evaluation of porphyrinogenesis and enzyme induction in workers exposed to PCB." Med Lav **75**(3): 188-199.
Masjosthusmann, S., D. Becker, B. Petzuch, J. Klose, C. Siebert, R. Deenen, M. Barenys, J. Baumann, K. Dach, J. Tigges, U. Hubenthal, K. Kohrer und E. Fritsche (2018). "A transcriptome comparison of time-matched developing human, mouse and rat neural progenitor cells reveals human uniqueness." Toxicol Appl Pharmacol **354**: 40-55.
Miettinen, P. J., J. R. Chin, L. Shum, H. C. Slavkin, C. F. Shuler, R. Derynck und Z. Werb (1999). "Epidermal growth factor receptor function is necessary for normal craniofacial development and palate closure." Nat Genet **22**(1): 69-73.
Milbrath, M. O., Y. Wenger, C. W. Chang, C. Emond, D. Garabrant, B. W. Gillespie und O. Jolliet (2009). "Apparent half-lives of dioxins, furans, and polychlorinated biphenyls as a function of age, body fat, smoking status, and breast-feeding." Environ Health Perspect **117**(3): 417-425.
Mimura, J. und Y. Fujii-Kuriyama (2003). "Functional role of AhR in the expression of toxic effects by TCDD." Biochim Biophys Acta **1619**(3): 263-268.
Montano, L., C. Pironti, G. Pinto, M. Ricciardi, A. Buono, C. Brogna, M. Venier, M. Piscopo, A. Amoresano und O. Motta (2022). "Polychlorinated Biphenyls (PCBs) in the Environment: Occupational and Exposure Events, Effects on Human Health and Fertility." Toxics **10**(7).
Moore, M. C., H. L. Greene, H. M. Said, F. K. Ghishan und D. N. Orth (1986). "Effect of epidermal growth factor and artificial feeding in suckling rats." Pediatr Res **20**(12): 1248-1251.
Morgan, A. (2024). "White Paper: Fire Retardancy: What, Why and How." Retrieved 06.09.2024, from https://www.isola-group.com/wp-content/uploads/Fire-Retardancy-What-Why-and-How.pdf.
Murray, I. A., A. D. Patterson und G. H. Perdew (2014). "Aryl hydrocarbon receptor ligands in cancer: friend and foe." Nat Rev Cancer **14**(12): 801-814.
Mutoh, S., M. Sobhany, R. Moore, L. Perera, L. Pedersen, T. Sueyoshi und M. Negishi (2013). "Phenobarbital indirectly activates the constitutive active androstane receptor (CAR) by inhibition of epidermal growth factor receptor signaling." Sci Signal **6**(274): ra31.
Nagayoshi, H., K. Kakimoto, S. Takagi, Y. Konishi, K. Kajimura und T. Matsuda (2015). "Benzotriazole ultraviolet stabilizers show potent activities as human aryl hydrocarbon receptor ligands." Environ Sci Technol **49**(1): 578-587.
Nakatsuru, Y., K. Wakabayashi, Y. Fujii-Kuriyama, T. Ishikawa, K. Kusama und F. Ide (2004). "Dibenzo[A,L]pyrene-induced genotoxic and carcinogenic responses are dramatically suppressed in aryl hydrocarbon receptor-deficient mice." Int J Cancer **112**(2): 179-183.

Nebert, D. W. und C. L. Karp (2008). "Endogenous functions of the aryl hydrocarbon receptor (AHR): intersection of cytochrome P450 1 (CYP1)-metabolized eicosanoids and AHR biology." J Biol Chem **283**(52): 36061-36065.
Noma, T., A. Lemaire, S. V. Naga Prasad, L. Barki-Harrington, D. G. Tilley, J. Chen, P. Le Corvoisier, J. D. Violin, H. Wei, R. J. Lefkowitz und H. A. Rockman (2007). "Beta-arrestin-mediated beta1-adrenergic receptor transactivation of the EGFR confers cardioprotection." J Clin Invest **117**(9): 2445-2458.
Oda, K., Y. Matsuoka, A. Funahashi und H. Kitano (2005). "A comprehensive pathway map of epidermal growth factor receptor signaling." Mol Syst Biol **1**: 2005 0010.
Oenga, G. N., D. C. Spink und D. O. Carpenter (2004). "TCDD and PCBs inhibit breast cancer cell proliferation in vitro." Toxicol In Vitro **18**(6): 811-819.
Orth, J. D., E. W. Krueger, S. G. Weller und M. A. McNiven (2006). "A novel endocytic mechanism of epidermal growth factor receptor sequestration and internalization." Cancer Res **66**(7): 3603-3610.
Panteleyev, A. A. und D. R. Bickers (2006). "Dioxin-induced chloracne--reconstructing the cellular and molecular mechanisms of a classic environmental disease." Exp Dermatol **15**(9): 705-730.
Paris, A., N. Tardif, F. M. Baietti, C. Berra, H. M. Leclair, E. Leucci, M. D. Galibert und S. Corre (2022). "The AhR-SRC axis as a therapeutic vulnerability in BRAFi-resistant melanoma." EMBO Mol Med **14**(12): e15677.
Park, J. Y., M. K. Shigenaga und B. N. Ames (1996). "Induction of cytochrome P4501A1 by 2,3,7,8-tetrachlorodibenzo-p-dioxin or indolo(3,2-b)carbazole is associated with oxidative DNA damage." Proc Natl Acad Sci U S A **93**(6): 2322-2327.
Passarini, B., S. D. Infusino und E. Kasapi (2010). "Chloracne: still cause for concern." Dermatology **221**(1): 63-70.
Patel, R. D., D. J. Kim, J. M. Peters und G. H. Perdew (2006). "The aryl hydrocarbon receptor directly regulates expression of the potent mitogen epiregulin." Toxicol Sci **89**(1): 75-82.
Pavanello, A., M. Gomez-Mendoza, V. A. de la Pena O'Shea, M. A. Miranda und M. L. Marin (2022). "Degradation of Benzotriazole UV-stabilizers in the presence of organic photosensitizers and visible light: A time-resolved mechanistic study." J Photochem Photobiol B **230**: 112444.
Peters, A. K., S. Nijmeijer, K. Gradin, M. Backlund, A. Bergman, L. Poellinger, M. S. Denison und M. Van den Berg (2006). "Interactions of polybrominated diphenyl ethers with the aryl hydrocarbon receptor pathway." Toxicol Sci **92**(1): 133-142.
Poland, A., E. Glover und A. S. Kende (1976). "Stereospecific, high affinity binding of 2,3,7,8-tetrachlorodibenzo-p-dioxin by hepatic cytosol. Evidence that the binding species is receptor for induction of aryl hydrocarbon hydroxylase." J Biol Chem **251**(16): 4936-4946.
Raaschou-Nielsen, O., M. Pavuk, A. Leblanc, P. Dumas, J. Philippe Weber, A. Olsen, A. Tjonneland, K. Overvad und J. H. Olsen (2005). "Adipose organochlorine concentrations and risk of breast cancer among postmenopausal Danish women." Cancer Epidemiol Biomarkers Prev **14**(1): 67-74.
Reed, L., V. M. Arlt und D. H. Phillips (2018). "The role of cytochrome P450 enzymes in carcinogen activation and detoxication: an in vivo-in vitro paradox." Carcinogenesis **39**(7): 851-859.
Ren, M., P. Peng, Y. Cai, D. Chen, L. Zhou, P. Chen und J. Hu (2011). "PBDD/F impurities in some commercial deca-BDE." Environ Pollut **159**(5): 1375-1380.
Ronan, T., J. L. Macdonald-Obermann, L. Huelsmann, N. J. Bessman, K. M. Naegle und L. J. Pike (2016). "Different Epidermal Growth Factor Receptor (EGFR) Agonists

Produce Unique Signatures for the Recruitment of Downstream Signaling Proteins." J Biol Chem **291**(11): 5528-5540.
Roskoski, R., Jr. (2014). "The ErbB/HER family of protein-tyrosine kinases and cancer." Pharmacol Res **79**: 34-74.
Rothhammer, V. und F. J. Quintana (2019). "The aryl hydrocarbon receptor: an environmental sensor integrating immune responses in health and disease." Nat Rev Immunol **19**(3): 184-197.
Safe, S., U. H. Jin, H. Park, R. S. Chapkin und A. Jayaraman (2020). "Aryl Hydrocarbon Receptor (AHR) Ligands as Selective AHR Modulators (SAhRMs)." Int J Mol Sci **21**(18).
Saito, T., S. Okada, K. Ohshima, E. Yamada, M. Sato, Y. Uehara, H. Shimizu, J. E. Pessin und M. Mori (2004). "Differential activation of epidermal growth factor (EGF) receptor downstream signaling pathways by betacellulin and EGF." Endocrinology **145**(9): 4232-4243.
Sakuragi, Y., H. Takada, H. Sato, A. Kubota, M. Terasaki, S. Takeuchi, A. Ikeda-Araki, Y. Watanabe, S. Kitamura und H. Kojima (2021). "An analytical survey of benzotriazole UV stabilizers in plastic products and their endocrine-disrupting potential via human estrogen and androgen receptors." Sci Total Environ **800**: 149374.
Sandermann, W. (1974). "[Polychlorinated aromatic compounds as environmental poisons]." Naturwissenschaften **61**(5): 207-213.
Sandermann, W. (1984). "Dioxin. Die Entdeckungsgeschichte des 2,3,7,8-Tetrachlordibenzo-p-dioxins (TCDD, Dioxin, Sevesogift) (Dioxin. Discovery history of 2,3,7,8-tetrachlorodibenzo-p-dioxin (TCDD, dioxin, Seveso toxin))." Naturwissenschaftliche Rundschau **37**: 173-178.
Santos, E. D. S., K. A. B. Nogueira, L. C. C. Fernandes, J. R. P. Martins, A. V. F. Reis, J. B. V. Neto, I. Junior, C. Pessoa, R. Petrilli und J. O. Eloy (2021). "EGFR targeting for cancer therapy: Pharmacology and immunoconjugates with drugs and nanoparticles." Int J Pharm **592**: 120082.
Scaltriti, M. und J. Baselga (2006). "The epidermal growth factor receptor pathway: a model for targeted therapy." Clin Cancer Res **12**(18): 5268-5272.
Schecter, A., L. Birnbaum, J. J. Ryan und J. D. Constable (2006). "Dioxins: an overview." Environ Res **101**(3): 419-428.
Schlessinger, J. (2000). "Cell signaling by receptor tyrosine kinases." Cell **103**(2): 211-225.
Schreiber, T., K. Gassmann, C. Gotz, U. Hubenthal, M. Moors, G. Krause, H. F. Merk, N. H. Nguyen, T. S. Scanlan, J. Abel, C. R. Rose und E. Fritsche (2010). "Polybrominated diphenyl ethers induce developmental neurotoxicity in a human in vitro model: evidence for endocrine disruption." Environ Health Perspect **118**(4): 572-578.
Shao, J., S. B. Lee, H. Guo, B. M. Evers und H. Sheng (2003). "Prostaglandin E2 stimulates the growth of colon cancer cells via induction of amphiregulin." Cancer Res **63**(17): 5218-5223.
Sharkey, M., S. Harrad, M. Abou-Elwafa Abdallah, D. S. Drage und H. Berresheim (2020). "Phasing-out of legacy brominated flame retardants: The UNEP Stockholm Convention and other legislative action worldwide." Environ Int **144**: 106041.
Shimizu, Y., Y. Nakatsuru, M. Ichinose, Y. Takahashi, H. Kume, J. Mimura, Y. Fujii-Kuriyama und T. Ishikawa (2000). "Benzo[a]pyrene carcinogenicity is lost in mice lacking the aryl hydrocarbon receptor." Proc Natl Acad Sci U S A **97**(2): 779-782.

Sibilia, M., J. P. Steinbach, L. Stingl, A. Aguzzi und E. F. Wagner (1998). "A strain-independent postnatal neurodegeneration in mice lacking the EGF receptor." EMBO J **17**(3): 719-731.
Sigismund, S., E. Argenzio, D. Tosoni, E. Cavallaro, S. Polo und P. P. Di Fiore (2008). "Clathrin-mediated internalization is essential for sustained EGFR signaling but dispensable for degradation." Dev Cell **15**(2): 209-219.
Sigismund, S., T. Woelk, C. Puri, E. Maspero, C. Tacchetti, P. Transidico, P. P. Di Fiore und S. Polo (2005). "Clathrin-independent endocytosis of ubiquitinated cargos." Proc Natl Acad Sci U S A **102**(8): 2760-2765.
Singh, B., G. Carpenter und R. J. Coffey (2016). "EGF receptor ligands: recent advances." F1000Res **5**.
Son, Y., S. Kim, H. T. Chung und H. O. Pae (2013). "Reactive oxygen species in the activation of MAP kinases." Methods Enzymol **528**: 27-48.
Sondermann, N. C., S. Fassbender, F. Hartung, A. M. Hatala, K. M. Rolfes, C. F. A. Vogel und T. Haarmann-Stemmann (2023). "Functions of the aryl hydrocarbon receptor (AHR) beyond the canonical AHR/ARNT signaling pathway." Biochem Pharmacol **208**: 115371.
Sondermann, N. C., A. A. Momin, S. T. Arold und T. Haarmann-Stemmann (2024). "Benzotriazole UV stabilizers disrupt epidermal growth factor receptor signaling in human cells." Environ Int **190**: 108886.
Sorg, O. (2014). "AhR signalling and dioxin toxicity." Toxicol Lett **230**(2): 225-233.
Sorg, O., M. Zennegg, P. Schmid, R. Fedosyuk, R. Valikhnovskyi, O. Gaide, V. Kniazevych und J. H. Saurat (2009). "2,3,7,8-tetrachlorodibenzo-p-dioxin (TCDD) poisoning in Victor Yushchenko: identification and measurement of TCDD metabolites." Lancet **374**(9696): 1179-1185.
Streicher, K. L., N. E. Willmarth, J. Garcia, J. L. Boerner, T. G. Dewey und S. P. Ethier (2007). "Activation of a nuclear factor kappaB/interleukin-1 positive feedback loop by amphiregulin in human breast cancer cells." Mol Cancer Res **5**(8): 847-861.
Sueyoshi, T., L. Li, H. Wang, R. Moore, P. R. Kodavanti, H. J. Lehmler, M. Negishi und L. S. Birnbaum (2014). "Flame retardant BDE-47 effectively activates nuclear receptor CAR in human primary hepatocytes." Toxicol Sci **137**(2): 292-302.
Sung, Y., S. T. Hong, M. Jang, E. S. Kim, C. Kim, Y. Jung, I. Youn, I. Chan Kwon, S. W. Cho und J. H. Ryu (2023). "Predicting response to anti-EGFR antibody, cetuximab, therapy by monitoring receptor internalization and degradation." Biomaterials **303**: 122382.
Sutter, C. H., H. Yin, Y. Li, J. S. Mammen, S. Bodreddigari, G. Stevens, J. A. Cole und T. R. Sutter (2009). "EGF receptor signaling blocks aryl hydrocarbon receptor-mediated transcription and cell differentiation in human epidermal keratinocytes." Proc Natl Acad Sci U S A **106**(11): 4266-4271.
Ticiani, E., J. Gingrich, Y. Pu, M. Vettathu, J. Davis, D. Martin, M. G. Petroff und A. Veiga-Lopez (2021). "Bisphenol S and Epidermal Growth Factor Receptor Signaling in Human Placental Cytotrophoblasts." Environ Health Perspect **129**(2): 27005.
Ticiani, E., J. A. Villegas, C. Murga-Zamalloa und A. Veiga-Lopez (2023). "Binding sites in the epidermal growth factor receptor are responsible for bisphenol S effects on trophoblast cell invasion." Chemosphere **318**: 137960.
Tomas, A., C. E. Futter und E. R. Eden (2014). "EGF receptor trafficking: consequences for signaling and cancer." Trends Cell Biol **24**(1): 26-34.
Torres-Duran, M., A. Ruano-Ravina, K. T. Kelsey, I. Parente-Lamelas, V. Leiro-Fernandez, I. Abdulkader, M. Provencio, J. Abal-Arca, O. Castro-Anon, C. Montero-Martinez, I. Vidal-Garcia, M. Amenedo, A. Golpe-Gomez, C. Martinez, R. Guzman-

Taveras, M. J. Mejuto-Marti, A. Fernandez-Villar und J. M. Barros-Dios (2017). "Environmental tobacco smoke exposure and EGFR and ALK alterations in never smokers' lung cancer. Results from the LCRINS study." Cancer Lett **411**: 130-135.
UNEP. (2001). "Stockholm Convention on Persistent Organic Pollutants (POPs). Text and Annexes. Revised in 2019.", from http://chm.pops.int/Convention/ConventionText/tabid/2232/Default.aspx.
UNEP. (2023a). "The new POPs under the Stockholm Convention." Retrieved 05.09.2024, from https://chm.pops.int/TheConvention/ThePOPs/TheNewPOPs/tabid/2511/Default.aspx .
UNEP. (2023b). "Report of the Conference of the Parties to the Stockholm Convention on Persistent Organic Pollutants on the work of its eleventh meeting." from https://chm.pops.int/TheConvention/ConferenceoftheParties/Meetings/COP11/tabid/9310/Default.aspx.
UNEP (2023c). "Third global monitoring report. Global monitoring plan for persistent organic pollutants under the Stockholm Convention Article 16 on effectiveness evaluation." Secretariat of the Basel, Rotterdam and Stockholm conventions, United Nations Environment Programme, Geneva.
Uribe, M. L., I. Marrocco und Y. Yarden (2021). "EGFR in Cancer: Signaling Mechanisms, Drugs, and Acquired Resistance." Cancers (Basel) **13**(11).
Vafeiadi, M., S. Agramunt, M. Pedersen, H. Besselink, L. Chatzi, E. Fthenou, S. Fleming, L. J. Hardie, J. Wright, L. E. Knudsen, J. K. Nielsen, J. Sunyer, R. Carreras, G. Brunborg, K. B. Gutzkow, U. C. Nygaard, M. Lovik, S. A. Kyrtopoulos, D. Segerback, D. F. Merlo, J. C. Kleinjans, M. Vrijheid, M. Kogevinas und C. NewGeneris (2014). "In utero exposure to compounds with dioxin-like activity and birth outcomes." Epidemiology **25**(2): 215-224.
Van den Berg, M., L. Birnbaum, A. T. Bosveld, B. Brunstrom, P. Cook, M. Feeley, J. P. Giesy, A. Hanberg, R. Hasegawa, S. W. Kennedy, T. Kubiak, J. C. Larsen, F. X. van Leeuwen, A. K. Liem, C. Nolt, R. E. Peterson, L. Poellinger, S. Safe, D. Schrenk, D. Tillitt, M. Tysklind, M. Younes, F. Waern und T. Zacharewski (1998). "Toxic equivalency factors (TEFs) for PCBs, PCDDs, PCDFs for humans and wildlife." Environ Health Perspect **106**(12): 775-792.
Viberg, H., A. Fredriksson, E. Jakobsson, U. Orn und P. Eriksson (2003). "Neurobehavioral derangements in adult mice receiving decabrominated diphenyl ether (PBDE 209) during a defined period of neonatal brain development." Toxicol Sci **76**(1): 112-120.
Vogeley, C., N. C. Sondermann, S. Woeste, A. A. Momin, V. Gilardino, F. Hartung, M. Heinen, S. K. Maass, M. Mescher, M. Pollet, K. M. Rolfes, C. F. A. Vogel, A. Rossi, D. Lang, S. T. Arold, M. Nakamura und T. Haarmann-Stemmann (2022). "Unraveling the differential impact of PAHs and dioxin-like compounds on AKR1C3 reveals the EGFR extracellular domain as a critical determinant of the AHR response." Environ Int **158**: 106989.
Vranic, S., O. Tawfik, J. Palazzo, N. Bilalovic, E. Eyzaguirre, L. M. Lee, P. Adegboyega, J. Hagenkord und Z. Gatalica (2010). "EGFR and HER-2/neu expression in invasive apocrine carcinoma of the breast." Mod Pathol **23**(5): 644-653.
Wahl, M., B. Lahni, R. Guenther, B. Kuch, L. Yang, U. Straehle, S. Strack und C. Weiss (2008). "A technical mixture of 2,2',4,4'-tetrabromo diphenyl ether (BDE47) and brominated furans triggers aryl hydrocarbon receptor (AhR) mediated gene expression and toxicity." Chemosphere **73**(2): 209-215.

Wang, C., X. Liu, J. Zhai, C. Zhong, H. Zeng, L. Feng, Y. Yang, X. Li, M. Ma, T. Luan und J. Deng (2024). "Effect of oxidative stress induced by 2,3,7,8- tetrachlorodibenzo-p-dioxin on DNA damage." J Hazard Mater **472**: 134485.
Wang, F., X. J. Ruan und H. Y. Zhang (2015). "BDE-99 (2,2',4,4',5-pentabromodiphenyl ether) triggers epithelial-mesenchymal transition in colorectal cancer cells via PI3K/Akt/Snail signaling pathway." Tumori **101**(2): 238-245.
Wang, S., Z. Zhang, H. Peng und K. Zeng (2019). "Recent advances on the roles of epidermal growth factor receptor in psoriasis." Am J Transl Res **11**(2): 520-528.
Wang, W. L., W. Porter, R. Burghardt und S. H. Safe (1997). "Mechanism of inhibition of MDA-MB-468 breast cancer cell growth by 2,3,7,8-tetrachlorodibenzo-p-dioxin." Carcinogenesis **18**(5): 925-933.
Watanabe, M. und Y. Noma (2010). "Behavior of 2-(3,5-di-tert-butyl-2-hydroxyphenyl)benzotriazole (DBHPBT) and 2-(3,5-di-tert-butyl-2-hydroxyphenyl)-5-chlorobenzotriazole during incineration of solid waste contaminated with thousand mg/kg levels of DBHPBT." J Hazard Mater **178**(1-3): 1065-1069.
WHO (2019). "Exposure to dioxins and dioxin-like substances: a major public health concern. Preventing disease through healthy environments. ." World Health Organization.
Wilson, K. J., C. Mill, S. Lambert, J. Buchman, T. R. Wilson, V. Hernandez-Gordillo, R. M. Gallo, L. M. Ades, J. Settleman und D. J. Riese, 2nd (2012). "EGFR ligands exhibit functional differences in models of paracrine and autocrine signaling." Growth Factors **30**(2): 107-116.
Wu, D., N. Potluri, Y. Kim und F. Rastinejad (2013). "Structure and dimerization properties of the aryl hydrocarbon receptor PAS-A domain." Mol Cell Biol **33**(21): 4346-4356.
Xie, G., Z. Peng und J. P. Raufman (2012). "Src-mediated aryl hydrocarbon and epidermal growth factor receptor cross talk stimulates colon cancer cell proliferation." Am J Physiol Gastrointest Liver Physiol **302**(9): G1006-1015.
Xue, W. und D. Warshawsky (2005). "Metabolic activation of polycyclic and heterocyclic aromatic hydrocarbons and DNA damage: a review." Toxicol Appl Pharmacol **206**(1): 73-93.
Yang, J., J. Zhu und K. M. Chan (2016). "BDE-99, but not BDE-47, is a transient aryl hydrocarbon receptor agonist in zebrafish liver cells." Toxicol Appl Pharmacol **305**: 203-215.
Yao, N., C. R. Wang, M. Q. Liu, Y. J. Li, W. M. Chen, Z. Q. Li, Q. Qi, J. J. Lu, C. L. Fan, M. F. Chen, M. Qi, X. B. Li, J. Hong, D. M. Zhang und W. C. Ye (2020). "Discovery of a novel EGFR ligand DPBA that degrades EGFR and suppresses EGFR-positive NSCLC growth." Signal Transduct Target Ther **5**(1): 214.
Yasuda, K. und M. Takahashi (1998). "The Emission of Polycyclic Aromatic Hydrocarbons from Municipal Solid Waste Incinerators during the Combustion Cycle." J Air Waste Manag Assoc **48**(5): 441-447.
Ye, W., R. Chen, X. Chen, B. Huang, R. Lin, X. Xie, J. Chen, J. Jiang, Y. Deng und J. Wen (2019). "AhR regulates the expression of human cytochrome P450 1A1 (CYP1A1) by recruiting Sp1." FEBS J **286**(21): 4215-4231.
Yemele, O. M., Z. Zhao, J. N. Nkoh, E. Ymele und M. Usman (2024). "A systematic review of polycyclic aromatic hydrocarbon pollution: A combined bibliometric and mechanistic analysis of research trend toward an environmentally friendly solution." Sci Total Environ **926**: 171577.

Zhang, F., L. Peng, Y. Huang, X. Lin, L. Zhou und J. Chen (2019). "Chronic BDE-47 Exposure Aggravates Malignant Phenotypes and Chemoresistance by Activating ERK Through ERalpha and GPR30 in Endometrial Carcinoma." Front Oncol **9**: 1079.
Zhang, W., H. Q. Xie, Y. Li, M. Zhou, Z. Zhou, R. Wang, M. E. Hahn und B. Zhao (2022). "The aryl hydrocarbon receptor: A predominant mediator for the toxicity of emerging dioxin-like compounds." J Hazard Mater **426**: 128084.
Zhuang, S., X. Lv, L. Pan, L. Lu, Z. Ge, J. Wang, J. Wang, J. Liu, W. Liu und C. Zhang (2017). "Benzotriazole UV 328 and UV-P showed distinct antiandrogenic activity upon human CYP3A4-mediated biotransformation." Environ Pollut **220**(Pt A): 616-624.
Zota, A. R., S. D. Mitro, J. F. Robinson, E. G. Hamilton, J. S. Park, E. Parry, R. T. Zoeller und T. J. Woodruff (2018). "Polybrominated diphenyl ethers (PBDEs) and hydroxylated PBDE metabolites (OH-PBDEs) in maternal and fetal tissues, and associations with fetal cytochrome P450 gene expression." Environ Int **112**: 269-278.

6 Anhang

Anhang I: Übersicht aller kolorimetrischer BrdU Inkooperationsassays, welche im Rahmen dieser Dissertation angefertigt wurden. Die Assays wurden dem Material/Methoden-Teil von Sondermann et al. (2024) entsprechend in HaCaT AHR KO-Zellen zur Bestimmung des Einflusses verschiedener Substanzen auf die AREG-induzierte DNA-Synthese durchgeführt. n = 4-7. *, p ≤ 0.05 im Vergleich zu DMSO. n.s. = nicht signifikant. Graues Feld = Konzentration nicht getestet.

Substanz	0,1 nM	1 nM	10 nM	100 nM	1 µM	10 µM
Aroclor 1254			*	*	*	
PCB126			n.s.	n.s.	*	
PCB 118	*	*	*	*	*	
PCB 77				n.s.	*	*
PCB 47			*	*	*	
TCDD				*	*	
Bifenox				n.s.	n.s.	*
Atrazin				n.s.	n.s.	n.s.
4,4-DDT				n.s.	n.s.	*
UV-320				n.s.	n.s.	*
UV-326				n.s.	*	*
UV-327		n.s.	n.s.	*	*	*
UV-350				n.s.	n.s.	n.s.
UV-PS				n.s.	n.s.	n.s.
BDE-47				n.s.	*	*
BDE-99				n.s.	*	*
			25 nM	**250 nM**	**2.5 µM**	
B[a]P			n.s.	n.s.	n.s.	
B[k]F			n.s.	n.s.	n.s.	
				200 nM	**2 µM**	**20 µM**
Bisphenol A				*	*	*

7 Danksagung

An dieser Stelle möchte ich mich noch herzlich bei allen bedanken, die zum Gelingen dieser Arbeit beigetragen haben.

Mein besonderer Dank gilt meinem Doktorvater, Dr. Thomas Haarmann-Stemmann, für die fachkundige Betreuung, das entgegengebrachte Vertrauen und die stetige Unterstützung während meiner Promotionszeit. Deine wertvollen Anregungen und das Vertrauen in meine Fähigkeiten haben mich durch die Höhen und Tiefen dieser Arbeit begleitet und maßgeblich zu ihrem Erfolg beigetragen.

Auch meiner Mentorin Frau Prof. Dr. Henrike Heise möchte herzlich danken. Ich schätze es sehr, dass Sie sich der Betreuung meines Promotionsvorhabens und der Begutachtung dieser Dissertation angenommen haben.

Ebenso möchte ich der gesamten Arbeitsgruppe Haarmann-Stemmann danken. Ohne eure kollegiale Unterstützung, die anregenden Diskussionen und die freundliche Arbeitsatmosphäre wäre diese Arbeit nicht in der Form möglich gewesen! Ein riesengroßes Dankeschön geht außerdem an Etta Zühr für die wiederholte Unterstützung am CellInsight.

Darüber hinaus bedanke ich mich ausdrücklich bei meinen Kooperationspartnern Prof. Stefan Arold und Afaque Momin, welche mich bei den flexiblen *in silico*-Dockinganalysen unterstützt haben.

Mein besonderer Dank gilt außerdem der Jürgen Manchot-Stiftung, die mir diese Arbeit durch eine dreijährige Finanzierung meines Projekts überhaupt ermöglicht hat.

Auch allen anderen, die auf direktem Weg oder Umwegen zu dieser Arbeit beigetragen haben, gebührt mein aufrichtiger Dank: Alina, Jenny, Timo, Katie, Mutter, Schwesterherz - danke, dass ihr immer da seid!

8 Eidesstattliche Erklärung

Hiermit versichere ich an Eides statt, dass die vorliegende Dissertation „Identifizierung des epidermalen Wachstumsfaktor-Rezeptors als Zielstruktur für Umweltgifte“ von mir selbständig und ohne unzulässige fremde Hilfe unter Beachtung der „Grundsätze zur Sicherung guter wissenschaftlicher Praxis and der Heinrich-Heine-Universität Düsseldorf“ erstellt worden ist. Die Dissertation wurde in der vorgelegten oder einer ähnlichen Form noch bei keiner anderen Institution eingereicht. Ich habe bisher keine erfolglosen Promotionsversuche unternommen.

Düsseldorf, den 20.11.2024

Natalie C. Sondermann